Feasibility of Tall Timber Buildings
Master Thesis - Structural Engineering

S.G.C.Timmer

October 2011

Tall Timber Buildings

Feasibility Study

Author:
Ing. S.G.C. Timmer

Graduation Committee:

Prof.Ir. R. Nijsse	Chairman
Prof.dipl.-ing. J.N.J.A. Vambersky	Former Chairman
Ir. G.J.P. Ravenshorst	Board Member
Ir. K.C. Terwel	Board Member
Dipl.-Ing Carmen Sandhaas	Former Board Member
Ir. L.J.M. Houben	Supervisor

Delft University of Technology
Faculty of Civil Engineering and Geosciences
Structural Engineering

October 2011

Picture on the cover: cover picture of att. zuschnitt Vielgeschossiger Holzbau im urbane Raum Dokumentation Forschungsprojeckt 8+ proHolz Austria [5]

Abstract

The choice of the subject of this thesis was initially motivated on two issues, namely the current social momentum for finding solutions for sustainable building and the authors personal interest in large structures like bridges and tall buildings. The subject tall timber buildings answer to both issues.

The objective of this thesis is twofold. The first objective is to determine the influence factors on the height of buildings. The second objective of this thesis is to verify the structural feasibility of a timber office building of 100 m high, with acceptable architectural performance, within a reasonable set of conditions

An analysis of the problem was conducted within the preliminary study of this thesis. Within the literature several definitions of tall timber buildings were found. It was also found that the building height itself does not determine the feasibility of an acceptable design solution, and that the height of a building design is one of the many architectural performance characteristics. If a definition of a tall timber building exists, it would be the combined part of the definitions of tall buildings and timber buildings, which results in:

Tall timber building: *A building of which most of the engineered parts constitute out of timber products, that is constructed according to modern requirements and in which the effects of the lateral loads is reflected in the structural design.*

The influence factors on the height of a tall timber building were determined within a problem analysis. The main factors are part of architectural requirements, structural issues, fire safety and building physics. In this thesis the influence factors are quantified to achieve the highest potential, within realistic limits.

Architectural influence factors are worked out to a set of requirements which result in the design of a feasible universal floor plan, a minimum wall-window ratio of 15% and a building slenderness of 1:4.

Structural influence factors are the foundation, the comfort experienced by occupants and the load bearing structure. The behavior of the load bearing structure is in fact responsible for comfort perception, associated problems. The influence of the properties of wood on the structural characteristics of the building was theoretically investigated. It was found that the specific properties of wood could be counteracted with, and defined by, the terminology:

- *Wood Quality*
- *Stability System*
- *Joint Detailing*
- *Foundation*

Wood Quality: The assumed wood quality is based on what is believed to be maximum achievable. Handpicked sawn timbers of a wood species that resemble a strength class D70, as graded according to EN 338, were found to be used in the Yingxian Pagoda [30]. Based on a recently developed traffic bridge project [14], it is known that the timber engineering industry has machinery and workshops that are able to produce and handle large sections of laminated timber. When these facts are combined a maximum virtual timber lamination of strength class D70 is possible, however not available on the current market. Still, this virtual material is used for the calculation in this thesis to investigate the maximum potential.

Stability System: The stability system is broken down into system principle, horizontal layout and type of bracing. The stability system consists of a tube-in-tube structure, braced system with three possible types of bracing, namely a Diagid geometry, diagonal bracing and a solid timber shear wall.

Joint Detailing: The joint detailing was chosen consistent with the type of bracing of the stability system and are: balloon framing joints for cross laminated timber shear wall systems and either steel-timber joints, or glued in rods for other stability systems.

Foundation: The load bearing capacity of the foundation is not expected to be a problem for tall timber buildings. The stiffness of the foundation does influence the lateral deflection at the top of a tall building and is therefore included in the calculations.

Fire safety influence factors are derived from the consequences of a fire which are counteracted by satisfying a number of fire safety objectives. These objectives are covered when evacuation is safely possible, building collapse does not occur and spread of fire and smoke is limited. The universal floor plan is verified to comply with the Dutch building code to satisfy the fundamental objectives of evacuation. The remaining objectives are satisfied by establishing compartment burn out through the use of fire concepts in combination with fire suppression measures. The fire concepts are:

- Building Encapsulation
- Finite Charring

Building Encapsulation: The concept of building encapsulation is to protect the structural wooden parts for the whole duration of a fire by non-combustible materials, with inclusion of the condition that wooden part do not start charring. The application of non-combustible surface materials also limits the production of fire and smoke.

Finite Charring: The concept of finite charring protects the structure by the charcoal layers forming on wooden parts and by the massiveness of timber members themselves, until all other combustible material inside the considered compartment has burned. The high wood quality of structural members satisfies the regulations with respect to the production of fire and smoke for the majority of the building.

Relevant building physical influence factors are acoustic vibrations in vertical partitions, i.e. timber floor structures. This problem is solved by using a suitable floor lay-up solution.

To quantify the problem, a case study was conducted in which all relevant parameters determined earlier on in this thesis are taken into account. The universal tall building acted as a template for four variants. This template building is 112 m high divided over 32 storey's, consists of a building core and a tube structure which are coupled by the intermediate floor structure. Variants embedded the proposed stability systems, i.e. types of bracing, and consist of the set:

- Diagrid Geometry
- Diagonal Braced Frame
- Solid Shear Wall
- Mega Frame

Two laminated timber materials of a deciduous wood base of strength class D70 are applied to variants in the case study. These materials are called D70-LAM and D70-CLT to distinguish between unidirectional laminated timber and cross laminated timber respectively. The material properties of D70-LAM are equal to the base material while for D70-CLT some stiffness modifications are taken into account.

Finite element models are created of variants. Of these models, parameters are modified in order to investigate: the influence of the joint stiffness; the building core stiffness; and the support stiffness on the global behavior. The investigation on the global behavior of the systems focused on the deflection at the top, the development of bending moments within members and the dynamical behavior.

An optimization was conducted on the size of members for all variants. The optimization focused on the buckling force of members because no significant stress increase occurred caused by internal bending moments. The applied joint type of the first two variants where believed to influence the behavior. The stiffness of these joints was determined by a joint optimization design procedure. The joints where designed to match the buckling capacity of adjacent members. In this way a list could be created and used to chose sections within an optimization procedure while the verification of joint strength is satisfied.

The stiffness of the core was calculated with a 2D finite element model and reduced to section properties which could be applied in 1D element models. The foundation was assumed to consist of bored piles and the stiffness of those piles was transformed into spring stiffness values used in the calculation models.

In the fire safety analysis, variants where subdivided into categories based on the size of windows, or rather the opening factor. The fire load and other parameters where determined in order to calculate the effective charring rates and subsequently the charring depth of the proposed solutions. Based on these calculations it was found that buildings with a large opening factor resulted in relatively high peak temperatures but shorter lasting fires. The desperation of heat energy released in a fire, is higher for of buildings with large windows, which is more favorable in terms of charring depth. It was concluded that buildings with small window openings, i.e. the solid shear wall solution, within the configuration it was proposed, can only be feasible in terms of fire safety when the concept building encapsulation is applied. The maximum effective charring depth for other solutions was 41 mm without taking active fire measures into account, which resulted into a reduction of square sections of 82 mm.

The buckling verification of members under basic ultimate limit state load combinations, was conducted simultaneous with the optimization of members for all variants. The forces in members under load combinations applied for fire verifications showed that timber members are certainly protected by the massiveness themselves, because the reduced sections of relatively small members fail.

The deflection at the top of the timber building satisfied the limits of the building code for all variants. It was derived that the influence on the deflection of the joint stiffness was between 14% and 20%, of the core stiffness was between 39% to 56% and the foundation was between 16% to 23%. The difference in influence between doweled joints and tube-fasteners joints on the deflection is insignificant.

The joints stiffness of the first two variants did not result in higher bending moments then when a hinged connection is assumed. A rigid joint interface with rotational and translational fixations in all directions results in higher bending moments but does not reduce the deflection at the top significantly.

The dynamical analysis was conducted with two methods, namely: a finite element analysis and a manual calculation method according to the Dutch standard which served as a verification on the first. For both methods the relevant modes and associated eigen frequencies where determined first. The dynamic part of the wind load was imposed on the model within a linear time history analysis for the finite element method to determine the acceleration.

The dynamic behavior results were verified against the frequency-acceleration curve stated in the Dutch standard NEN 6702. The scatter between solutions is larger and less conservative for the finite element method then the manual calculation method. It was found that not all solutions satisfied the requirements.

The support reactions of ultimate limit state combinations showed that the stiffness of the assumed foundation was correct, because the load bearing capacity of the foundation was close or equal to the magnitude of the forces.

In the last part of the thesis a feasibility analysis was carried out for all variants. In this analysis, characteristics of the variants where graded. The first criterion is the stiffness of the building over the mass of raw material necessary to create the building structure, to determine the efficiency of the material use. The second criterion was a production analysis based on the number of components and their opportunity cost. The rating of the last three criteria is based on an assessment of the entry of daylight, the fire safety and the comfort correlated with their economic implications.

In can be concluded that a tall timber building is possible within the definition that was stated earlier. For this thesis a building structure of 112 m high was proven to be possible on a fundamental level. Several structural systems can be applied in combination with an appropriate fire concept.

It can be concluded that a mega-frame is less feasible, because additional devices like trusses have to be applied to redirect the dead load to the windward mega-columns to compensate for uplift under latteral wind loading. Moreover, the size of elements used in the mega-frame makes lifting more difficult and expensive.

A cross laminated timber shear wall frame is most cost effective because construction speed is high. This is mainly due to the simplicity of connecting and placing the elements descending from the simple screwed joint interface and the semi-balloon framing method. This variant can be made more interesting when windows are chosen larger then is assumed in this thesis, while trading of some lateral structural stiffness.

The Diagrid geometry tube structure is the preferred choice because its combined evaluation in a multi criteria analysis results in the highest grade when compared to other alternatives. A common braced frame is also a sound and frequently proven solution.

Furthermore it is recommended that some detailed research must be done on the properties of laminated timber of hardwood species, the combination of this with tube-fasteners and dowels and the verification of the finite charring concept as it was suggested in this thesis. Furthermore could the science of structural engineering benefit from further investigations of prestressing timber for application in trusses of beams. The last recommendation made in light of this thesis is the necessity to investigate micro and macroeconomic implications of hardwood application to a tall timber building project.

Preface

This master thesis is the crowning glory of my study at the faculty of Civil Engineering and Geosciences at Delft University of Technology. I can remember when I just was registered for the Master program at the university, that Wout Luites and I agreed walking on the campus: "Now we can die in peace". I have to explain here that we were fellow students at the academy from which we graduated earlier that same year. It has been both our wish to study and graduate in Delft for some time before.

It has been a longer road then I anticipated especially during this last phase of my study. On the other hand, I got myself to blame and congratulate at the same time. During this phase I have also explored other activities that where part of a personal development. Especially at the beginning of writing this thesis, I was rather passionate about playing the piano and trying to master this art. A man can dream. It was also in this period that I took an deeper interest then before in social studies like psychology, and found online lectures on the study of non-violence by coincidence on a lazy day browsing the internet.

It is therefore that I would first like to thank my parents and family for being accommodating, and supporting in anything I would like to embark on. I could never have done this on my own and therefore, I thank you.

It is one thing to chase your interests as you go along, but like everything in live there is always the other side of the coin. Scattering your attention like I did, can eventually result in academic procrastination. It is therefore that I would like to thank the entire graduation committee, and within that sense in particular Karel Terwel who contacted me several times to motivate and discuss my thesis. I would also like to thank Carmen Sandhaas for sharing her knowledge and sources in the field of timber engineering, and getting my thesis (finally) organized. Which brings me to Geert Ravenshorst who inspired me on some occasions to be practical in my approach, and showing me that I must stop looking when the answer is already showing. Furthermore I would like to thank both professor Jan Vambersky and Rob Nijsse for being chairman of the graduation committee during different phases of my study, and their valuable input.

Not to forget, Jos Wolters and Hans van Vliet of ABT consultancy, for their input at an early stage, of which parts still resonate within the underling rational of my thesis, thank you both.

I also would like to express my gratitude to my brother in law, Martin van Breukelen who took on the effort of rereading, making notes and discussing parts of my thesis when I was becoming weary. And my sister for inviting me on many occasions to dinners and parties. In that last sense I would like to thank all my friends, for both taking my mind off the study and pear pressuring me into completion.

October 2011

Index

1 Introduction

1.1 Problem Description

The ultimate height limit for tall buildings in general will probably be unknown indefinitely, because of ever advancing building technology and developments in the field of structural engineering. Several attempts have been made in the past to gain insight into the limit of high rise structures and several buildings have been constructed accordingly. In the recent past, similar efforts have emerged for timber buildings. Because of recent developments in the field of timber engineering and technology new insights and possibilities have risen for tall buildings with wood as the main material of use.

To investigate the height limitation of tall timber buildings one has to deal with a set of many variables that influences the design. In general, the decision making process associated with designing tall buildings results in a defined set of these variables. Apart from recent developments the experience with tall timber buildings is limited, while large timber structures like bridges are more common.

The combination of the confusion associated with many variables making up the design of a tall building, and the limited experience with tall timber buildings create a void of understanding what can be achieved with wood based materials. Therefore the height limit of tall timber buildings is not established proportionally compared to other building materials.

The most common challenges for tall timber buildings are the lateral stiffness, the dynamic behavior in wind conditions, acoustic vibrations and the fire safety.

1.2 Objective

The objective of this thesis is twofold. The first objective is to determine which factors influence the height of timber buildings. The second objective of this thesis is to verify the structural feasibility of a timber office building of 100 m high, with acceptable architectural performance, within a reasonable set of conditions.

The following sub questions have to be answered for a timber building structure of at least 100 m high:

- Can the building be designed stiff enough to satisfy the requirements on lateral deflection?
- Is the dynamic behavior of the building within the requirements of human comfort?
- Can the building be designed fire safe?

1.3 Outline of the Thesis

This thesis is build-up out of two main parts. The first is the preliminary study, in a discussion takes place and some solutions are proposed and analyzed. The second part consists of chapters 3 to 9 and embodies the case study. In chapter 10 conclusions and recommendations are given.

The basic solutions proposed in the preliminary study are worked out in the case study into research parameters and boundary conditions. These parameters are the basis of models presented and worked out in the chapters 4 to 6. In the fire safety analysis in chapter 7, calculations are made on the charring depth for different solutions which are used in the verification of sections in chapter 8. The results of calculations with finite element models are presented in chapter 8, which also includes some basic limit state verifications in graphic form. In chapter 9 the results are used to do a feasibility study based on the issues encountered during this study.

2 Preliminary Research

2.1 Introductory Statement

Using timber for the structural buildings systems up to 120 m with 40 storey's seem mind altering to some, while nature creates these cantilever wonders, people worry about them [1]. Low-rise light-timber frame dwellings are the 'standard' in North America and to some extend still popular in Europe. The position of mid-rise buildings have been held by steel and concrete for so long that wood multi-storey construction strikes many people as ancient and impractical [2].

Until the resent past this was the case, and some dominant paradigms are still held inside regulatory regimes and building codes of today. There are some historical and modern examples of buildings and structures erected entirely out of timber that have survived the ravages of time like Gliwice Radio Transmission Tower and the Yingxian Pagoda. A modern example is the nine-storey high apartment block housing development in the suburb of London, called the Murray Grove Tower, finished in the year 2008, which is built entirely out of solid cross laminated timber panels.

Arguments against wood as a construction material for buildings are usually superficial observations of inferior strength and stiffness properties compared to other building materials, that wood is combustible material and timber buildings have poor acoustic characteristics. There is some truth in all these arguments. However, their truth depends on the perspective of these observations.

Wood has some specific characteristics that are encountered when studying tall timber buildings with respect to their height. In this paragraph the relationship between these material specific characteristics and the building structure are explained. The characteristics consist of the timber material properties as they are known from the building codes and timber handbooks.

Structural performance

Timber graded according to EN 388 into strength-class C24 is comparable to the strength of commonly used concrete. Compared to steel, the tensile strengths of timbers are in the order of 10-20% of the yield strengths of commonly available grades of structural steel. In terms of stiffness, steel and concrete are respectively in the order of 10 to 20 times and 3 to 5 times stiffer than sawn timber. These comparisons are made on timber properties parallel to the grain.

Thereby, when the comparison is normalized to the difference in mass per volume, different conclusions emerge. Some modern wood-based composites are commonly at least twice the strengths of sawn timber. To make comparisons conservative, an average deciduous wood species has a density of about 530 kg/m^3. Compared to commonly used concrete with a density of about 2400 kg/m^3 and structural steel with a density of 7850 kg/m^3 sawn timber is about 4 ½ times lighter than concrete and about 15 times lighter then steel in terms of mass. Using steel grade S355 as the benchmark for strength and stiffness comparison, and concrete C55 with 5% reinforcement as another competitor, timber in bending performs at a level of 133% in terms of strength while reinforced concrete performs at 99%. In terms of tension and compression parallel to the grain the timber strength ratio levels are respectively 48% and 70%, where concrete levels are at 4% and 38%. In terms of stiffness, normalized to weight, assuming the mean modules of elasticity, comparisons produce levels of 78% for timber and 55% for concrete. In that sense, timber has some strength and stiffness qualities that are comparable or superior to steel and concrete.

Naturally, this assumes that the section geometry of timber in these comparisons are at least 4 to 15 times larger than those of concrete and steel. Still there is a wide range to be explored within the discrepancy of weight and volume, where large sections are acceptable, e.g. intergraded walls, and mass reduction is preferable. Moreover, available cross-sections of sawn timber, usually rectangular, are inefficient while some modern wood-based composites are deliverable in highly structural efficient sectional geometries.

Sawn timber is about thirty times weaker in its direction perpendicular to the grain then parallel to the grain, which is well known and can be taken into account when designing a structure. Timber building structures should exploit the inherent high strength-to-mass ratio of timber while simultaneously have the ability to develop alternative load paths, prevent the propagation of damage and absorb energy associated with inertial forces when close to collapse [3].

Several requirements and expectations of a building are dependent on the performance of the load bearing structure. For timber buildings, like any other, sufficient stiffness, strength, stability and robustness should be achieved for particular purposes [3].

Fire safety

The combustibility of wood based materials is undeniable. However the casualties worldwide caused by war-induced, or other firestorms has been significantly less than those of earthquake-collapsed reinforced concrete buildings that were poorly constructed. This observation contextualizes the risks involved in disaster and stochastic occurring events. There is also circumstantial evidence that in the city of Istanbul, people caused arson to qualify for modern spacious concrete apartments [2].

Most views of regulatory regimes and regulations are based on statistically analysis of historical events, which take place in a different era where fire safety science and technology where underdeveloped in comparison to today. The absence of effective fire compartments, fire detection and suppression and fire-fighting technologies in those historic events are not representative as arguments for modern regulations. Unfortunately complete paradigm shift has still to come, but fortunately, it is unenviable.

Light-frame structures perform poorly under fire conditions, while heavy laminated timbers have excellent fire resistance, far exceeding steel. Standard procedures to calculate the fire resistance of timber members are generally accepted and available [4]. New performance-based regulatory paradigms, applying all aspects of building design, are beginning to emerge. These recognize that ensuring satisfactory fire performance of buildings is not achievable through discriminatory blanket prohibitions of certain materials from certain uses. [3].

Historically speaking, it was necessary that conflagration of timber buildings took place to create momentum for scientific fire safety research and technology, which takes where we are today and tomorrow, creating safer buildings.

Acoustics

Before and during the industrial revolution, almost every floor of every building was constructed out of swan timber. When later, concrete floor solutions came into play they turned out to be good acoustic barriers. Hence, since then the quality of acoustic comfort performance expectations have risen, creating a problem for timber building construction. This problem, like fire safety, has to be seen in the light of new technologies and engineering knowledge. Nowadays, with solid timber solutions and acoustic insulation materials, one can find the optimal floor lay-up solution through analytical analysis, computer model analysis and laboratory testing.

Summery

The line of reasoning given in the augmented statement above, strengthen the principle that more is possible with wood based materials then is the case in the current situation, even when modern timber buildings are considered. Obsolete paradigms about structural performance, fire safety and acoustics of timber buildings will fade out to allow the use of wood based materials for tall buildings under influence of science and technological development. With this change in thinking, market demand will grow and increase benefit to society, of which the latter is discussed in the following paragraph.

2.2 Motivation of this Study

It the authors intention that, architects, builders and engineers become more comfortable choosing wood as a building material for medium-rise and high-rise building structures by reading this thesis. Because advantages of tall timber buildings are social, economical and ecological as is outlined in this paragraph.

2.2.1 Social relevance of this study

Here an illumination is given on the question why tall timber buildings are important to modern society. The relevance of tall buildings and tall timber buildings in city centers is best summarized by, Peter Krabbe who writes in his contribution to ref. [5]:

> " From an investigation performed by the European Commission of 1997 it can be derived that 80% of all Europeans live in agglomeration i.e. in cities of at least 10,000 inhabitants. The city is a growing, changing, more attractive, culturally and economically interesting area. These must be designed taking the conditions of social and economical life and the challenge of an ecological development of our world, equally into account. "

Timber buildings, like any others, exhibit exemplary performance when material is used appropriately, when structural forms and construction details address overload and serviceability requirements, and when geometry and interior layouts address fire safety. The development of urban construction with timber is cultural interesting, economical relevant and a ecological way for prudent urban needs [3].
Timber building in Europe has developed more and more in height in recent years which also means that the building material timber is more and more established in the cities core. Three- to five story wood frame buildings offer economical housing through low construction cost and high speed of construction.

2.2.2 Social-Economical advantages

Widely spread housing occurs in cities around the world and generally results in increasing cost to the local government in providing streets, water, sewer services and public transportation [7]. The obvious solution to this problem is condensation of housing development of in-fill projects in the suburban town centers, reducing the cost of infrastructure to society.

Tall buildings in general have advantages when living in a dense demographic environment. Tall buildings accommodate centralized utilities with respect to living and working in a city socially and culturally.

2.2.3 Micro-Economical advantages

For real-estate developers, owners, shareholders and tenants, tall timber buildings can create financial advantages through low building cost, high speed of construction and flexibility of the design.

Cost aspect: From some cases in the USA [6,7] it is known that the cost of a timber building relative to the steel alternative is 75% lower. Although the feasibility of a timber alternative always depends on the architectural context and other requirements. Because timber is a relatively low density material, the self weight of structural elements is low and allows for a lighter foundation and requires less lift capacity during construction [10]

Speed of construction: Not totally unrelated to the cost of a building is the speed of construction. Timber parts are increasingly becoming prefabricated and thus allowing a short construction period, dry and cleaner construction sites in the city, which only produce a fraction of the noise of conventional construction [5]. Examples of housing projects in Vienna [6] and the UK provide empirical proof of short construction times through prefabrication of only two weeks and nine weeks respectively. Short construction periods directly relate to increase of interest revenue.

Flexibility: Timber buildings can easily be renovated. With changing demands, they can relatively easy be adapted so that the useful life of the building can be extended [5].

2.2.4 Ecological advantages

Most multiple story buildings or tall buildings are build out of concrete or steel. Much energy is needed to produce the materials concrete and steel compared to timber. Cement is a main component of concrete. Cement is produced from calc that is heated to a temperature of 1450° C and than cooled again to 100° C. The use of energy to heat material relates directly to CO_2 emissions and hence to global warming. In figure 2.1 an overview is given on the amount of energy required to produce one metric ton of material for several building materials. Wood is shown in the figure on the left side of the spectrum with 5-7,5 kWh/t while cement and aluminum alloy are positioned on the right side with 1000 kWh/t and 72000 kWh/t respectively, which indicates that wood is a sustainable material at least by comparison of raw material.

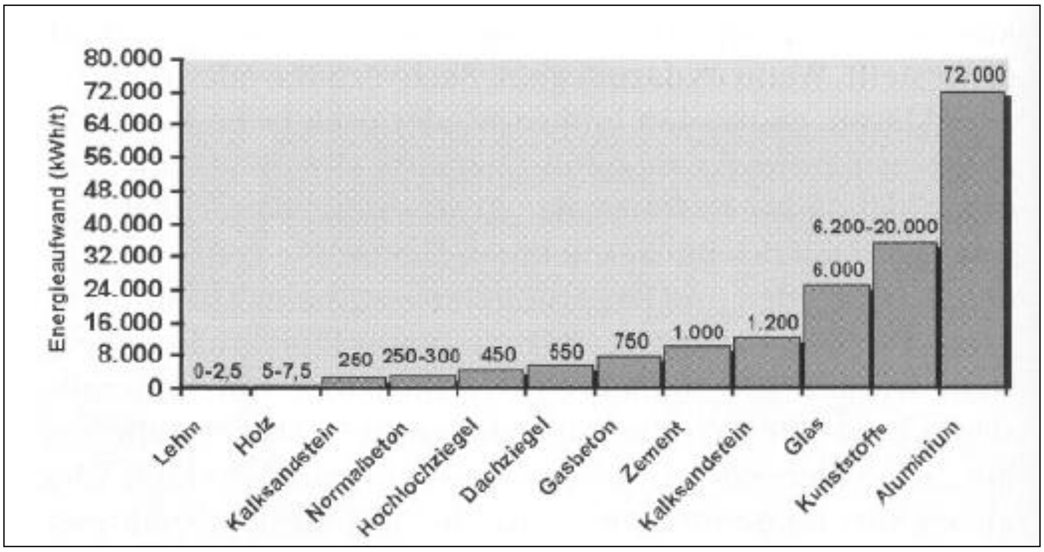

figure 2.1: Required Amount of Energy for the Production of the Plotted Materials [8]

The energy needed to produce wood from trees comes directly from the sun and is optimized through millions of years of evolution. When harvested, wood gets processed into wood based materials and sawn timber which demands just a fraction of the energy needed to produce steel or concrete [8].

Hence, timber is a ecologically sustainable building material, i.e. it stores carbon dioxide, which is beneficial to the ecological balance of the building, a factor which in the future is becoming increasingly important.

2.3 Historical and Recent Examples

In this paragraph some historical and recent examples of timber structures and buildings are given. Traditional types of framing are mainly based on experience, and are therefore a valuable reference to modern timber engineering.

2.3.1 Historical structures

In the table below and in figure 2.2 some historical wood structures and buildings of significant heights are presented. These structures are empirical proof of wood engineered possibilities.

Name	Location	Height	Year of Completion	Year of Demolition
Mühlacker Radio Transmission Tower	Germany	190 m	1933	1945
Gliwice Radio Tower	Poland	118 m	1935	N/A
Yingxian Pagoda (Sakyamuni Pagoda)	China	67 m	1056	N/A
St. Georges Anglican Cathedral	Guyana	43,5 m	1890	N/A
St. Paulus Lutheran Church	USA	75 m	1893	1995
Sapanta-Peri Monastery	Romania	75 m	2003	N/A

Measuring towers and spires of religious structures, give no sense of possible heights of modern (inhabitable) timber buildings in general, but it gives an indication of timber engineering possibilities.

Mühlacker Radio Transmission Tower [31]

Gliwice Radio Tower [32]

Sapanta-Peri Monastery [2]

figure 2.2: Historical tall timber structures

Because the structures given in the above are not subjected to demands concerning modern performance characteristics associated with inhabitable buildings, the following subparagraph is dedicated to reference projects of timber buildings.

2.3.2 Reference projects

In order to get a feeling for the design of tall timber buildings, a number of projects with affinity to this subject are summarized and analyzed in this thesis. This produces insight into realistic solutions for the design issues of modern tall timber buildings. Except for the Yingxian Pagoda, all of the project discussed are recently developed buildings. Here an overview is given on the projects studied.

Project	E3 Berlin, Germany	Murray Grove Tower London, Great Britten	Yingxian Pagoda Yingxian, China
Architects	Kaden – Klingbeil	Waugh Thistleton	building method: Yingzao Fashi by Li Jie
Type	Residential	Residential	Religious/monumental
Nr of storey's	7 storey's	9 storey's	5 (+4) storey's
Height	23 m	29 m	67 m
Slenderness	1:1.8	1:1.7	1:1.9
Year of completion	2008	2008	1056 A.D

E3 Berlin [33]

Murray Grove Tower [34]

Yingxian Pagoda [35]

figure 2.3: Reference projects

In the tables below the structural, fire safety and building physical solutions are summarized for these reference projects whenever relevant. More information on these projects is given in appendix A.1.

Structural solutions

Project: **Design issue:**	**E3, Berlin**	**Murray Grove Tower, Londen**	**Yingxian Pagoda, China**
Structural design, Stability system	Primary diagonal bracing on a heavy timber frame	Shear frame through honeycomb frame (panelized frame) of solid timber shear walls	Internal and external stacked Dou Gong beam and column frames.
Wood quality *	Base material graded at strength class C24	Base material graded at strength class C24	Hand picked, high quality resembles strength class D70 [30]
- Joints/ Connections	Welded steel nodes, bolted to steel-timber joints at members and braces.	Platform framed, mechanical fixing: screwed interface with steel angel brackets and steel ties	Dou gong, interlocking carpentry joints
- Columns	360 x 280 mm Glue laminated timber members	N/A	600 mm sawn timbers,
- Beams	Glue laminated timber members	N/A	600 x 300 mm sawn timbers, hand picked, high quality
- Walls	Stacked boards (Brettstapeldecke)	Cross laminated Timber Combined load baring & shear wall function	Dou gong stacks and non structural cladding
- Floors	Timber concrete composite: - Stacked timber - Concrete top layer	Cross laminated Timber Combined Load baring & diaphragm function	Planks an beams of solid timber

* Strenght classes are based on EN 338

Fire safety solutions

The Yingxian Pagoda is excluded from this table because the building was not designed to modern standards of fire safety engineering, therefore no comparable engineered solutions are present.

Project: **Design issue:**	**E3, Berlin**	**Murray Grove Tower, London**
Fire safety design	Fire protection design strategy, with the objective to obtain planning permission which liberate the regulations with respect to a design of combustible materials, resulting in fire resistance class F 90	Design relies on charring rates and surplus material is provided to give adequate time for a fire to be controlled. The design meets UK standards which is: within units: 30 min between units: 60 min units - vertical circulation: 120 min
- Compartments	Each floor has two units: - Living unit - Vertical circulation	Each floor has five units: - Four living units - Vertical circulation
- Resistance	Appropriate sizing of load bearing components results in 30 minutes fire resistance	Appropriate sizing of load bearing components and certified fire resistance of CLT elements
- Layout (Escape Routing)	Fire escape (separate): - Steel –Concrete - Dethatched from building - Short escape routes (< 13 m) Secondary escape (redundant): - 1st - 3rd floor ladder - 4nd – 7th floor spiral staircase	120 min fire resistant: - 2x12.5 mm Gypsum board (60 min) - 60 mm Mineral wool - 128 mm (3 layers) CLT (30 min) - 40 mm Mineral wool - 117 mm (3 layers) CLT (30 min)
- Interior Walls	Encapsulated (K 60 = 60 min.) - 2 x 18 mm gypsum board (60 min)	Between units (90 min): - 2 x 12.5 mm gypsum board (60 min) - 128 mm (3 layers) CLT (30 min)
- Exterior Walls	Encapsulated (K 60): - 8 mm mineral plaster; - Mineral wool (ρ = 70 kg/m^3); - 18 mm gypsum board (30 min)	Exterior Class A (Non-combustible): - Fiber cement panels - Mineral wool;
- Floors	Top: Class A (Non-combustible): - 100 mm concrete composite Bottom: 90 minutes fire resistance (F 90-B): - Stacked timber lamella (30 min) - 2 x 18 mm Gypsum board (kitchen area, F 60) - Fire resistant paint (remaining area, B1, flame resistant)	Top: Class A (Non-combustible): - 55 mm concrete screed Bottom: 90 minutes fire resistance: - 146 mm (5 layers) CLT (60 min) - 1 x 12.5 mm Gypsum board (30 min) - Additional mineral insulation
Technical systems (active)	Fire alarms Smoke detectors (redundant): - According to DIN 14675 - Fire brigade respond time: 60 minutes	N/A

Acoustics

The Yingxian Pagoda is not included for the same reasons it was excluded from fire safety solutions.

Building Physics: Acoustics - Vibrations	Design meets German standards	Design meets UK standards
Exterior Walls	- 18 mm Gypsum board - 210 mm Solid Timber lamella - 12.5 mm Gypsum board - 100 mm Mineral wool - Plaster	- 2 x 12.5 Gypsum board - 128 mm CLT - 100 mm Mineral wool - Fiber cement panels
Interior Walls	N/A (one unit per floor)	Between Units: - 2 x 12.5 mm Gypsum board - 128 mm (3 layers) CLT
Floors	Concrete screed on elastic foundation: - 45mm Concrete screed - 20 mm Sound insulation - 100 mm Concrete - 160 mm Stacked timber lamella	Concrete screed on elastic foundation: - 55mm Concrete screed - 25 mm Sound insulation - 146mm CLT Suspended ceiling: - 75 mm Void - 50 mm Insulation

2.3.3 Previous studies

In the last decade some other studies with affinity to the subject or tall timber buildings are conducted at university's in the Netherlands. The most recent is the graduation project of E.C. Woudenberg with the title "Hoogbouw in hout" (Tall timber buildings) of the year 2006. The other study is the graduation project by H. Kuijpers with the same title. Furthermore, some resent studies have been done in the field of tall timber buildings like the research project "Projekt 8+" and the Feasibility study "Dock Tower". The latter is a timber-concrete composite building and this sollution will not be pursued in this thesis. Here an overview is given of these studies of which pictures are shown in figure 2.4.

Project	Research project: Projekt 8+	MSc Thesis E.C. Woudenberg	MSc Thesis H. Kuipers	Vision Dock Tower
Architects\Design\ Auteur	Schluder architektur	Van Aken Architektuur	H. Kuipers	Hermann Blumer
Type	Office utility building	Residential	Residential	Residential
Nr of storey's	20 storey's	10 storey's	12 storey's	40 storey's
Height	75 m	34 m	37 m	120 m
Slenderness	1:4.2	1:1.8	1:1.2	1:4
Year of completion	2008	2006	1998	2001

Project 8+ [36]

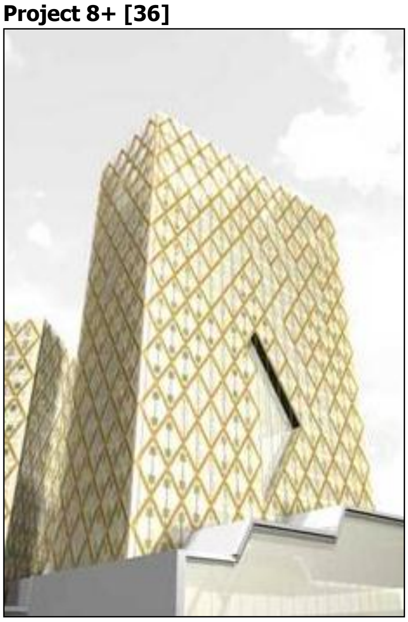

MSc project H.Kuipers [37]

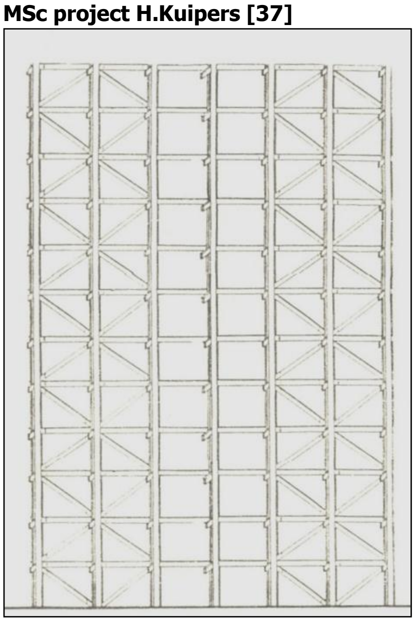

Dock Tower [18]

figure 2.4: Previous studies

In the tables below the structural, fire safety and building physical solutions are summarized for these previous studies whenever relevant. More information on these projects is given in appendix A.1.

Fire Safety Solutions

Project **Design issue**	**Research project Projekt 8+**	**MSc Thesis E.C. Woudenberg**	**Feasibility study Dock Tower**
Fire safety design	The fire resistance according to ONR 22000 was reached without consideration of the sprinkler system	Design according to Dutch building regulations which requires a fire resistance of 120 minutes for the structure.	Fire concept based on a central core and four external staircases in reinforce concrete.
Compartments	Internal compartments possible	Seven compartments per floor: - six living units - one vertical circulation	Projecting concrete slabs every three storeys. Slabs and timber walls fulfill burn-out requirement.
- Layout (Escape Routing)	Two external staircases constructed out of concrete	Distance escape route to fire escape smaller than 45 m. Distance to fire brigade elevator smaller than 90 m	Four Staircases: - Two open to the outside environment - Two pressurized
- Interior Walls	Glass and associated building materials throughout a conventional design	Gypsum fiber board encapsulation	Timber
- Exterior Walls	Glass façade	Glass façade	Timber
- Floors	- 50 mm Dry screed (stone chipping) - 162 mm CLT	- Floor plate of Gypsum fiber board (Fermacell) - Lignatur elements - Suspended ceiling of gypsum fiber board (Fermacell)	Non combustible: Composite Timber-Concrete
Technical systems (active)	Sprinkler system	N/A	High pressure water mist system (sprinkler) Alarm systems etc.

Acoustics

Building Physics: Acoustics - Vibrations	**8+ ATT, Swiss**	**MSc Thesis E.C. Woudenberg**
Exterior Walls	Glass façade	N/A
Interior Walls	Glass and easily associated building materials in a thoroughly conventional design	Gypsum fiber board (Fermacell)
Floors	- Raised floor (Nortec) - 25 mm Gypsum fiber board - 29 Floorrock HP30-1 - 50 mm stone chipping - 162 mm CLT	N/A (Solution failed)

Structural solutions

Project **Design issue**	**Research project Projekt 8+**	**MSc Thesis E.C. Woudenberg**	**MSc Thesis H. Kuipers**	**Feasibility study Dock Tower**
Structural design, Stability system	Tube structure. Four different structural systems are investigated	Diagonal Braced at interior and exterior planes	Diagonal Braced at interior planes	Stability Core of Concrete Residential area: Timber
- Joints/ Connections	Steel plate connections	DVW reinforced joints with expanded tube connectors.	DVW reinforced joints with expanded tube connectors.	N/A (unknown)
- Columns	GLT	GLT	LVL	N/A
- Beams	GLT	GLT	LVL	N/A
- Walls	No structural walls inside building (tube structure)	Light timber frame	N/A (Unknown)	Concrete core and staircase, timber walls.
- Floors	GLT	Lignatur elements	N/A (Unknown)	Composite Timber-Concrete

2.4 Analysis of the Problem

2.4.1 Field of research

As indicated in the introduction, discussion of the heights of buildings is an imprecise delineation of whether or not it is difficult to design and construct them. Adding the dimensions of geometric proportioning and structural form to delineations enables some generalized statements about design complexity [3]. The definition tall timber buildings can be derived if the following statements are taken in consideration:

- Tall buildings: "A building can be considered as tall when the effect of the lateral loads is reflected in the design" [9].
- Timber buildings, are those buildings of which most of the engineered parts of the structure constitute out of timber products [3].
- Tall timber buildings are those timber buildings that are larger then has been constructed according to modern requirements. Currently tall timber buildings can be defined as timber buildings of approximately 10 floor levels with a maximum of 20 floor levels [3].

The field of research lies within the section between tall buildings and timber buildings as shown in figure 2.5. Within this field of research, design issues of both tall buildings and of timber buildings come into play. The relevance of these issues to this thesis, have to be verified by the question if they influence the structural height of a building.

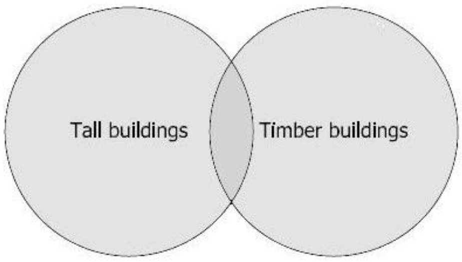

figure 2.5: Field of research

Base on a combination of what is presented above a definition for a tall timber building can be formulated.

> ***Tall timber building:*** *A building of which most of the engineered parts constitute out of timber products, that is constructed according to modern requirements and in which the effects of the lateral loads is reflected in the structural design.*

It must be noted that the building height itself does not determine the feasibility of arriving at an acceptable engineering design solution. The height of a building design is part of the many architectural performance characteristics and economical feasibility.

In the following text of this paragraph the relevant factors are given for tall buildings. After eliminating irrelevant factors, remaining factors are described and categorized. Then the way in which these factors are processed and quantified is explained subsequently.

2.4.2 Influence factors

A scientifically wide supported statement is, that, in order to regain acceptance for multi-storey timber buildings, the three aspects that have to be addressed are vibration, fire resistance and acoustic transmission [10]. In addition to those three aspects there are several factors that influence the design of a tall building. In ref. [11] initially 14 challenges where proposed that potantialy limit the height of a high-rise design. Here, these challenges and will be evaluated within the context of the current thesis with a timber building perspective.

Based on the above combined with the distinctive charateristics of timber, a list is composed of posible influence factors. These are sorted within five categories, namely Architectural requirements, Economical issues, Structural issues, Fire safety and Building physical issues as shown below:

Architectural requirements:
1. Influence on surroundings
2. Vertical transportation
3. Slenderness

Economic issues:
4. Economic feasibility
5. Sufficient Economical Support
6. Market Instability

Fire safety:
7. Fire Safety
8. Evacuating the Building

Structural issues:
9. Foundation
10. Load Bearing Structure
11. Comfort
12. Organizing the building site
13. Earthquakes
14. Terrorist Attacks

Building physical issues
- Acoustics
- Vibrations
- Thermal insulation

2.4.3 Elimination of factors

Below a number of influence factors are discussed and eliminated from the list of challenges for reasons of relevance and the manageability in order to create a delineation of the thesis.

Influence on surroundings
Considering the objective of this thesis, namely the height of a timber building itself it is unnecessary to include this challenge, and preferable with eye on manageability of the problem. The scale of the intended tall timber building is of a magnitude from which it is not expected that it imposes on its surroundings. Above all, this is highly dependent on the location of the building. To keep the present thesis manageable this challenge is not included for study.

Economical issues
The challenges sufficient economical support and market instability lie outside the influence of architects and engineers and therefore are not relevant to this thesis. Economical feasibility issues are treated through engineering problems like simple and economical detailing and respecting the a Gross-Net floor area ratio. The Gross-Net floor area ratio is a parameter defined by the ratio between the Gross area and Net area i.e. lettable area of the floor plan. The economical issues can therefore be accounted for by the gross-net floor area ratio of the building because this determines the relation between the cost of the footprint and the revenue of one storey of the building.

Organizing the building site
In the real world this is always a design issue. The thesis objective is looking for a theoretical limit that mainly include, structural, fire safety and building physical challenges, confined to the building itself, therefore it is assumed there is no deficiency of space on the building site.

Earthquakes
Very tall building structures are, because of their lower natural frequency, in general more susceptible to wind loadings then earthquake-induced loadings. Therefore, and because earthquakes only occur in a small part of the world, it is chosen not include earthquake loading. Moreover, the most favorable theoretical location with respect to earthquakes can be assumed.

Terrorist attacks
is a problem on a social-political level and/or national or private security level and therefore a domain which will not be discussed in light of this thesis.

Evacuating the building
This challenge has associations with fire safety challenges and similar events and will therefore be linked with fire safety issues. According to [11] the evacuation of the benchmark skyscraper that was studied is limited to 154 m. The intended height of a tall timber buildings in this thesis is not of the scale that it will be confronted with this challenge of this magnitude which emerges at modern high-rise design.

2.4.4 Processing factors

After elimination of the challenges and factors in the previous subparagraph the remaining factors have to be processed. This processing of factors is done within separate paragraphs. How this is done is described here per category in general.

Architectural requirements
To make the problem manageable the challenges sorted within this category will have effect on the layout and the size of the floor plan. The entry of daylight is also added as a separate requirement to complete the brief of design for the case study. Elimination and further breakdown of these topics will be conducted in a separate paragraph "Architectural requirements" which will delineate the brief for the floor plan design which is executed in the paragraph "Universal floor plan". The remaining topics within the architectural requirements set hold:

- Vertical transportation
- Daylight entry
- Slenderness

Structural issues
Structural issues will become more significant when timber buildings become tall. Wood has some characteristics that are different from other materials. When tall buildings are studied with respect to their height these material specific properties become more important then is usual with low-rise timber structures. The refinement of factors will be conducted in the paragraph "Structural problems". The structural issues are confined to a remaining set of factors which holds:

- Foundation
- Load Bearing Structure
- Comfort

Fire safety
The fire safety will be dependant on the fire resistance of the building structure, and the possibility to evacuate the building in compliance with the building regulations and fire safety objectives.

Building physics
The height of the building is indirectly related to the building physical challenges. The space needed for insulation in floors and walls is effecting the layout and the remaining space to facilitate load bearing functions and effective floor space. This is especially true for wood because is possesses different physical properties, like low density and high thermal qualities compared e.g. concrete.

2.4.5 Quantifying factors

In general, all factors have to become quantified with realistic values. The universal principle that is maintained for choosing a value is best depicted in figure 2.6.

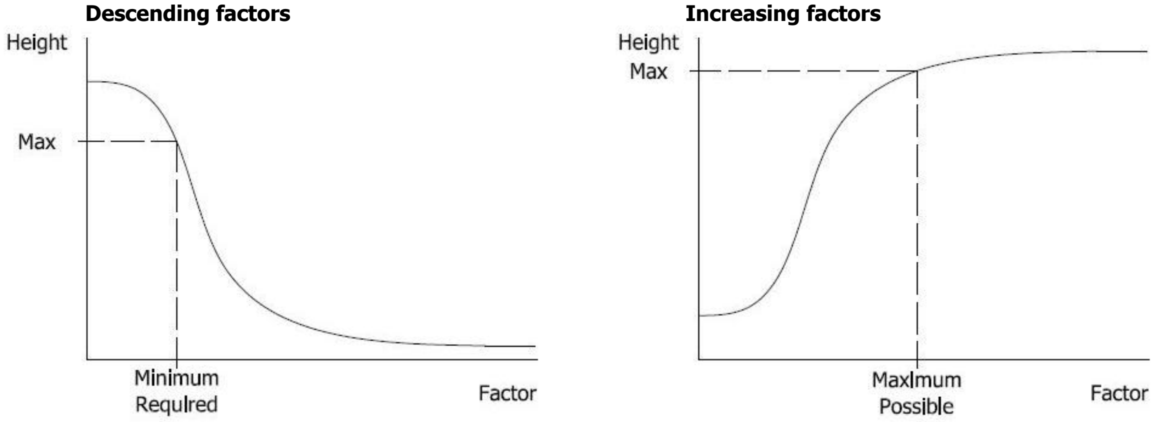

figure 2.6: Decision principle for factors

Dependant on the nature of influence on the height of the building, either decreasing or increasing, individual factors can be chosen within the range of possibilities to result in the greatest building height. As an example the entry of daylight is discussed. The entry of daylight is predominantly regulated by the size of windows in the façade. When large windows are chosen, then the space to facilitate load bearing elements becomes smaller, hence the possible building height becomes smaller.

To achieve maximum building height, the optimum set of variables that influence the building height have to be chosen within realistic boundaries.

2.4.6 Intermediate summary

The relevant factors have been categorized in general topics and will be processed within the associated paragraphs of this thesis. These factors will be quantified according to the universal principle as was described above. Below a schematic representation is given of the four remaining issues that delineate the boundaries of this thesis.

Architectural requirements	- Vertical transportation - Daylight entry - Slenderness
Structural Issues	- Foundation - Load bearing structure - Comfort
Fire safety	
Building Physics	

2.5 Architectural Requirements

In this paragraph the architectural requirements of a building are summarized, their relevance is discussed and when possible and applicable, quantified. The list of architectural issues is partially originating from Ref. [11] and contains the following topics:

- Vertical transportation
- Daylight entry
- Slenderness

2.5.1 Vertical transportation

The objective height of this thesis for a tall timber building consequentially makes vertical transportation neglectable as a main criteria in the broad sense. The challenge "evacuation of the building", is decisive in this case when consulting ref. [11]. The facilities for vertical transportation must be incorporated in the layout of the floor plan, inside the building core. This challenge, therefore, is enclosed in the floor plan design and will fulfill the requirements by reserving space for lift and staircases.

To achieve this the gross-net floor area ratio has to be established. This parameter defines the ratio between the gross and net area of the floor plan and determines the available space on the floor plan that facilitates technical services and structural elements, i.e. the building core. In case of a high-rise project, real estate experts aim for a net floor area in the range of 70% and 80% of the gross floor area [11]. The net floor area is chosen to be approximately 75% of the gross floor area.

-Gross-Net floor ratio-

> The net floor area is chosen to be 75% of the gross floor area, to facilitate space in the core for vertical transportation and simultaneously create an economic feasible project.

2.5.2 Daylight entry

The entry of daylight into the internal space of a building is collected in the term floor-to-window area ratio, combined with an acceptable floor depth. The floor-to-window area ratio is a parameter defined by the ratio between floor area and window area within a confined space. This parameter is directly related to the wall-to-window area ratio which determines the available space in the tube façade that facilitates stabilizing and load bearing elements, i.e. influences the virtual section modules of the building. Hence, good architectural daylight performance is in conflict with structural performance. The floor height and ceiling height necessary for relevant calculations are assumed to be respectively 3,50 m and 3,00 m.

-Floor depth-

Another important factor defining the daylight entry is the floor depth. The global limitation to floor depth in relation to daylight entry is very subjective to national regulations, where e.g. the United States has more lenient rules about access of daylight for workspaces, European countries have strict time limitations to which a person may work in spaces without available daylight. Based on empirical evidence of European buildings, the floor depth is limited to a range of 7,2 to 9,0 m [11]. To keep the floor span feasible for an all timber design the floor depth is chosen to be 7,2 m for the case study design.

> The maximum floor depth of the building is chosen to be 7,2 m.

-Regulations-

The floor-to-window ratio is highly dependant on the area of the floor that needs access to daylight, i.e. lounges and workspaces inside an office building demand a certain entry of daylight. According to Dutch Health and Safety regulations for the workplace "ARBO", the window surface of a room must be at least 5% of the floor area in which people work for periods longer than two hours. This criteria is decisive when compared to the Dutch building regulations which demand a 2,5% window area surface for office spaces. Not all spaces in an office building need entry of daylight, like lifts, staircases and utilities. For the assumed ceiling height and floor depth the regulations result in a minimum wall-to-window ratio of 10,2% .

-Acceptable daylight performance-

A number of observations are made in a study written by Eero Vartiainen [12] which focused on optimal division between the window area and the photovoltaic solar area of various façade layouts. From this study it can be derived that the minimum acceptable window area for offices in Europe is 14%. The annual lighting requirement during office hours, provided by daylight, for Northern Europe (60°N) is plotted against the façade-to-window ratio in the table below.

facade-to-window ratio	Daylight availability
14%	44%
24%	61%
38%	71%

According to Vartiainen an optimum layout of photovoltaic panels and window area can be found of 24%, considering both available daylight entry and the electric lighting requirement replaced by daylight.

For the case study design of this thesis the possibility of photovoltaic panels is not taken into account and focuses on the structural behavior. The optimum division found by Vartiainen is of less concern. The acceptable minimum found by Vartiainen is more important because it exceeds the statutory standard. For the case study a minimum wall-to-window ratio of 15% is chosen, which is above the regulatory minimum and the acceptable minimum according to Ref [12]

Wall-to-window ratio

The wall to window area ratio is chosen to be at least 15%, which is larger the statutory minimum and above the acceptable minimum for office buildings according to Vartiainen .

2.5.3 Slenderness

The slenderness is a parameter defined by the ratio between the width and the height of the building. Buildings with squat shapes and many internal divisions are the simplest to design and construct. Squat shapes buildings are those with modest ratio of height to footprint dimensions [3]. Therefore the slenderness is a very important parameter that limits the buildings height. High slenderness also results in more daylight penetration but less stiffness and stability and therefore creates a more flexible system which is susceptible to wind induced vibrations and P-delta effects.

Because the slenderness is part of a tall buildings identity, it is necessary to choose a high slenderness for the case study design, which will assumed to be 1:4. A slenderness of 1:4 is assumed to be a realistic value based on the reference project 8+. Currently, the ultimate slenderness for skyscrapers is 1:8 – 1:9 according to [11].

The slenderness for the case study building is chosen to be 1:4, which is believed to be the minimum to keep the identity of a tall building while resulting in an acceptable base footprint.

2.5.4 Relevant parameters

The vertical transportation and evacuation of the building are relevant, but are embedded in the floor plan design through proper choice of the gross net floor ratio. Daylight entry is best confined to the parameters floor-depth and wall-to-window ratio. The relevant architectural parameters leading from the preceding discussion can now be summarized in the following quantified subset:

- Gross-Net floor ratio = 0,75 [-]
- Wall-to-window ratio > 0,20 [-]
- Floor depth = 7,20 [m]
- Slenderness < 1:4 [-]

2.5.5 Influence of parameters

To discuss the height limit theoretically, the relation between the relevant parameters and their influence on the height limit are analyzed. To do this a cantilever beam model is assumed to be representative for the building structure.

A tall building can be considered as a vertical cantilever beam with certain cross-section properties. Parameters originating from architectural demands, influence the virtual cross section of the building, e.i. the section modules. The section modules, in turn, will influence the strength and stiffness characteristics of the building. The architectural building characteristics associated with the section modules are Gross-Nett floor area ratio, Slenderness, and Wall-to-Window area ratio. Minimum and maximum values were assigned to the parameters previously, to quantify the problem. Below the theoretical influence is indicated per factor and visualized in figure 2.7.

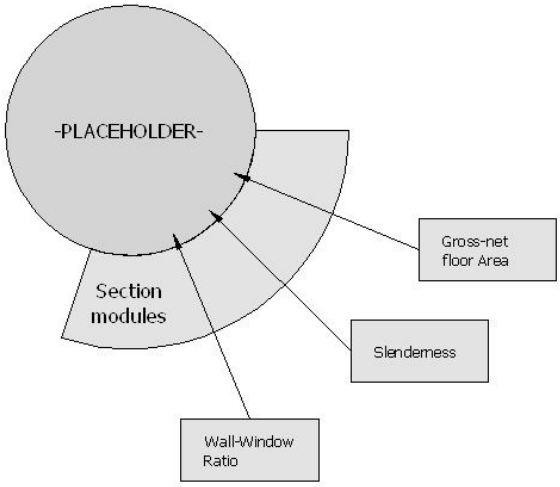

figure 2.7: Influence diagram section-modules

Gross-net floor area ratio: determines the available space in on the floor plan that facilitates stabilizing and load bearing elements, i.e. influences the section modules of the building. Here the influence of the gross net floor area only exists in theory because the value is already assigned by assumption of realistic economical and architectural boundaries.

Slenderness: influences the section modules of a building of a certain height. High slenderness results in a relatively small section modules in comparison to the lateral wind – loads and vertical floor loads. While the minimum slenderness of 1:4 was assumed for the case study building there is still freedom when system capabilities appear higher then expected.

Wall-to-window ratio: determines the available space in the facade that facilitates stabilizing and load bearing elements, i.e. influences the virtual section modules of the building. This factor is limited at a lower bound of 20%. In order to produce a general statement of the height limit for timber buildings without compromising architectural freedom, several possibilities have to be considered for the case study enabling variable daylight entry, i.e. structural solutions have to be found that facilitate this possibility.

Architectural objective

> In order to preserve architectural freedom, cases have to be analyzed that define opposite sets of minima and maxima possibilities in terms of architectural requirements versus structural building height.

2.6 Universal Floor Plan

In this part of the study the floor plan for the case study is chosen. The dimensional limitation originating from architectural requirements are used to design the floor plan. A design formula is written out to establish the dimensions.

2.6.1 Plan limitations

Some general and national limitations to the dimensions of the floor plan are discussed throughout this paragraph. These limitations are implemented in the case study floor plan design.

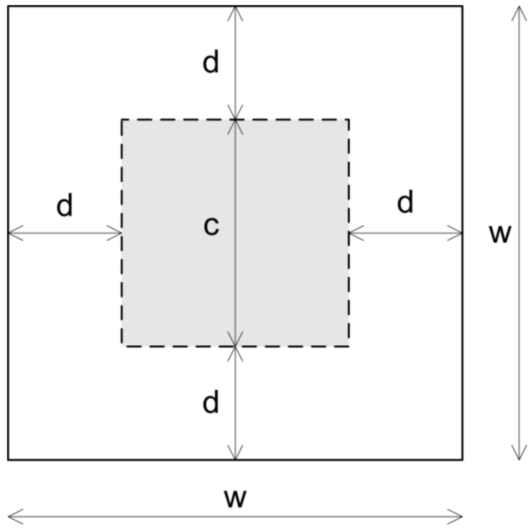

figure 2.8: Floor plan variables assignment [11]

Footprint shape: To keep the problem simple, and eliminate any noise associated with oddly shaped building structures, a square footprint is chosen for the shape of the floor plan of the case study building. Rectangular and square shapes are common shapes for tall buildings located in city centers, probably because they maximize the use of space within the plot of land shaped by the surrounding infrastructure. Changing the shape of the building also does not increase the height limit significantly [11]. Therefore, by using a square shaped floor plan, the most common case can be studied without compromising the height potential for a tall timber building much.

Core dimensions: Within a regular design the dimensions of the core are usually dependant on the demand for spaces that facilitate vertical services, such as lift shafts, staircases and ventilation. Through the use of a common gross-net floor area ratio for the case study design this demand will probably be satisfied. Economical feasibility was established by choosing a gross-net floor ratio of 75% for the case study design.

Outer dimensions: The outer dimensions is dependant on the floor depth and the dimensions of the core.

Modular grid: The modular grid is based on a accepted measure of 1,8 x 1,8 m for office buildings.

Core layout: Inside the core spaces are reserved for staircases, lifts, sanitary facilities and technical shafts. The dimensions of these spaces are calculated proportionately to the net floor area based on another tall building project in the Netherlands, namely: staircases (3,5%), Lifts (1/200 m^2), sanitary space (2,1%) and technical spaces (2,0%).

2.6.2 Design formula

1st design formula: The quantification of the gross-net floor ratio and the square form of the building gives rise to an algebraic approach for the design of the floor plan. The author of this thesis deduced the following equation that describes the relation between the dimensions of the core and the gross floor area:

$$A_{core} = \left(1 - R_f\right) \cdot A_{gross} \quad \rightarrow \quad c^2 = \left(1 - R_f\right) \cdot w^2 \quad \rightarrow \quad c = \sqrt{1 - R_f} \cdot w$$

In which (figure 2.8):
A_i = Area with index
c = the dimensions of the core
R_f = the gross-net floor ratio
w = the outer building dimensions.
d = the depth op the floor

2nd design formula: The relation between the linear dimensions of the building is easily described and rewritten as follows:

$$w = c + 2 \cdot d \quad \rightarrow \quad c = w - 2 \cdot d$$

Rewriting Design formula: Through the rewriting of the first and second equation and putting them into a set, one variable, can be eliminated from the set through substitution.

$$\left.\begin{aligned} c &= \sqrt{1 - R_f} \cdot w \\ c &= w - 2 \cdot d \end{aligned}\right\} \quad \rightarrow \quad \sqrt{1 - R_f} \cdot w = w - 2 \cdot d$$

Rewriting of this, and quantifying the variable R_f with 75%, the following simple set of equations is created.

$$w = \frac{2 \cdot d}{1 - \sqrt{1 - R_f}} \quad \xrightarrow[R_f = 0{,}75]{} \quad \begin{cases} w = 4 \cdot d \\ c = 2 \cdot d \end{cases}$$

These equations can be used for the calculations of all floor plan design with a square shape. For the case study floor plan, in which the building depth is 7,20 m the dimensions become:

$$\begin{aligned} w &= 4 \cdot 7{,}20 = 28{,}80m \\ c &= 2 \cdot 7{,}20 = 14{,}40m \end{aligned}$$

2.6.3 Floor plan

The floor plan dimensions are shown in figure 2.9. The core walls are initially assumed to be 400 mm thick Cross Laminated Timber, which is the current maximum on the market. The walls of the core can also be of another format, like a truss-frame or a diagonal-braced frame.

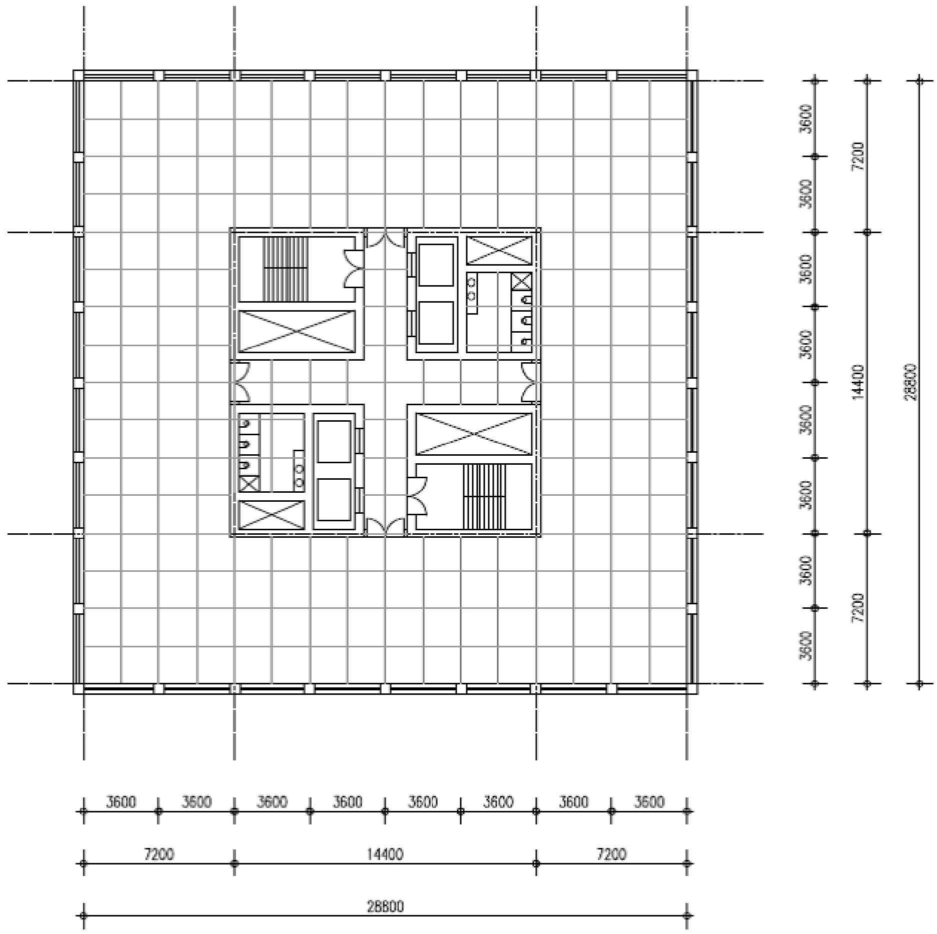

figure 2.9: Floor plan dimensions

This floor plan will be used for the case study. This design will lead to a building height of about 115 m, when a slenderness of 1:4 will be maintained, which satisfies the target height for this thesis.

2.7 Structural Problems

In this paragraph the structural problems encountered when designing a tall building are summarized, their relevance is discussed and when possible, quantified. The list of structural issues is partially originating from Ref. [11] and contains the following topics:

- Foundation
- Load bearing structure
- Comfort

Foundation

Because timber is a very light material no real problems with the vertical load-bearing capacity of the building's foundation will be expected. On the other hand the light weight structure can be pushed over under lateral wind load. In order to reach realistic results the stiffness of the foundation and associated soil will be estimated through calculation. If unusual forces have to be transferred through the foundation, like axial tension forces in piles, than this will either proof failure of the system or will give rise to find solutions.

Comfort

Because wood has different dynamic properties and due to the high slenderness of tall buildings, different dynamic behavior can be expected in tall timber buildings. Vibrations and movements of the building have a negative effect on the comfort felt by the building's occupants. The building design inherently possesses a dynamic Eigen-frequency which gives an indication of the comfort of the building as it is experienced by occupants. The comfort criteria is therefore subject of the dynamic behavior of the load-bearing structure.

Load-bearing structure

As it is equally true for skyscrapers as for timber buildings, the load-bearing structure limits the height of a tall buildings. This is also one of the most important subject of the present thesis. The challenge load-bearing structure can be further differentiated to horizontal and vertical load-bearing devices. Further more the load-bearing structure characteristics can generally be divided in to strength, robustness, movement, stability, stiffness and dynamic behavior of the building. A diagram of the relations between the challenge load-bearing structure and its underlying properties is given in figure 2.10 as is described in the below.

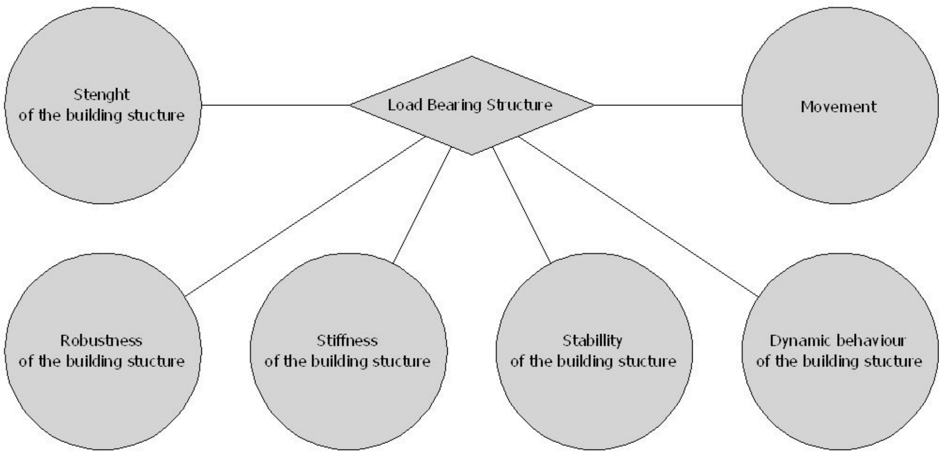

figure 2.10: Relations Load-Bearing Structure

Within the following subparagraphs the split up characteristics of the load bearing building structure, building structure for short, their intermediate relations and the relations with material specific properties are explained. The relationship between their factors and their influence is discussed, in order to establish relevant structural factors that influence the height limit.

2.7.1 General influence diagram

Here, parameters are discussed that generally apply to all relevant building structure characteristics. For this subparagraph, parameters are defined as material specific properties and stability system. Material specific properties are used as they are known from codes and literature on timber. In figure 2.11 an overview is given of the relations, with in the center of the diagram a placeholder to indicate universal applicability to multiple building structure characteristics.

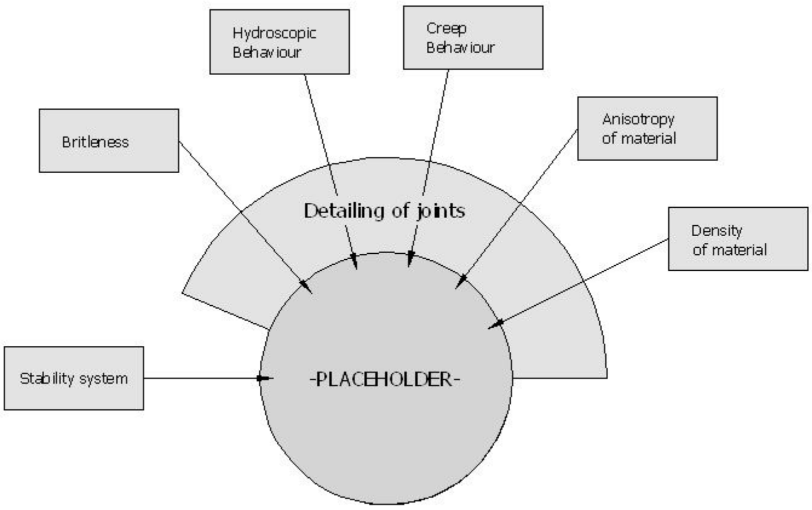

figure 2.11: General influence diagram

Stability system: The stability system is a parameter that possesses characteristics about the lateral stiffness and strength of the building structure. The choice of structural load bearing and stabilizing system is limited to the possibilities that are available in timber, which has consequences for the building height.

Brittleness: Wood is a brittle material or non ductile material, which means it does not show enough deformation before collapse. Therefore timber buildings have to be designed in such a way that steel fasteners yield before the wood crushes. Brittle material behavior influences the structural detailing of the structure and therefore influences multiple aspects of the building structure.

Anisotropy of wood: The anisotropic properties of wood have consequences for the way in which the structure will be designed, i.e. in order to avoid high stresses perpendicular to the grain and the associated deformations, the detailing has to be designed around those issues. Therefore it influences the building structure through the structural detailing of the joints.

Hygroscopic behavior: Wood is a hygroscopic material, this impies that, dependant on the moisture content, timber will expand and contract. The moisture content of the material is dependant on the climate of the environment. When the climate is stable no expansion and contraction will be expected. This property is very specific to timber when compared to steel and concrete. The hygroscopic behavior is subject of anisotropy. The deformation caused by swelling and shrinkage parallel to the grain is limited, but can be rather large perpendicular to the grain and therefore needs special attention in some cases. The hygroscopic behavior has consequences for the way in which the structure will be designed, i.e. in particular the detailing has to be designed around those issues. Therefore shrinkage influences the behavior aspects of the building structure through the structural detailing of the joints.

Creep behavior: The creep of timber is also subject of anisotropy and is rather large in the direction perpendicular to the grain. The joints have to be detailed around creep issues which influences the detailing of the structure and therefore influences multiple aspects of the building structure.

Density of wood: The specific density of wood and wood based products does influence the embedment strength of fasteners and the stiffness of that embedment. Therefore it influences the building structure through the detailing of joints.

2.7.2 Strength (ULS)

The strength of the building structure is visualized with a circular diagram. There are four main factors that influence the global strength of the building structure, which are:

- Strength of the material
- Stability system
- Structural detailing (detailing)
- Section modulus

The strength of timber: The ultimate strength is a decisive factor for the ultimate load on a member, hence determines the maximum load bearing capacity of all members of the building structure, and therefore influences the strength of the building structure directly. The material choice is for the problem of this thesis is limited to possible timber products. Anisotropy and the moisture content of the timber can influences the strength properties of the timber. Anisotropy is well known and is usually resolved through proper detailing. The moister content of the timber can be overcome by the use of prefabrication in controlled shop conditions, which is usually the case.

Stability system: The stability system governors the way in which the structure transfers (lateral) loads to the foundation, i.e. the material stresses are influenced by the choice of the stability system. The global strength of the building structure is therefore influenced by this choice, as was stated earlier.

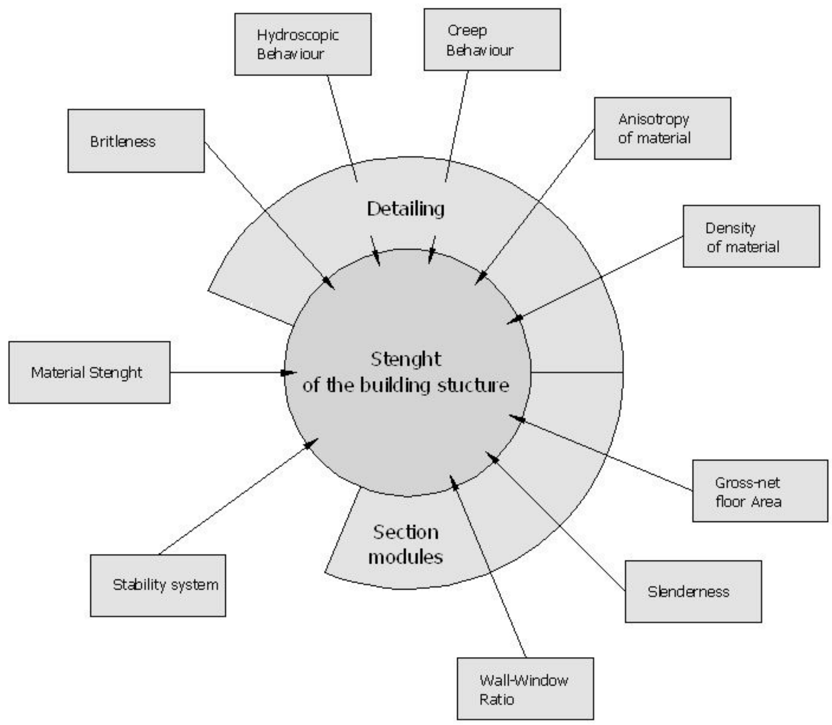

figure 2.12: Influence diagram building strength

Structural detailing: The structural detailing can be a weak link in a building structure. Under influence of several material specific characteristics, the design of the detailing can result in smaller load bearing resistance compared to the full cross section of the adjacent member.

Section modules: To create a complete picture, the influence of architectural parameters are also included in this diagram through the hemisphere "section modules" shown in figure 2.12.

2.7.3 Stiffness (ULS)

Similar to the building strength, the relations between influence factors and global building stiffness is indicated in figure 2.13. The five main factors that influence the building stiffness are:

- Stiffness of the material
- Stability system
- Foundation stiffness
- Structural detailing
- Section modulus

The stiffness of timber: The magnification of scale will increase the structural problems for tall timber buildings, of which the majority is dedicated to the low inherent material stiffness. The modulus of elasticity (E) and shear modules (G) are the main cause of problems with horizontal stiffness in multiple story timber buildings. Anisotropic material stiffness can be resolved through proper detailing.

Stability system: The stability system possesses inherent stiffness qualities, dependant on its geometry. The stability of the building structure is influenced by the choice of the stability system. The stiffness of the stability system, can compensate for the relatively low inherent material stiffness of timber products.

Foundation stiffness: The deformation of the foundation contributes to the deformation of the building at the top. The stiffness of the foundation is limited, especially when the soil is of poor quality, and therefore influences to the stiffness of the building structure on a global level.

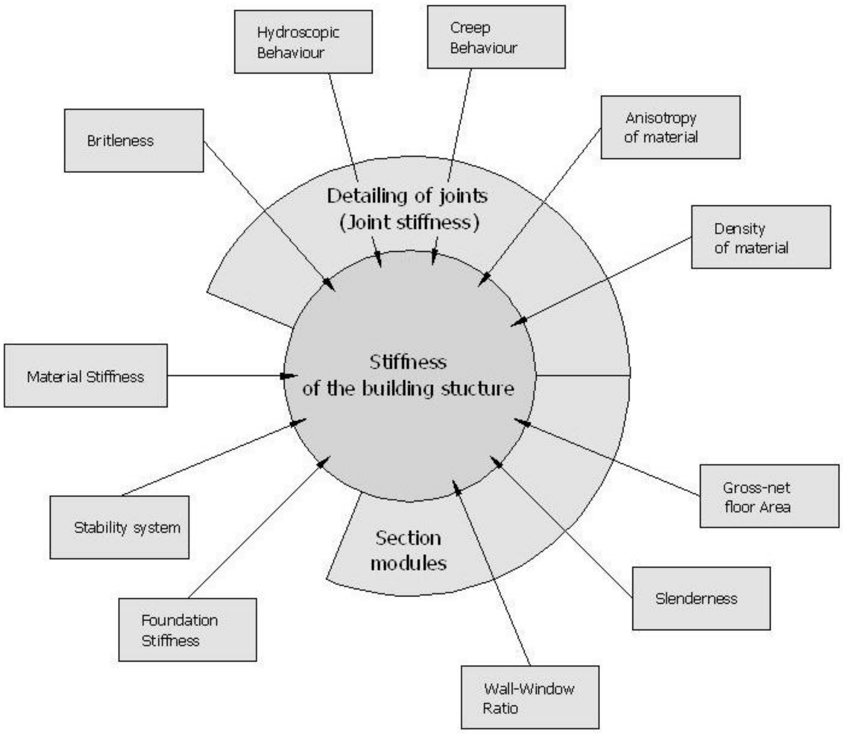

figure 2.13: Influence diagram building stiffness

Structural detailing: The structural detailing contributes to the deformation of the building structure. The design of joints posses inherent stiffness qualities. Furthermore, while serviceability considerations are decisive factors affecting the sizing of structural members, the consequential stiffness of certain members can result in compatibility constraints. When a member is designed based on the yield capacity of fasteners, and the deformation under corresponding loading is higher than the compatibility of its connection, that system will fail. Thus, instability of the system is a consequence of designing connections based on the yield capacity that are in essence to flexible.

Section modules: similar to the strength of the building structure, the influence of architectural parameters are included in this diagram through the hemisphere "section modules" shown in figure 2.13.

The quantity stiffness of the building structure determines its static behavior, namely the deflection under static loading and the distribution of the loads, which has consequences for the serviceability limit state, the dynamic behavior and the stability of equilibrium.

2.7.4 Stability (ULS)

The high ratio of strength and stiffness related to the specific gravity of timber, makes timber-frame building relatively light. Therefore the building is vulnerable to being pushed over when exposed to wind forces [10]. Problematic second order effects emerge when horizontal sway of tall buildings arises through wind loading, which is mainly a consequence of the stiffness of the building structure as shown in figure 2.14, which also indicates the second order loading influencing the strength of the building.

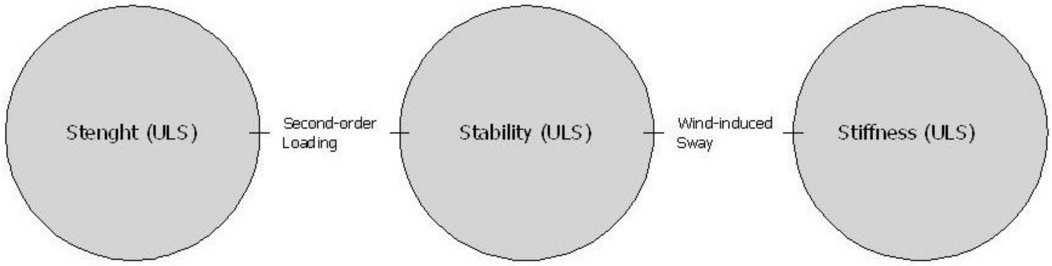

figure 2.14: Influence diagram building stability

Push-over and second order effects through sway are stability problems that can be addressed possibly by making the building non-sway, or sway-limited through choice of proper stability devices. This is a challenge because there is relatively little experience in tall timber building while simultaneously design codes for timber structures do not provide any drift criteria for multi-story timber buildings. The drift limits proposed for steel structures (Euro Code 3) can potentially be used for this particular problem. [4].

2.7.5 Movement (SLS)

Creep and shrinkage through loading perpendicular to the grain is problematic when a certain height is desired with platform framing. Beam-column framing is less sensitive to creep and shrinkage. Hence, the severity of movement problems are dependant on the system used including its detailing.

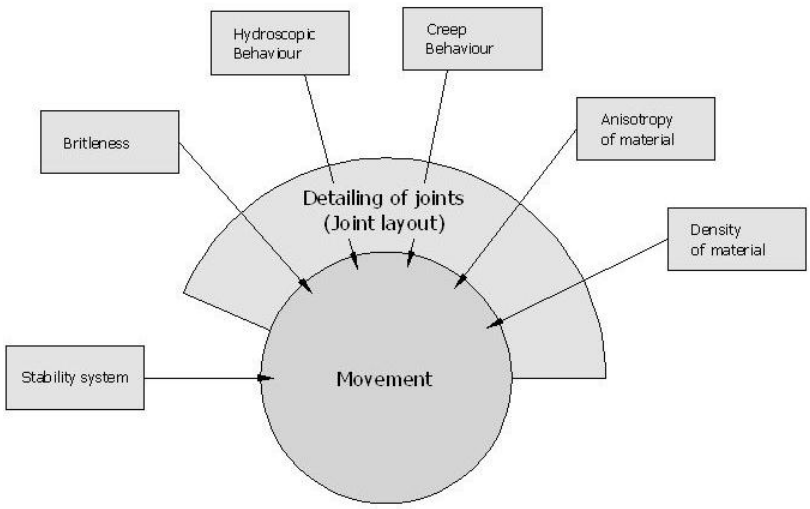

figure 2.15: Influence diagram building movement

Because the building structure is not restrained in vertical and horizontal direction, and because most structural timber elements behave similar to climate change, i.e. expand and contract, no real structural problems can be expected with hygroscopic behavior issues. Hygroscopic behavior of the material can be avoided entirely by creating a stable climate inside the curtain wall façade on the perimeter of the building

2.7.6 Vibration (SLS)

Vibration of the building structure is a consequence of the dynamic characteristics of the structure. As is indicated in figure 2.16, the dynamic behavior is basically determined by the crucial combination of stiffness and mass of the structure.

Stiffness/mass of the structure: The density of wood is relatively low compared to other structural building materials. The properties of the material result in high stiffness/mass ratios for timber frames which result in low natural frequency of the system and may lead to a dynamic response induced by wind loads [4]. From medium-rise buildings up, especially with taller timber buildings, problems arise with both vertical and horizontal motion transmission between units [3]. Therefore, wind dynamic effects can only be neglected for low- or medium-rise buildings with heights of less than 22 m [4].

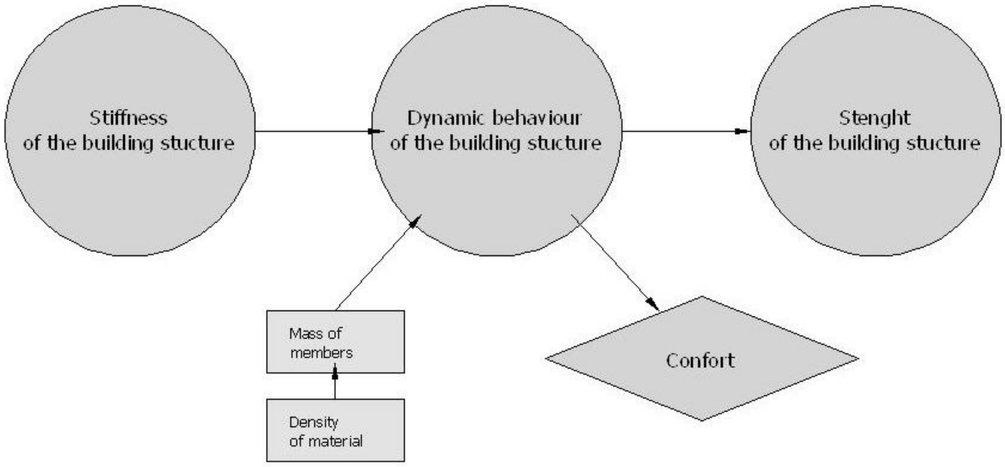

figure 2.16: Influence diagram dynamic behavior

The dynamic behavior, in turn, has consequences for strength of the building structure and the comfort as it is experienced by occupants.

Strength of the building structure: Vibrations originating from wind loading and the dynamic properties of the building can result in material stresses, which has consequences for the ultimate load bearing capacity and stability of the building structure.

Comfort: The dynamic behavior of the building structure determines its comfort, namely the acceleration under excitations like wind loading. Tall timber buildings also must be designed against the potential for local and vibration and sound transmission, with emphasis on isolation, provision of damping and appropriate placement of relatively massive elements as key components of good solution strategies. [3]

2.7.7 Robustness (ULS)

The robustness is a performance characteristic that is a consequence of the buildings design and is always an issue that has to be addressed, independent of the material choice. The brittleness of the timber itself does not allow for plastic redistribution of forces to the secondary path when compared to e.g. steel.
However there are compelling arguments why structures should be designed within the elastic range [3]. Moreover when plastic deformation is desirable the yielding of fasteners are always possible, but are also dependant on geometric-fit-constraints which where discussed in the preceding subparagraph.

Taking account for robustness is possible with timber buildings when incorporating well known timber characteristics and systematic design.

2.7.8 Summary

The above analysis can be imagined as a course from a centre diverging outward, with on the inside the load-bearing structure and on the outside material specific parameters. This results in a list of material properties and building features which can be housed as follows:

Material properties:
- Strength
- Stiffness
- Density

Detailing:
- Brittleness
- Hygroscopic
- Creep
- Anisotropy

Stability system

Foundation stiffness

Section modules:
- Gross-net floor ratio
- Slenderness
- Wall-Window Ratio

When the quality of performance of these envelopes increase, consequently the potential building height increases. Therefore the following statements can be made concerning these envelopes.

Material properties: The inherent material properties, strength, stiffness and density all increase when the quality of the wood based material increase. By increasing the density of wood, the mass of the structure increases, making the structure less susceptible to wind induced push-over, hence increasing the stability. The eponymous characteristics of the building structure, namely strength and stiffness, increase proportionally with the wood quality and consequently the stability of the building structure also increases. The relation between wood quality and dynamic behavior is uncertain because the increase of wood inherent density and stiffness seems proportional.

> The quality of the wood based material should be chosen as high as possible.

Detailing: The type of joint and proper detailing should address the aforementioned material specific characteristics. The choice should also maximize the strength and stiffness qualities.

> Joints should be chosen to maximize strength and stiffness qualities, while simultaneously addressing brittleness, hygroscopic behavior, creep and anisotropic behavior.

Section modules: Most of the section modulus parameters are defined and quantified except for the wall-to-window ratio, which was limited by a lower bound of 20%. It was stated earlier that architectural freedom can be preserved when several possibilities are analyzed.

Stability system

> The choice of stability system should enable flexibility concerning entry of daylight, i.e. transparency and simultaneously maximize strength and stiffness properties of the structure.

Foundation stiffness: The stiffness of the foundation should be sufficient to limit the deflection of the building or compensate for the stiffness of the building structure.

In general the problems with timber as a building material for tall buildings are to be addressed through application of a raised level of timber engineering design knowledge. Additional to this statement the proper choices of material, joint detail and system can maximize the outcome, as is proposed in the following paragraph.

2.8 Structural Solutions

The structural solutions suitable for tall timber buildings can be split up in levels of material choice, the stability system and the associated joint principles. In this paragraph the solutions are presented sequential in eponymous subparagraphs.

2.8.1 Material choice

To generate a theoretical limitation to the material strength and stiffness of timber the strength class's for sawn timber and wood based products are considered. The most common laminations concern mainly the following: Glue Laminated Timber (GLT), Structural Composite Lumber (SCL) which includes Laminated Veneer Lumber (LVL) and Cross Laminated Timber (CLT). The strength of wood based composites depends on the base material and the processing. The dimensional limitations of structural timber products can be a challenge for the feasibility of a timber tall building.

Glue Laminated Timber (GLT)
There are five standard strength classes for GLT. To get an indication of the strength, the bending strength ($f_{m,k}$) of the different strength classes varies between 20 and 36 N/mm^2. The ultimate load capacity of poplar GLT exceeds that of sawn timber beams by 39.0%, while the stiffness does not increase significantly [13]. Some empirical proof of achievable dimensions is based on a bridge project in Sneek, the Netherlands, in which some laminated timber elements are as large as 1500 x 1080 mm [14]. This leads to believe that the dimensional limitation is at least 1500 mm. This example project gives rise to use the design and principles of this project as a realistic assumption for the maximum allowable dimensions of structural elements for a timber building. Moreover, treatment of the material, as it was applied in this project, is resistant against environmental influence like fungi.

Laminated Veneer Lumber (LVL)
The length of LVL beams can go over 20 m. The cross-section dimensions vary between 27 x 200 mm and 75 x 900 mm up to 75x2500 mm in special cases. To get an indication of the strength, the bending strength ($f_{m,k}$) of standard products varies between 32 and 42 N/mm2. The ultimate load of poplar LVL beams exceeds that of swan timber beams by 62.6% to 90.0%, while the bending stiffness increases by 35.0% to 45.0%. [13] Laminations are usually orientated in the longitudinal direction of the element but can be applied perpendicular to increase the strength and stiffness in that direction.

Cross Laminated Timber (CLT)
CLT plate elements do not distort when the moister content changes. Maximum dimensions depend upon the manufacturer, and usually is within in the range of 2,95 m in width, 16,5 m in length and 400 mm in thickness. The bending strength of CLT increases for laminations of four layers or more with about 10%, while through the perpendicular arrangement of the boards decrease the strength with 6% when compared to Glue Laminated Timber. Cross laminated timber panels are in particular useful applied as shear wall- and floor elements.

Summary wood based products
Wood based products discussed here range from Glue Laminated Timber (GLT), Structural Composite Lumber (SCL), which includes Laminated Veneer Lumber (LVL), and Cross Laminated Timber (CLT). These are in general the available products in the current market. Compared to sawn timber the ultimate strength and mean modulus of elasticity increases [13], namely:

- Compared to sawn timber the ultimate strength increases with 39.0% for Glue Laminated Timber and with 62.0%~90.0% for Laminated Veneer Lumber.
- The stiffness of Glue Laminated Timber does not increase significantly while the stiffness of Laminated Veneer Lumber increases with 35.0% to 45.0% when compared to the base material sawn timber.
- For Cross Laminated Timber the lamination effect does increase the ultimate strength but the effective section reduces with a factor, e.g. the effective cross section reduces to $^3/_5$ for a plate of five vertical laminations.

Dimensional limitations of timber products range from 1500 mm for GLT, 2500 mm for LVL and 400 mm in thickness for CLT. Because it is uncertain if LVL products are also available in square sections, because they are predominantly used as bending elements, it is safer to assume the maximum dimensions of GLT.

Base material
There are many different deciduous wood species available all with different properties. Therefore a strength class of graded wood must be used to confine the problem. The highest strength class according to EN 338 is D70. It can be shown that hand-picked timbers of certain wood species with characteristics similar or better then strength class D70 exist [30]. Irrespective of economic issues like market price and market availability this base material is assumed to be the structural limit.

Ultimate material

When the above is combined it is expected that a theoretical lamination or veneer exists that has high capabilities when a base of deciduous wood with D70 grading is used. This theoretical product will effectuate the limit for the inherent material strength and stiffness for this thesis with dimensional limitations of 1500 mm

2.8.2 Stability System

The structural system can be broken down in the systems principle, and if applicable, the type of bracing and the configuration of the system. The combination of these three levels will determine the capacity to resist lateral forces. Proper choice will result in a stability system with high capabilities, with the objective to design a tall timber building. The three levels, system principle, bracing and layout are explained here.

Systems principle: The system can be braced, moment resisting (un-braced) or semi-rigid.

Bracing: Bracing systems provide lateral stability to the framework when a braced principle is chosen. Bracing can be in the form of triangulated bracing or shear components. The most common types of bracing are discussed with special attention to timber applications.

Configuration: The efficiency of a building to resist lateral forces depends on the location and the types of the bracing systems employed and the presence of shear walls, and cores around lift shafts and stair wells.

2.8.2.1 System principle

In order to get in insight in how stability systems can be applied when designing a tall timber building, some explanation is given below on the mechanisms and the advantages of possible principal systems.

Braced frames: A simple frame refers to a structural system in which the beams and columns are pin connected and the system itself is not capable of resisting any lateral loads. The stability of the entire structure must be provided by attaching the simple frame to some forms of bracing systems. The lateral loads are resisted by the bracing systems while the gravity loads are resisted by both the simple frame and the bracing system. In most cases, the lateral load response of the bracing system is sufficiently small such that second order effects may be neglected for the design of the frames. Thus, the simple frames that are attached to the bracing system may be classified as non sway frames [9]. It is easier to design and analyze a building structure that can be separated into system resisting vertical loads and system resisting horizontal loads. For example, if all the girders are simply supported between the columns, the sizing of the simply supported girders and the columns is a straightforward task. It is more cost-effective to reduce the horizontal drift by means of bracing systems added to the simple framing than to use un-braced frame systems with rigid connections.

Semi-rigid frames: Actual connections in structures do not always fall within the categories of pinned or rigid connections. Practical connections are semi-rigid in nature and therefore the pinned and rigid conditions are only idealizations. Modern design codes allow the design of steel semi-rigid frames using the concept of wind moment design. In wind moment design, the connection is assumed to be capable of transmitting only part of the bending moments (those due to the wind only).

Moment resisting (MR) frames: A moment frame derives its lateral stiffness mainly from the bending rigidity of frame members interconnected by rigid joints. The deformation of a moment frame is a result of the flexural stiffness of the members and the axial stiffness of the columns. The detailing of the rigid connections results in a less economic structure. Rigid unbraced frame systems perform better in load reversal situation, i.e. earthquakes. From the architectural and functional points of view, it can be advantageous not to have any triangulated bracing systems or solid wall systems in the building.

In general, laminated wood frames are relatively flexible and prone to large horizontal drifts. This is due to their topology and low rotational stiffness of the beam-to column connections. To prevent excessive drifts, moment-resisting frames require nearly rigid connections and/or additional stiffening devices. Producing rigid moment connections between beams and columns of timber structures is nearly impossible due to the anisotropy of wood and need for mechanical fasteners. [4]

Some systems such as glued-in rods can provide high rotational stiffness, but the with low strength perpendicular to the fibers of wood still limits the capacity of such connections. [4] An innovative high-capacity moment transmitting connection, known as the tube connection, was developed at Delft University in 1998, which suits this type of structure very well [10]

Ultimate system principle

A braced system is the most economic principle and has highest potential of all possibilities, while moment resisting type of framing system is unsuitable for the design of a tall timber building because of its height limitations and uneconomic properties. The performance in earthquake conditions is not important within the boundary of this thesis

2.8.2.2 Triangulated bracing

In steel structures, it is common to have triangulated vertical truss to provide bracing. This type of bracing is common in timber buildings. The general principle of the bracing system is based on equilibrium of axial forces through the geometrical orientation of linear structural elements. There are many possible geometric shapes thinkable for structural bracing, like diagonal bracing, triangular (Diagrid) shapes and quadrangular shapes as suggested in the project 8+ (see A.1). These grid structures enable maximum daylight entry.

Diagonal bracing
The diagonal braced system is structurally minimal through use of merely necessary static braces calculated to withstand the external load development by wind or earthquakes. A bracing system that consists of diagonal bracing is common in heavy timber structures as shown in figure 2.17. Steel elements can be applied for the diagonal bracing eliminating creep, shrinkage and other compatibility constraints that emerge when structures are erected completely out of timber. However, shrinkage and creep do occur in the bracing elements as well when timber bracing is considered, canceling out the compatibility constraints.

Diagrid
The Diagrid geometry, sometimes called Auermann principle, is a net structure that consists of a diagonal crossing grid of linear elements forming a triangular appearance. The geometry is very efficient and system is statically flawless. The geometry is applied in modern steel structures like the Hearst Tower in New York (figure 2.18) and 30 St Mary Axe in London (figure 2.19, [40]). The geometry is esthetically attractive, the structural system is therefore left in sight and becomes part of the façade. The Diagrid frame is one possible alternative for the case study design.

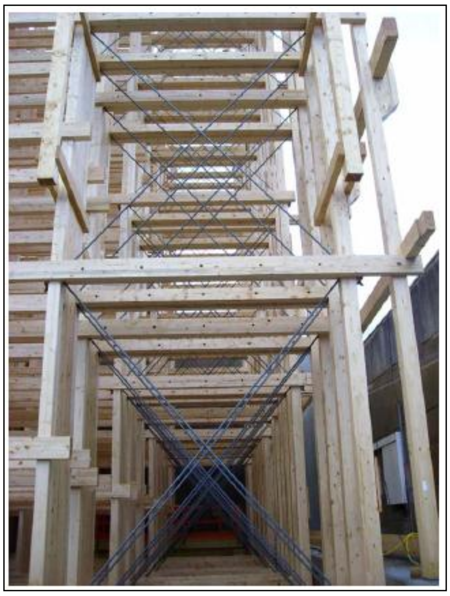
figure 2.17: Diagonal braced [38]

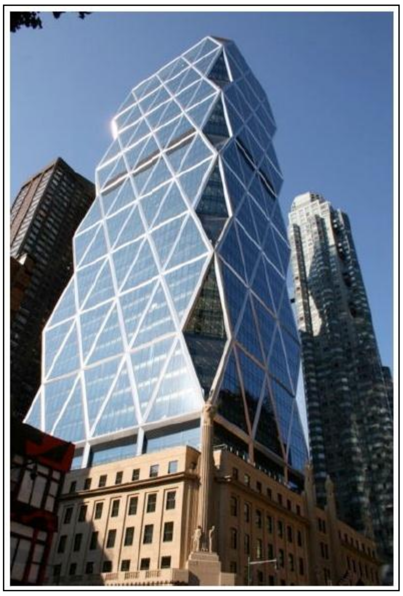
figure 2.18: Hearst Tower [39]


figure 2.19: 30 St Mary Axe

Cranked quadrangle
The Cranked quadrangle is made from diagonal framework where the connection is offset from the intersection of the gridline. Architecturally it is a attractive solution, but the complex intersections must be made statically effective and is therefore less efficient.

Ultimate triangulated bracing

The most promising type of bracing is the simple diagonal braced system and the Diagrid geometry structure. The quadrangular geometry is less efficient and therefore disqualified. It is not possible at this point, to say which remaining type of bracing is most effective.

2.8.2.3 Shear wall bracing

In regular tall buildings shear walls or core walls are often used when very stiff structures are necessary. The application of shear walls in a timber design is quite common in light timber frames and at the time of writing a growing solution for solid timber (CLT) platform framing. Research on the shear capacity and stiffness of CLT has been conducted in the recent past referring to [15]. The two types of shear wall bracing discussed here are light timber frame bracing and honeycomb framing. The entry of daylight of this type of bracing can be controlled by the size of windows to any desired value.

Light timber framing

Consist of two basic concepts of framing, namely: Platform framing and Balloon framing. This type of framing is suitable for low timber multiple storey buildings up to five storey's. The most common form of timber-frame building in the Netherlands is the light timber frame platform method. This method, however, is limited to about four storey's due to limited capacity of the perpendicular to the grain strength of timber and the effects of material shrinkage [10]. For light timber framing overturning is a problem when the building height increases, because of difficulties with axial loaded nailed connections and absence of mass.

Honeycomb framing

The structural engineering company Techniker, that was involved in the design of the Murray Grove Tower, investigated the theoretical and current practical limits on cross laminated timber platform construction. Inherently the strength capacity of panels could be further exploited. For economic wall thicknesses, this resulted in some general conclusions:

- If the current form is not modified, the upper bound limit reaches 15 storey's
- If bearing points where locally strengthened the limit reaches 18 storey's

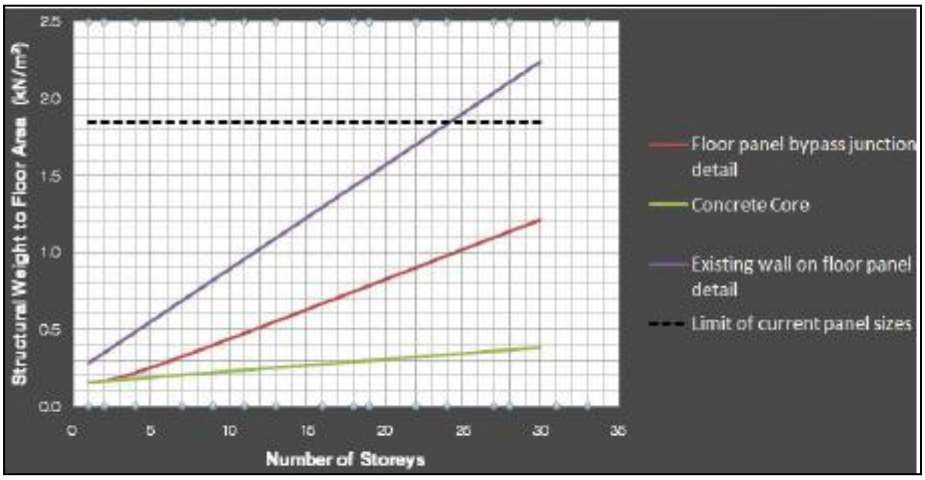

figure 2.20: Structural weight to floor area [41]

According to Techniker the economic viability hinges on both quantity of material and simplicity of detailing in more or less equal measure. An indication of structural weight to floor area provided for increased height is shown in figure 2.20.

Some improvements suggested by Techniker for ties and baring details are addition of hardwood margins, nail plates at bearings and side plates which enhance robustness and additional loading. The designs would then display behavior where p/delta effect begins to govern wall thicknesses and hence costs. With the materials now in use the upper bound limit then reaches 25 storey's retaining economic wall thickness.

To limit horizontal drift and accompanied second order effects must be resisted by additional stiffness. In figure 2.21 a graph is shown of the stiffness requirement of a core stabilized apartment building plotted against the number of floor levels.

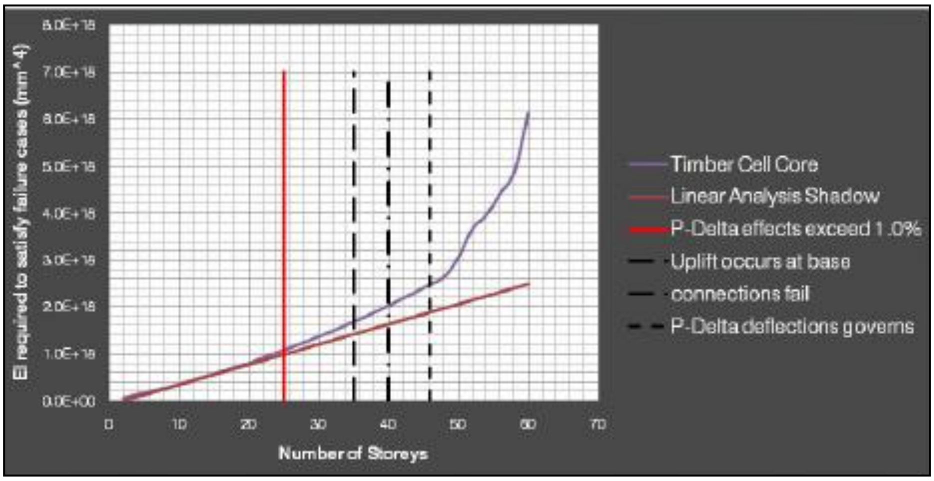

figure 2.21: Stiffness requirement [41]

Ultimate shear wall bracing

> Light timber framing is limited to five storey's and therefore disqualified. The remaining solution for shear-wall framing is the heavy timber honeycomb like system with solid cross laminated timber elements, which is limited to 25 storey's according to investigations by Techniker with materials now available.

2.8.2.4 Structural bracing

In summary, the type of structural bracing suitable for tall timber buildings with unprecedented heights are either triangulated braced systems with diagonal braces or a Diagrid structure, or a solid- heavy timber shear wall system of cross laminated timber panels. Because no research is available that quantifies the potential of timber frames braced with linear elements, no judgment can be made on the most potential bracing system.

Ultimate bracing system

> The set of ultimate bracing systems includes the diagonal braced system, the Diagrid geometry and the solid timber shear wall system. Each bracing system has specific properties concerning structural stiffness, economic feasibility and daylight entry.

2.8.2.5 System configuration

The layout of bracing for lateral load can be configured in different ways. The most common layout is the core braced system, while in tall buildings or high-rise structures usually a combination of devices is applied. The possible configurations are:

- Core braced systems
- Frame-tube systems
- Tube-in-tube systems
- Outriggers

Core braced systems
The majority of the buildings with a core braced system is erected out of structural concrete. Because tall timber buildings higher than eight storey's are scarce, timber core braced systems are also not common, however, designs exist that implemented a concrete core in a predominantly timber building. There are solutions thinkable of a solid timber core of CLT or heavy truss elements.

Tube-frame system
The tube-frame structure is in general by far the stiffest solution available in terms of configuring structural bracing. A tube-frame system consists of a braced frame that is placed on the perimeter of the building. In steel structures, the frame tube is constructed of large columns with small centre to centre spacing connected by deep beams resulting in a punched wall appearance. The interior space of the frame tube system consists of a simple gravity frame. The exterior frame provides resistance for lateral loading of wind and earthquakes while the interior gravity frame only resists its share of the gravity load.

Under action of lateral loading the overturning moment will be resisted by the compression of the leeward and tension on the windward columns, these are called flange columns. The columns and beams parallel to the direction of the lateral load provide resistance to shear by bending and are called web frames. On the wind- and leeward side of the frame tube, shear-lag may occur in the frame. The magnitude of the shear lag is dependant on its shear rigidity of the frame. This results in an uneven distribution of strain deformation and therefore an uneven distribution axial forces between columns.

Tube-in-tube system
A frame-tube can be transformed into a tube-in-tube system through addition of internal cores and columns and floor framing, which enhances the lateral stiffness when this is required (i.e. very tall buildings). Special design additions to this system are internal shear frames or walls that reduce the shear-lag by coupling the leeward and windward exterior frames in several places. There are many geometric solutions thinkable when a frame-tube is applied, including the bracing devices discussed above like: triangulated frames, shear walls, moment resisting frames, etc.

Outriggers
An significant improvement of lateral stiffness can be achieved by the application of a outrigger. The outrigger is a vertical truss placed in between floors to connect the core with the shear frame on the perimeter of the building. On the perimeter of the building a belt truss is located to activate the columns, reducing the shear leg. The outrigger stiffening effect is twofold, namely: the external columns are activated to participate in the cantilever mode of the core and the external façade gets stiffened by the belt truss to act as a three-dimensional tube. In steel structures outriggers can improve the global stiffness by 25%. [9] Outriggers can be constructed out of timber in the form of trusses or solid shear walls.

Ultimate system configuration

The tube-in-tube system configuration is the most promising layout orientation of a stability system, which can be accompanied by timber outriggers when necessary.

2.8.2.6 Summary

From what is known about steel frames, a classification exists on the economic feasibility of different stability systems. These categories are visualized in figure 2.22 and from what can be observed, the exterior diagonalized tube is most promising system for tall steel buildings. The principle involved is also applicable to timber building design because it involves linear elements.

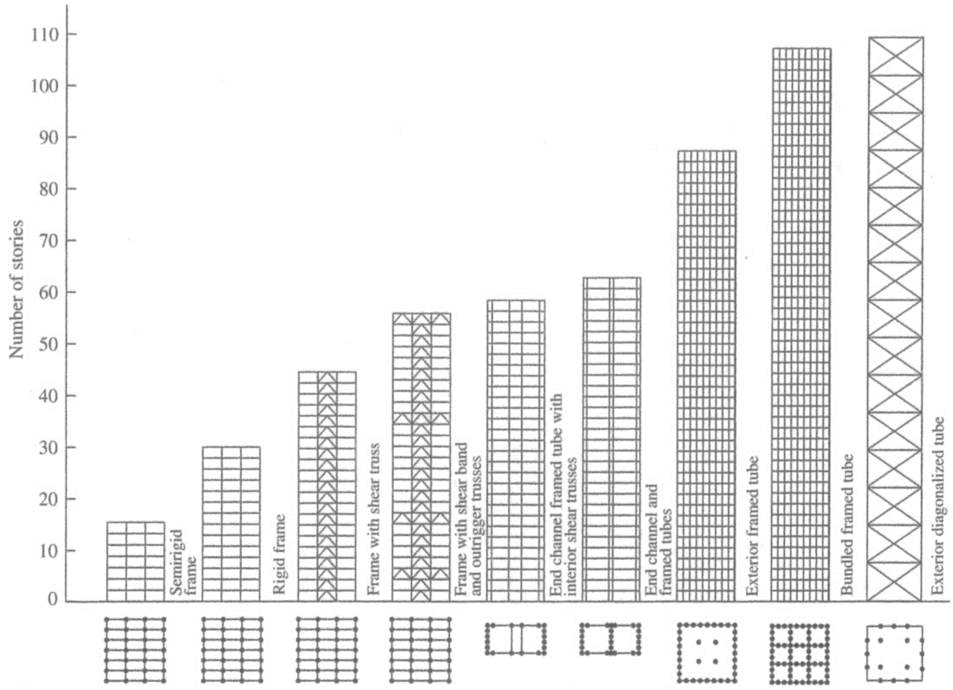

figure 2.22: Categorization of building systems (for steel structures) [9]

The two main characteristics of an exterior diagonalized tube possesses is in the name, i.e. the system consists of an exterior tube structure that is braced by diagonal bracing. The diagonal bracing can be replaced by solid shear walls or other types of bracing that have similar or higher shear strength and stiffness capabilities.

From what is described above a categorization for timber stability system applications can be made. Such an assessment of the possible solutions is difficult to make at this point, because no specific quantification to economical height limits are known for tall timber building systems. It is therefore part of the scientific void within timber engineering. Consequently this is part of the objective to investigate the maximum building height of which the ultimate stability system is subject.

Ultimate stability system

System principle:	Braced-system
Horizontal layout:	Tube-in-tube frame
Structural bracing:	- Diagonal bracing;
	- Diagrid geometry;
	- Solid heavy-timber shear walls;
Additional devices:	Outriggers

The ultimate stability system is believed to create the highest potential. In light of this thesis different bracing systems where chosen to create sets of possibilities regarding daylight entry versus strength and stiffness qualities, while simultaneously investigating the feasibility of different systems. By doing so, an opportunity is created to investigate the quality of different solutions on multiple criteria. Within the line of this thesis this enables architectural freedom versus building height.

2.8.3 Joint solutions

The relevant issues for tall timber buildings like creep, shrinkage and stress perpendicular to the grain can be overcome by proper detailing of the connection which avoid stress perpendicular to the grain. There are in principle two different type of joints thinkable with timber connections, the timber to timber joints and steel to timber joints. The investigation splits up in two parts that result from the chosen bracing systems, namely cross laminated timber joints and beam-column frame joints.

2.8.3.1 Cross laminated timber joints

The conventional way to connect cross laminated timber is with "of the shelf" steel plate brackets and screws using the platform building method as shown in figure A.7 of appendix A.1.1.2. To recapitulate, with the platform method, floor elements are placed directly on top of wall elements which in turn carry the wall element for the next floor above. The platform method is not used for the case study design, because of high stress perpendicular to the grain within horizontal elements, especially when the building height is increasing. The semi-platform method shown in figure 2.23 and the quasi balloon-framing method (figure 2.24) is therefore preferable, however these have not been used before for cross laminated timber.

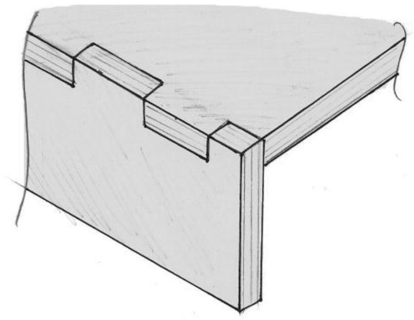

figure 2.23: Semi platform-framing

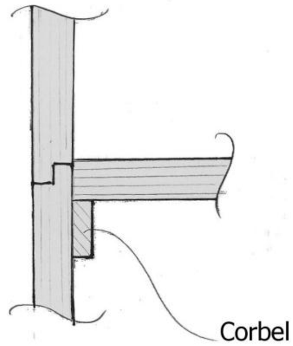

figure 2.24: Quasi balloon-framing

The semi-platform method, or the quasi balloon-framing method can be applied to the the wall-floor and/or wall-beam connection. The wall-to-wall connection, i.e. the joint between vertical elements, can be realized in the same manner, which is shown in figure 2.25. When two plate elements are, notched or toothed cut, a perfect fit between the two could realize an optimum shear connection. But it also leaves less room for error in the workshop, which could result in low performance in final execution on site through last minute modifications.

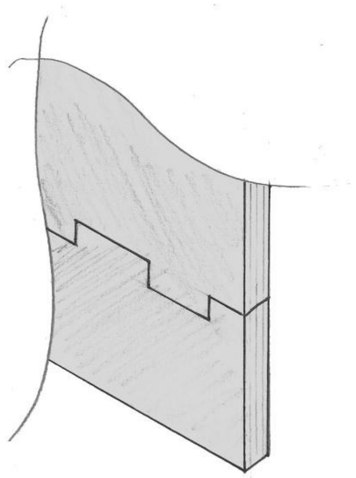

figure 2.25: Toothed-Cut Wall

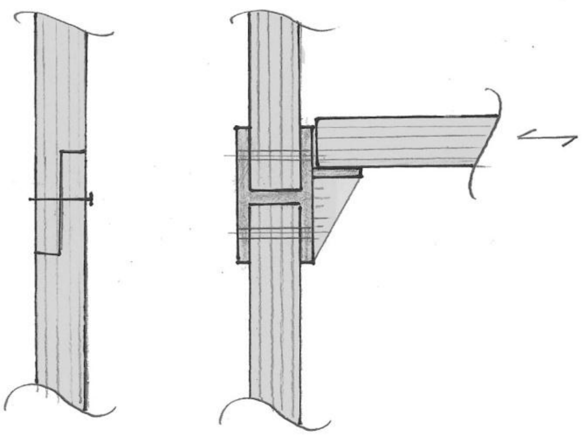

figure 2.26: conventional and steel saddle solution

The conventional and proven method for connecting plates in the longitudinal direction is realized with screws over half the width of each plate shown on the left side of figure 2.26. The other option to realize a connection is through the use of welded steel plate saddles combined with dowel fasteners shown on the right side of figure 2.26.

Evaluation of proposed solutions

The semi-platform method with tooth cut elements is rejected because it can result in a doubled shear stress concentration in the joint seam, where only half the material is present within the horizontal section. The same analogy holds for wall-to-wall connections. Moreover, the geometrical fit error as noted above, can result in uncertainty regarding joint stiffness.

For wall to wall connection this leaves only the steel plate saddle option which is expensive because for every joint seam a steel member has to be welled, predrilled for fasteners ect. This solution can also result in a steel frame with timber shear wall infill, rather then a timber frame with steel joints.

Solution CLT-joint

The best possible solution which is believed to be most economical is presented in figure 2.27 and figure 2.28. This is not the standard solution as it was used in practice of the "Murray Grove tower", but found in the process of writing this thesis. The solution is a balloon framing method with platform method execution quality. Both options make use of a timber line which functions as a corbel that is glued on in shop on the side of a wall element later in production. This corbel mimics the advantage of the platform framing method resulting in high construction speed through fast and simple connection.

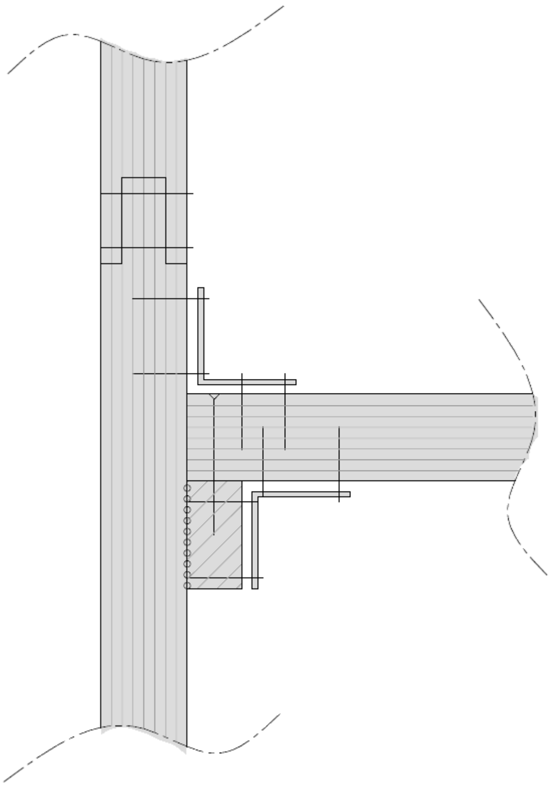

figure 2.27: Balloon framing solution I

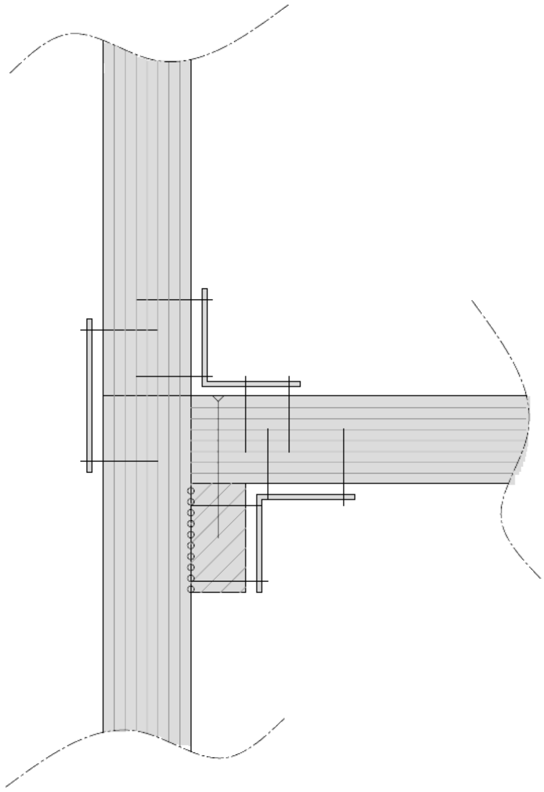

figure 2.28: Balloon framing solution II

For the option in figure 2.27 the wall elements are milled around the edge of the plate to create a joint in double shear that can transfer tension, compression and shear in plane. For clarity of presentation figure 2.27 is not an actual representation of the joint, because the wall-to-wall joint seam must in reality be closer to the corbel (timber line) to prevent instability. The second option shown in figure 2.28 is equipped with a steel tie on the outside to take care of any tension within the element.

Like the platform method, both options make use of steel angle brackets that are used to transmit shear between wall elements, and wall and floor elements fixed with large screws. Mechanical fixing between wall and floor elements is realized with the use of long screws through the floor element and either through the corbel or the wall, i.e. askew or vertical.

2.8.3.2 Beam-column joints

Triangulated braced, Diagrid and diagonal braced systems, make use of a similar type of joint. For all joint types the Blumer-System-Binder (BSB) is proposed. These can either be realized with dowels or expended-tube-fasteners. Below some description is given on the Blumer-System-Binder and fasteners.

Blumer System Binder
The multiple-shear dowel connection with slotted-in steel plates is one of the most efficient joints for heavy timber structures. The Blumer-System-Binder is well known in Europe for its high-performance in combination with glue laminated timber and high strength composite lumber products. An example of a multiple shear steel-to-timber connection is shown in figure 2.29. The solution makes use of Computer Numerical Control (CNC) machinery to drill holes in wood and steel for reasons of accuracy.

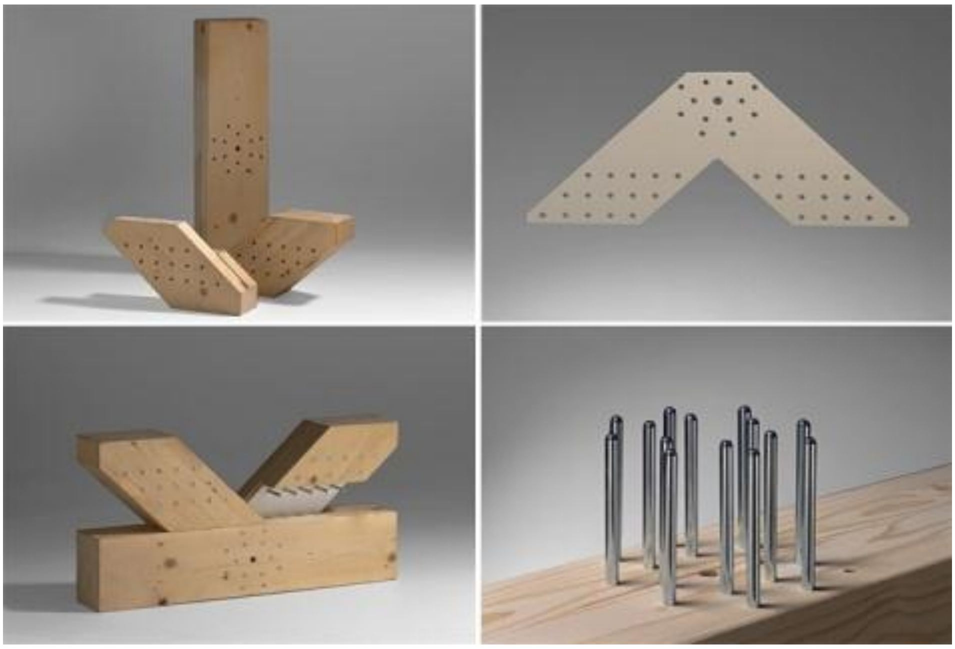

figure 2.29: Blumer System Binder [42]

This type of joint has several advantages over conventional timber-to-timber joints. The joint saves space in the thickness direction, i.e. the interface area in BSB steel-timber joints does not require an overlap between timber elements. Consequently, eccentricity of load introduction into members is avoided. Secondly the initial slip is absent through use of slender dowels and very tight fabrication tolerances through CNC implementation.

2.8.3.3 Fasteners

When manufacturing common steel-to-timber connections, steel and timber parts usually have to be predrilled separately, which is unfavorable for both load bearing capacity and stiffness performance of the final joint, mainly because even small tolerances effect the behavior. These disadvantage can be avoided when either self-drilling dowels or expended-tube-fasteners are used. Glued-in rods are used when high strength solution are necessary, which are only used in exceptional cases because of associated cost.

Self drilling dowels
The initial slip is absent when using self drilling dowels. These dowels are provided with a drill head that allows a continues drilling operation through the steel and timber parts. An alternative to these types of dowels is a steel gas-tube fastener.

Expended tube fastener
When multiple fastener joints are considered, conventional dowels usually are difficult to insert due to misalignment of holes. The oversize holes of bolted connections give problems with stiffness and ductility of the joint. Based on jointing techniques in steel (i.e. the pop-nail) the expanded tube fastener was developed. Expanded tube fasteners joints are reinforced with densified veneer wood.

Glued-in rods
When joints have to transfer relatively large forces, the best joint solution involves the use of glued in bolts. The stiffness associated with glued in rods or bolts is large [16] and is considered to have no influence on the global stiffness behavior. Glued-in rod joints are relatively expensive when compared to other solutions and demand special attention during on site assembly. Glued-in bolts where also used in the Krusrak bridge in Sneek, the Netherlands [14]. A detail of such a connection for this bridge is given in figure 2.30 which was assembled on the building site and partially prepared in workshop.

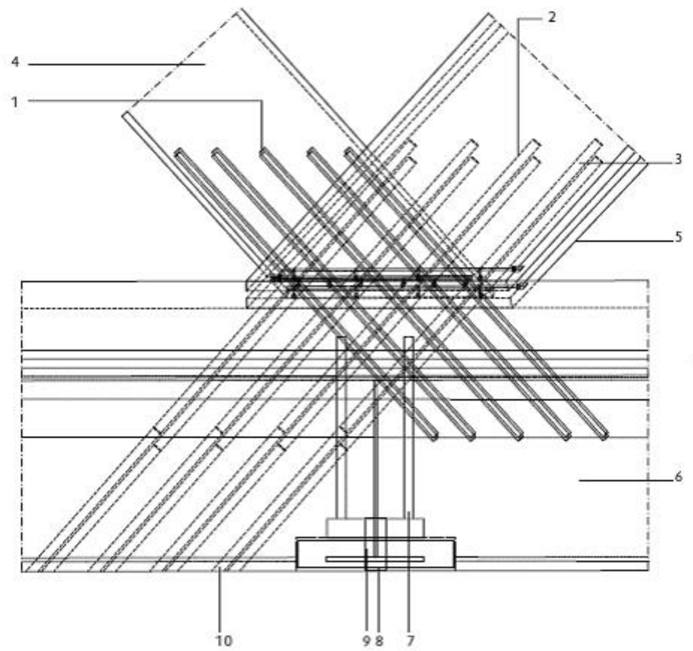

figure 2.30: Glued-in rods detail "Krusrak" bridge [14]

The bolt treads that were used in the Krusrak bridge project range between M36 and M48. Based on this project it is assumed that jointing of large elements is not an issue.

Reinforcement of joints
The general principal of reinforced joint is to prevent crushing of the wood in load introduction. The reinforcement plate is glued on a timber beam which prevents splitting of the timber. The forces applied through the fastener enter this compound through the reinforcement plate and are gradually introduced into the timber element through a glued surface. Glued steel plate reinforcement is rejected by the timber industry for a number of reasons [17]. Historically, plywood was used to reinforce timber joints. Nowadays Densified Veneer Wood (DVW) is used as reinforcement of timber joints.

2.8.3.4 Summary

A timber line corbel glued on the side of wall elements, combined with double shear connection for wall-to-wall connections is proposed as solution for cross laminated timber joints. The two main possibilities considered for bracing systems using linear elements are the Blumer System Binder and glued in rods. The BSB solution can be executed with either dowels or expended-tube-fasteners. Glued in rods can be used without intervention of an steel interface but are usually more expensive and more difficult to make on site.

For Cross Laminated Timber elements; a timber line is used for wall-to-floor joints, and a milled-out tongue and groove solution in double shear is created for wall-to-wall joints.

The default joint used to connect linear elements is the steel-to-timber BSB solution, while for large force connections and special cases glued-in rods are proposed.

2.9 Fire Safety Problems

Combustible building materials like timber burn on their surface, release energy and thus contribute to fire propagation and the development of smoke in case of fire. Because timber is a combustible material, fire safety is one of the most frequently discussed topics when tall timber building comes to order. The fire safety demands of a building could therefore limit the height of a timber building structure.

2.9.1 Fire action

To understand the behavior of a fire, the fire action as it is known by fire safety engineers is visualized in figure 2.31 for a typical space. After ignition a fire can grow very rapidly, very slowly (as in a smoldering fire) or extinguish, depending on the arrangement of combustible materials in the vicinity of the ignition source, based on the type of combustible material as well as on the geometry, dimensions and ventilation of the room. Growing fires not controlled by fire-fighting actions may lead to rapidly rising temperatures and to flashover, a scenario in which all unprotected combustible material burns.

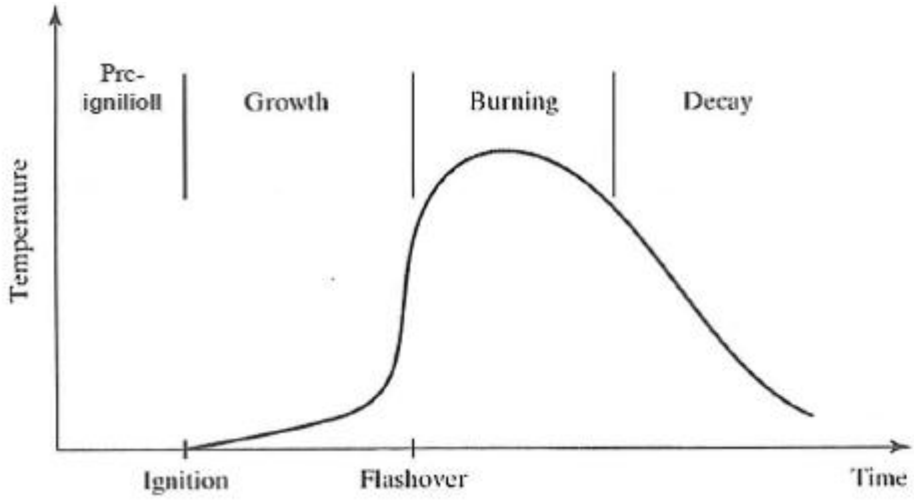

figure 2.31: Development of a fire [18]

The fire action model for building structures is visualized in figure 2.32. Four major components that play part in the fire action model are: fire load, firefighting action, ventilation of a space and thermal properties of the enclosures. Fire load and thermal properties are dependent on the material choice and are therefore relevant to the discussion, while firefighting action and ventilation are not specific for timber structures.

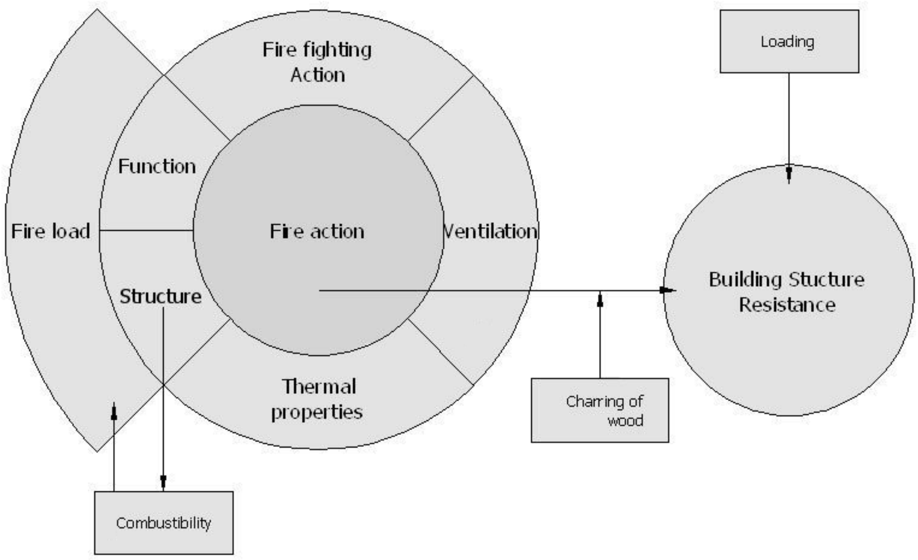

figure 2.32: Model of fire action

Fire load
As can be observed from the diagram in figure 2.32 the fire load can be separated into the contribution that originates from the function of the building and the contribution of combustible materials that embody the structure of the building, including lining and finishing. Only materials that start charring during a fire have to be included, according to NEN-EN 1991-1-2 Appendix E.

Thermal properties of enclosures
For timber buildings the thermal properties of separating elements, like walls and floors, are different compared to tall concrete buildings for which a long lasting experience is known. It is therefore relevant to include this influence in the analysis.

Material unspecific factors
The fire fighting action and ventilation of a space are not specific to the discussion of tall timber buildings, however, to achieve a realistic approach these have to be incorporated into the fire action.

In order to quantify the influence of the fire action of a fire within the analysis of a tall timber building for the case study, a calculation model has to be used that includes all relevant factors. The modeling of fires can be achieved through simplified models, more realistic models or through detailed analysis. The modeling of the fire action for timber buildings is different from others mainly because timber is a combustible material and therefore contributes to the fire load.

Simplified models: Some examples of simplified models are nominal fire curves like: ISO 834 fire curve and ASTM El19 fire curve. Nominal fire curves provide a simple relationship for the temperature of the gases in a compartment as a function of time. They represent the phase of the fully developed fire and grow monotonically in time.

Realistic models: More realistic models are parametric fire curves, which take into account the most important parameters for temperature development, namely:

- the fire load (amount, type and arrangement of combustible material);
- the ventilation conditions in the room;
- the thermal properties of the enclosures and;
- the fire-fighting action.

Detailed analysis: Computer simulations are based on parameters of multiple space zone models and the interface between those spaces or computational fluid dynamics models of the layout. These simulations can incorporate all relevant factors within the fire analysis mind frame.

Simplified models are disqualified for use in this thesis because these do not include the influence of the used material and are based on the unrealistic assumption that fires never extinguish. Parametric fire curves include all factors relevant for the discussion in this thesis, while less time consuming than fluid dynamics computer simulations. Therefore parametric fire curves are proposed.

2.9.2 Consequences of fire

In general two problems can be distinguished when discussing fire safety. The first and foremost problem regarding fire safety is the safety of people. This first problem can be divided into occupants of a building, the fire brigade present in case of a fire and neighbors. The second problem is the material damage caused by a fire. The importance of the first problem is self-explanatory, the second problem has emphasis on financial los through destruction of the building and its contents.

Safety of people: The main cause of fatalities in case of a fire is due to gases and smoke, namely approximately 80% [18], which are released during the combustion process.

Material damage: The release of heat energy during the combustion process, is the primary reason for the damage to the structure of a building and its surrounding infrastructure and environment. The general principle that leads to failure of timber buildings is shown in figure 2.32 and is basically the charring of timber during a fire, reducing the cross section of members which can fail under mechanical loading.

The problems that originate from a fire can be limited or prevented by realizing fire safety objectives, that have to be formulated in the beginning of the design process.

2.9.3 Fire safety objectives

In order to develop a satisfying fire safety design that reduces the consequences of fire, one has to formulate objectives with respect to fire safety. The basic objectives for tall buildings [18] are a direct deduction from the consequences of a fire and are:

- Safety of occupants and fire brigade
- Safety of neighbors and their property
- Limitation of financial los
- Protection of the environment in case of fire

These objectives are general of nature and are therefore broken down in: evacuation, building collapse and fire spread. The possibility to evacuate people from a fire hazardous situation relates directly to the first basic objective. Building collapse and fire spread envelope all basic objectives because they effect occupants, owners, neighbors and the environment. The three keywords: evacuation, building collapse and fire spread are discussed below for tall timber buildings.

Evacuation: The height of tall buildings results in a longer evacuation time for occupants and a longer period of time for fire fighters to reach the fire. Alternative routes of evacuation and rescue may be blocked, in case of a fire. These reasons contribute to the assumption that evacuation of people in a tall building is not feasible and even can contribute to the severity of the problem. It must therefore be possible that people can stay in a safe place inside the building until compartment burn-out occurs.

Building collapse: Building collapse in case of a fire is not allowed for several now following reasons. Building collapse makes evacuation impossible. Because the collapse is not controlled it can damage or destroy neighboring infrastructure and the environment. With respect to financial loss, building collapse is generally not accepted.

Fire spread: To ensure the possibility to evacuate and to prevent building collapse the fire spread must be limited to compartments. In the broad sense, fire spread must be limited to the outside to ensure safety of neighbors. Therefore it is generally not accepted that the fire spreads to another part of the building.

> Fires must be contained to a single part of the building as such that damage caused by a fire is limited to that part, resulting in safe evacuation and limited material damage.

Since achieving absolute safety is impossible, the level of acceptance must be quantified by the authorities or with regard to financial losses by the owner or insurance companies. The fire safety problem can be addressed by respecting regulations stated in building codes and standards. Fire safety regulations made by the authorities are different between countries and cities.

2.9.4 Regulations

Some regulations seem to discriminate against wood as a structural material compared to steel or concrete in fire conditions. In Germany for example, the building regulations state that buildings in class 5, those are buildings higher than 13 meters and/or with a net floor area over 400 m^2, are not allowed to be build out of combustible materials, which includes wood. While Austria has similar regulations, the United Kingdom and the Netherlands have no limitations of such form. For this thesis the analysis of the case study design is limited to regulations in the Netherlands with respect to fire safety.

Besides requirements on the use of combustible material for building elements, the fire regulations give mandatory rules for the design of escape routes consisting of corridors and staircases, emergency exits, and necessary organizational and technical measures like smoke detectors, alarm systems, fire hydrants, sprinkler systems, smoke exhaust systems, etc. All these measures are required independent of the type of construction material used, and are therefore not specific problems for timber buildings [3, 18]. There are in fact several regulations concerning the limitation of fire hazardous situations and fire fighting stated in the Dutch building code under sections §2.11.1 and §2.21.1 thereof. Except for demands concerning shafts and roofs, these are omitted for aforementioned reasons.

For the delineation of the case study however, it is necessary to proof that the layout of the floor plan potentially satisfies demands stated in the building code. Remaining requirements are influenced by the choice of combustible building materials.

The fire safety analysis concerns a timber office building of at least 100 m high. Below, Dutch building regulations [19] are discussed for this particular case divided into regulations effecting layout and material related regulations.

2.9.5 Regulations effecting layout

Articles within §2.17.1 to §2.20.1 of the building code [19] concern typical demands with respect to the layout of the building. In figure 2.33 the universal layout is given for all floor levels. For this analysis it is necessary to indicate the separation of fire areas and compartments. To preserve architectural freedom with respect to the layout, it is assumed that no divisions are present except for those between the lettable floor area and the core interior. This results in one coincident fire and smoke compartment consisting of the lettable floor area bound by the perimeter of the building and the building core walls.

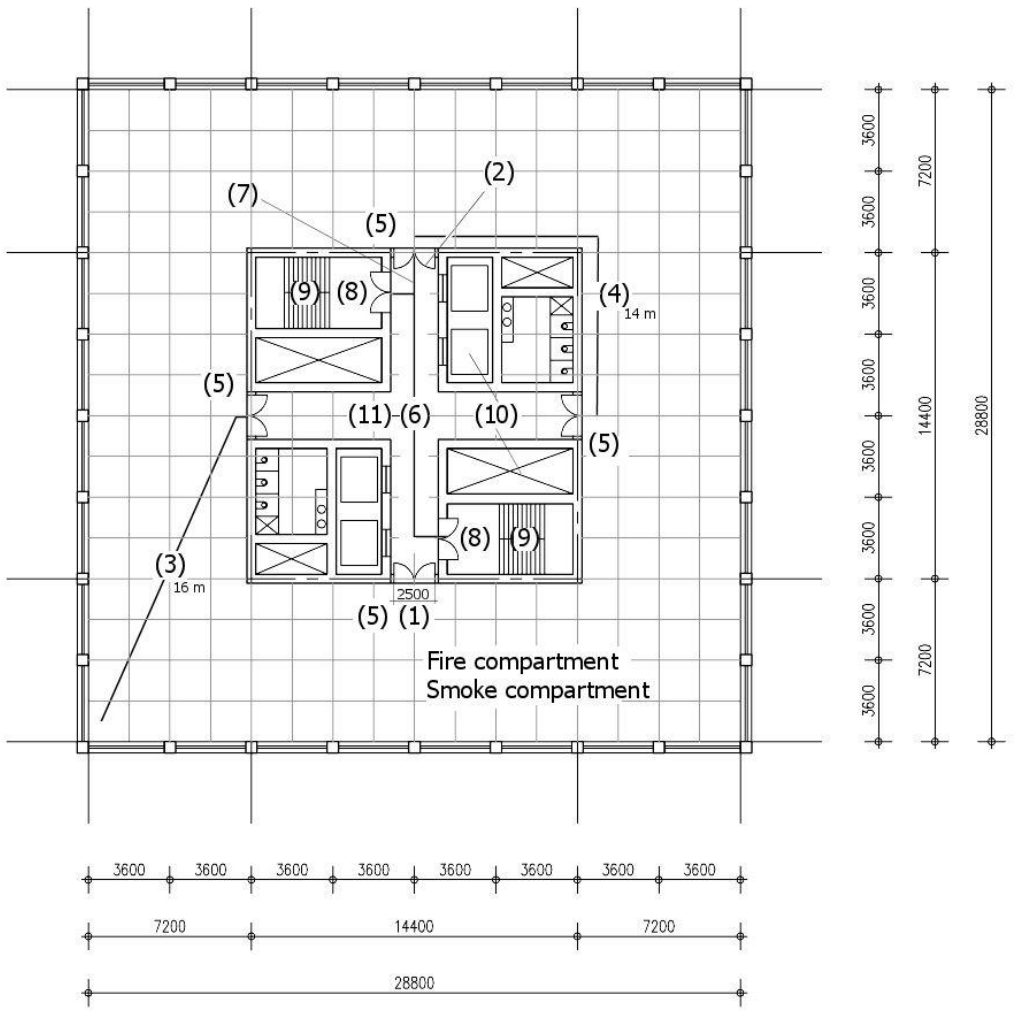

figure 2.33: Layout fire safety

In the following items the floor plan is verified to the different articles of which the numbers correspond with the numbering between parenthesis in figure 2.33. The maximum occupancy rate (B1) [19] of the floor area is used for calculations of the layout. The lettable area of one floor level is about 622 m^2.

(1) Width of free passage: Article 2.146 subsection 8, which is decisive over article 2.148 subsection 3 of [19] states that the total width of free passage for office spaces has to be at least 8553 mm for this case. Since there are four entrances of at least 2500 mm the condition is satisfied.

(2) Rotation of doors: Article 2.146 subsection 9 and Article 2.148 subsection 4 and 5 of [19] states that doors may not rotate in the direction of flight, which can be satisfied because fire and smoke compartments have coincident flight directions. This door has to be self closing in accordance with article 2.107 of [19].

(3) Distance to entrance: Article 2.146 subsection 10 of [19] states that the distance between a arbitrary point in the room and the entrance of that room is no more than 20 m, which is 16 m. Meanwhile article 2.147 subsection 16 states that the distance between the entrance of a room inside a smoke compartment and the entrance to that smoke compartment is at least 15 m, which can be satisfied since office space dimensions are larger than 1,80 m.

(4) Multiple entrances: Article 2.146 subsection 14 and Article 2.148 subsection 7 of [19] state that entrances must be located at least 5 m apart from each other, which is satisfied since the distance between entrances is at least 14 m.

(5) Exit smoke compartment: Article 2.148 subsection 2 of [19] states that at least two entrances have to be present, since there are four entrances this demand is redundant.

(6) Escape route: Article 2.156 subsection 1 of [19] states that at least two escape routes are available at the entrance of a smoke compartment, which is the case. Consequently, the circulation space inside the core must be free of smoke.

(7) Coincident escape routes: Article 2.156 subsection 7 of [19] states that escape routes as in (6) can coincide over a length of no more than 30 m, which is the case since the mutual part is only 1,80 m.

(8) Entrance smoke free escape: Article 2.167 subsection 1 of [19] states that the width and height of free passage to the smoke free escape are respectively at least 0,85 m and 2,30 m, which can be satisfied.

(9) Smoke free escape: The flight staircase must satisfy demands of a fire and smoke safeguarded space, according to Article 2.158.

(10) Fire fighting lift: Article 2.184 subsection 1 of [19] states that a fire fighting lift has to be present, which can be satisfied either by sacrificing one conventional lift or using space reserved for technical shafts.

(11) Distance staircase: Article 2.185 subsection 5 of [19] states that the distance between the entrance of a smoke compartment and the staircase is no more then 30 m, which is the case since this is either 1,80 m or 14 m with reference to (6).

Other subsections of articles within §2.17.1 and §2.20.1 of the building code [19] are either not applicable to office buildings, trivial or are satisfied by default when preceding subsections are satisfied.

> The layout itself of the universal floor plan can satisfy the regulations without the use of additional internal divisions, thereby providing a range of possible architectural arrangements.

2.9.6 Material related regulations

Articles within §2.2.1 and §2.12.1 to §2.16.1 of the building code [19] state material related regulations which are discussed below. Solutions must be found later to satisfy these demands. Dutch building code state regulations with regard to: strength during a fire, limiting development and expansion of a fire and limiting development and expansion of smoke. Articles concerning these issues are relevant to timber buildings, but are no different for building heights upward of 13 m.

Strength during a fire ([19], §2.2.1)
For buildings with floor levels above 5 m the structural resistance of the building structure is at least 90 minutes. When the fire load is smaller then 500 MJ/m^2 this may be reduced with 30 minutes. The objective of this demand is, that in case of fire, a building can be abandoned and searched for a reasonable amount of time without any risk of collapse.

Limiting development of fire ([19], §2.12.1)
The use of materials is limited with regard to their fire propagation. The contribution to fire propagation of materials is sorted into classes 1 to 4 for horizontal separations, of which class 1 is incombustible material like stone and class 4 combustible material like low density wood. The requirements depend on location of the division concerned, i.e. either division between inside spaces or bordering outside air and/or adjacent to fire and smoke proof escapes. The requirements for the case study are given in table 2.1 in which both the Dutch classes and Euro classes are indicated.

Regulations state exceptions to table 2.1 for elements bordering outside air located between ground level and 2,5 m high and elements located higher than 13 m measured from ground level, which must satisfy respectively class 1 and class 2. For purpose of uniformity and simplicity, it is decided that elements bordering outside air higher than 2,5 m, must satisfy class 2.

Structural part adjacent to:	Escapes free of fire and smoke	Escapes smoke free	Other spaces
Inside air	Dutch class 2 Euro class B	Class 4 Euro class D	Class 4 Euro class D
Outside air	Class 2 Euro class B	Class 4 Euro class D	Class 4 Euro class D
Inside air, Vertical divisions	Class T1 Euro class C_{fl}	Class T2 Euro class C_{fl}	Class T3 Euro class D_{fl}

table 2.1: fire class for divisions

Limiting expansion of fire ([19], §2.13.1)
To limit the expansion of fire, the building has to be dividend into fire compartments of less than 1000 m^2. This demand does not apply to sanitary spaces and fire escapes. The in-between fire delay between compartments, fire safety corridors and fire safety staircases is at least 60 minutes. The fire compartments are 622 m^2 which satisfies the first statement of this demand. In §2.11.1 it is stated that shafts adjacent to multiple fire compartments have to be non-combustible on the inside over a thickness of at least 10 mm.

Limiting development of smoke ([19], §2.15.1)
The use of materials is limited with regard to their smoke development in a fire. Building parts on inside spaces should have a maximum smoke density of 10 m^{-1}. When this building part is adjacent to an escape that is free of fire and smoke, then the maximum allowed smoke density is 2,2 m^{-1} and 5,4 m^{-1} for building part that satisfy respectively class 2 and class 1. These rules do not apply to floor and staircase elements.

Limiting expansion of smoke ([19], §2.16.1)
To limit the expansion of smoke, fire compartments have to be dividend into one or more smoke compartments. There is at least one smoke compartment. The resistance of smoke between a smoke compartment and a secluded space inside the fire compartment has to be at least 30 minutes. Strictly speaking, this statement leaves a void. The actual article 2.137 of [19] does not state any demands regarding resistance of smoke to other fire compartments or spaces enclosing escapes free of fire and/or smoke. By using common sense one could say that this resistance has to be at least 30 minutes.

The circulation space inside the building core is a smoke compartment by default, but not a fire compartment. This corridor must have a distance of at least 2 m between the entrance and the flight staircase access, which is approximately the case, dependant on the exact location of the doors and the wall thickness of the building core. To avoid these uncertainties, the staircase could be shifted with the adjacent technical shaft.

Graphic summary
As mentioned before, most regulatory measures apply to all buildings and are independent of the choice of material. To make a realistic fire safe design, rules on applying wood as a building material where summarized here. figure 2.34 graphically summarizes the requirement of the applied materials in the plan.

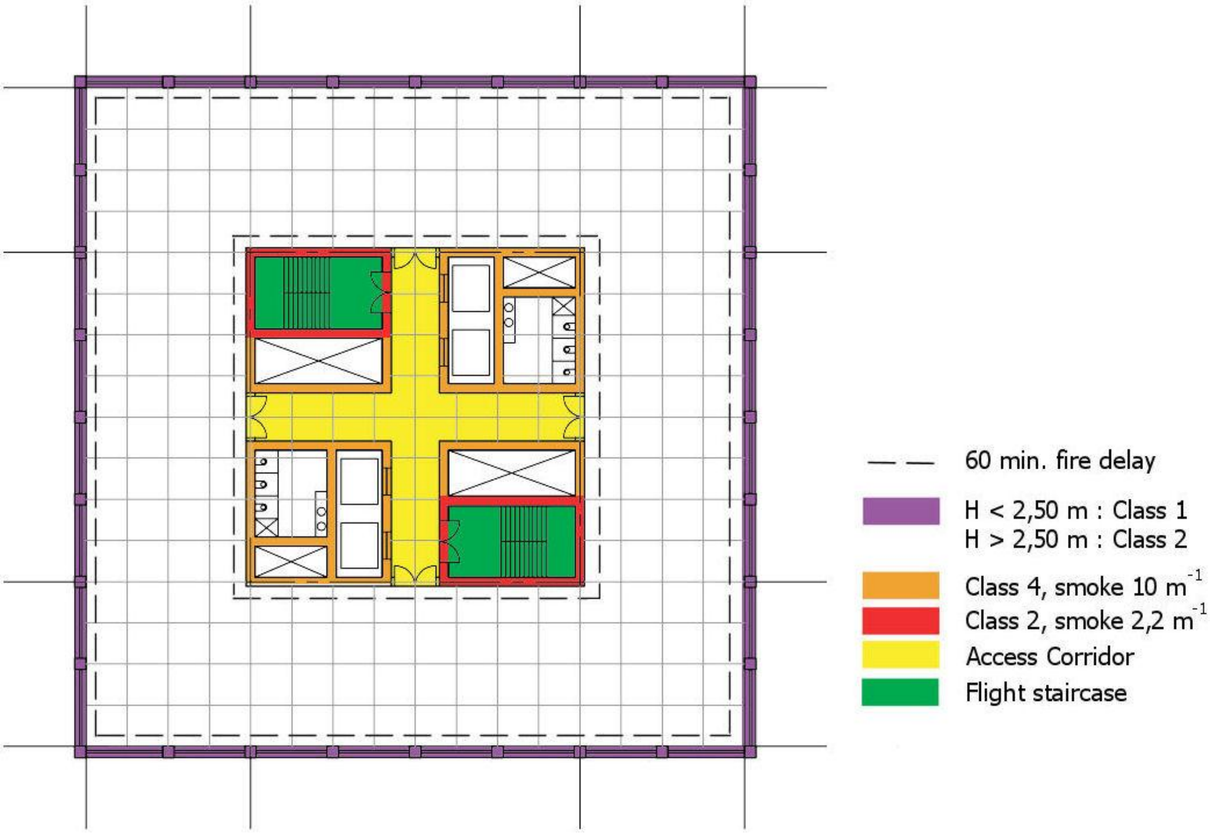

figure 2.34: Demand applied materials

2.9.7 Summary

The consequences of fire where determined to be: the safety of people and material damage. Fire safety issues specific to timber buildings are the contribution to the fire load and smoke production. Thermal properties also can influence on the fire action which are specific to timber buildings. To model the fire action, a parametric fire curve is suggested in order to take all relevant influence factors into account.

Fire safety objectives where described to limit the consequences of a fire. These objectives resulted in the demand that evacuation of people to a safe place inside the building is possible, while the building does not collapse in a fire and the fire spread is limited to predetermined boundaries.

It was proven that the universal floor plan layout is compatible with the Dutch regulations, which are believed to be a sound quantification of basic fire safety objectives regarding evacuation. While basic fire safety objectives originating from ref. [18] constrain building collapse entirely, the Dutch building regulations demand a structural resistance of 90 minutes. It is safe to say that stakeholders prefer the first.

Development of fire and smoke is limited by using materials in accordance with the building code. According to Dutch regulations expansions of fire between spaces is limited to at least 60 minutes and for smoke respectively 30 minutes. The basic fire safety objective is to contain fires to a limited part of the building to ensure evacuation within the building in a worst case scenario.

It can be concluded that the basic fire safety objectives, as they where described, are more demanding then the Dutch regulations. A reasonable fire safety concept is situated between the minimum safety demands stated by regulations and the stated fire safety objectives in absolute sense. Part of the fire safety problem analysis in this paragraph was also part of the solution. In the next paragraph solutions will be presented and a choice of a applicable fire concept will be made.

2.10 Fire Safety Solutions

The consequences of a fire and associated safety objectives and regulatory demands where analyzed in the previous paragraph. To address these fire safety issues some fire safety concepts are presented in this paragraph. These concepts possess qualities that will lead to a design of a tall buildings in which occupants can survive a full burn-out of the fire compartment while remaining in another part of the building. Before these concepts are presented the fire safety demands are summarized into compressed parts.

2.10.1 Fire Safety Demands

The demands that where encountered during the fire safety analysis can be summarized in the keywords: Evacuation, Building collapse, material classes, fire expansion and smoke expansion. Some elaboration:

Evacuation: The evacuation demand is satisfied when all items below are satisfied. Furthermore, it was proven in the previous paragraph the layout addressed evacuation within limits of the building code [19].

Building collapse: The collapse of the building structure is not allowed in a fire related circumstance.

Material classes: The use of materials is limited in accordance with the building code, in order to quantify the limitation to development of fire and smoke (figure 2.34).

Fire expansion: The expansion of fire to other parts of the building is limited to 60 minutes, undiminished the building collapse demand.

Smoke expansion: The expansion of smoke to other parts of the building is limited to 30 minutes. This demand can within reason be accomplished by satisfying the previous.

2.10.2 Fire Safety Concepts

There are two basic concepts emerging from different philosophies to address fire safety issues. The premise of these philosophies are either that wooden members of a timber building keep burning, or self extinguish. The first premise is trivial to anyone who ever build a fire, while the other is implicitly suggested in EC 1995-1-2 when making use of parametric fire curves. The two different fire safety concepts belonging to these fire safety philosophies are:

- Building encapsulation
- Finite charring

There is a reason for these two different approaches. Because architects and other stakeholders of the building sometimes want to leave timber surfaces in sight, the concept of finite charring can be applied. On the other hand, when the building encapsulation concept is used, it is assumed that the building cost are lower and authorities are easier to persuade.

While the two basic concepts differ in principle, their mutual objective is to establish compartment burn out. Compartment burn-out occurs when all combustible content has completely burned and the fire therefore extinguishes. In general, compartment burn-out satisfies at least three basic demands, which are; building collapse, fire expansion and smoke expansion. The remaining demand that safety concepts must address are the use of material to limit the development of fire and smoke.

> Fire safety concepts for tall timber buildings must result in compartment burn out using materials that limit fire and smoke development in accordance with regulations. This can be established with building encapsulation or finite charring of timber elements.

2.10.3 Building encapsulation concept

The principle of the building encapsulation concept is to protect structural timber elements for the whole duration of a fire a by non-combustible material. This results in a complete burn-out of the compartment of ignition, whereby the structural and separating timber elements shall not start charring and therefore do not contribute to the fire load. This can be achieved by protecting the timber structure with a sufficient number of non-combustible claddings like gypsum plasterboards or cement bonded panels and additional insulation materials present between spaces and within the façades.

Gypsum board: From a conservative and simplified approach it is allowed, based on tests according to the Construction Products Directive (CPD), to add 30 minutes to the fire resistance for every layer of gypsum fiber board with a thickness of about 15 mm, dependant on the manufacturer of the material. Gypsum board material usually meets requirements of non-flammable building material class A2.

Cement-bonded panels: From test results it can be derived that a cement-bonded wood fiber panel with a thickness of 15 mm can result in 60 minutes fire resistance, dependant on the underlying construction and manufacturer. Most cement-bonded wood fiber panels are non-flammable building materials which can be classified into class A1 of the euro class scale.

Insulation material: It is important to note that the presence of insulation with melt point ≥ 1000°C inside the wall can improve the fire resistance of an element, only if the insulation remains in place after the failure of the fire side cladding. [18]. A simple calculation example according to EN 1995-2 confirms that a relatively common mineral wool insulation layer of 100 mm with a density of 50 kg/m^3 increases the fire resistance with 40 minutes. Most mineral wool insulation materials meet the requirements of non-flammable building material class A1 of the euro class scale.

Experimental proof

A study conduced in Berne and Zurich, Switzerland concluded that there was no difference in fire damage for modern timber buildings compared to incombustible constructions [18]. Fire experiments were conducted in august of the year 2000 at the Institute of Structural Engineering, ETH in Zurich consisting of real-life fire tests of stacked modular hotel units.

The fire load was mimicked with 11 wooden pallets located inside the module and a PU-foam mattress was added. One to three layers of non-combustible gypsum plasterboard cladding were used and present sprinklers where disabled. For these configurations the fire load was estimated to be about 366 MJ/m^2.

One test in particular, resulted in a complete burn-out of the lower module, without significant damages to the timber structure and fire propagation to the upper module. The timber structure of this module was protected by three layers of gypsum plasterboards on the ceiling and two layers of gypsum plasterboards on the walls. No elevated temperatures were measured in the fire compartment of the room above and even the smoke concentration was at normal level until the breaking of the windows.

The fire test conducted by the Institute of Structural Engineering, ETH in Zurich confirmed that it is possible for timber structures to limit the fire spread to one compartment with only passive measures.

> Non-combustible materials protecting timber surfaces can establish compartment burn-out with inclusion of the condition that charring of timber does not occur. The application of high class non-combustible layers satisfies regulatory demands on development of fire and smoke. The building encapsulation concept can operate without intervention of automated fire suppression systems of which is scientific evidence referring to [18].

Building encapsulation eliminates the difference between combustible and non-combustible structures, i.e. the fire safety performance is equal to a concrete structure. When applying building encapsulation one can arrive a feasible fire safety concept that transcends building code and fire safety regulations.

2.10.4 Finite charring concept

Because wood itself is a poor conductor of heat and protective charcoal layers form on members in a fire, modern structural systems are properly protected by the massiveness of timbers themselves [3]. As mentioned before the self extinguishing property of fires is implicitly suggested when using parametric fire curves accompanied by parametric charring rates of timber. This can be established by making use of the appendices of the Eurocode. When the finite charring depth is established the fire resistance verification does not differentiate from other safety checks like strength, stability and stiffness under load conditions.

Fire load

The main difference between the 'finite charring' concept and 'building encapsulation' is that the structure contributes to the fire load because the wooden members start charring. There is some discussion whether or not the burning timber self extinguishes. One way to eliminate this doubt is by using automated fire suppression systems, however these are not mandatory. For calculation of the fire load only the parts that start charring have to be included. The depth of charring is linear dependent on the charring rate.

Charring rates

There is a difference between 'apparent' and 'parametric' charring rates used in the Eurocode. Apparent charring rates are assumed constant over time, while parametric charring rates are proportional to the parametric fire curve. This is effectuated by a bi-linear curve which is constant over one third of fire duration and decreases to zero simultaneous with the decay phase. The magnitude of the parametric charring rate is dependant on the fire load, which in turn is dependant on the charring depth, hence the charring rate. This results in an iterative calculation problem.

Material quality

There are indications of strong correlations between the inherent density of wood based products and their fire performance [20]. Solid timber with a density larger than 790 kg/m^3 can be classified in class 2 of the Dutch class scale which is equivalent to class B of the European class scale. Because it was chosen to use a high strength class of about D70 as a base material for structural composites the demand for development for smoke and fire can be satisfied.

Geometric oversize

To achieve a feasible fire concept based on finite charring, the reduced size of structural members after charring have to be sufficient to carry the residual loads under fire conditions. When, for example, a apparent charring rate of 0,70 mm/min for glue laminated timber is assumed, a 43 mm element oversize is equivalent to 60 minutes of fire resistance. When the duration of this fire is smaller then 60 minutes, compartment burn out would be established.

Metal components

Metal structural parts are potentially vulnerable links in completed structural systems and need to be protected by timber fire stops or putty, coated with fire retardant paint when necessary. The thickness of the protecting timber has to be sufficient to insulate the metal during charring.

> Massive timber members develop a layer of charcoal that protects the remaining cross section during a fire until burn-out, and must be sufficiently strong to carry the reduced loads. Making use of high density wood for structural and separating components, regulatory demands on development of fire and smoke can be satisfied. The fire load originating from the charred components must be determined iteratively. Uncertainty about the self extinguishing quality of this fire concept can be overcome by application of an automated fire suppression system.

2.10.5 Active fire protection

Modern technologies for detection and suppression of building fires suggest that there is no continuing reason to prescriptively limit permissible heights of timber buildings [3]. Because active fire safety systems are common practice in tall buildings and the present paradigm is cautious using timber for tall buildings it is chosen to make use of the available systems within the reasons of realism.

Automatic fire suppression systems: The presence of automatic fire suppression systems like sprinklers can be quantified in fire load reduction. These systems also guarantee that the fire extinguishes. The presence and configuration of independent water supplies determines the magnitude of the reduction. It is chosen to make use of sprinkler systems, because they are highly common in tall buildings. Independent water supplies are omitted to establish a realistic ground outlining the thesis case boundaries.

Fire detection: Modern fire detection systems can measure the composition of air in the building and trigger an alarm when any indicator of a growing fire is present. This assists an early evacuation and alarms fire fighters at an early stage. EN 1991-1-2 incorporates this through a reduction in the fire load. Fire detection systems either respond to temperature or smoke. Temperature detection is used which results in a smaller but substantial reduction when combined with automatic alarm at the fire brigade.

Fire fighting installations: Because the higher storey's of tall buildings are not easy accessible for fire brigade the following installations are mandatory: fire hydrants or other extinguishing devices, smoke exhaust systems, fire-fighters lifts and safe approaches for the fire brigade. These measures are independent of the material choice, but when these installations are absent they can magnify the fire load considerably. There is no reason why these installations should be omitted, therefore they are assumed present in the building in accordance with the regulations. Dependant on the type of fire brigade a reduction can be applied to the fire load. Private fire brigades usually operate within fire hazardous places industry. It is chosen to make use of the public fire brigade which is more common for office buildings.

Experimental proof

Sprinkler tests where carried out additional to the experiments of the study conduced in Berne and Zurich, Switzerland [18]. For two modules, the sprinkler system was enabled and the room linings consisted of combustible orientated strand board (OSB). For these configurations the fire load was estimated to be about 855 MJ/m^2. Temperature was measured at the window, in the back of the rooms and at the neighboring units above.

The temperature measurements inside the units during the experiments, varied between 50°C and 200°C until the sprinkler was automatically activated after three minutes of ignition. Therefore, flashover did not occur and it was found that combustible room linings did not contribute to the fire load within that period. Ventilation conditions, i.e. open or closed windows, did not influence the activation time of the sprinklers.

Based on the experiments described in ref. [18], sprinkler systems provide enough protection against fire for combustible compartments without any additional measures. Quantification in design, according to EC 1991-1-2 of sprinkler systems however, just reduce the fire load and do not guarantee total protection. Sprinkler systems can furthermore be economically desirable when insurance premiums come into play.

> Active fire protection is common in tall buildings. Automatic sprinklers, fire detection systems and fire fighting installations are assumed to be a realistic possible maximum on active fire protection present to reduce the fire load when necessary.

2.10.6 Summary

It was found that all fire safety demands stated in the building code, regulations and transcending fire safety objectives can be satisfied with two different concepts. The two concepts proposed are 'building encapsulation' and 'finite charring'.

The first concept is believed to protect the building structure sufficiently without the use of additional active fire protection measures. The effectiveness of second concept, finite charring, can be discussed because no accurate information is available on the self extinguishing property of massive timber members and associated thick protective charcoal layers. Since this is implicitly suggested in EC 1995, calculation can be made based on the philosophy of finite charring. To be absolutely certain that a fire extinguishes, application of active fire measures can be suggested.

Dependant on the used concept, active fire safety measures can be applied. Two extreme possibilities are suggested, either all active fire protection measures are present within realistic boundaries, or just the minimum required fire measures. The difference between the two options manifests in the presence of automatic fire suppression systems like sprinklers and fire detection measures.

Concluding the above a two dimensional combination can be made between the two concepts and the possible active fire protection measures. In table 2.2 these four possibilities are visualized and an estimation of their feasibility indicated.

Automatic fire suppression:	**Present**	**Absent**
Building encapsulation concept	Redundant	Possible
Finite charring concept	Possible	Unknown

table 2.2: Feasibility fire concepts – active fire measures

The solutions of table 2.2 provoke the investigation of their feasibility and their differences. It is therefore suggested that these solutions are quantified through calculation for the different structural systems suggested earlier in this thesis.

The solutions that where discussed above in general, are described for different reference projects and previous efforts in appendix A.1. Their layout and national regulations differ from the case discussed in this thesis, however, give a good indication of realistic possibilities.

2.11 Building Physical Problems

Desirable building physical characteristics are important to buildings in general, and include the separation between spaces inside a building and on the facade. The most common solutions for the façade are a cavity-wall or a curtain wall construction. Proper functioning of curtain-wall solutions is usually independent of the underlying structural material. Wood based material can influence the characteristics of a building through the convection density and the mass, thermal, acoustic and hydrothermal properties. The necessary solutions to address these issues take up space which will compromise the lettable floor area. The relevance and influence in light of this thesis is discussed below.

> Curtain-wall solutions overcome most building physical problems concerning separation of inside and outside space.

2.11.1 Air tightness

The air tightness, actually better known as the convection density is an essential building physics design parameter of modern separation constructions. Dependant on the system used, wood based material should be capable of performing within the demands of the building code through architectural detailing. For cavity wall solutions, barrier films and cladding could be applied when necessary, which are thin and therefore do not effect the use of space. Measured convection density of cross laminated timber panels [21] can be in the order of 750 Pa, which is assumed to be enough for separation elements. For these reasons it is assumed convection density does not influence the building height.

> Barrier films and cladding can solve convection density issues. Cross laminated timber panels are sufficiently air tight to for practical use.

2.11.2 Thermal insulation

Factors that influence the thermal insulation quality of a separation wall are particularly the thermal conductivity and the convection density. Assuming absolute convection density the thermal conductivity remains as the key parameter. Thermal conductivity depends mainly on the density and the moisture content of the used wood based material. When a vapor barrier is applied and convection density is guaranteed the inside climate can be assumed stable, hence the moister content is low. In general wood possesses good thermal insulation properties when compared to mineral materials e.g. concrete or steel.

> Wood based materials have a positive effect on thermal insulation qualities of buildings.

Light timber frames have good thermal insulation characteristic because the thermal contact area is small over the total area. Solid timber building systems are homogenous, which result in homogenous temperature fields, hence larger heat transfer, but compensate with more material and mass resulting in good insulation barriers and heat storage in summertime [21]. This difference has to be dealt with through common detailing of façade and separation walls. When absolute convection density is assumed, thermal insulation is not expected to cause unusual problems with tall timber buildings when this is taken into account through architectural detailing.

2.11.3 Sound insulation

From an acoustic point of view, wood is a light building material. The propagation of sound though air usually does not cause problems in timber buildings. Contact noise however is decisive, originating from the small mass-stiffness ratio of timber. The vibrations are induced by footfall of people using the floor surface. Horizontal acoustic separation between units is usually not a problem.

> Vertical acoustic separation is one of the main issues in timber building and should be resolved to perform within the limits of the building code

2.11.4 Hydrothermal aspects

Controlling the humidity is important for the timber structure to maintain durability of the material. Scientifically the rule to be followed is that timbers are unlikely to decay if the ambient drying rate exceeds the ambient wetting rate [3]. The hydrothermal characteristics of wood differs from other building materials. The storage of moister in wood and its diffusion through walls is therefore influenced by the material choice but also highly dependent on the architectural detailing of the wall and façade that incorporate such a choice. Constructions including a vapor barrier film can be applied to overcome problems with moister when necessary. Issues with vapor and moisture do not influence the height of a tall timber building significantly, because solutions do not require a significant amount of space.

> Vapor barrier films can solve hydrothermal issues.

2.11.5 Other issues

Other basic building physical issues like: ventilation and light issues are not specific for timber buildings and lie outside the boundaries of this thesis. Ventilation infrastructure is assumed to be embedded inside the core of the buildings layout. Entry of daylight was discussed in the paragraph 2.5.

2.11.6 Summary

The problems that are related to the building physical aspects of design have been discussed in the above. Building physical characteristics of wood as a building material that could influence the height are eliminated when using a curtain wall solution. Cavity wall solutions that include walls of wood based materials can influence building physical aspects of the building but are either easily overcome or do not influence the building height significantly.

Problems with air tightness and hydrothermal aspects can be overcome by using vapor barrier films and cladding materials. Wood based materials poses relatively good thermal properties and therefore do not require more space for additional insulation materials then other buildings. Because these problems can be solved within the space that is usually available for building physical measures, they do not influence the height of a tall timber building. Problems with contact noise sound insulation however are more difficult to overcome. Once this problem is solved there is no need for excluding wood as a modern building material for tall buildings based on building physical performance.

2.12 Building Physical Solutions

From the problem analysis it has become clear that most issues in the field of building physics do not influence the height of timber buildings with the exception of impact sound transmission of timber floor solutions.

2.12.1 Façade solutions

The construction of a curtain wall façade is believed to be no different for timber buildings than others, except when heat storage comes into play in summer. On this subject investigation is done in the field of cross laminated timber and generally good results are established for its characteristics [21].

2.12.2 Floor systems

Usually, effective solutions involve combinations of high-frequency tuning and proper selection of construction details [3]. Other solutions suggested are avoiding continues girders and floors to eliminate sound wave propagation between spaces.

Generally, floor lay-up solutions consist of a top layer with a relatively high mass, succeeded by a elastic foundation material with vibration damping qualities, on top of a structural timber floor with eventual mass additions. Solid timber plates are in general preferable over joisted floors. This solution can be equipped with a suspended ceiling. A cross-section of the floor lay-up is shown in figure 2.35 and described below.

(1) Topping, arbitrarily
(2) Cement screed
(3) Separation (eg PE-foil)
(4) Sound insulation (damping layer)
(5) Concrete tiles or blocks
(6) Bearing and bracing planking/plates
(7) Structural timber
(8) Spring bracket for ceiling
(9) Ceiling, such as gypsum board

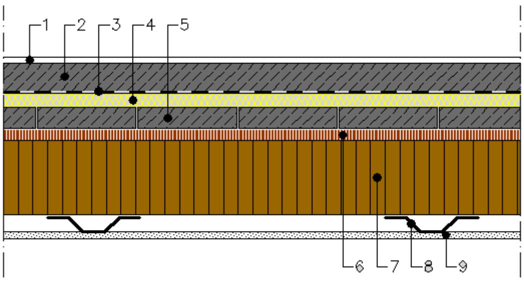

figure 2.35: Floor solution principle [43]

The topping (1) can be chosen as desired by the tenant and does not to influence the construction. The cement screed (2) is usually poured in situ on a foil (3) and functions as fire protection and adds mass to the floor. Beneath the cement screed a sound and vibration insulation layer (4) is placed. This layer functions as a elastic bedding between the above and underlying mass (5) (concrete tiles, bricks or blocks) to create a spring mass system which reduces contact sound. Beneath the concrete layers bracing planking or plates (6) can be used, in combination with the timber floor system (7). Then either battens or spring brackets can be used to fasten the ceiling of gypsum board that provides acoustic insulation and additional fire protection. In figure 2.36 a simpler and cheap way to create a floor solution is shown.

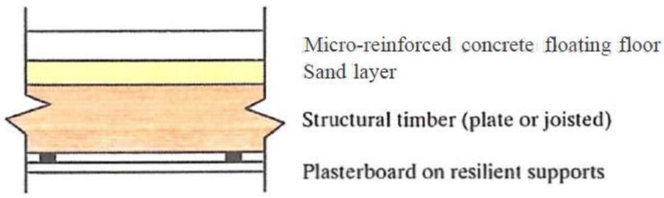

figure 2.36: Simple floor solution [3]

A combination of layers can satisfy demands on contact noise acoustics of structural timber floor systems.

2.13 Summary Preliminary Study

It was found in the preliminary study that the building height must be accompanied by a number of boundary conditions in order to investigate the structural height limit of timber buildings. These boundary conditions consist mainly of architectural performances and safety concerns. Economical limitations are left out of the equation within a realistic range. To achieve maximum building height, the optimum set of variables that influence the building height has to be chosen.

Elimination was conducted on a broad list of thinkable challenges, remaining relevant influence factors on the design of tall timber buildings. The remaining issues where categorized within architectural, structural, fire safety and building physical subsets. In this summary the challenges of these boundary conditions are summarized and their proposed solutions are given.

2.13.1 Summary Architectural Requirements

Three factors of concern for the category architectural requirements are vertical transportation, daylight entry and slenderness. It was found that vertical transportation issues could be solved through facilitation of sufficient amount of space in the building core by respecting a gross-net floor ratio of 75%. Sufficient entry of daylight is more complex to indicate exactly, but a floor depth of 7,2 m and a minimum wall-window ratio of 15% was found to quantify the minimum requirements. It was found that the slenderness is an important part of the identity of a tall building, while in contradiction with the height potential. The slenderness was therefore chosen to be 1:4 as a compromise. In figure 2.37 the determination of aforementioned factors is presented schematically.

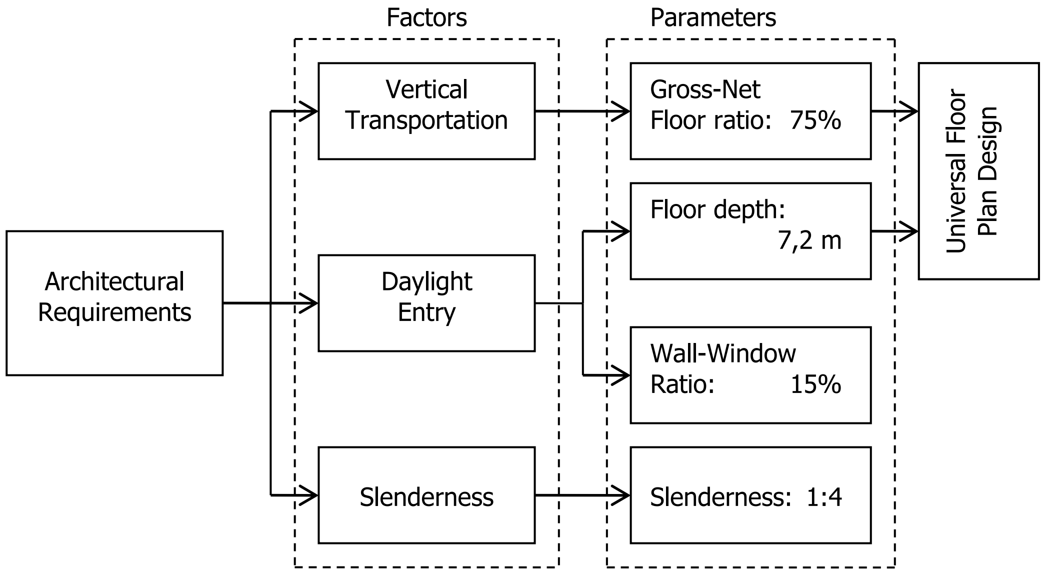

figure 2.37: Determination of architectural requirements and factors

The defined set of parameters shown in figure 2.37 radiate from factors which represent the boundary conditions. Within this set there are several possibilities concerning the daylight entry by variations of the wall-window ratio, preserving some architectural freedom. These can be actualized by the investigation of different structural systems which are summarized in the following paragraph.

2.13.2 Summary Structural Issues

The structural issues that were found to be of concern are foundation, comfort and load bearing structure. The comfort experienced by occupants is strongly correlated with the characteristics of the load bearing structure and therefore not treated separately.

It was assumed that the load bearing capacity of the foundation would not result in problems with the condition that no tension forces will enter the foundation. The stiffness of the foundation should be incorporated through an on calculations based assumption.

The load bearing structure was determined to consist of several sub factors which could be hosted under: the properties of the applied material, the choice of stability system and the structural detailing.

It was found that all desired properties of the material increase with the quality of the base material. The dimensional limitations of laminations are at least 1500 mm. The chosen material is therefore a theoretical, but possible lamination of a deciduous wood base with strength class D70. Assuming the properties of the lamination are the same as the base material is conservative, because any wood lamination process was found to increase the strength, stiffness and density.

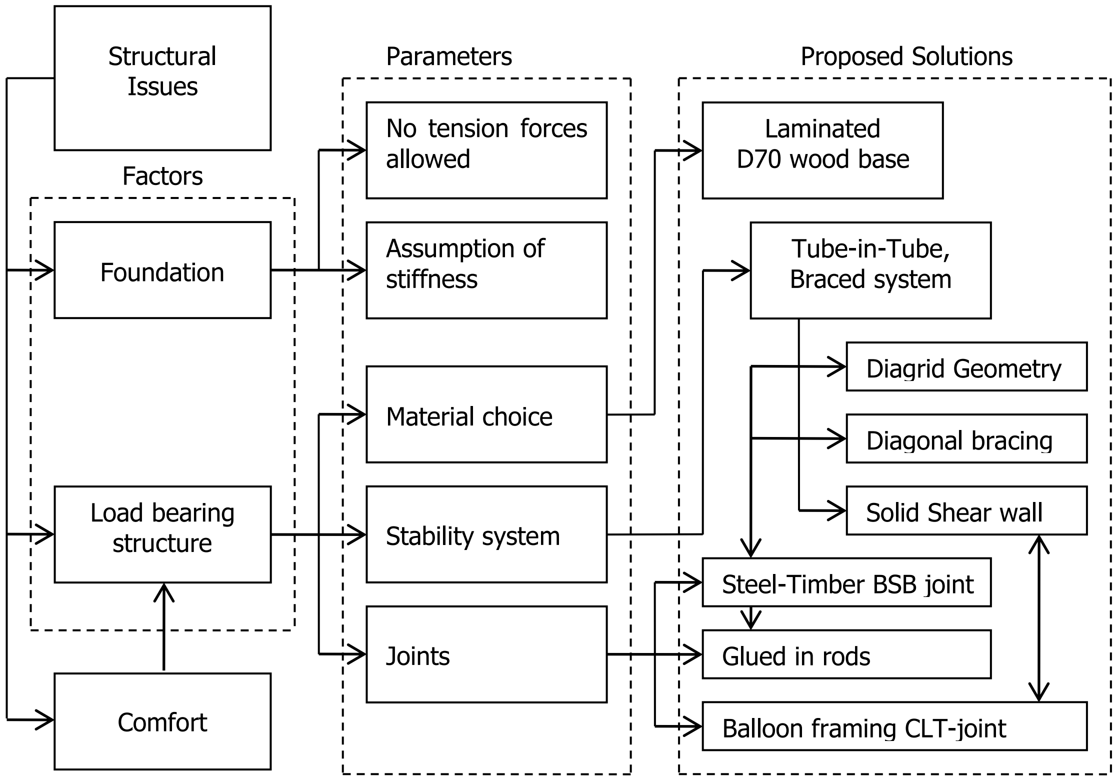

figure 2.38: Determination of structural issues and factors and solutions

The stability system is a combination of the horizontal layout and the principle of the system. The ultimate solution is believed to consist of a tube-in-tube braced system. Diagonal bracing, the Diagrid geometry and a solid shear wall are proposed options for the structural bracing. In special circumstances outriggers can be applied to increase the stiffness of the system. The reason to investigate several stability systems is to enable flexibility concerning entry of daylight, referring to the wall-window ratio and determining which is most feasible.

Structural detailing of joints is primarily dependent on the chosen stability system. The ultimate joint solutions should maximize strength and stiffness qualities, while simultaneously addressing brittleness, hygroscopic behavior, creep and anisotropic behavior. The shear wall system is equipped with a timber line corbel facilitating floor supports and a milled-out tongue and groove in double shear for wall connections, naming this a cross laminated timber balloon framing joint. For other systems either steel-to-timber BSB joints or glued-in rods are proposed.

In figure 2.38 a schematic representation is shown of the determination of the aforementioned factors and proposed solutions concerning the structural issues.

2.13.3 Summary Fire Safety Problems

It was found in the preliminary research that the necessity to evaluate the fire safety of a tall timber building is evident because wood is a combustible material. It was also found that special attention to the fire safety of tall buildings is recommended and mandatory in some cases.

To counteract the consequences of fire, certain fire safety objectives must be pursued which can be met by ensuring safe evacuation, avoiding building collapse and limiting fire spread. The quantification of these objectives is dependent on the demands set by clients and authorities. The Dutch building code was chosen as a framework of minimum requirements for this thesis.

Safe evacuation is achieved through respecting the regulations about layout, while evidently dependent on the satisfaction of the other fire safety demands like building collapse. The global layout of the universal floor plan complied with the regulations, thus providing different possibilities of architectural arrangements.

Building collapse, development and expansion of fire and smoke is limited through a combination of a chosen fire safety concept, affiliated material use and active fire suppression measures. These solutions will establish compartment burn-out, hence, avoid building collapse and limit the expansion of fire and smoke. The use of material affiliated with the concept, suppress or limit the development of fire and smoke transcending the regulatory demands.

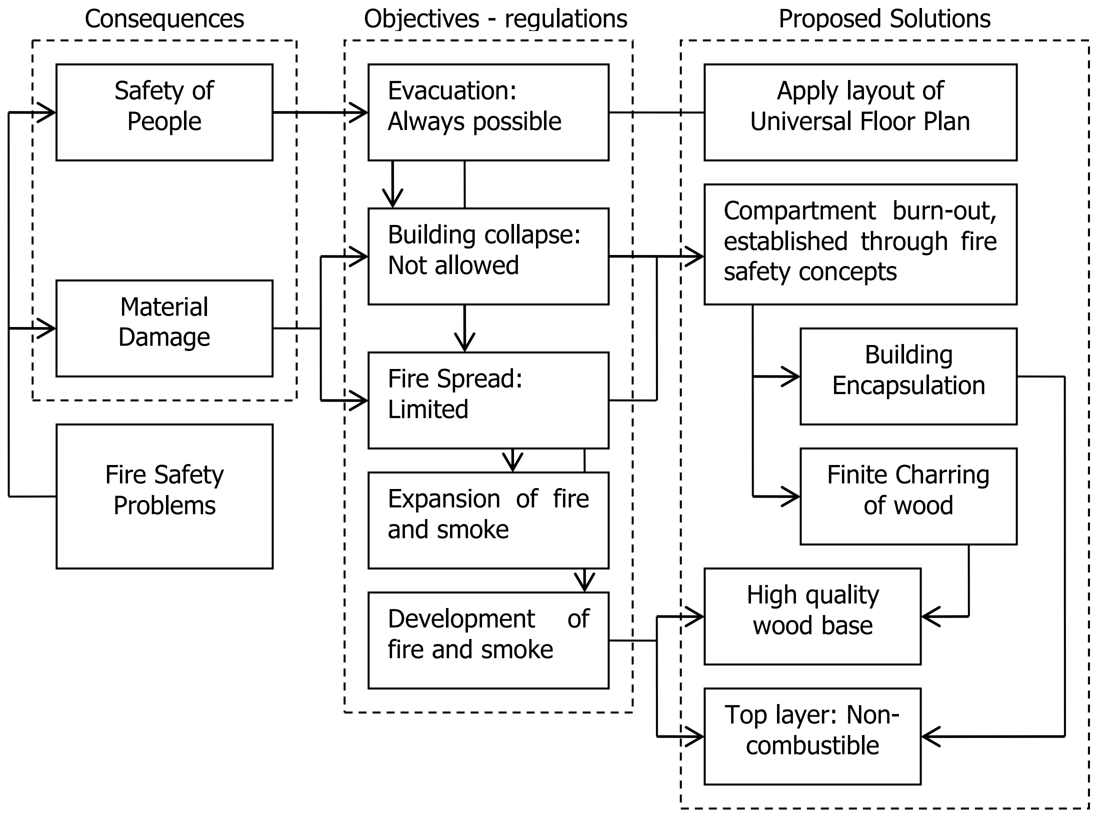

figure 2.39: Determination of fire safety problems and solutions

Suggested concepts for fire safety applicable to tall timber buildings are building encapsulation and the finite charring of timber elements. Building encapsulation concepts apply non-combustible materials to protect timber surfaces during a fire without intervention of automated fire suppression systems, provided that the wood does not start charring. Finite charring concepts depend on the development of charcoal layers that protect the remaining cross section during a fire until burn-out. Uncertainty about the self-extinguishing quality of the finite charring concept can be overcome by application of an automated fire suppression system.

The fire safety problems, the quantification of these problems and the proposed solutions are schematically presented in figure 2.39.

2.13.4 Summary Building Physical Problems

The field of building physics consist of a large list of topics of which some where found relevant to the problem of this thesis. The functioning of curtain wall solutions in building physical terms is believed to be independent of the underlying structural material. Most building physical problems concerning separation of inside and outside space are therefore overcome when a curtain wall solutions is applied.

Barrier films and cladding can solve convection density issues hydrothermal issues. Wood based materials have a positive effect on thermal insulation qualities of buildings. The remaining issue concerning timber buildings is the vertical acoustic separation of structural timber floor systems. Acoustic contact noise transition can be reduced with optimized combination of layers which create a mass spring system. No further attention will be paid to building physical issues in this thesis from here on out. The solution will be incorporated through calculating additional dead load and thickness to the floor.

2.13.5 Preparation for case study

In the following chapters the proposed solutions and fixed parameters are forged into a case study with several options concerning structural system and fire safety. These different options are called variants and will be compared with each other on their unique qualities.

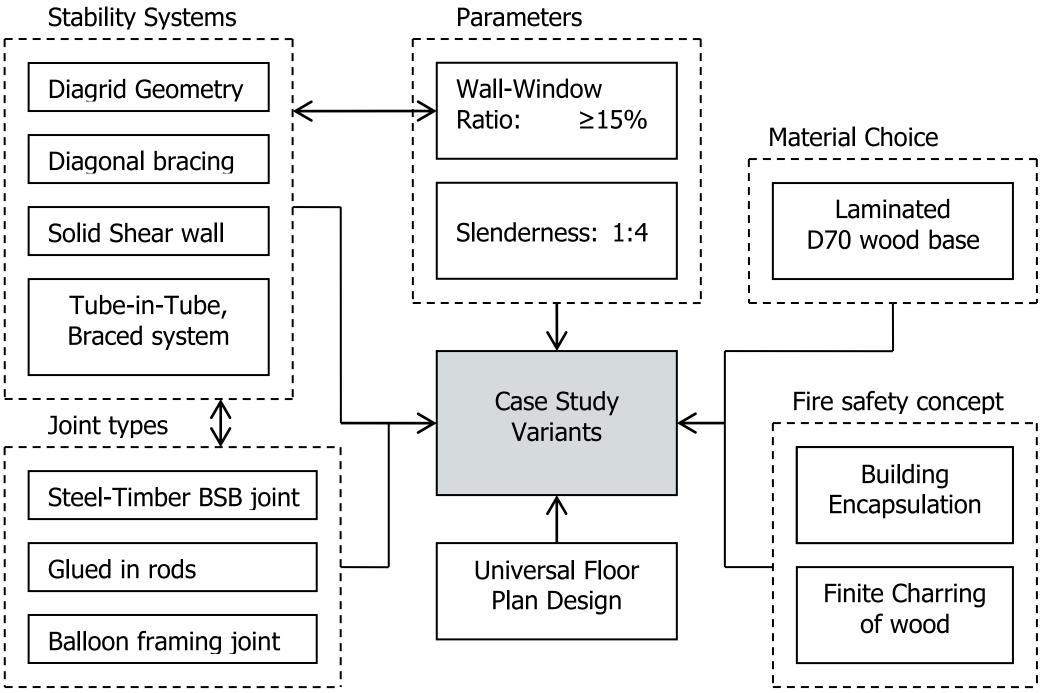

figure 2.40: Case Study Variants – Visualization of Origin

The scheme shown in figure 2.40 shows the basic characteristics of the Case Study Variants. In summery there are three different stability systems, with three affiliated joint types and two fire safety concepts to be combined and create variants. The floor plan, the chosen base material and the slenderness are basically the same for all variants. The wall-window ratio is dependent on the chosen stability system as indicated.

3 Case Study Introduction

3.1 Objective

The main objective of this case study is to proof the feasibility of a tall timber building of at least 100 m high, within the limits of regulations and certain boundary conditions. One secondary objective is to study the effect of different stability systems and determine the most feasible. Another objective is to investigate the difference between two proposed fire safety concepts in combination with fire suppression measures. Other secondary objectives are to investigate the influence on the global behavior of: the joint stiffness, the stiffness contribution of central building core and the stiffness of the foundation.

Some boundary conditions were determined in the preliminary study, while others are basic structural requirements. With these boundary condition an elementary design specification can be created which is:

- The spring stiffness of supports is a realistic representation of the foundation.
- No vertical tension forces are allowed in the supports;
- The wall to window ratio is larger than or equal to 15%;
- The slenderness of the building is about 1:4;
- The universal floor plan is used for the building design;
- The material properties resemble strength class D70 according to EN 338;
- The maximum cross-sectional dimensions of laminated members is 1500 mm;
- The maximum thickness dimension of cross laminated members is 400 mm;
- Additional floor loads will be added for acoustic separation based on common solutions;
- The fire safety of the building is achieved through application of a fire safety concept;
- The global deformation of the building is within the limits of the Dutch standard (NEN 6702);
- The material stresses are within allowable limits of the Eurocode (EN-1995-1-1).

3.2 Approach

The approach of the case study consists of creating models of variants with finite element software to calculate all relevant forces, deflections and vibrations. To analyze and verify the fire safety of the variants the proposed solutions are checked through calculation of the charring depth. To expand the above:

- Different variants are created based on the stability systems with Diagrid geometry, diagonal bracing and solid shear wall bracing.
- Joint types are chosen in association with the stability system from steel-timber BSB joints, glued in rods and cross laminated timber balloon framing joints.
- The fire safety of the building is achieved through application of a fire safety concept 'building encapsulation' or 'finite charring' with or without active fire suppression measures.

3.3 Method

Designing a structure is always a iterative process. Usually a rule of thumb is applied to estimate the dimensions of a section within a certain system, e.g. floor beams. For the structural system that is analyzed here, such a simple rule does not exist. In order to arrive at a realistic and feasible solution for a tall timber building an optimization procedure has been applied.

The optimization process consists of minimizing the cross sections of the structure to a required minimum, within reasonable limits and includes only tube structure elements. Other optimization approaches like minimizing the number of elements and changing the shape of the base geometry are omitted. All elements on the perimeter of the building, called tube structure elements, are assumed to have a cross-section with a rectangular shape to simplify the problem. After creation of the models the general process can be described with the following steps:

1) Input: estimated member sections;
2) Run linear-elastic calculation;
3) Organizing results;
4) Adjust member sections using a design list;
5) Loop procedure from step 2 until an reasonable optimum is reached.

In order to make the models and subsequently conduct such a optimization, a number of parameters has to be known in advance. To summarize:

- Geometry of the building;
- Material properties;
- Geometry of models;
- Design list;
- Stiffness of the Joints;
- Stiffness of the building core;
- Stiffness of the foundation;
- Stiffness of the floor.

Geometry of the building: In the next paragraph (3.4) the global dimensions and the shape of the universal tall building is given which serves as a template for all the variants.

Material properties: The materials that are used in the analysis of different models are described in paragraph 3.6.

Geometry of models: The variants are introduced in paragraph 3.5 from which the geometry of the models can be extracted.

Design list: Elements are primarily loaded axially with a compression force, which is caused by the geometry of the systems applied to the case study variants. The buckling resistance of these elements are given in paragraph 3.9, based on the section properties given in paragraph 3.7 and 3.8.

Stiffness of the Joints: The buckling resistance of elements is used to calculate the necessary resistance of the joints. While force transfer in compression can be accommodated by the contact surface between members and nodes, joints are assumed to transfer these forces through the fastener interface. The stiffness of the joints is discussed in paragraph 3.10, in which also the arrangement of the joints is chosen. The elimination of the stiffness influence of cross laminated timber joints is given in paragraph 3.11.

Stiffness building core: The joint stiffness assumption concluded in paragraph 3.11 is used to calculate the stiffness of the applied building core in paragraph 3.12.

Stiffness Supports: The stiffness of the foundation that is applied to the supports in the models is calculated in paragraph 3.13. Additionally, the load bearing capacity of the assumed foundation is calculated to be used as verification with the result to justify this assumption.

Loads on the Structure: In paragraph 3.14 and 3.15 the load cases and the load combinations are given.

Stiffness of the floor: In paragraph 3.16 the floor structure is calculated based on the bending behavior, which will prove the possibility of a timber floor span. The dimensions of the floor are used to calculate the axial stiffness of the floor which is used to model the interface conditions between the core and structural tube elements.

The models are described in full based on the above parameters. With these models calculations are conducted, which are shown in the following chapters. The results of these calculations are used to draw up some general conclusions completing the objective of this thesis.

3.4 Universal Tall Building

The universal tall building is a template for all variants, which implies that all characteristics described for this template apply to all variants. Here a description is given of the Universal Tall Building.

Global geometry: The global geometry of the universal tall building is shown in figure 3.1. On the left side of this figure an quasi-isometric perspective is given of the building with a partially cutaway transparent façade. On the right side of this figure the floor plan is shown corresponding with the universal floor plan. It is clearly visible that the building consists of a tube structure and a building core. The Diagrid geometry projected on the façade in this figure is just a figurative suggestion.

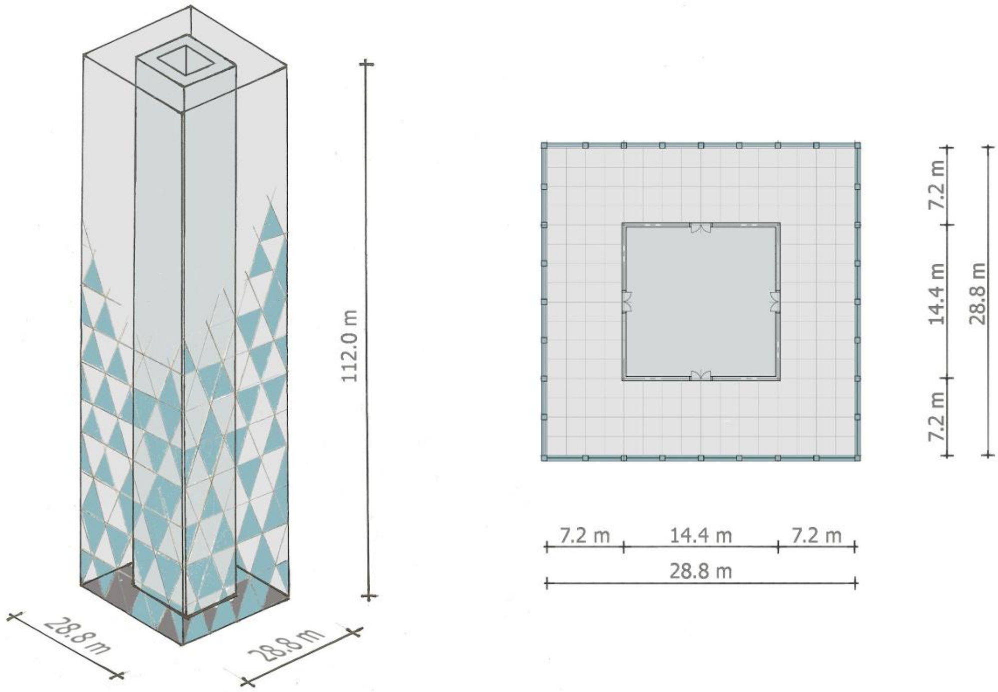

figure 3.1: Geometry of the Universal Tall Building.

Building height: The building height is chosen to be 112,0 meters, which exceeds the target height and approximately results in a building slenderness satisfying the boundary conditions. This compromise originates from the chosen center to center distance of tube structure elements.

Storey height: The average storey height or floor-to-floor height is assumed to be 3,5 meters.

Number of storey's : As a direct deduction of the storey height, the building consists of 32 storey's.

Tube structure: The tube structure is located at the perimeter of the building. The tube structure can be imagined as a cantilever beam that consist of a stiff shear frame between axial loaded elements [9].

Building core: The core structure is located at the centre of the building and is made of cross laminated timber elements. The thickness of these elements is 387 mm which is equivalent to nine board layers.

Translational coupling: The floor elements between the tube structure and the core structure effectuate kinematic coupling in the horizontal direction. This coupling is justified because the axial strain deformation within floor elements is assumed to be neglectable.

3.5 Variants

The variants of this case study are basically different tube structure geometries. Four variants are proposed in order to investigate the most relevant influence factors. Variants distinguish the following properties: structural tube geometry, pattern size, wall-window ratio, applied material and joint type.

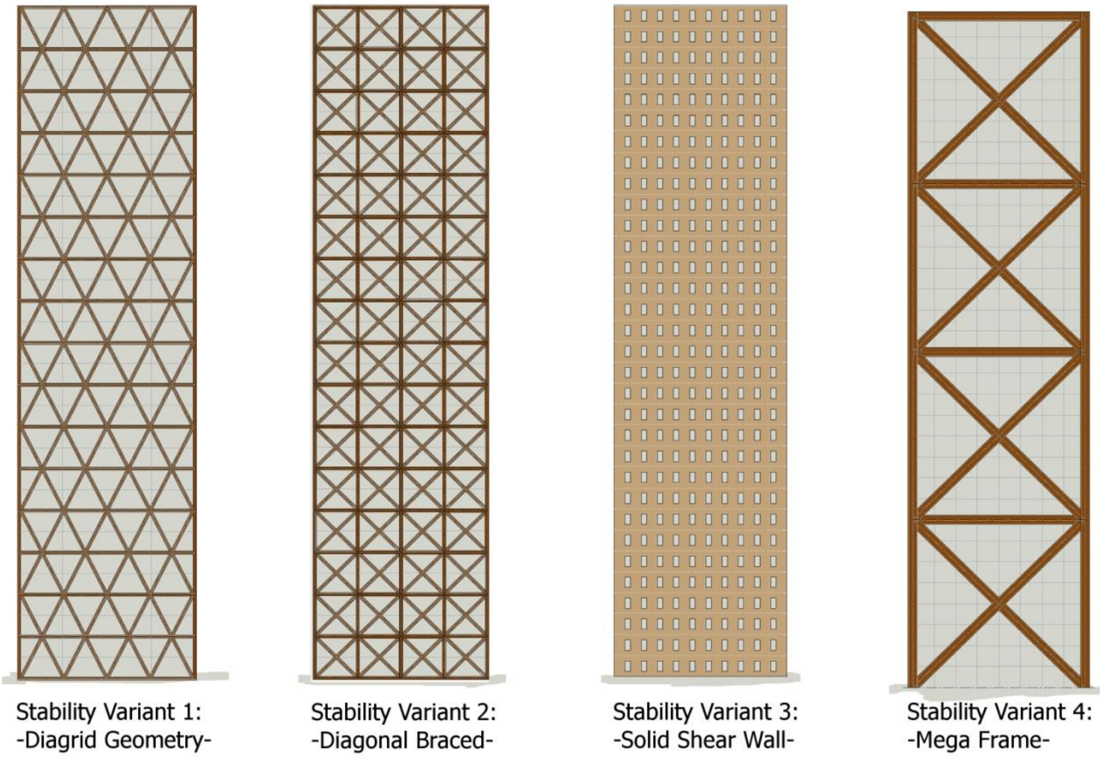

figure 3.2: Geometry of Variants

3.5.1 Primary grid pattern

For all variants the horizontal grid corresponds with a the modular grid of the floor plan and the vertical grid is a coincident with the floor height spacing. The center to center distance of the primary grid is based on an estimation of economic performance. Large centre to centre distances reduce the number of nodes and joints, while simultaneously dimensions of structural elements increase under influence of increasing forces and buckling lengths. Economically it is beneficial to choose large elements because it results in less crane operations and handling of workmen, but is also structural inefficient in some cases. Numerical optimization of this issue is not pursued further. Instead the spectrum is represented by the extreme values of the variants one through four.

For the first and second variant, respectively the Diagrid Geometry and the Diagonal Braced Frame, the pattern consists of a horizontal grid with a 7,20 m interval and a vertical grid with a 7,00 m interval. For the Diagrid Geometry this results in quasi-isosceles triangles. Section dimensions of tube structure elements are on average 500 mm for both the first and second variant.

For the third variant, the Solid Shear Wall frame, elements are basically 2,70 m wide and 7,00 m high (long) with cut outs for windows. The decisive criteria for the maximum dimensions is handling of elements during erection under wind conditions. Within the dimensional limitations stated in paragraph 3.6.4 of this thesis, it would theoretically be possible to make elements three storey's high, that is 10,50 m long. This is avoided because of expected problems with temporarily bracing of wall elements when floor elements are not present yet.

For the fourth and last variant, the "wildcard" Mega Frame, the grid pattern dimensions are based on maximization of the internal lever arm which implies the total width of the building. This is realized through introduction of mega columns on the four corners of the building. This results in a horizontal grid of 28,8 m and a vertical grid of 28,0 m.

A mega-frame is basically a structure that takes account of the lateral loads in large building structures. Part of the vertical loads is be carried by the mega-frame as well. Section dimensions for the Mega Frame range from 1000 mm to 1350 mm for column elements and from 650 mm to 750 mm for brace elements. The mega-beam elements, spaced between column-brace intersections, where transformed into mega-trusses as will be explained later in this thesis. Because this structural alternative is expected to have high potential with respect to building height it is interesting to investigate

3.5.2 Secondary grid pattern

A secondary grid, which is not visible in figure 3.2, is present to support the intermediate floors and is assumed not to contribute to the global structural behavior. A representation of the secondary structures is shown in figure 3.3 and could also accommodate support for window frames or a curtain wall facade placed on, or between structural elements. The architectural façade is assumed to be placed on the outside of the tube structure in order to overcome any problems with environmental influence on the tube structure. The justification of this solution can be discussed because it can compromise the net (lettable) floor area.

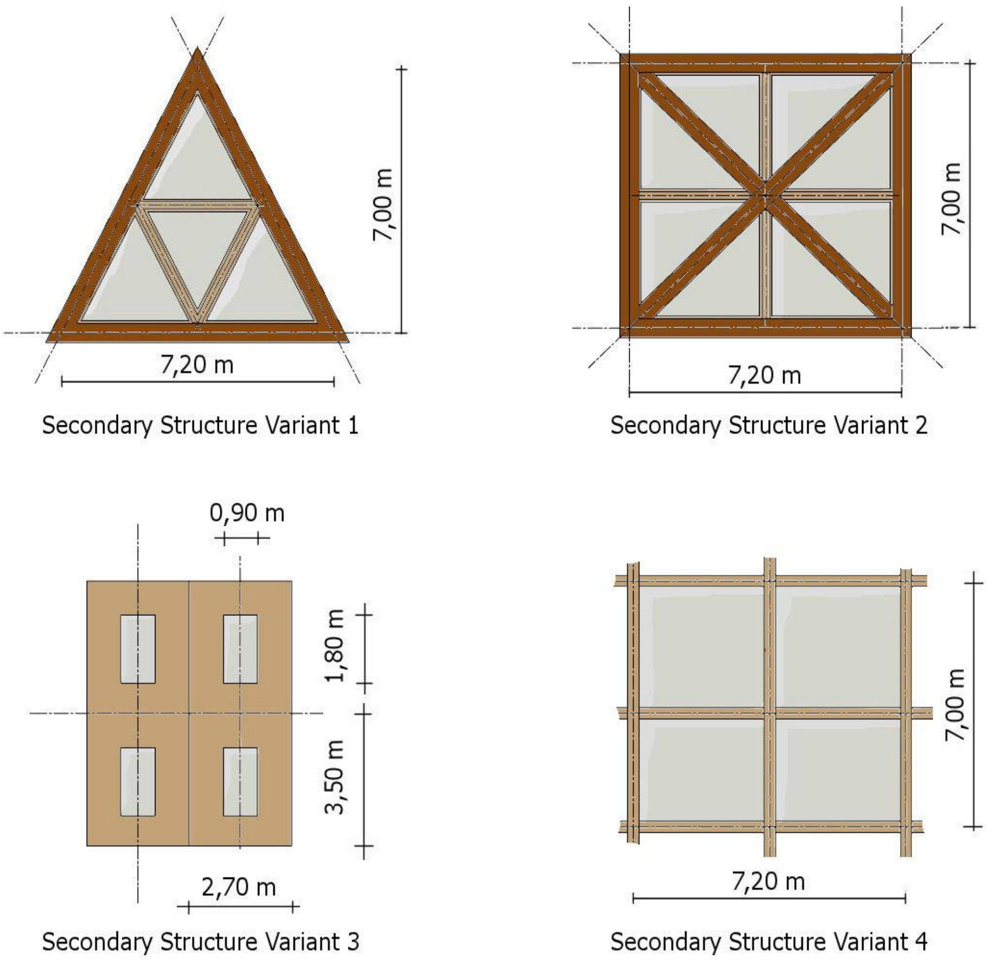

figure 3.3: Secondary Structure

Cross sections of elements of the secondary structure are small compared to the load bearing tube structure because of their smaller span and loads acting on the structure. Variant 3 does not have to incorporate a secondary structural grid to support floors intermediately. Variant 4 is equipped with a gravity frame of which the columns are larger compared to other variants because they carry eight floor levels. All secondary frames, including the gravity frame of variant 4, are carried by the primary tube structure.

The cross sectional dimensions of secondary beam elements that support the floor are 175 mm x 175 mm for all variant. The column sections of variant 1 and 2 are also 175 mm x 175 mm. The column sections of the gravity frame of variant 4 range between 150 mm x 150 mm and 400 mm x 400 mm. With these section dimensions, calculations can be carried out to determine the wall- window ratio.

3.5.3 Wall-Window ratio

The openings that are reserved for daylight entry must be of an acceptable size from a building physical and architectural point of view in order to arrive at a realistic case study design. Based on area calculations with AutoCAD ® software of the geometries shown in figure 3.3, the wall to window ratio is determined.

3.5.4 Summary of Variants

The specifications of variants 1 to 4 are given in the frames below under the bold eponymous headings.

Variant 1: Diagrid Geometry
The Diagrid Geometry tube structure is shown on the left side of figure 3.2.

Structural tube	Diagrid Geometry
Applied material	Laminated Timber of a D70 Wood Base
Joint type	Steel-Timber Joint
Pattern size	7,2 x 7,0 m grid
Secondary pattern size	3,6 x 3,5 m grid
Wall-window ratio	63 %

Variant 2: Diagonal braced
The diagonal braced tube structure is shown in figure 3.2 on the second from the left.

Structural tube	Diagonal Braced Frame
Applied material	Laminated Timber of a D70 Wood Base
Joint type	Steel-Timber Joint
Primary pattern size	7,2 x 7,0 grid
Secondary pattern size	3,6 x 3,5 grid
Wall-window ratio	58 %

Variant 3: Solid Shear Wall
The Solid Shear Wall tube structure is shown in figure 3.2 on the second from the right.

Structural tube	Shear Wall Braced
Applied material	Cross Laminated Timber of a D70 Wood Base
Joint type	Balloon Framing Joint
Pattern size	2,7 x 7,0 m plate design
Wall-window ratio	17 %

Variant 4: Mega Frame
The Mega Frame tube structure is shown on the right side of figure 3.2

Structural tube	Diagonal Braced Mega Frame
Applied material	Laminated Timber of a D70 Wood Base
Joint type	Glued-in Rods
Pattern size	28,8 x 28,0 m grid
Secondary pattern size	3,6 x 3,5 grid
Wall-window ratio	83 %

3.6 Material Properties

Two materials are used in the calculation models of this theses, and will be referred to by the names: D70-LAM and D70-CLT, which are laminations of a deciduous base material graded to strength class D70. The properties of the base material and the laminations are given in this paragraph.

3.6.1 Base material D70

The properties of the base material D70 are given below.

Strength properties of D70 class

$f_{m,k}$	$f_{t,0,k}$	$f_{t,90,k}$	$f_{c,0,k}$	$f_{c,90,k}$	$f_{v,k}$
N/mm²					
70	42	0,6	34	13,5	6

Stiffness properties of D70 class

$E_{0,mean}$	$E_{0,05}$	$E_{90,mean}$	G_{mean}
kN/mm²			
20	16,8	1,33	1,25

3.6.2 D70-LAM

It was determined in the preliminary study that a lamination has higher capabilities than the base material. This was based on tests [13] of softwood species. The theoretical lamination D70-LAM is therefore conservatively assumed to be equal to the applied base material D70, because specific data of such improvements are unknown for hardwood species.

Material modification factors for this glue laminated timber are derived from EN 1991-1-1. The size effect for bending and tension of the lamination is not taken into account, because this assumption simplifies the calculation, and because most members are larger than 600 mm anyway.

3.6.3 D70-CLT

D70-CLT is cross laminated timber of a base material graded to strength class D70. An important material property of this material is the rolling shear stiffness and strength. According to ref. [25] the rolling shear stiffness ($G_{R,mean}$) is equal to 10% of the mean shear strength (G_{mean}) for softwoods. The rolling shear strength ($f_{R,k}$) is equal to 1,0 N/mm^2 independent of the strength class [25]. For this theoretical lamination these values are adopted by default, because of insufficient knowledge about the properties of hardwood.

Dimensional limitations

Most European manufacturers of cross laminated timber are equipped with machinery and infrastructure than can deliver elements up to 16 m in length, 2,95 m wide and 400 mm thick. The individual boards that are glued together to create these elements have maximum board thickness of 43 mm with a board width of 200 mm. To realize an economic design it is necessary to keep board width and thicknesses as large as possible, because this results in a smaller number of actions handling individual boards during production of the material.

Reduction of stiffness moduli

The build-up in the thickness direction of cross laminated timber plates has influence on the global strength and stiffness parameters of the material. For the calculations with the computer software used for this thesis, these reductions are best accounted for through reduction of the stiffness moduli, because the software features orthotropic material properties. The software is not able, however, to assign effective cross sections to different directions of 2D-elements, hence this unconventional approach. The modification of the material properties of D70-CLT consist of axial reduction and shear reduction and are explained in the following subparagraphs. The reduction of the strength and stiffness in bending effectuates on a system level and is therefore not included within these material properties.

3.6.3.1 Axial Reduction

The reduction of the stiffness of the cross laminated timber cross section in the axial direction is straight forward. The effective (equivalent) modulus of elasticity (E_{eff}) section is calculated though averaging the modulus of elasticity over individual layers. Equation (3.1) is deduced by the author based on this theory and holds for all plate configurations.

$$E_{eff} = \frac{\sum_1^n t_i \cdot b_i \cdot E_i}{\sum_1^n t_i \cdot b_i} \quad \textbf{(3.1)}$$

Because the layer thickness (*t*) and the width (*b*) are assumed to be equal for all layers, a simplified method shown in equation (3.2) is used. Additionally, for a symmetric build-up of (*m*) uneven number of layers equations (3.3) and (3.4) are true for plates respectively loaded parallel and perpendicular to the board grain direction that is visible on the face. The equations (3.2) to (3.4) are all deduced by the author.

$$E_{eff} = \frac{n_0 \cdot E_0 + n_{90} \cdot E_{90}}{n_0 + n_{90}} \quad \textbf{(3.2)}$$

$$E_{eff,\parallel} = \frac{(m+1) \cdot E_0 + (m-1) \cdot E_{90}}{2 \cdot m} \quad \textbf{(3.3)}$$

$$E_{eff,\perp} = \frac{(m-1) \cdot E_0 + (m+1) \cdot E_{90}}{2 \cdot m} \quad \textbf{(3.4)}$$

In which:
n_0= number of layers parallel to the load
n_{90}= number of layers perpendicular to the load
E_0= Modulus of elasticity parallel to the grain
E_{90}= Modulus of elasticity perpendicular to the grain
m= total number of layers

According to the informative annex of Eurocode EN-338 stiffness properties perpendicular to the grain of timber are calculated with equation (3.5) for hardwoods. Substitution of (3.5) into (3.3) and (3.4) results in equations (3.6) and (3.7) which calculate the axial reduction factor originating from the plate buildup.

$$E_{90} = \frac{E_0}{15} \quad \textbf{(3.5)}$$

$$\boxed{\frac{E_{eff,\parallel}}{E_0} = \frac{m+1}{2 \cdot m} + \frac{m-1}{30 \cdot m}} \quad \textbf{(3.6)}$$

$$\boxed{\frac{E_{eff,\perp}}{E_0} = \frac{m-1}{2 \cdot m} + \frac{m+1}{30 \cdot m}} \quad \textbf{(3.7)}$$

3.6.3.2 In-Plane Shear Reduction

The geometric build-up of the plate with boards, i.e. the width and thickness of boards and intended spacing between boards, has influence on the shear modulus of the plate. This influence is documented in ref. [15] of which conclusive graphs are shown in figures 3.4 (a) and (b)

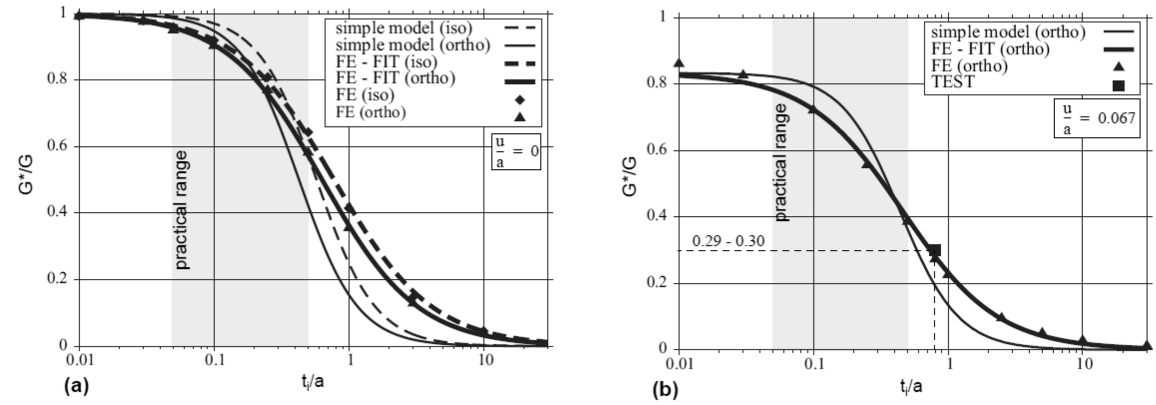

figures 3.4: Shear reduction – thickness ratio [15]

There are two different configurations possible for cross laminated timber, the standard and the non-standard configuration [15]. The standard is configuration, without intended spacing and without being glued to each other by the narrow side of boards results in a larger shear modulus. Equation (3.8) gives the general simplified model corrected to the FE- results from the research of ref. [15].

$$\frac{G_{FE-FIT}}{G}=\left(1+\frac{u}{a}\left(1+2\frac{G}{G_Q}\right)+\alpha_{FE-FIT}\cdot 3\frac{G}{G_T}\left(1+\frac{u}{a}\right)^2\left(\frac{t_i}{a}\right)^2+2\frac{G}{E}\left(\frac{u}{a}\right)^3\right)^{-1} \tag{3.8}$$

For the correction factor to the FE-results two models where used, one isotropic plate and one orthotropic plate model, which are shown in equation (3.9) of which the second is used for D70-CLT.

$$\alpha_{FE-FIT,iso}=0.45\cdot\left(\frac{t_i}{a}\right)^{-0.80} \qquad \alpha_{FE-FIT,ortho}=0.32\cdot\left(\frac{t_i}{a}\right)^{-0.77} \tag{3.9}$$

The standard configuration is used for D70-CLT, which implies the simplification through u=0 as shown in equation (3.10).

$$\boxed{\frac{G_{FE-FIT}}{G}\xrightarrow{u=0}\left(1+\alpha_{FE-FIT}\cdot 3\frac{G}{G_T}\left(\frac{t_i}{a}\right)^2\right)^{-1}} \tag{3.10}$$

Substitution of the used board dimensions and the shear modulus - torsional shear modulus ratio, results in the reduction calculation of the shear modulus given below. The value of the torsional shear modulus (G_T) is assumed to be equal to the averaged shear modules ($½\cdot(G_{||}+G_{\perp})$).

$$\frac{G_{FE-FIT}}{G}=\left(1+0.32\cdot\left(\frac{43}{200}\right)^{-0.77}\cdot 3\cdot\frac{2}{1{,}1}\cdot\left(\frac{43}{200}\right)^2\right)^{-1}=0{,}79$$

3.6.3.3 Reduced Stiffness Properties D70-CLT

The axial reduction according to equations (3.6) and (3.7) and the shear reduction according to equation (3.10) results in the values given in table 3.1 for the considered number of layers of D70-CLT. The definition of these properties is given in figure 3.5.

Stiffness Properties of D70-CLT

layers: t=43 mm	3	5	7	9
		kN/mm^2		
$E_{eff,\|\|}$	13,8	12,4	12,0	11,8
$E_{eff,\perp}$	7,6	8,8	9,4	9,6
E_{90}		1,33		
G_{eff}		0,99		

table 3.1:Stiffness properties for D70-CLT

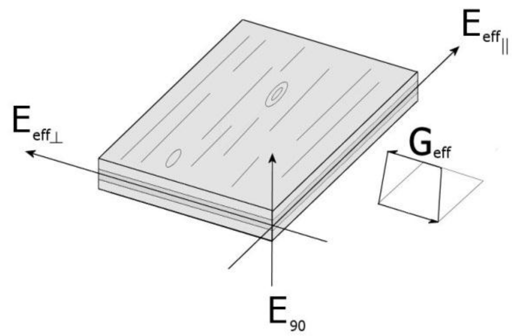

figure 3.5: Definition of Stiffness properties

3.6.3.4 Effective Cross Sections

For the assumed board thickness which is equal for all layers the effective cross sections of D70-CLT are calculated according to equations (3.11) and (3.12) in which the contribution of boards orientated perpendicular to the grain are neglected. The calculated effective cross sections of D70-CLT are shown in table 3.2 for plate thicknesses of 3 to 9 layers.

$$A_{eff,\|\|} = t \cdot \frac{(m+1)}{2 \cdot m} \quad \textbf{(3.11)}$$

$$A_{eff,\perp} = t \cdot \frac{(m-1)}{2 \cdot m} \quad \textbf{(3.12)}$$

In which:
$A_{eff,\|\|}$= Effective cross section parallel to face grain
$A_{eff,\perp}$= Effective cross section perpendicular to face grain
t= board thickness
m= total number of layers

Section Properties of D70-CLT

layers: t=43 mm	3	5	7	9
		mm^2/m^1		
$A_{eff,\|\|}$	$86 \cdot 10^3$	$129 \cdot 10^3$	$172 \cdot 10^3$	$215 \cdot 10^3$
$A_{eff,\perp}$	$43 \cdot 10^3$	$86 \cdot 10^3$	$129 \cdot 10^3$	$172 \cdot 10^3$

table 3.2: Effective Cross Sections D70-CLT

3.6.3.5 Stiffness Reduction to include Openings

The stiffness parameters of the material are modified in the below to include the influence of openings in the tube structure of variant 3. The plate arrangement of the tube structure of variant 3 is shown in figure 3.6. The in-plane shear stiffness and axial stiffness modifications are calculated below.

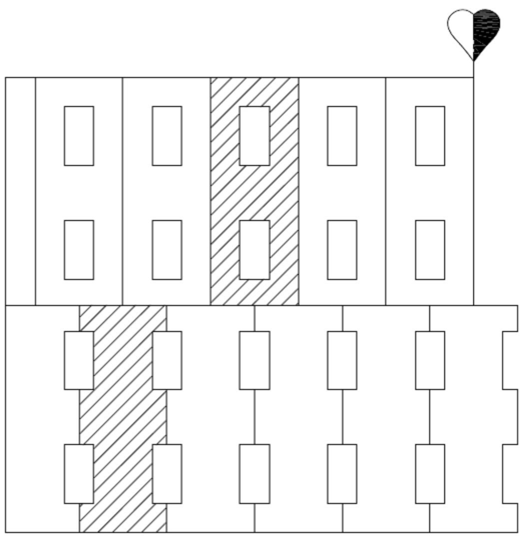

figure 3.6: Primary Grid of Variant 3

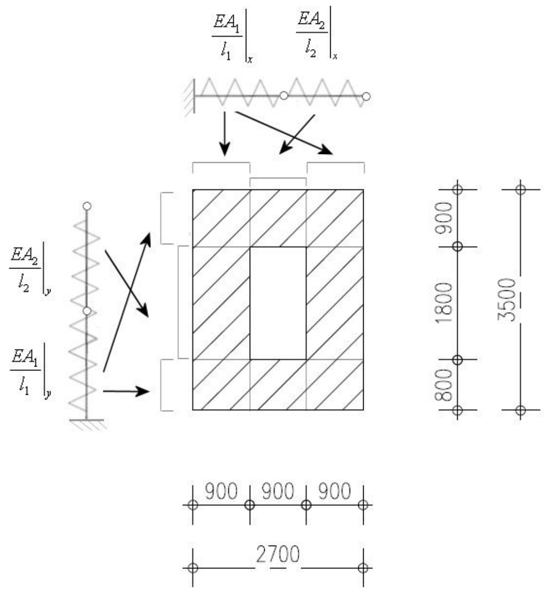

figure 3.7: Representative Plate Part

Axial reduction

The axial reduction of the cross section due to openings in the tube structure is incorporated in two models of variant 3 through modification of the modules of elasticity. A representative plate part of the tube structure is shown in figure 3.7. In this figure are also two series of two springs shown that represent strips of this plate, indicated with arrows. The spring series are shown for the horizontal (x), and the vertical (y) direction. The two outer strips are not affected by the opening, while the inner strip is. Based on the theory of serial springs, the stiffness of the total spring system can be derived to the right hand side of equation (3.13). When the plate part shown in figure 3.7 is imagined without an opening, the representative spring stiffness for such a plate can be derived as the left hand side of equations (3.13). The left hand side includes the effective modulus of elasticity (E_{eff}) of which a formula must be found through deduction.

$$\frac{AE_{eff}}{L} = \left(\frac{l_1}{EA_1} + \frac{l_2}{EA_2} \right)^{-1} \tag{3.13}$$

In which, for the arbitrary direction considered:

A = theoretical cross section area of plate without openings
E_{eff} = effective modulus of elasticity (to include the effect of openings)
L = total length of the representative plate part
l_1 = total length of the outer strips of the plate
A_1 = cross section area representative for the outer strips of the plate
l_2 = length of the inner strip of the plate
A_2 = cross section area representative inner strip of the plate
E = modulus of elasticity of the material

To establish a reduction factor for the modulus of elasticity equation (3.13) is rewritten to equation (3.14) by multiplying both sides with L and dividing both sides by E and A .

$$\frac{E_{eff}}{E} = \frac{L}{A} \cdot \left(\frac{l_1}{A_1} + \frac{l_2}{A_2} \right)^{-1} \tag{3.14}$$

The equations (3.15) and (3.16) are special cases of equation (3.14) and discribe the reduction of the modulus of elasticity respectively in the horizontal (x) and vertical (y) direction with variables filled in as they are defined in figure 3.9.

$$\frac{E_{eff,x}}{E} = \frac{B}{t \cdot H} \cdot \left(\frac{(B-b)}{t \cdot H} + \frac{b}{t \cdot (H-h)} \right)^{-1} \rightarrow \frac{B \cdot (H-h)}{B \cdot (H-h) + b \cdot h} \tag{3.15}$$

$$\frac{E_{eff,y}}{E} = \frac{H}{t \cdot B} \cdot \left(\frac{(H-h)}{t \cdot B} + \frac{h}{t \cdot (B-b)} \right)^{-1} \rightarrow \frac{H \cdot (B-b)}{H \cdot (B-b) + h \cdot b} \tag{3.16}$$

Evaluation of the reduction factors using the dimensions given in figure 3.7 result in:

$$\frac{E_{eff,x}}{E} = 0{,}74, \qquad \frac{E_{eff,y}}{E} = 0{,}80$$

These values are used to modify the material parameters of variant 3, in order to model with 1D elements and 2D elements without having to reduce sections properties to take into account the effect of openings.

In Plane Shear reduction

The openings of the solid tube-structure are equally spaced. This motivates the use of an equation documented in ref. [15] which are valid for square plate shapes with square openings. The equation was created through the fit of data from orthotropic material modeling of a CLT wall element as shown in figure 3.8 (solid line). The dimensions are defined as in figure 3.9 where *B* and *H* are the outer width and the height of the plate respectively, and *b* and *h* are the dimensions of the openings subsequently.

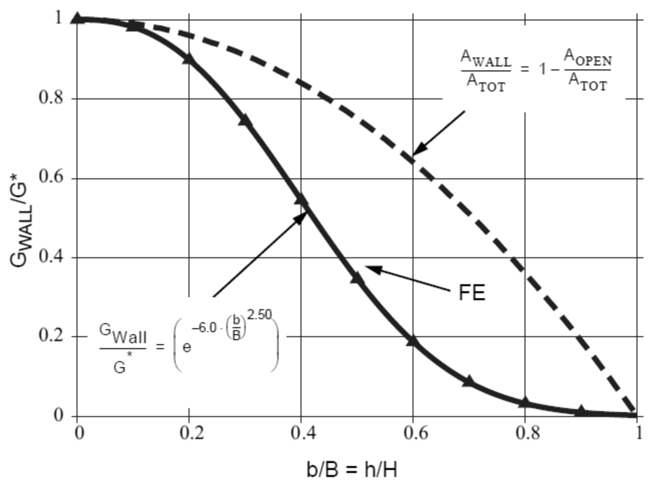

figure 3.8: Shear reduction of CLT with Openings

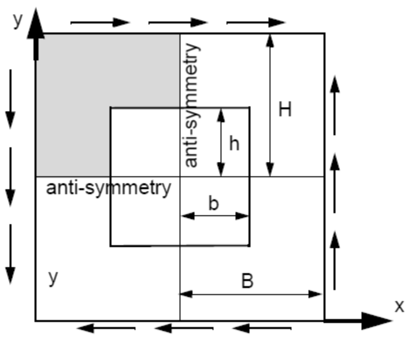

figure 3.9: Definition of Opening

Based on previous inquiries within this thesis the plate dimensions where established. With figure 3.9 as constitution the values for plate dimensions are defined as in figure 3.7. Because these dimensions are not actually squared, a conservative approach would be to use the largest ratio which is h/H as in equation (3.17). For comparison the smallest ratio is calculated in equation (3.18) which indicates a wide range. This suggests the use of the square root averaged opening-to-plate ratio as calculated in equation (3.19).

$$\frac{G_{WALL}}{G} = e^{-6,0\cdot\left(\frac{h}{H}\right)^{2,50}} \xrightarrow{\frac{h}{H}=\frac{1,80}{3,50}} \frac{G_{WALL}}{G} = 0,32 \tag{3.17}$$

$$\frac{G_{WALL}}{G} = e^{-6,0\cdot\left(\frac{b}{B}\right)^{2,50}} \xrightarrow{\frac{h}{H}=\frac{0,90}{2,70}} \frac{G_{WALL}}{G} = 0,68 \tag{3.18}$$

$$\frac{G_{WALL}}{G} = e^{-6,0\cdot\left(\sqrt{\frac{b\cdot h}{B\cdot H}}\right)^{2,50}} \xrightarrow{\frac{b\cdot h}{B\cdot H}=\frac{0,90\cdot 1,80}{2,70\cdot 3,50}} \frac{G_{WALL}}{G} = 0,52 \tag{3.19}$$

The results of equation (3.19) is convenient to use to correct the model material of 1D models and 2D models that do not include openings in the analysis otherwise. In other words: the structure can be modeled through correction with the shear modulus reduction factor without shaping openings with elements.

3.6.4 Dimensional limitations

Besides the limitation on dimensions of structural components due to fabrication, the materials are limited through transport limitations and erection under wind conditions.

3.6.4.1 Transportation limitations

Road transport in the Netherlands is a decisive factor on the dimensional limitation for transportation in general, i.e. oppose to transport over water. The legal limitations for motor vehicles is 4,00 m high 18,75 m long and 2,55 m wide. Cargo space dimensions of a large trailer are 13,60 m long, 2,55 m wide and 3,00 m high. These limitations influence the choice of dimensions.

3.6.4.2 Erection under wind conditions

The lift capacity under wind conditions can influence the choice of the dimensions of single elements. This can apply to linear elements like columns and beams but especially to plate elements.

Timber elements are relatively light weight when compared to precast concrete elements. From experience with formwork for concrete, which are slightly lighter then structural timber elements, controlling the load can sometimes cause trouble. Hoisting and lifting of with cranes is controlled by the use of tables, which states that at winds of 6 Beaufort magnitude or higher all crane activities should stop, which is approximately at wind speeds of 10.8 m/s. Controlling the hoist load is usually done by two crew members who each can exercise a force of 300 N horizontally. Based on Bernoulli equations, this leads to the following calculation for the maximum area of the object under wind load.

$$\left.\begin{aligned} F &= S \cdot v \\ S &= \rho_{air} \cdot Q \\ Q &= A \cdot v \end{aligned}\right\} \quad F = \rho_{air} \cdot A \cdot v^2$$

$$\rightarrow$$

$$A = \frac{F}{\rho_{air} \cdot v^2}$$

In which:

F = stabilizing force	N
S = mass flow	kg/ s
Q = flow	m^3/ s
ρ = density (air)	kg/ m^3
A = plate area	m
v = wind speed	m/ s

The statistical data of de Royal Dutch Meteorological Institute (KNMI) gives average annual wind speeds of 4,9 m/s and 5,1 m/s from stations Rotterdam and Schiphol (Amsterdam) with a standard deviation of 0,9 and 0,8 respectively. This leads to assume an expected value of 5,0 m/s with 0,85 standard deviation for the case study. Therefore the 95-percentile of the wind speed, based on a normal t-distribution, is calculated to be 6,5 m/s.

However, the data is based on 24 hour measurements seven days a week, while one workweek only lasts 40 hours on average, which means that only 23,8% of the time construction takes place. This assumption leads to a wind speed of 4,4 m/s. Based on the assumption that only 60 % of one workweek (3/5) is used for lifting elements into place as with the Murray Grove tower project, the wind speed can even be reduced to 4,0 m/s on which a reasonable dimension of elements can be chosen.

The density of air (ρ_{air}) is 1,293 kg/m^3 where the wind speed (v) is smaller than 4.0 m/s for most of the time. The wind loaded area can be reduced to the net area through multiplication of a factor that incorporates the opening of windows, which is assumed to be at least 15% in case of plate elements. Based on these parameters the calculation of the area and the width results in the following.

Plate elements: $$A \leq \frac{1}{(1-R_w)} \frac{F}{\rho_{air} \cdot v^2} = \frac{1}{(1-0{,}15)} \frac{600}{1{,}293 \cdot 4^2} = 34{,}1 \cdot \left[m^2\right]$$

Other elements: $$A \leq \frac{F}{\rho_{air} \cdot v^2} = \frac{600}{1{,}293 \cdot 4^2} = 29{,}0 \cdot \left[m^2\right]$$

3.7 Sections D70-LAM

The first second and last variant are lattice frame structures and consist of D70-LAM. The cross sections of members for these frames range from 100 mm to 1500 mm. The necessary properties of these sections are calculated with 50 mm interval steps size in order to create a selection list for optimization purposes. The properties of these sections are calculated with equations (3.20) and (3.21) and shown in table 3.3.

$$I_z = \frac{1}{12} \cdot b \cdot h^3 \tag{3.20}$$

$$A = b \cdot h \tag{3.21}$$

b	h	A [mm²]	EA [N]	EI [Nmm²]	b	h	A [mm²]	EA [N]	EI [Nmm²]
100	100	10000	$2{,}00 \cdot 10^{8}$	$1{,}67 \cdot 10^{11}$	1050	1050	1102500	$2{,}21 \cdot 10^{10}$	$2{,}03 \cdot 10^{15}$
150	150	22500	$4{,}50 \cdot 10^{8}$	$8{,}44 \cdot 10^{11}$	1100	1100	1210000	$2{,}42 \cdot 10^{10}$	$2{,}44 \cdot 10^{15}$
200	200	40000	$8{,}00 \cdot 10^{8}$	$2{,}67 \cdot 10^{12}$	1150	1150	1322500	$2{,}65 \cdot 10^{10}$	$2{,}92 \cdot 10^{15}$
250	250	62500	$1{,}25 \cdot 10^{9}$	$6{,}51 \cdot 10^{12}$	1200	1200	1440000	$2{,}88 \cdot 10^{10}$	$3{,}46 \cdot 10^{15}$
300	300	90000	$1{,}80 \cdot 10^{9}$	$1{,}35 \cdot 10^{13}$	1250	1250	1562500	$3{,}13 \cdot 10^{10}$	$4{,}07 \cdot 10^{15}$
350	350	122500	$2{,}45 \cdot 10^{9}$	$2{,}50 \cdot 10^{13}$	1300	1300	1690000	$3{,}38 \cdot 10^{10}$	$4{,}76 \cdot 10^{15}$
400	400	160000	$3{,}20 \cdot 10^{9}$	$4{,}27 \cdot 10^{13}$	1350	1350	1822500	$3{,}65 \cdot 10^{10}$	$5{,}54 \cdot 10^{15}$
450	450	202500	$4{,}05 \cdot 10^{9}$	$6{,}83 \cdot 10^{13}$	1400	1400	1960000	$3{,}92 \cdot 10^{10}$	$6{,}40 \cdot 10^{15}$
500	500	250000	$5{,}00 \cdot 10^{9}$	$1{,}04 \cdot 10^{14}$	1450	1450	2102500	$4{,}21 \cdot 10^{10}$	$7{,}37 \cdot 10^{15}$
550	550	302500	$6{,}05 \cdot 10^{9}$	$1{,}53 \cdot 10^{14}$	1500	1500	2250000	$4{,}50 \cdot 10^{10}$	$8{,}44 \cdot 10^{15}$
600	600	360000	$7{,}20 \cdot 10^{9}$	$2{,}16 \cdot 10^{14}$	1350	1350	1822500	$3{,}65 \cdot 10^{10}$	$5{,}54 \cdot 10^{15}$
650	650	422500	$8{,}45 \cdot 10^{9}$	$2{,}98 \cdot 10^{14}$	1400	1400	1960000	$3{,}92 \cdot 10^{10}$	$6{,}40 \cdot 10^{15}$
700	700	490000	$9{,}80 \cdot 10^{9}$	$4{,}00 \cdot 10^{14}$	1450	1450	2102500	$4{,}21 \cdot 10^{10}$	$7{,}37 \cdot 10^{15}$
750	750	562500	$1{,}13 \cdot 10^{10}$	$5{,}27 \cdot 10^{14}$	1500	1500	2250000	$4{,}50 \cdot 10^{10}$	$8{,}44 \cdot 10^{15}$
800	800	640000	$1{,}28 \cdot 10^{10}$	$6{,}83 \cdot 10^{14}$					
850	850	722500	$1{,}45 \cdot 10^{10}$	$8{,}70 \cdot 10^{14}$					
900	900	810000	$1{,}62 \cdot 10^{10}$	$1{,}09 \cdot 10^{15}$					
950	950	902500	$1{,}81 \cdot 10^{10}$	$1{,}36 \cdot 10^{15}$					
1000	1000	1000000	$2{,}00 \cdot 10^{10}$	$1{,}67 \cdot 10^{15}$					

table 3.3: Section Properties Lattice Structures

3.8 Sections D70-CLT

The length and the thickness of D70-CLT sections influences the effective bending stiffness. There are two different (span/buckling) lengths and four different thicknesses applied in the case study. Therefore, eight different sections properties are determined below.

3.8.1 Bending and Buckling Reduction

There are several ways to calculate the bending behavior of cross laminated timber (CLT). Because the layers of CLT are placed perpendicular to each other, the shear deformation of layers that are perpendicular to the span direction may not be neglected. The so called rolling shear stiffness (modules) is believed to be between 50 N/mm^2 and 200 N/mm^2 or 10% of the in-plane shear for soft wood [25].

Dependant on the slenderness of the element in bending, different methods for calculation of CLT can be used. For a slenderness (L/h) larger than 30 the shear deformation can be neglected, for which the plate build-up factor [22] can be used. Research at the TU Graz [26] have shown that for a plate slenderness larger then 10, the Kreuzinger beam model [27] is appropriate, which will be used here.

Kreuzinger beam

The Kreuzinger beam model is a combination of two beams that take different properties of the total beam into account. The stiffness of the first beam, named beam A, takes into account the own bending stiffness of the layers with infinite shear stiffness (equation (3.22)), which is logical because no relevant shear deformation takes place within the individual layers.

$$(EI)_A = \sum_{i=1}^{n} E_i \cdot I_i \tag{3.22}$$

Beam B, the second beam, takes into account the Steiner part of the layers with finite shear stiffness as in equation (3.23). Because the layers act in series the reciprocal sum of the shear stiffness of individual layers is equal to the total shear stiffness. The first term of the first summation between parentheses on the right hand side in equation (3.24) deals with the slip deformation between layers when these are not rigidly connected i.e. not glued but nailed or otherwise flexible connected. For cross laminated timber, which is usually glued, this term is equal to zero.

$$(EI)_B = \sum_{i=1}^{n} E_i \cdot A_i \cdot z_i^2 \tag{3.23}$$

$$\frac{1}{(GA)_B} = \frac{1}{S} = \frac{1}{a^2} \cdot \left(\sum_{i=1}^{n-1} \frac{1}{c_i} + \frac{d_1}{2 \cdot G_1 \cdot b_1} + \sum_{i=2}^{n-1} \frac{d_i}{G_i \cdot b_i} + \frac{d_n}{2 \cdot G_n \cdot b_n} \right) \tag{3.24}$$

The deflection of the two beams is coupled in a framework model, the loads and boundary conditions are set and the calculation is executed. The moments and forces of the beams A and B can now be proportionally distributed back down towards their individual parts. More explanation is given in ref. [28].

Beam section properties

The equations (3.22) to (3.24) are used to calculate the beam section properties with a programmed procedure with maple shown in appendix B.2. Assumptions to simplify calculations have been made on the thicknesses of individual board layers, which all are 43 mm.

The beam section properties are calculated for a three, five, seven and nine layer thick element. This resulted in the section properties given in table 3.4. The input for finite element model beam are calculated through dividing the section properties by the appropriate stiffness modules used in the final element software. The shear stiffness or effective shear area for beam A is infinite.

t =43mm	BEAM A		BEAM B			
Layers	**EI**	**(Input) I**	**EI**	**(Input) I**	**GA_S**	**(Input) A_S**
	[Nmm^2]	[mm^4]	[Nmm^2]	[mm^4]	[N]	[mm^2]
9	$6{,}89 \cdot 10^{11}$	$3{,}45 \cdot 10^7$	$6{,}57 \cdot 10^{13}$	$3{,}29 \cdot 10^9$	$1{,}56 \cdot 10^8$	125093
7	$5{,}56 \cdot 10^{11}$	$2{,}73 \cdot 10^7$	$3{,}27 \cdot 10^{13}$	$1{,}63 \cdot 10^9$	$1{,}17 \cdot 10^8$	94307
5	$4{,}15 \cdot 10^{11}$	$2{,}08 \cdot 10^7$	$1{,}29 \cdot 10^{13}$	$6{,}47 \cdot 10^8$	$7{,}82 \cdot 10^7$	62547
3	$2{,}74 \cdot 10^{11}$	$1{,}37 \cdot 10^7$	$3{,}18 \cdot 10^{12}$	$1{,}59 \cdot 10^8$	$3{,}91 \cdot 10^7$	31387

table 3.4: Section Properties for Beam Model Input into Framework Software

Finite element modeling

Eight beam structures where created in GSA Oasys software. Each structure consists of two parallel beams, each beam has 11 intermediate nodes spaced at $1/10^{th}$ of the span and supported at the end, as depicted in figure 3.10. The beams where loaded with vertical forces at the nodes which are equivalent to the appropriate distributed load. The values calculated for the separate beams (A and B) of table 3.4 are assigned to the model elements. This is only possible with software that is capable of incorporating shear deformation, which is the case (GSA Oasys). Because the deflection of the beams must be coupled, the beams are kinetically connected at intermediate nodes with pinned link elements, as shown in figure 3.10. Described in the program fundamentals, the software takes into account shear deformation if the shear factors (K_y, K_z) are not set to zero, which are assigned accordingly.

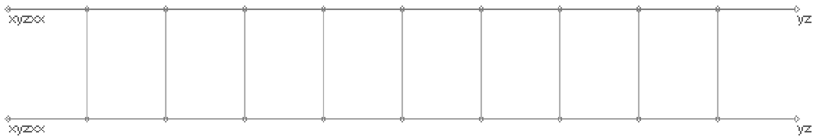

figure 3.10: Picture of the Kreuzinger Beam Framework Model

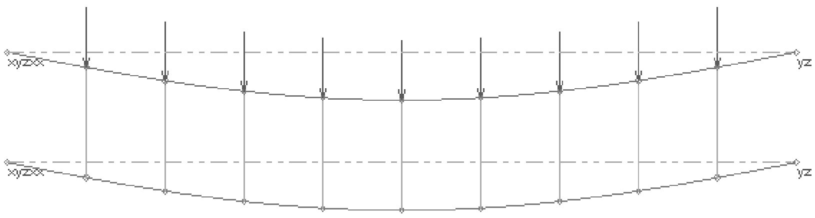

figure 3.11: Deflection under Loading of the Framework Model

Effective bending stiffness

The effective bending stiffness, oppose to the virtual shear-stiff bending stiffness, was calculated back from the deflection of the coupled beam model with equation (3.25) which is based on classical mechanics.

$$EI_{eff,i} = \frac{5}{384} \cdot \frac{q \cdot l^4}{w_i} \quad \textbf{(3.25)}$$

The results are displayed in table 3.5. In the last column of the table the ratio is given between the effective bending stiffness and the sum of the bending stiffness without shear reduction.

Length:	**3500 mm**			**7200 mm**		
Number of Layers	**w**	**EI_{eff}**	**EI_{eff}/EI**	**w**	**EI_{eff}**	**EI_{eff}/EI**
	[mm]	[Nmm2]	[-]	[mm]	[Nmm2]	[-]
9	0,37	$5{,}253 \cdot 10^{13}$	79%	5,63	$6{,}219 \cdot 10^{13}$	94%
7	0,71	$2{,}753 \cdot 10^{13}$	83%	11,00	$3{,}181 \cdot 10^{13}$	96%
5	1,63	$1{,}20 \cdot 10^{13}$	90%	26,77	$1{,}31 \cdot 10^{13}$	98%
3	5,94	$3{,}29 \cdot 10^{12}$	95%	101,90	$3{,}43 \cdot 10^{12}$	99%

table 3.5: Effective Bending Stiffness Properties of D70-CLT sections

Ironically, the reduction of the bending stiffness decreases with the slenderness of an element, while in conflict with the buckling reduction factor and the deflection of the beam. This implies that increasing the elements thickness, in case of buckling and deflection, does not reduce stiffness associated problems linearly as compared to homogenous and parallel laminated sections. The reduction must be evaluated case by case, because the slenderness is a dominant factor.

3.9 Buckling Resistance

3.9.1 General Calculation Procedure

The calculation of the buckling resistance is done with the equations stated in 1995-1-1, section 6.3. Bending stresses of members under compression are neglectable, as will be shown in the results of model calculations later in this thesis, and are therefore not included in the calculation. The general calculation is given in equation (3.26) to (3.31).

$$F_{buc} = f_{c,0,d} \cdot k_{c,z} \cdot A \tag{3.26}$$

$$k_{c,z} = \frac{1}{k_z + \sqrt{k_z^{\,2} - \lambda_{rel,z}^{\,2}}} \tag{3.27}$$

$$k_z = 0,5 \cdot \left(1 + \beta\left(\lambda_{rel,z} - 0,3\right) + \lambda_{rel,z}^{\,2}\right) \tag{3.28}$$

$$\lambda_{rel,z} = \frac{\lambda_z}{\pi} \cdot \sqrt{\frac{f_{c,0,k}}{E_{0,05}}} \tag{3.29}$$

$$\lambda_z = \frac{l_{buc}}{i_z} \tag{3.30}$$

$$i_z = \sqrt{\frac{EI_z}{EA_z}} \tag{3.31}$$

3.9.2 Material Factors

The relevant material properties for the calculation are given below. The design value of the compression strength is calculated with equation (3.32).

β_c=	0,1	[-]
k_{mod}=	0,70	[-]
y_M=	1,25	[-]
$f_{c,o,d}$=	19,0	[N/mm2]

$$f_{c,0,d} = \frac{f_{c,0,k}}{\gamma_M} \cdot k_{\text{mod}} \tag{3.32}$$

3.9.3 Buckling of plates

The calculation of the buckling resistance of a cross laminated timber plate is, according to ref.[22], no different from a timber column except for the effective bending stiffness. The calculation of the effective bending stiffness was set out in paragraph 3.8.1. The buckling calculations are made with the bending stiffness reduction derived from the Kreuzinger beam model for plates which span the buckling length of 3500 mm, i.e. the floor-to-floor height.

The buckling resistance is calculated by universal buckling equations stated in the EN 1995-1-1 as suggested in ref. [22]. The cross section area is reduced to layers acting parallel to the grain. In table 3.14 the results of the buckling calculation are given for a plate strip of one meter wide.

3.9.4 Sections Variant 1: Diagrid

The cross section dimensions of all elements in the Diagrid structure range from 300 mm to 700 mm. The maximum buckling length (l_{buc}) for members under compression is 7871 mm.

Members, 300 mm- 700 mm, l_{buc}=7871 mm

b	h	i_z [mm]	λ_z [-]	λ_{relz} [-]	k_z [-]	k_{zc} [-]	δ_{buc} [N/mm2]	F_{buc} [kN]
300	300	87	90,89	1,30	1,40	0,52	10	900
350	350	101	77,91	1,12	1,16	0,67	13	1563
400	400	115	68,17	0,98	1,01	0,79	15	2398
450	450	130	60,59	0,87	0,90	0,86	16	3320
500	500	144	54,54	0,78	0,83	0,90	17	4300
550	550	159	49,58	0,71	0,77	0,93	18	5348
600	600	173	45,45	0,65	0,73	0,94	18	6476
650	650	188	41,95	0,60	0,70	0,96	18	7691
700	700	202	38,95	0,56	0,67	0,96	18	8998

table 3.6: Buckling Resistance Member Sections Variant 1

3.9.5 Sections Variant 2: Braced Frame

The cross section dimensions of the Braced Frame range from 300 mm to 800 mm. The buckling length of columns is 7000 mm and respectively 5021 mm for braces which are assumed to be supported laterally at half span by the floor.

Columns, 300 mm - 800 mm, l_{buc}=7000 mm

b	h	i_z [mm]	λ_z [-]	λ_{relz} [-]	k_z [-]	k_{zc} [-]	δ_{buc} [N/mm2]	F_{buc} [kN]
300	300	87	80,83	1,16	1,21	0,64	12	1088
350	350	101	69,28	0,99	1,03	0,77	15	1806
400	400	115	60,62	0,87	0,91	0,86	16	2622
450	450	130	53,89	0,77	0,82	0,91	17	3497
500	500	144	48,50	0,69	0,76	0,93	18	4441
550	550	159	44,09	0,63	0,72	0,95	18	5468
600	600	173	40,41	0,58	0,68	0,96	18	6584
650	650	188	37,31	0,53	0,65	0,97	18	7792
700	700	202	34,64	0,50	0,63	0,97	19	9095
750	750	217	32,33	0,46	0,62	0,98	19	10494
800	800	231	30,31	0,43	0,60	0,98	19	11988

table 3.7: Buckling Resistance Column Sections Variant 2

Braces, 300 mm - 600 mm, l_{buc}=5021 mm

b	h	i_z [mm]	λ_z [-]	λ_{relz} [-]	k_z [-]	k_{zc} [-]	δ_{buc} [N/mm2]	F_{buc} [kN]
300	300	87	57,98	0,83	0,87	0,88	17	1510
350	350	101	49,69	0,71	0,77	0,93	18	2164
400	400	115	43,48	0,62	0,71	0,95	18	2898
450	450	130	38,65	0,55	0,67	0,97	18	3722
500	500	144	34,79	0,50	0,63	0,97	19	4639
550	550	159	31,62	0,45	0,61	0,98	19	5651
600	600	173	28,99	0,42	0,59	0,99	19	6761

table 3.8: Buckling Resistance Brace Sections Variant 2

3.9.6 Sections Variant 4: Mega Frame

The cross section dimensions of the Mega Frame range from 1000 mm to 1350 mm. The buckling length of columns is 28000 mm and respectively 20084 mm for braces which are assumed to be supported laterally at half span by the building core through the floor.

Mega-Columns, 1000 mm - 1350 mm, l_{buc}=28000 mm

b	h	i_z	λ_z	λ_{relz}	k_z	k_{zc}	δ_{buc}	F_{buc}
		[mm]	[-]	[-]	[-]	[-]	[N/mm2]	[kN]
1000	1000	289	96,99	1,39	1,52	0,47	9	8922
1050	1050	303	92,38	1,32	1,43	0,51	10	10717
1100	1100	318	88,18	1,26	1,35	0,55	11	12732
1150	1150	332	84,34	1,21	1,27	0,59	11	14966
1200	1200	346	80,83	1,16	1,21	0,64	12	17412
1250	1250	361	77,60	1,11	1,16	0,67	13	20054
1300	1300	375	74,61	1,07	1,11	0,71	14	22868
1350	1350	390	71,85	1,03	1,07	0,74	14	25827

table 3.9: Buckling Resistance Column Sections Variant 4

Mega-Braces, 650 mm - 800 mm, l_{buc}=20084 mm

b	h	i_z	λ_z	λ_{relz}	k_z	k_{zc}	δ_{buc}	F_{buc}
		[mm]	[-]	[-]	[-]	[-]	[N/mm2]	[kN]
650	650	188	107,03	1,53	1,74	0,39	7	3152
700	700	202	99,39	1,42	1,57	0,45	9	4185
750	750	217	92,76	1,33	1,43	0,51	10	5428
800	800	231	86,97	1,25	1,32	0,57	11	6891

table 3.10: Buckling Resistance Brace Sections Variant 4

The beams of the mega frame trusses are orientated in-line with the adjacent floor, which justifies the assumption that these beams are unable to buckle. Other elements of the mega-trusses are columns and braces of which the buckling lengths are respectively 3500 mm and 5021 mm.

Columns of Mega-Truss, 100 mm - 200 mm, l_{buc}=3500 mm

b	h	i_z	λ_z	λ_{relz}	k_z	k_{zc}	δ_{buc}	F_{buc}
		[mm]	[-]	[-]	[-]	[-]	[N/mm2]	[kN]
100	100	29	121,24	1,74	2,08	0,31	6	59
150	150	43	80,83	1,16	1,21	0,64	12	272
200	200	58	60,62	0,87	0,91	0,86	16	656

table 3.11: Buckling Resistance Column Sections of Truss Variant 4

Braces of Mega-Truss, 300 mm - 550 mm, l_{buc}=5021 mm

b	h	i_z	λ_z	λ_{relz}	k_z	k_{zc}	δ_{buc}	F_{buc}
		[mm]	[-]	[-]	[-]	[-]	[N/mm2]	[kN]
300	300	87	57,98	0,83	0,87	0,88	17	1510
350	350	101	49,69	0,71	0,77	0,93	18	2164
400	400	115	43,48	0,62	0,71	0,95	18	2898
450	450	130	38,65	0,55	0,67	0,97	18	3722
500	500	144	34,79	0,50	0,63	0,97	19	4639
550	550	159	31,62	0,45	0,61	0,98	19	5651

table 3.12: Buckling Resistance Brace Sections of Truss Variant 4

The gravity frame on the secondary grid of the mega frame consists of columns and beams. The columns are assumed pined connected between floors and their buckling length is therefore 3500 mm.

Columns of gravity frame, 100 mm - 400 mm, l_{buc}=3500 mm

b	h	i_z	λ_z	λ_{relz}	k_z	k_{zc}	δ_{buc}	F_{buc}
		[mm]	[-]	[-]	[-]	[-]	[N/mm2]	[kN]
100	100	29	121,24	1,74	2,08	0,31	6	59
150	150	43	80,83	1,16	1,21	0,64	12	272
200	200	58	60,62	0,87	0,91	0,86	16	656
250	250	72	48,50	0,69	0,76	0,93	18	1110
300	300	87	40,41	0,58	0,68	0,96	18	1646
400	400	115	30,31	0,43	0,60	0,98	19	2997

table 3.13:

3.9.7 Sections Variant 3: Solid Shear Wall

The thickness dimensions of wall sections of the solid shear wall variant range from 129 mm to 387 mm respectively 3 to 9 layers. The buckling length of walls is 3500 mm based on the vertical floor spacing.

Wall plates, 3 to 9 layers CLT, b=1000 mm, l_{buc}=3500 mm

n	Σt	i_z	λ_z	λ_{relz}	k_z	k_{zc}	δ_{buc}	F_{buc}
	[mm]	[mm]	[-]	[-]	[-]	[-]	[N/mm2]	[kN]
3	129	44	80,04	1,15652	1,2116	0,636	12,106	1041
5	215	68	51,41	0,74284	0,7980	0,918	17,472	2254
7	301	89	39,13	0,56534	0,6731	0,963	18,337	3154
9	387	111	31,67	0,45758	0,6126	0,981	18,670	4014

table 3.14: Buckling Resistance Wall Sections of Variant 3

Based on these results the dimensions of the elements used in the solid façade variant of the case study design are chosen.

3.10 BSB Joint Properties

The BSB joints apply to the first and second variant. The properties of this type of joint are parameters assigned to the calculation models.

3.10.1 BSB Nodes Geometry

For lattice framework structures as the case study variants 1 and 2, members are jointed at central nodes. Here two possible solutions are presented, compared and evaluated for feasibility.

Proposed solutions
The concept of the proposed solutions are shown in figure 3.12 for the first variant. Similar concepts could be drawn up for the second variant. The first central node solution consist of welded steel plates in a hexagonal shape as shown on the left side in figure 3.12 with central steel plates and edge plates similar to the node design of the reference project "E3 Berlin". The second central node solution is shown on the right side of figure 3.12 and is made of laminated timber in multiple directions.

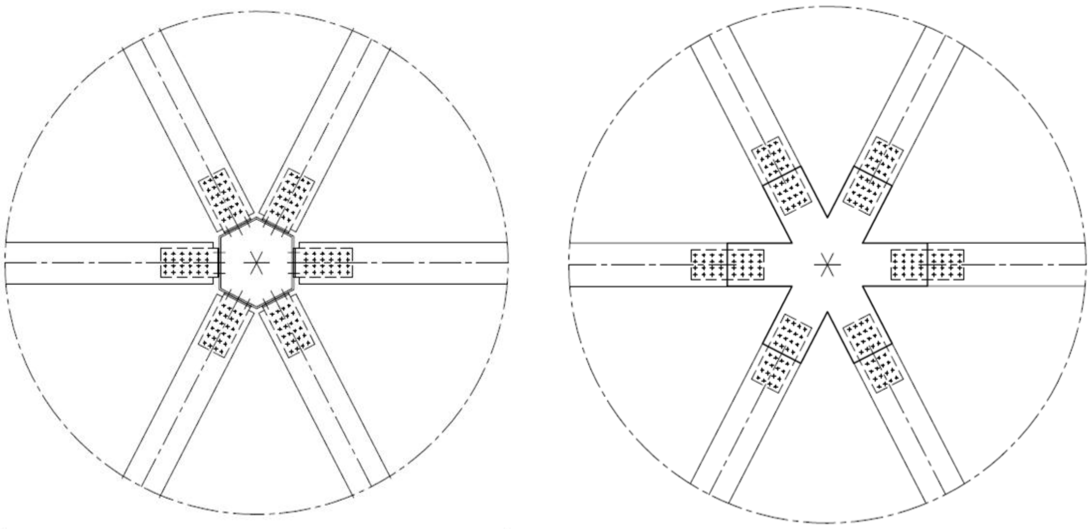

figure 3.12: Node Solution Concepts

Strength
The strength of the steel node is relatively unlimited in terms of available space because steel S355 has relatively high yield strength when compared to timber. The only concern with steel nodes is the local out of plane buckling of central plates, which can be avoided through use of local plate stiffeners if necessary.

The other solution, the laminated timber or laminated veneer joint is less strong in terms of available space. This is because the grain orientation of laminated layers has to be divided over three directions which implies that the effective cross section is close to 33% of the gross area. This has implications when connected to members of which the dimensions are chosen based on the buckling stress with low relative slenderness, hence a k_c reduction factor close to 1,00 which is the case. Solutions for this problem are either increasing the strength or the cross-section by three, while the first is impossible because all members are of strength class D70 the second gives a very heavy cubbish unattractive appearance.

Stiffness
The steel node is relatively stiff in comparison to the adjacent members and joint interface, also because the node is small by comparison. A steel timber interface also appears only once per jointed member, which makes the node four times stiffer when a force passes through to the opposite side when compared to the laminated node. Furthermore the laminated node suffers from additional stiffness problems that are similar to the strength related complications.

Fire resistance
The timber laminated node has better fire resistance properties then the steel node because all steel plates are embedded in a sufficiently thick layer of timber, which is not the case for an exposed central steel node. If the steel node is small enough in the thickness direction, this problem could be solved by encapsulating the node with a timber layer of sufficient thickness to improve the fire resistance.

Aesthetics
The appearance of the steel node is quite industrial while the laminated node is more natural and continuous. While the second is probably more attractive to some, the industrial appearance could be an architectural choice. The same appearance for the steel node could be achieved by covering the node with a timber layer which was mentioned earlier to improve the fire resistance.

Economics
The number and complexity of actions that has to be taken to manufacture these nodes is analyzed to make an estimation of the cost of production. For steel nodes at least six edge plates and three center plates have to be cut and welded together to create the central node. Furthermore, BSB joints have to be provided with edge plates which include further cutting and welding. Holes have to be created for bolting the steel node and the steel timber (BSB) joint together. These actions do not have to be executed for the laminated timber node.

For the steel node all fasteners of the steel-to-timber joints are applied in workshop conditions, while the laminated timber node only one half of the interface is finished. The prefabricated steel node can therefore be assembled relatively fast by fitting bolts on-site in a steel-to-steel connection, similar to steel frames, while during the on-site assembly of the laminated timber node a larger number of fasteners has to be fitted in a timber to steel connection, which also has stiffness complications when dowels are used.

Summary
Because most issues for the steel node, like fire resistance and aesthetics can be tackled, the steel node is preferable. While the manufacturing of this node is still more expensive then the laminated timber node, the erection cost on site are believed to compensate for the additional in-shop activities.

3.10.2 BSB Joint Stiffness

The joints between linear elements, i.e. columns, beams and braces, will be realized with steel-timber (BSB) joints. The stiffness of the joint is dependent on two dominant variables, namely the density of the wood, and the fastener diameter. However, when the diameter of fastener increases the spacing between dowels and the end distances increase also, resulting in a decreasing number of dowels per area.

To design an optimum joint, the relation between the fastener diameter and its stiffness is studied. The investigated principle of the joint is relevant to the case study, and is represented by an end connection of a linear element to a node.

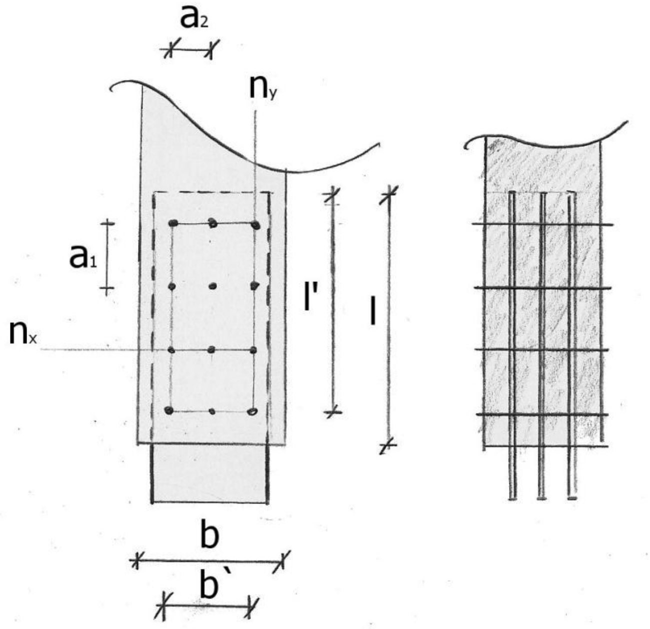

figure 3.13: Joint geometry linear elements

Based on the geometry shown in figure 3.13 the assumptions for the fastener stiffness can be formulated for one shear plane. The stiffness of the joint per shear plane is calculated through multiplication of the number of fasteners and the fastener stiffness as shown in equation (3.33). The fastener stiffness of a single dowel is given in equation (3.34) where the factor 2 takes into account the steel-timber configuration. The number of fasteners is determined by the dimensions of the joint and the spacing between the fasteners and are derived in equation (3.35) to (3.36). Through substitution of equations (3.33) to (3.36) the relation between the joint stiffness and the other parameters is created, shown in equation (3.37)

$$K_j = K_{ser} \cdot n_x \cdot n_y \tag{3.33}$$

$$K_{ser} = 2 \cdot \frac{1}{20} \cdot \rho_k^{1.5} \cdot d \tag{3.34}$$

$$n_x = \frac{l`}{a_1} \qquad l` = l - a_3 \tag{3.35}$$

$$n_y = \frac{b`}{a_2} \qquad b` = b - 2 \cdot a_4 \tag{3.36}$$

$$K_j = \frac{\rho_k^{1.5} \cdot d \cdot (l - a_3) \cdot (b - 2 \cdot a_4)}{20 \cdot a_1 \cdot a_2} \quad \textbf{(3.37)}$$

The values of a_i, *i={1..4}* are based on the Eurocode, (EC 5-1 1995) and are chosen most conservative. For this comparison the wood-fastener interface is assumed to be reinforced with densified veneer wood (DVW) with a density of 1300 kg/m^3 all shear planes. The assumed values for a indicative calculation are:

a_1 = 7·d
a_2 = 3·d
a_3 = 3·d
a_4 = 4·d
ρ= 1300 kg/m^3
b = 500 mm
l = 750 mm

For these values equation (3.10) results in a relation between the joint stiffness and the diameter of the dowel, which is plotted in the graph shown in figure 3.14. What immediately becomes clear form the graph in this figure is the descending stiffness with increasing diameter of the dowels.

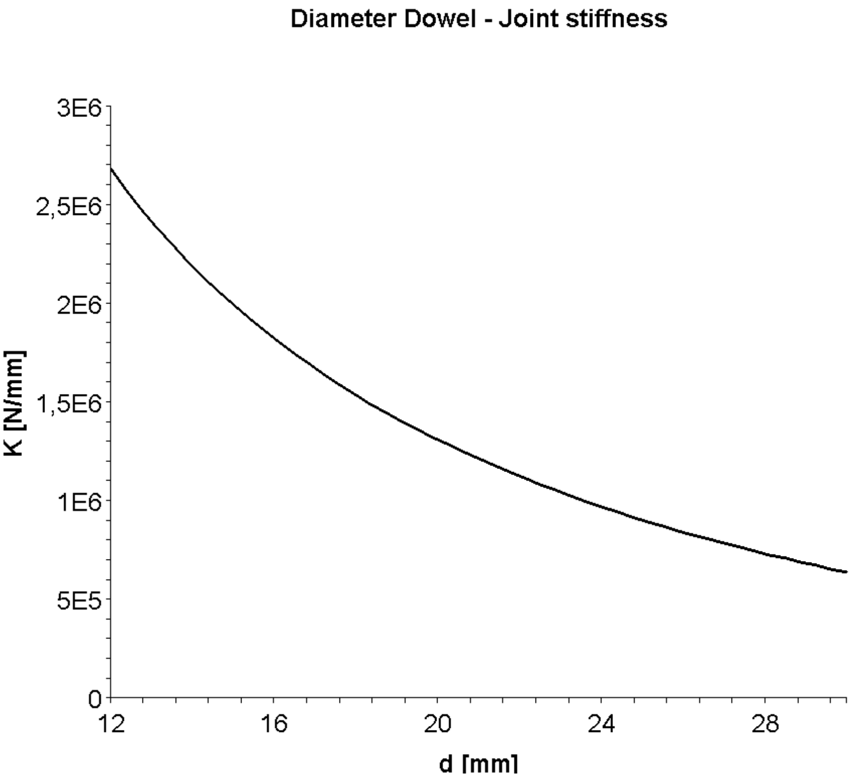

figure 3.14: Dowel diameter -Joint stiffness

For expended tube fasteners the relation between the diameter and the stiffness is derived from ref. [17]. From some discrete design values a linear least square regression can be made to enable the same calculation procedure as for dowels. In figure 3.15 the relation through regression between fastener stiffness and tube diameter and the design values is shown in one graph. The analytical relation between the equivalent stiffness and the diameter of the tube-fastener is shown in equation (3.38), which is assumed to be valid for a diameter between 20 and 36 mm (figure 3.15).

$$K_{tube\_eq} = 32187 + 969 \cdot d \quad \textbf{(3.38)}$$

As for the dowel, a similar relation of the total joint stiffness can be deduced, in which the edge distance and fastener spacing is defined as in NEN6770 TGB1990 resulting in $a_3 = a_4 = 3d$ and $a_1 = a_2 = 5d$, the other dimensions are preserved. The density of the wood is incorporated in the design data from tests in ref. [17], which was 1300 kg/m^3. The relation between the joint stiffness and the diameter of an expended tube is given in equation (3.39), where the factor 2 is due to the steel-timber joint layout. This relation is plotted in the graph of figure 3.16.

$$K_{j,tube} = 2 \cdot K_{tube\_eq} \cdot \frac{(l - a_3) \cdot (b - 2 \cdot a_4)}{a_1 \cdot a_2} \tag{3.39}$$

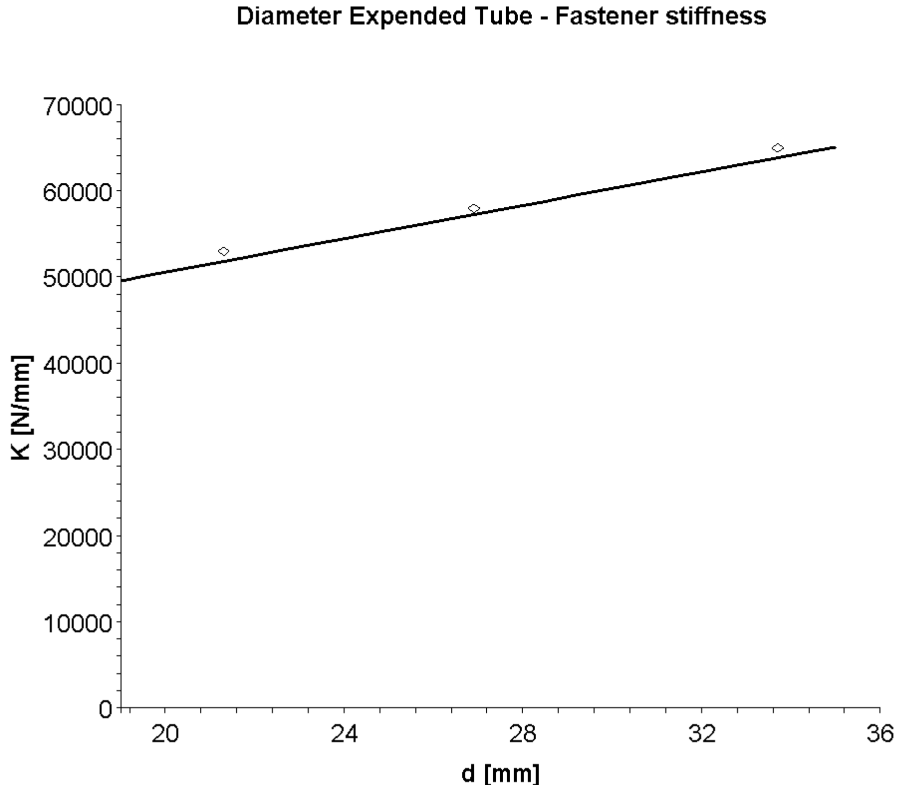

figure 3.15: Regression line of Tube-Fastener

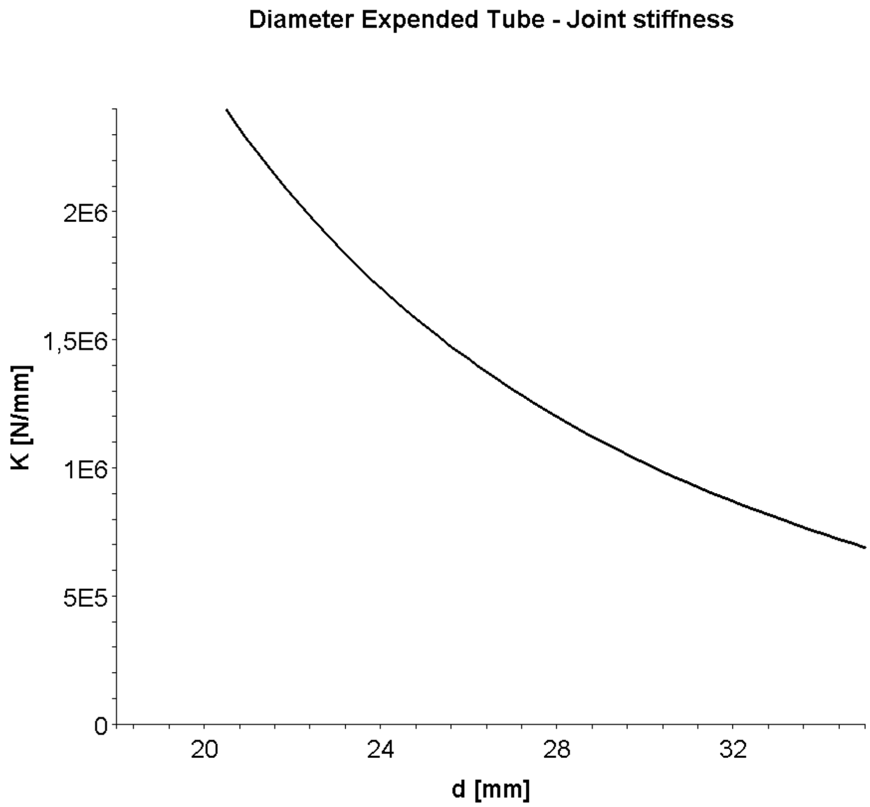

figure 3.16: Joint Stiffness Plotted against the Diameter of the Fastener

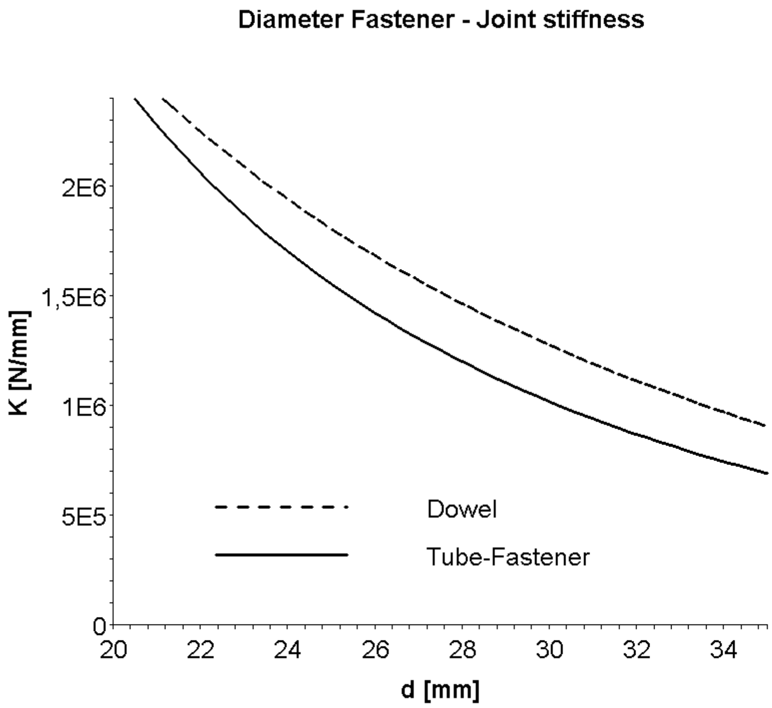

figure 3.17: Comparison of Joint Stiffness Fastener Types

When a comparison is made between the dowel and the expended-tube-fastener the difference in stiffness is becoming larger when the diameter increases (figure 3.17) in favor of the dowel. This is because a dowel itself is solid and therefore stiffer than tube-fasteners. The ratio between the stiffness of the dowel and the stiffness of the tube-fastener joint, given in figure 3.18, shows a clearer picture of the stiffness benefit of a dowel in relation to a tube fastener.

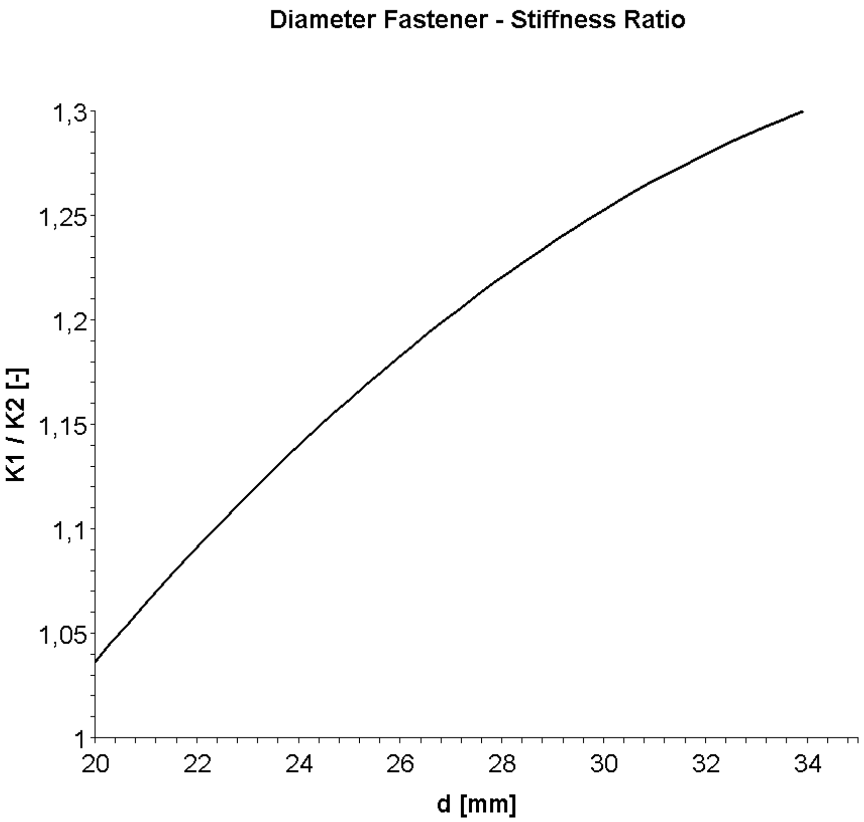

figure 3.18: Joint Stiffness Ratio between Dowel and Tube-Fastener

While the fastener stiffness for dowels increases with the diameter the number of fasteners decreases slightly when normalized to the tube-faster joint. The number of fasteners per joint can influence the economical choice between a smaller and a larger diameter, because it relates to the number of operations manufacturing a joint.

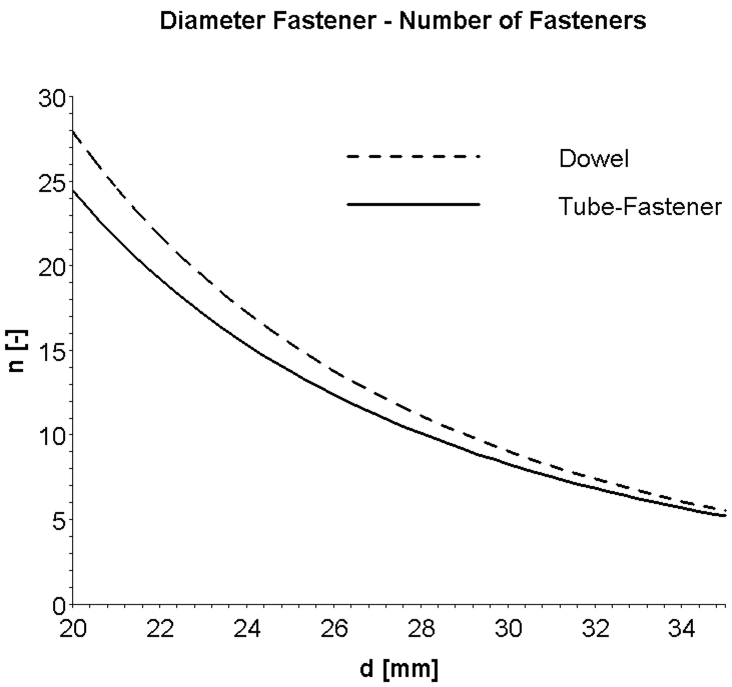

figure 3.19: Number of Fasteners Plotted against Diameter

Rotational stiffness
The rotational stiffness of the joint is of little importance for the case study, because elements are primarily loaded axial for all systems investigated. However, due to the joint geometry, rotational stiffness is present and will be calculated in order to take into account any accidental influence on the global behavior. The rotational joint stiffness is calculated with the equations by Kessel, 1991 [16].

Summary
From the above it has become clear that, in general, the joint stiffness decreases with the diameter of the fastener. The number of fasteners per shear plane also decreases with the diameter because of a hyperbolic relation between the diameter and the area available for the connection. The difference in stiffness between dowels and tube-fasteners, however indicative, is close to 30% for large fasteners.

This last observation is not decisive, because of other probable benefits to the tube-fastener. Furthermore, the assumed density of the material was chosen to be 1300 kg/m^3 for both fasteners, which could be problematic for the ductility of a doweled joint.

3.10.3 BSB Joint Strength

Joints suggested for variant 1 and 2 consists of steel-to-timber joints with multiple shear planes. The possible kinematical failure mechanisms for three slotted-in steel-plates, with six shear planes are shown in figure 3.20. The corresponding equations for the load bearing capacity of the total joint for the possible failure mechanisms are given below the figure. The normative material factors are not taken into account in these equations which is conservative and therefore justified for the objective of this thesis.

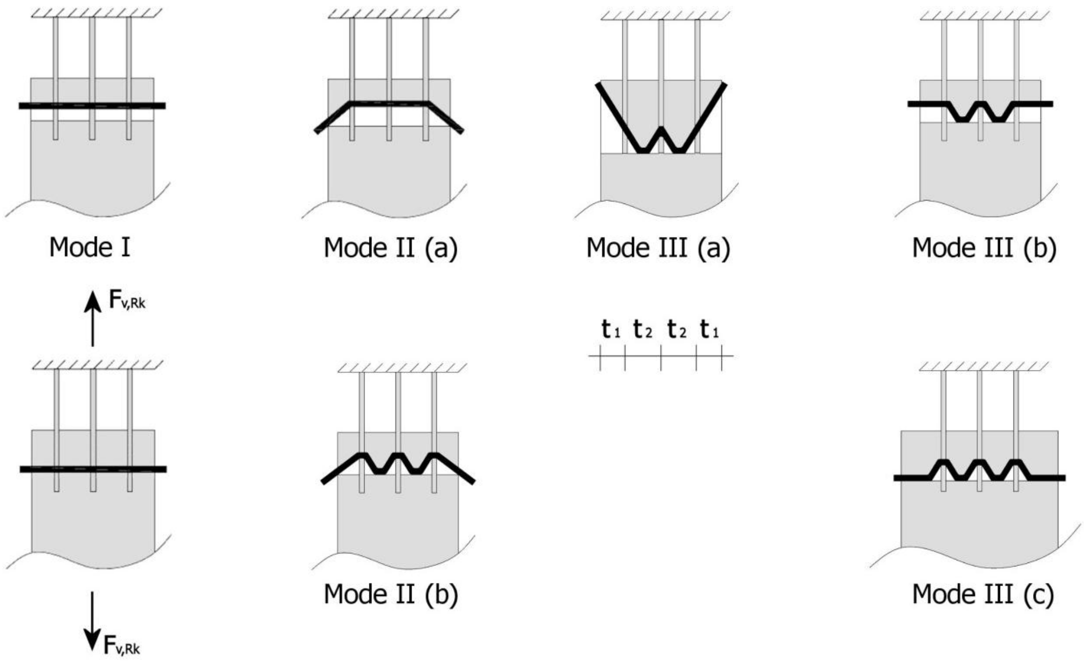

figure 3.20: Failure Mechanisms of Steel-Timber Joint

$$F_{v,Rk} = \min \begin{cases} 2 \cdot (t_1 + t_2) \cdot f_h \cdot d & I \\ 2 \cdot \left(t_2 + t_1 \cdot \left[\sqrt{2 + \dfrac{4 \cdot M_y}{f_h \cdot d \cdot t_1^2}} - 1 \right] \right) \cdot f_h \cdot d & II(a) \\ 4 \cdot \sqrt{4 \cdot M_y \cdot f_h \cdot d} + 2 \cdot t_1 \cdot f_h \cdot d \cdot \left[\sqrt{2 + \dfrac{4 \cdot M_y}{f_h \cdot d \cdot t_1^2}} - 1 \right] & II(b) \\ 2 \cdot t_1 \cdot f_h \cdot d + 2 \cdot \sqrt{2 \cdot M_y \cdot f_h \cdot d} + 1 \cdot \sqrt{4 \cdot M_y \cdot f_h \cdot d} & III(a) \\ 2 \cdot t_1 \cdot f_h \cdot d + 4 \cdot \sqrt{4 \cdot M_y \cdot f_h \cdot d} & III(b) \\ 6 \cdot \sqrt{4 \cdot M_y \cdot f_h \cdot d} & III(c) \end{cases}$$

The smallest value of these failure mechanisms is decisive.

The possible kinematic failure modes in the above can be reproduced by using the failure modes given in paragraph 8.2.3 of the Eurocode or applying the Johansen theory. Within the Eurocode the equations for the load-carrying capacity of modes are presented for the individual parts, as shown in figure 3.21 and are then considered for the force in the steel plate. For example, the load-carrying capacity of mode j/l according to EN 1995 is:

$$F_{v,Rk} = 0,5 \cdot f_{h,2,k} \cdot t_2 \cdot d$$

This is valid for one steel plate (shear plane) of the considered part, while the total of this part is twice this value in correspondence with the Johansson theory for kinematic failure mechanisms. Below a deduction is given for the failure modes I to III(c) that are shown in figure 3.20. The rope effect is not included in the calculation of modes which is conservative and therefore justified.

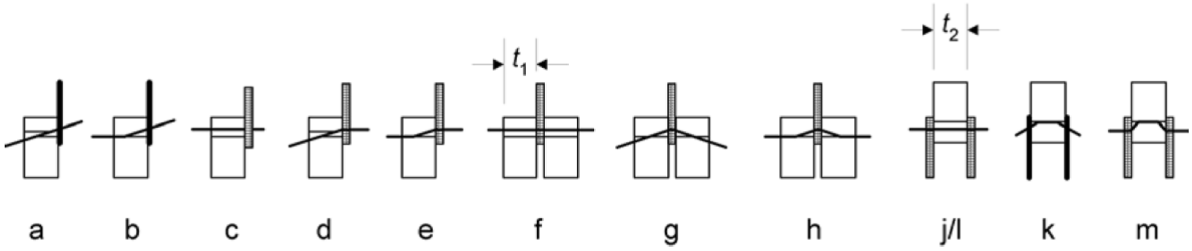

figure 3.21: Failure Mechanisms according to EN 1995-1-1: 2004

Mode I: This mode can be understood as two times Eurocode mode (c) for the edge wood parts, plus four times Eurocode mode (j/l) for the middle wood parts and is therefore equal to:

$$F_{v,Rk} = 2 \cdot \left[f_{h,k} \cdot t_1 \cdot d \right] + 2 \cdot 2 \cdot \left[0,5 \cdot f_{h,k} \cdot t_2 \cdot d \right]$$

Mode II(a): This mode can be understood as two times Eurocode mode (d) for the edge wood parts, plus four times Eurocode mode (j/l) for the middle wood parts and is therefore equal to:

$$F_{v,Rk} = 2 \cdot \left[f_{h,k} \cdot t_1 \cdot d \cdot \left[\sqrt{2 + \frac{4 \cdot M_y}{f_h \cdot d \cdot t_1^2}} - 1 \right] \right] + 2 \cdot 2 \cdot \left[0,5 \cdot f_{h,k} \cdot t_2 \cdot d \right]$$

Mode II(b): This mode can be understood as two times Eurocode mode (d) for the edge wood parts, plus four times Eurocode mode (k) for the middle wood parts and is therefore equal to:

$$F_{v,Rk} = 2 \cdot \left[f_{h,k} \cdot t_1 \cdot d \cdot \left[\sqrt{2 + \frac{4 \cdot M_y}{f_h \cdot d \cdot t_1^2}} - 1 \right] \right] + 2 \cdot 2 \cdot \left[\sqrt{4 \cdot M_y \cdot f_h \cdot d} \right]$$

Mode III(a): This mode can be understood as two times the embedment force over the total width of the edge wood parts, plus two times Eurocode mode (k) and once Eurocode mode (h) middle wood parts.

Mode III(b): This mode can be understood as two times Eurocode mode (c) for the edge wood parts, plus four times Eurocode mode (e) for the middle wood parts and is therefore equal to:

$$F_{v,Rk} = 2 \cdot \left[f_{h,k} \cdot t_1 \cdot d \right] + 2 \cdot 2 \cdot \left[\sqrt{4 \cdot M_y \cdot f_h \cdot d} \right]$$

Mode III(c): This mode can be understood as two times Eurocode mode (e) for the edge wood parts, plus four times Eurocode mode (m) for the middle wood parts.

$$F_{v,Rk} = 2 \cdot \left[\sqrt{4 \cdot M_y \cdot f_h \cdot d} \right] + 2 \cdot 2 \cdot \left[\sqrt{4 \cdot M_y \cdot f_h \cdot d} \right]$$

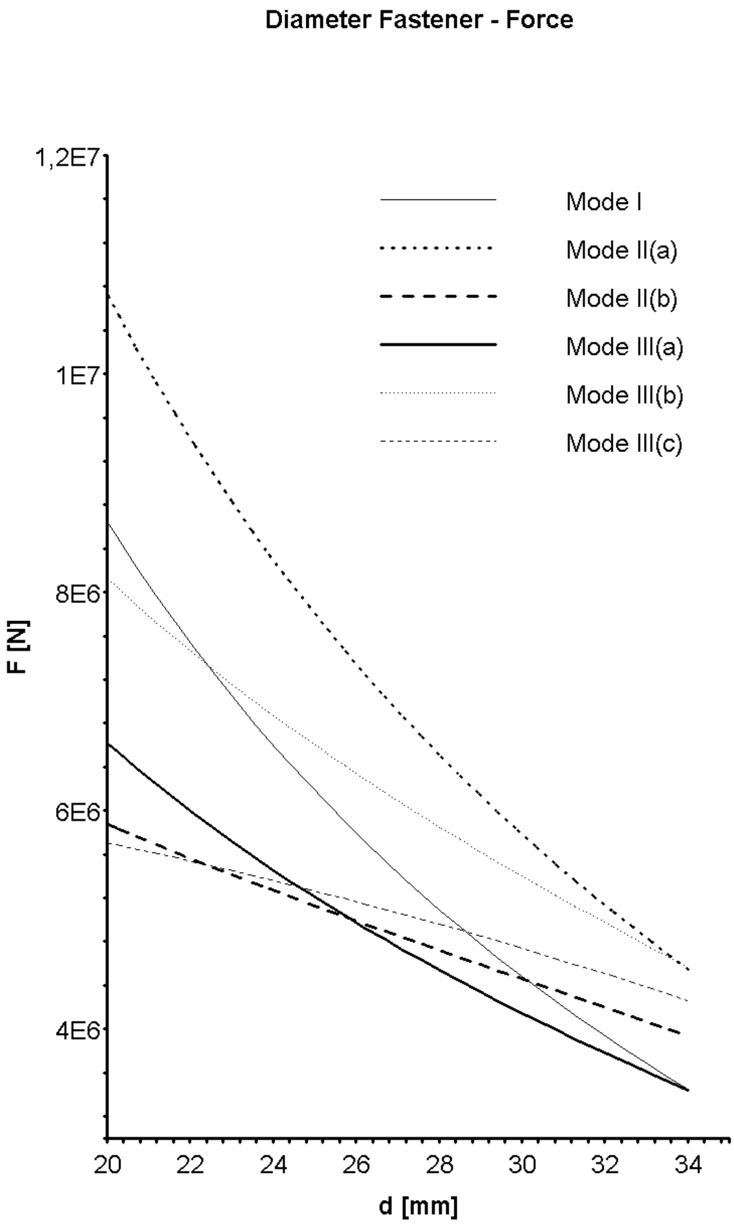

figure 3.22: Influence Diameter Dowel Joint Strength

To evaluate the strength of the joint through calculation of failure mechanisms some variables have to be defined. The number of dowels is slightly adapted to equation (3.40) based on the Eurocode (EC 5-1 1995), but is only valid for rows of six or more fasteners. End distances and fastener spacings are preserved, while the embedment strength is defined by equation (3.41) and the yield moment of the fasteners is defined as in equation (3.42). The wood density (ρ_k) of 500 kg/m^3 is based on a average deciduous wood species and the yield strength of the dowels is assumed to be $f_{u,k}$= 360 N/mm^2.

$$n_{ef} = n_x \cdot \left(6 + \frac{2}{3}\left(n_y - 6\right)\right) \quad \textbf{(3.40)}$$

$$f_h = 0,082 \cdot \left(1 - 0,01 \cdot d\right) \cdot \rho_k \quad \textbf{(3.41)}$$

$$M_y = 0,8 \cdot f_{u,k} \cdot \frac{d^3}{6} \quad \textbf{(3.42)}$$

The three steel plates are assumed to be 20 mm thick which is calculated to be sufficiently strong for the expected load. Initially the remaining 440 mm is equally divided over the timber member, which implies equal edge and middle wood thicknesses.

These assumptions of equations and values result in relations between the dowel diameter and the load bearing capacity for all individual failure mechanisms of which graphs are plotted in figure 3.22 for a joint. From these graphs it is observed that more brittle failure mechanism (Mode I) come into play when the diameter increases, while for dowels with diameters smaller then 30 mm the ductile Mode III (d) mechanism is decisive.

$$\alpha = \frac{t_1}{t_2} \tag{3.43}$$

Thickness ratio

To investigate the influence of the thickness ratio between the middle wood and the edge wood the thickness ratio is defined as in equation (3.43) and is displayed for a dowel of 20 mm in figure 3.23. It becomes clear that the thickness ratio (α) has influence on the decisive failure mode. For α > 1,0 no differences are observed, which implies that for this joint detail an equal divided spacing of steel plates is the strongest solution.

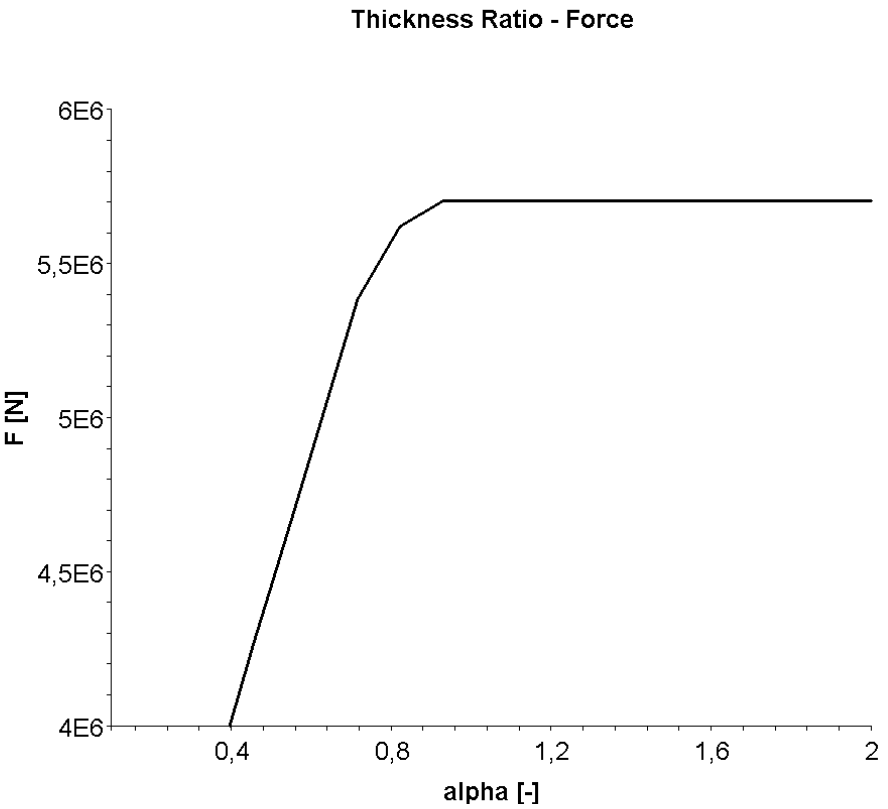

figure 3.23: Influence of Thickness Ration on the Capacity of the Joint

Combined influence
To give a complete overview of the influences of the thickness ratio and the dowel diameter, figure 3.24 shows a three dimensional graph of both variables and the capacity of the joint.

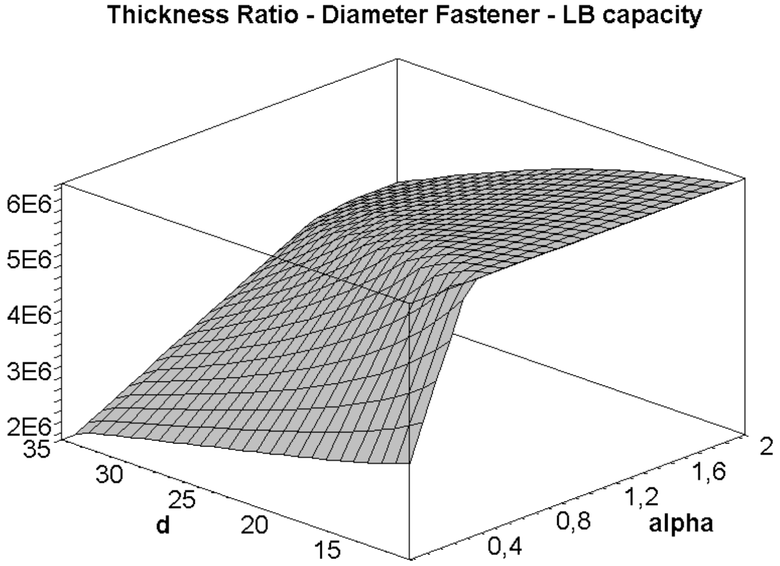

figure 3.24: Combined influence of Diameter and Thickness Ratio on the Joint Capacity

Expended tube fastener
For the expended tube similar relations can be established. From the available design data, a linear regression is made for the fastener strength per shear plane, which is shown in figure 3.25. The relation acquired through regression between the joint strength and the diameter of an expended tube is given in equation (3.44).

$$F_{tube\_eq} = 3517 \cdot d - 23394 \quad \textbf{(3.44)}$$

The number of fasteners is the same as for the fastener stiffness calculations of the expended tube. Oppose to dowels the fastener strength must be multiplied by the number of shear planes for the expended tube fastener, which is six for this joint. These alterations lead to a joint strenght depicted in figure 3.26.

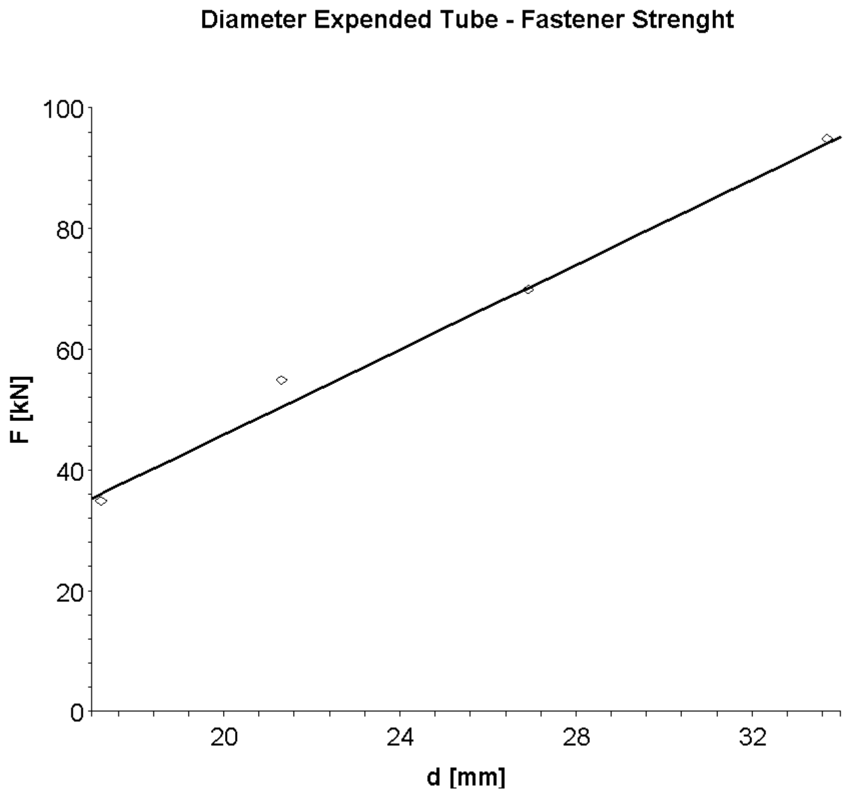

figure 3.25: Regression-Line Strength Tube-Fastener

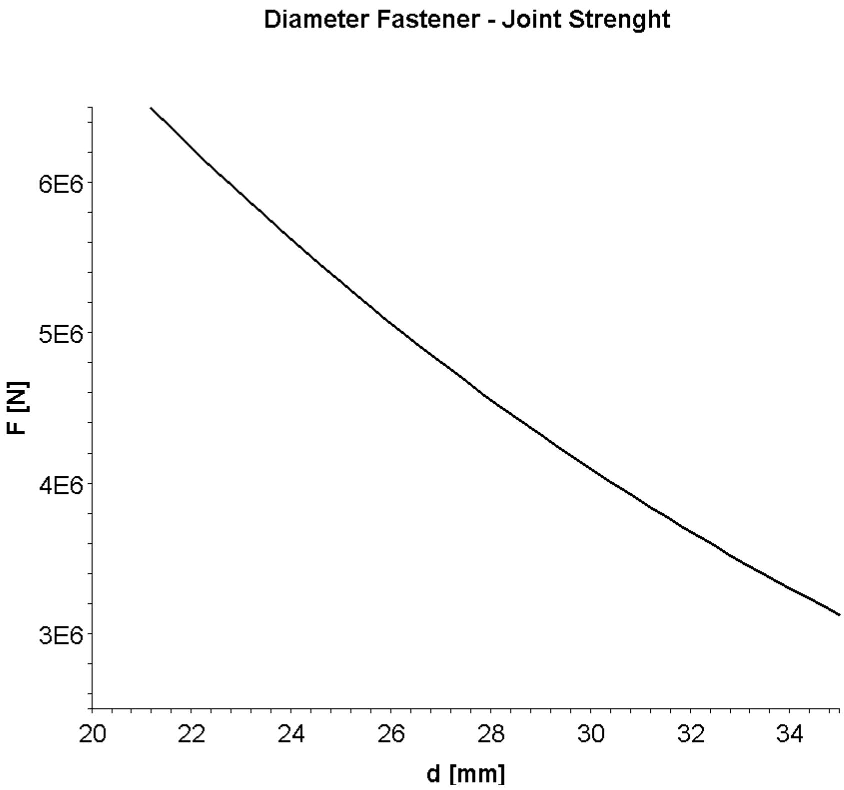

figure 3.26: Joint Strength Tube-Fastener

In order to compare the joint strength of the expended tube fastener with the dowel their graphs are plotted in figure 3.27. From the figure it becomes clear that tube fasters have a higher load bearing capacity then a doweled joint when fasteners are small. This difference can be attributed to the embedment strength of the densified veneer wood, which changes the behavior of the joint completely opposed to the conventional Johansen failure mechanisms.

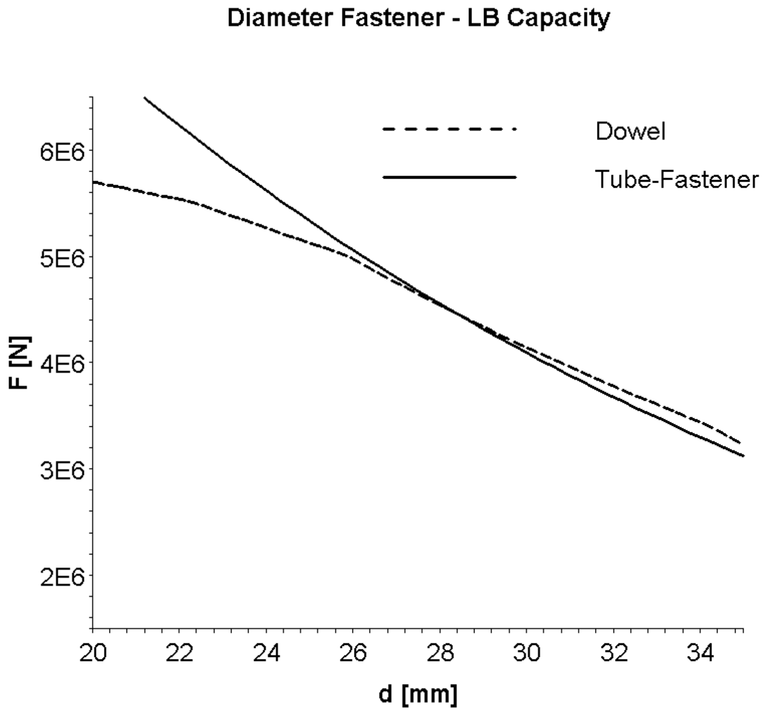

figure 3.27: Load-bearing Capacity of Joints

The tube fastener can be doubled to improve the capacity with 20% on average. From ref. [17] it is known that the industry rejects dowels combined with a densified veneer wood reinforcement because of misalignments resulting in low performance.

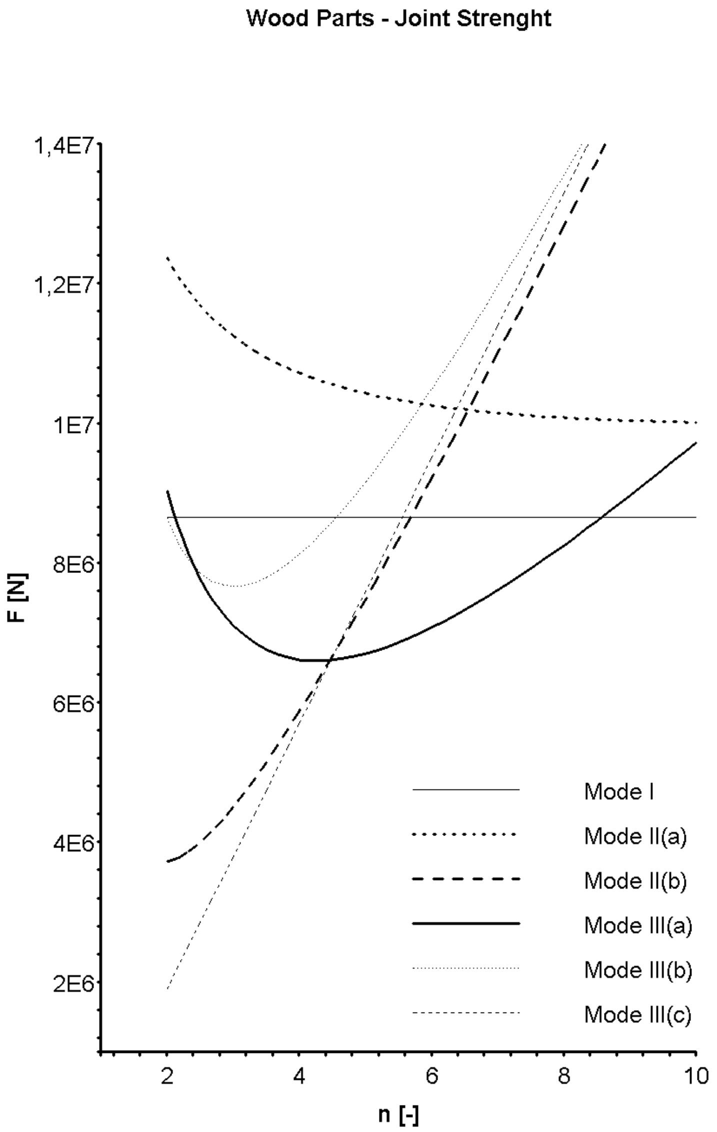

figure 3.28: Influence of Number of Shear Planes

Number of shear planes

To increase the strength of the joint, the number of shear planes could be increased to an optimum for the given dimensions. This can result into an increase of the capacity of modes III, especially for small dowels as can be observed in figure 3.28 combined with figure 3.22.

To investigate this phenomenon, it is assumed that α = 1,0. The total thickness of the timber is defined as "t", and is assumed to be constant, because the steel plates become thinner as the number of steel plates increase. The variable *"m"* is introduced which stands for the number of wood parts, i.e. the number of middle woods and edge woods together. This leads to an adaptation of the failure mechanisms as follows:

$$t \cdot f_h \cdot d \qquad I$$

$$\left((m-2) \cdot \frac{t}{m} + 2 \cdot \frac{t}{m} \cdot \left[\sqrt{2 + \frac{M_y}{f_h \cdot d \cdot \left(\frac{t}{n} \right)^2}} - 1 \right] \right) \cdot f_h \cdot d \qquad II(a)$$

$$2\cdot(m-2)\cdot\sqrt{4\cdot M_y\cdot f_h\cdot d}+2\cdot\left(\frac{t}{m}\right)\cdot f_h\cdot d\cdot\left[\sqrt{2+\frac{M_y}{f_h\cdot d\cdot\left(\frac{t}{m}\right)^2}}-1\right]\quad II(b)$$

$$2\cdot\left(\frac{t}{m}\right)\cdot f_h\cdot d+2\cdot\sqrt{2\cdot M_y\cdot f_h\cdot d}+(m-3)\cdot\sqrt{4\cdot M_y\cdot f_h\cdot d}\qquad III(a)$$

$$2\cdot t_1\cdot f_h\cdot d+2\cdot(m-2)\cdot\sqrt{4\cdot M_y\cdot f_h\cdot d}\qquad III(b)$$

$$\left[2+2\cdot(m-2)\right]\cdot\sqrt{4\cdot M_y\cdot f_h\cdot d}\qquad III(c)$$

The diameter of the dowels are assumed to be d = 20 mm. The total thickness of the timber is assumed to be t = 440 mm as mentioned before. Other parameters are preserved as previously mentioned. This leads to a relation between the failure mechanisms as depicted in figure 3.29.

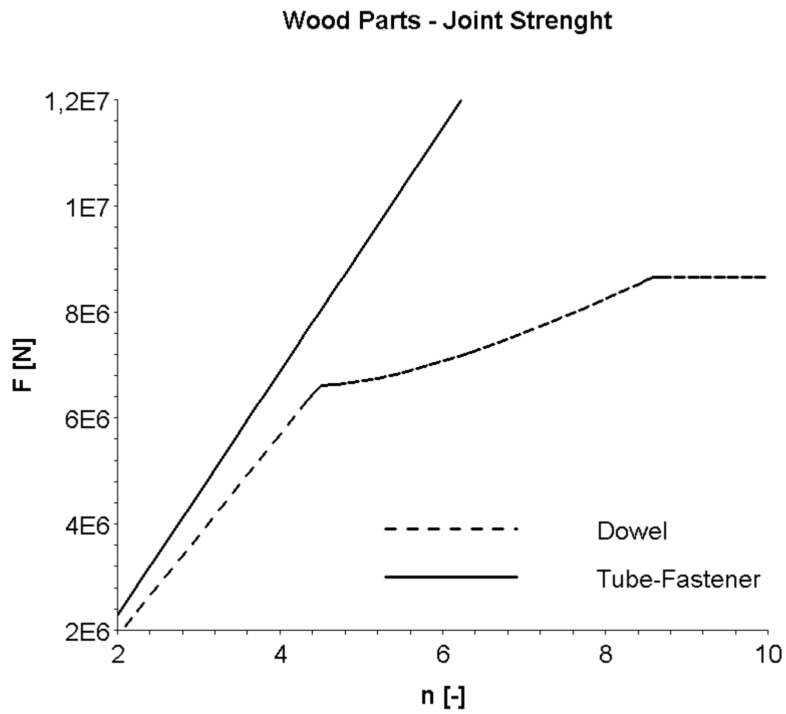

figure 3.29: Influence number of Shear Planes, Fasteners

Intermediate Summary
The load bearing capacity of the joint is inversely proportional with the diameter of the fastener, similar to the joint stiffness. In contrast to the joint stiffness, the load bearing capacity of tube-fasteners can be larger than dowels for the investigated joint geometry, primarily because the wood density is different. When load bearing capacity is a problem for doweled joints, then a tube-fastener can be chosen when otherwise the dimensions of the member had to be increased. Increasing the number of shear planes has a positive effect for strength and stiffness for the steel tube-fastener joint, bearing in mind that enough material is left to actually introduce the load into the timber member. Dowels do not benefit as much from an increasing number of shear planes (figure 3.29) because the failure mode changes from III (c) to III (a) to finally a brittle mode I. Reinforced tube-fastener joints always seem to fail in a ductile II or III type of mode because the embedment strength of the reinforcement is relatively high compared to the yield moment of the fastener.

The layout of the joint is different for tube-fasteners and dowels, through the DVW reinforcement of the timber member. The question remains if normal doweled joints can benefit from reinforcement. Reinforcement combined with normal dowels could invoke brittle failure modes, because the dowel is stout and solid, a different behavior could be expected then for tube-fasteners. Another question could be, if reinforcement is still necessary, since the density of the used base material is already high. This is subject for further investigation.

3.10.4 Economical Considerations

For the case study the two different types of fasteners are maintained. The arrangement of the joint, consists of the number of shear planes (wood parts), the number of fasteners associated with the width of the adjacent member and the length of the joint (steel plates). The joint arrangements are chosen based on economic considerations.

The cost of a single joint is dependant on the number of fasteners used and the number of shear planes in the joint. To process a single fastener within a joint during production, a hole has to be drilled through a number of steel and timber parts. As has become clear from figure 3.19, the number of fasteners decreases by increasing the diameter of the fasteners, but the length of the joint can increase because fastener spacing an edge distances also increase. For economic joints, a reasonable compromise has to be found between the number of fasteners and the length of the joint. The decision process is as follows:

First step: Create a spreadsheet (MS Excel) which calculates the number of fasteners and the joint capacity according to equations (3.35) to (3.36) and (3.40) and failure mechanisms shown in paragraph 3.10.3 adjusted for shear plane numbers. The embedment strength and the yield moment of fasteners is calculated using equation (3.41) and (3.42) respectively. Values of strength class D70 are assumed for the stiffness and embedment of dowels. The input variable of this spreadsheet is the joint length *"l"*, while the joint width is equal to the adjacent member.

Second step: Adjust the joint length to equalize the joint capacity with the buckling resistance of the adjacent member for all relevant sections calculated in paragraph 3.9. This is done for joints with dowels of 12 mm and 24 mm in diameter and tube-fasteners of 21,3 mm and 33,7 mm in diameter combined with for four and six wood parts, respectively six and 10 shear planes.

Third step: Calculate the total length *"L"* of the steel plates by multiplying the length of the joint *"l"* with the number of steel plates *"(m-1)"*. Also calculate the number of drilling actions *"N"* through multiplication of the parts *"m"* times the number of dowels *"n"*.

Last step: Make a choice between joint configurations based on the total length *"L"* and the number of drilling actions *"N"*. Most of the time the choice is obvious, e.g. when both criteria are smaller or one is extremely high. Joints with dowels and joints with tube-fasteners are kept separate during this process.

Results of the decision process are summarized in table 3.15 through table 3.20. The symbols used in table 3.15 through table 3.20 are assigned as shown below.

b_j = joint width
l_j = joint length
d = diameter fastener
F_u = load bearing capacity of single fastener
m = number of wood parts
N_{sp} = number of shear planes *(m-1)*
n_x = number of fasteners in the x direction
n_y = number of fasteners in the y direction
n_{eff} = total number of effective fasteners
t = thickness of wood parts
R_d = load bearing capacity of joint
K_{ser} = joint stiffness
$K_{r,ser}$ = joint rotational stiffness

From spreadsheet calculations it becomes clear than dowels usually fail in Mode III which is on one hand beneficial because it ensures a certain amount of ductility and therefore robustness of the structural system. On the other hand it does not exploit the full potential of the fastener.

3.10.5 Joints Variant 1

Dowel Joints

b_i	l_i	d	F_d	m	n_x	n_y	n_{eff}	t	R_d	$K_{ser,i}$	$K_{r,ser,i}$
[mm]	[mm]	[mm]	[kN]	[-]	[-]	[-]	[-]	[mm]	[kN]	[MN/mm]	[kNm/rad]
300	600	24	359	4	3	1	3	75	1076	1,17	709
350	600	24	359	4	3	2	6	88	2152	2,33	709
400	800	24	359	4	4	2	8	100	2869	3,11	709
450	450	24	598	6	2	3	6	75	3586	3,89	684
500	600	24	359	4	3	4	12	125	4304	4,67	1866
550	750	24	359	4	4	4	16	138	5738	6,22	1866
600	750	24	359	4	4	5	20	150	7173	7,78	3919
650	750	24	359	4	4	6	24	163	8607	9,33	3919
700	750	25	359	4	4	7	27	175	9564	10,89	7316

table 3.15: Properties for Doweled Joint, Variant 1

Tube Fastener Joints

b_i	l_i	d	F_d	m	N_{sp}	n_x	n_y	n_{eff}	R_d	$K_{ser,i}$	$K_{r,ser,i}$
[mm]	[mm]	[mm]	[kN]	[-]	[-]	[-]	[-]	[mm]	[kN]	[MN/mm]	[kNm/rad]
300	300	33,7	95	6	10	1	1	1	951	0,65	0
350	650	33,7	285	4	6	3	1	3	1712	1,17	787
400	550	21,3	412	4	6	4	2	8	2473	2,54	405
450	750	21,3	618	4	6	6	2	12	3709	3,80	1283
500	400	21,3	464	6	10	3	3	9	4637	4,75	2250
550	750	21,3	927	4	6	6	3	18	5564	5,71	3376
600	750	21,3	1236	4	6	6	4	24	7419	7,61	3376
650	550	21,3	824	6	10	4	4	16	8243	8,45	2250
700	550	22,3	1030	6	10	4	5	20	10304	10,57	5626

table 3.16: Properties for Tube-Fastener Joint, Variant 1

3.10.6 Joints Variant 2

Dowel Joints, Column Members

b_i	l_i	d	F_d	m	n_x	n_y	n_{eff}	t	R_d	$K_{ser,i}$	$K_{r,ser,i}$
[mm]	[mm]	[mm]	[kN]	[-]	[-]	[-]	[-]	[mm]	[kN]	[MN/mm]	[kNm/rad]
300	750	24	359	4	4	1	4	75	1435	1,56	709
350	600	24	359	4	3	2	6	88	2152	2,33	709
400	750	24	359	4	4	2	8	100	2869	3,11	709
450	450	24	598	6	2	3	6	75	3586	3,89	684
500	450	24	598	6	2	4	8	83	4782	5,18	684
550	750	24	359	4	4	4	16	138	5738	6,22	1866
600	750	24	359	4	4	5	20	150	7173	7,78	3919
650	750	24	359	4	4	6	24	163	8607	9,33	3919
700	750	24	359	4	4	7	27	175	9564	10,89	7316
750	600	24	598	6	3	7	20	125	11955	13,61	12193

table 3.17: Properties for Doweled Joint adjacent to Columns, Variant 2

Dowel Joints, Brace Members

b_j	l_j	d	F_d	m	n_x	n_y	n_{eff}	t	R_d	$K_{ser,j}$	$K_{r,ser,j}$
[mm]	[mm]	[mm]	[kN]	[-]	[-]	[-]	[-]	[mm]	[kN]	[MN/mm]	[kNm/rad]
300	400	12	96	4	4	5	20	75	1930	3,89	980
350	750	24	359	4	4	2	8	88	2869	3,11	709
400	600	24	538	6	3	2	6	67	3231	3,89	1182
450	750	24	359	4	4	3	12	113	4304	4,67	1866
500	450	24	598	6	2	4	8	83	4782	5,18	684
550	750	24	359	4	4	4	16	138	5738	6,22	1866
600	600	24	598	6	3	5	15	100	8966	9,72	6532

table 3.18: Properties for Doweled Joint adjacent to Brace Members, Variant 2

Tube Fastener Joints, Column Members

b_j	l_j	d	F_d	m	N_{sp}	n_x	n_y	n_{eff}	R_d	$K_{ser,j}$	$K_{r,ser,j}$
[mm]	[mm]	[mm]	[kN]	[-]	[-]	[-]	[-]	[mm]	[kN]	[MN/mm]	[kNm/rad]
300	550	33,7	190	4	6	2	1	2	1142	0,78	131
350	500	33,7	190	6	10	2	1	2	1903	1,30	219
400	650	33,7	285	6	10	3	1	3	2854	1,95	1311
450	800	33,7	381	6	10	4	1	4	3805	2,59	1311
500	1000	33,7	476	6	10	5	1	5	4756	3,24	4152
550	1150	33,7	571	6	10	6	1	6	5708	3,89	4152
600	1150	33,7	1142	4	6	6	2	12	6849	4,67	2491
650	550	21,3	824	6	10	4	4	16	8243	8,45	2250
700	1000	33,7	951	6	10	5	2	10	9513	6,48	4152
750	800	33,7	1142	6	10	4	3	12	11415	7,78	4370

table 3.19: Properties for Tube-Fastener Joint adjacent to Columns, Variant 2

Tube Fastener Joints, Brace Members

b_j	l_j	d	F_d	m	N_{sp}	n_x	n_y	n_{eff}	R_d	$K_{ser,j}$	$K_{r,ser,j}$
[mm]	[mm]	[mm]	[kN]	[-]	[-]	[-]	[-]	[mm]	[kN]	[MN/mm]	[kNm/rad]
300	400	21,3	155	6	10	3	1	3	1546	1,58	675
350	950	33,7	381	4	6	4	1	4	2283	1,56	787
400	1200	33,7	571	4	6	6	1	6	3425	2,33	2491
450	1300	33,7	666	4	6	7	1	7	3995	2,72	5769
500	1650	33,7	856	4	6	9	1	9	5137	3,50	11144
550	1900	33,7	951	4	6	10	1	10	5708	3,89	11144
600	800	33,7	761	6	10	4	2	8	7610	5,19	1311

table 3.20: Properties for Tube-Fastener Joint adjacent to Brace Members, Variant 2

The influence of the joint stiffness on the global system stiffness is incorporated by using values given in § 3.10.5 and § 3.10.6 in calculation model of the first and second variant

3.11 CLT Joint Properties

In this paragraph the stiffness of the proposed CLT joint and the influence on the total stiffness of the system is determined. The load bearing capacity of the proposed CLT joint is also calculated.

3.11.1 CLT Joint Geometry

The principle of the design is depicted in figure 3.30, the design is focused on a minimum number of joints or seems, hence maximum plate dimensions within allowable limits, and avoidance of coincident vertical joints. All elements are basically 2,70 m wide and 7,00 m long with cut outs for windows.

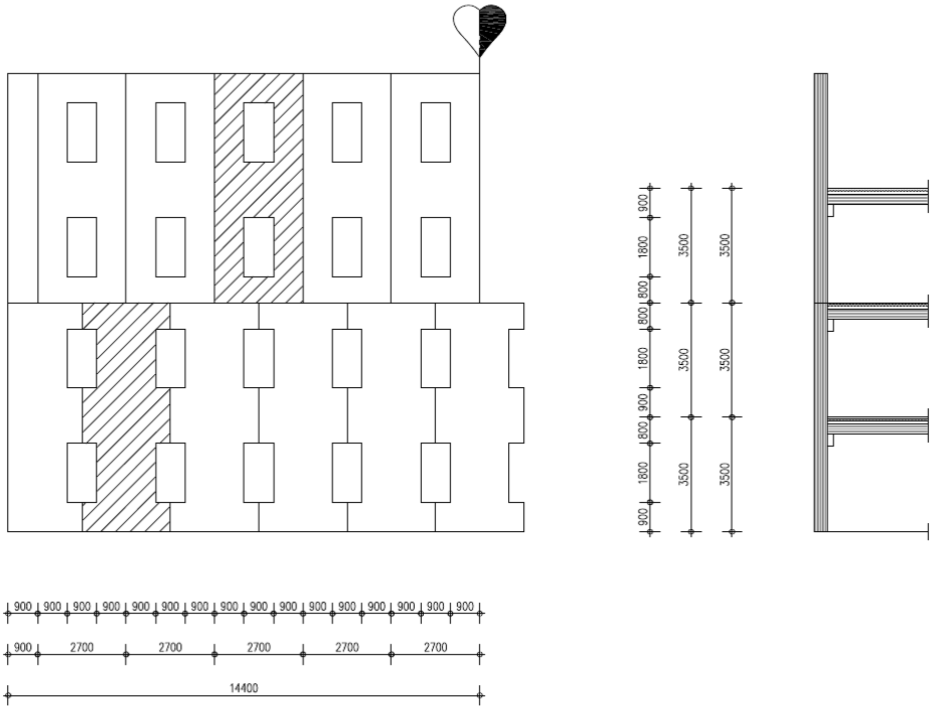

figure 3.30: Geometry Principle and Dimensions of Plates

The joint interface detail is shown in figure 2.27. The number of fasteners is determined by the fastener spacing and the number of rows. The fasteners are chosen to be screws of 12 mm in diameter which is common for cross laminated timber. According to ref. [23], the calculation of load beading capacity is conservative for a fastener spacing of 4·d and a edge distance of 6·d in tension. Because the load direction is diverse, and the stiffness calculated is used to determine the global stiffens, the maximum edge distance is used in all directions. The overlap of the joint is at least 200 mm, which implies there is space for two rows of 12 mm diameter screws. The maximum stiffness is achieved for a minimum fastener spacing of 4·d which is 48 mm. These assumptions results in 40 screws per meter length around the seam of an element. An estimation of a conventional configuration consists of one row of screws with a fastener pacing of 200 mm which results in 5 screws per meter length around the joint seam.

3.11.2 CLT Joint Stiffness

For the stiffness of a joint there is no difference between cross laminated timber elements, solid timber or other laminations, because the embedment stiffness is dependent on the mean material density and the fastener diameter. The stiffens of one fastener for one shear plane is calculated in equation (3.45) and (3.46) for the assumed material D70-CLT and the fastener diameter.

$$K_{ser} = \frac{1}{20} \cdot \rho_k^{\,1.5} \cdot d \tag{3.45}$$

$$K_{ser} = \frac{1}{20} \cdot 900^{1.5} \cdot 12 = 16200 N/mm \tag{3.46}$$

The joint stiffness is calculated for one seam or juncture per unit length with equation (3.47). Equation (3.48) shows the calculation of the joint stiffness for both fastener minimum and maximum spacing.

$$K_j = K_{ser} \cdot n_x \cdot n_y \tag{3.47}$$

$$K_j = 16200 \cdot \begin{bmatrix} 5 \cdot 1 \\ 20 \cdot 2 \end{bmatrix} = \begin{bmatrix} 81 \\ 648 \end{bmatrix} \cdot 10^3 N/mm/m^1 \tag{3.48}$$

The values in equation (3.48) are used for the calculation of the global system stiffness of the cross laminated timber in the next paragraph.

3.11.3 Influence of Joint Stiffness

The schematization of a plate combined with a joint seam loaded by a shear force is shown in figure 3.31. This model includes the shear deformation of the plate and an additional part at the top that represents the joint interface. The stiffness of the plate is indicated with (*GA*) and of the joint respectively with (*k*).

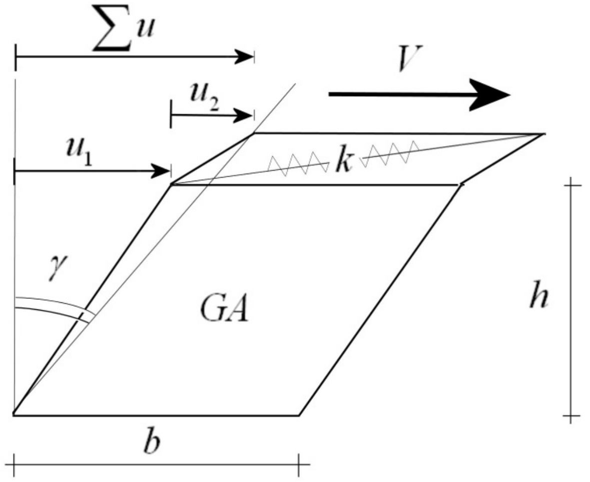

figure 3.31: Schematization of Plate in Shear

The total horizontal translation (Σu) under shear loading (V) is partly originating from the shear deformation of the plate itself (u_1) and partly of the deformation of the joint (u_2). This is formulated and combined in equation (3.49). The total shear deformation of the combined system can be derived by division of the total translation (Σu) over the height, equation (3.50). The effective shear stiffness (GA_{eff}) given in (3.51) is derived from the shear deformation of the model given in equation (3.50). In equation (3.52) this is solved for the effective shear modulus (G_{eff}). Substitution of the section area and the joint stiffness results in equation (3.53). Equation (3.53) can be validated by substitution of $K_{ser}=0$ and $K_{ser}=\infty$.

$$\left.\begin{aligned} u_1 &= V \cdot \frac{h}{GA} \\ u_2 &= V \cdot \frac{1}{k} \end{aligned}\right\} \rightarrow \qquad \sum u = V \cdot \left(\frac{h}{GA} + \frac{1}{k} \right) \tag{3.49}$$

$$\gamma = \frac{\sum u}{h} \rightarrow \qquad \gamma = V \cdot \left(\frac{1}{GA} + \frac{1}{h \cdot k} \right) \tag{3.50}$$

$$V = \gamma \cdot GA_{eff} \rightarrow \qquad GA_{eff} = \left[\frac{1}{GA} + \frac{1}{h \cdot k} \right]^{-1} \tag{3.51}$$

$$G_{eff} = \left(\frac{G \cdot k \cdot h}{GA + h \cdot k} \right) \tag{3.52}$$

$$\left. \begin{array}{l} A = t \cdot b \\ k = K_{ser} \cdot b \end{array} \right\} \rightarrow \qquad \frac{G_{eff}}{G} = \left(1 + \frac{G \cdot t}{K_{ser} \cdot h} \right)^{-1} \tag{3.53}$$

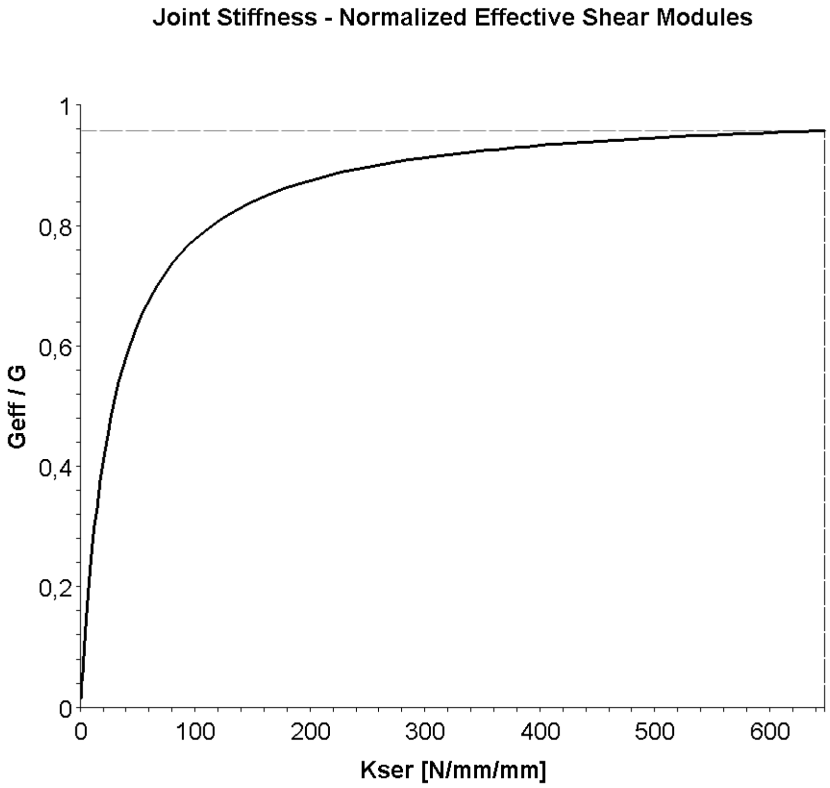

figure 3.32: Joint Stiffness – Normalized Effective Shear Module

To evaluate the influence some values are assigned to the variables in equation (3.53). The reduced shear modules modified for openings of D70-CLT is:

$$G = G_{mean} \cdot \frac{G_{eff}}{G} \cdot \frac{G_{WALL}}{G} = 1250 \cdot 0,79 \cdot 0,52 = 514 \, {}^{N}\!/\!_{mm^2}$$

The maximum plate thickness is 387 mm. The shear deformation is expected in the horizontal direction, which is corresponding with the height of 7000 mm for the plate geometry as shown in figure 3.30. In figure 3.32 the relation is shown between the stiffness of the joint interface per mm joint length and the shear modulus reduction factor.

In the second last paragraph it was determined that 40 screws of 12 mm in diameter is the maximum amount of fasteners along a joint line of one meter. Each screw has a serviceability stiffness of 16200 N/mm. The maximum joint stiffness per meter is therefore:

$$K_{ser} = 16200 \cdot \begin{bmatrix} 5 \cdot 1 \\ 20 \cdot 2 \end{bmatrix} = \begin{bmatrix} 81 \\ 648 \end{bmatrix} \cdot 10^3 N / mm / m^1$$

The calculation of the reduction factor for these parameters is then:

$$\frac{G_{eff}}{G}=\left(1+\frac{G\cdot t}{K_{ser}\cdot h}\right)^{-1}=\left(1+\frac{514\cdot 387}{648\cdot 7000}\right)^{-1}=0,96$$

The influence is not entirely negligible (G_{eff}/G = 0,96). From this model and quantification it can be concluded that the joint stiffness can influence the global shear stiffness of the structure, dependent on the number of screws along the joint line. However the assumed model does not include the positive influence of the masonry bond into the shear deformation as shown in figure 3.30.

The influence of the joint stiffness on the global shear stiffness is not entirely negligible, however for reasons of simplicity is the influence excluded in the stiffness calculation of cross laminated timber panels. The joints in the model of variant 3 and the model of the core are therefore assumed infinitely stiff.

3.11.4 CLT Joint Load Bearing Capacity

The strength of the joints is determined by the embedment strength of the fastener. For cross laminated timber elements the embedment strength of non-predrilled screws is independent of the loading direction. For dowels, the Johansen theory can be applied with the notion that some layers are loaded perpendicular to the grain. Therefore the embedment strength can be averaged over the thickness of the plate as in figure 3.33, which may only be applied when the assumption of characteristic values are sufficiently accurate or conservative [23].

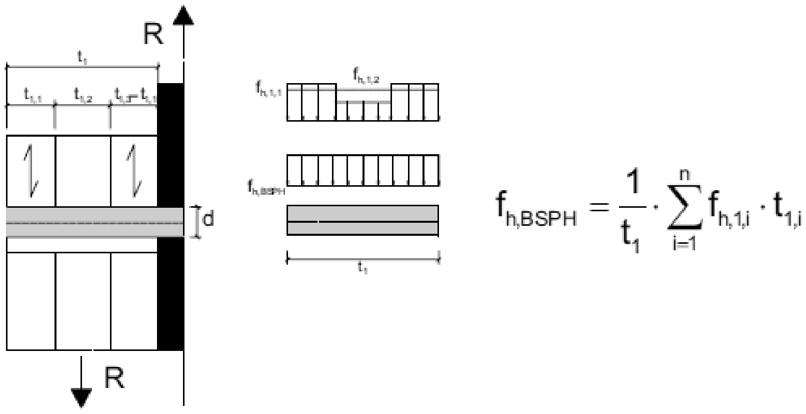

figure 3.33: Averaged Embedment Strength for Cross Laminated Timber [23]

For the joint solution shown in figure 2.27 the embedment strength must be equalized between the side and the middle wood. The calculation of the weighted average embedment strength for both parts is evaluated for both orthogonal loading directions. A 2-5-2 layer distribution of a 9 layer thick board of cross laminated timber is chosen, which practical for workshop milling. According to most standards the general formulation for the embedment strength parallel to the grain is as in equation (3.54). The mutation of the embedment strength in equation (3.55) takes into account the angle between the force and the grain direction. The definition of k_{90} is given in equation (3.56). Combining the above for an angle of 90° equation (3.57) emerges.

$$f_{h,0,k}=0,082\cdot\left(1-0,01\cdot d\right)\cdot\rho_k \tag{3.54}$$

$$f_{h,\alpha,k}=\frac{f_{h,0,k}}{k_{90}\cdot\sin\left(\alpha\right)^2+\cos\left(\alpha\right)^2} \tag{3.55}$$

$$k_{90} = 1,35 + 0,015 \cdot d \tag{3.56}$$

$$f_{h,90,k} = \frac{0,082 \cdot \left(1 - 0,01 \cdot d\right) \cdot \rho_k}{1,35 + 0,015 \cdot d} \tag{3.57}$$

Based on the equations (3.54) to (3.57) a calculation of the embedment strength can be executed for screws of 12 mm in diameter for layers loaded parallel and perpendicular to the grain of D70-CLT with a density of 900 kg/m^3 . This result in the values calculated in (3.58) and (3.59).

$$f_{h,0,k} = 0,082 \cdot \left(1 - 0,01 \cdot 12\right) \cdot 900 = 64,8 \tag{3.58}$$

$$f_{h,90,k} = \frac{28,8}{1,35 + 0,015 \cdot 12} = 42,5 \tag{3.59}$$

The cross laminated timber elements are assumed to be build up out of layers of an equal thickness. This leads to a generalization of equation (3.60) for the embedment strength of an arbitrary part cross laminated timber.

$$f_{h,k} = \frac{f_{h,0,k} \cdot n_0 + f_{h,90,k} \cdot n_{90}}{n_0 + n_{90}} \tag{3.60}$$

The 2-5-2 layer division of the joint shown in figure 2.27 results in approximately equal embedment strengths for both the side parts and middle parts, in both orthogonal directions of the board. This is demonstrated in equation (3.61) and (3.62).

$$f_{h,0,k,CLT,1} = \frac{64,8 \cdot 1 + 42,8 \cdot 1}{1 + 1} = 53,7 \approx f_{h,0,k,CLT,2} = \frac{64,8 \cdot 3 + 42,8 \cdot 2}{3 + 2} = 55,9 \tag{3.61}$$

$$f_{h,90,k,CLT,1} = \frac{64,8 \cdot 1 + 42,8 \cdot 1}{1 + 1} = 53,7 \approx f_{h,90,k,CLT,2} = \frac{64,8 \cdot 2 + 42,8 \cdot 3}{2 + 3} = 51,6 \tag{3.62}$$

According to Blaß and Uibel [24] the embedment strength for normal cross laminated timber of a C24 base material is given as in equation (3.63). Assuming a linear effect on the embedment strength of the material density, equation (3.63) can be adjusted to (3.64). This results for screws of 12 mm diameter in the range shown in (3.65) ,of which the actual value is dependent on the direction of loading.

$$f_{h,k} = \frac{32 \cdot \left(1 - 0,015 \cdot d\right)}{1,1 \cdot \sin\left(\alpha\right)^2 + \cos\left(\alpha\right)^2} \tag{3.63}$$

$$f_{h,k} = \frac{32 \cdot \left(1 - 0,015 \cdot d\right)}{1,1 \cdot \sin\left(\alpha\right)^2 + \cos\left(\alpha\right)^2} \cdot \left(\frac{900}{400}\right) \tag{3.64}$$

$$53,8 < f_{h,k} < 59,0 \tag{3.65}$$

Based on the above, the embedment strength for D70-CLT ($f_{h,k,CLT}$) is conservatively chosen to be 51,6 N/mm^2 for all directions and all parts of the proposed joint solution shown in figure 2.27.

$$
\left.
\begin{array}{ll}
t_1 \cdot f_h \cdot d & I(a) \\
0,5 \cdot t_2 \cdot f_h \cdot d & I(b) \\
\dfrac{f_h \cdot t_1 \cdot d}{2+\beta} \cdot \left[\sqrt{2 \cdot \beta \cdot (1+\beta) + \dfrac{4 \cdot \beta \cdot (2+\beta) \cdot M_y}{f_h \cdot t_1^2}} - \beta \right] & \\
\xrightarrow{\beta=1} \dfrac{f_h \cdot t_1 \cdot d}{3} \cdot \left[\sqrt{4 + \dfrac{12 \cdot M_y}{f_h \cdot t_1^2}} - 1 \right] & II \\
\sqrt{\dfrac{2 \cdot \beta}{1+\beta}} \cdot \sqrt{2 \cdot M_y \cdot f_h \cdot d} \xrightarrow{\beta=1} \sqrt{2 \cdot M_y \cdot f_h \cdot d} & III
\end{array}
\right\} \tag{3.66}
$$

Failure mechanisms
Based on the 2-5-2 layer division the embedment strength for side and middle wood parts is assumed to be the equal. The corresponding equations for the load bearing capacity of the possible failure mechanisms of the joint in figure 2.27 (a) per shear plane for one fastener, derived from EC 1995, are given above in equation (3.66).

Calculation
The calculation of the joint capacity is calculated in a maple file given in appendix B4 for both minimums and maximum fastener spacing. The decisive failure mechanism is mode III in which the screw develops plastic hinges, and is therefore ductile. The capacity for one shear plane per fastener is 10100 N and the capacity of the joint is given in equation (3.68) for both minimum and maximum configurations. These values of the will be used to verify the joint capacity of a tube structure of cross laminated timber later in the thesis.

$$F_{v,Rx} = 10100[N] \tag{3.67}$$

$$R_{v,j} = 10100 \cdot \begin{bmatrix} 20 \cdot 2 \\ 5 \cdot 1 \end{bmatrix} \cdot 2 = \begin{bmatrix} 810 \\ 101 \end{bmatrix} \cdot 10^3 \, N/m^1 \tag{3.68}$$

3.12 Universal Core Stiffness

The universal core section applies to all variants of the case study. In this paragraph the properties of the core section are determined. The core is build up out of cross laminated timber elements with a thickness of 387 mm. The dimensions of the cross section are given in the left side of figure 3.34, on the right side of this figure the vertical layout of the plate elements is given.

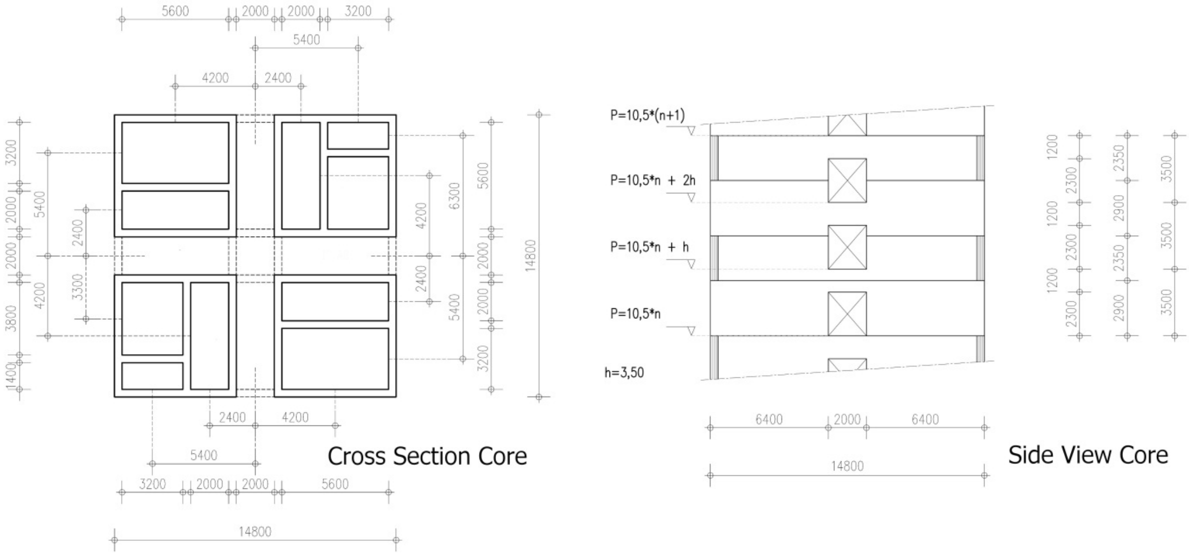

figure 3.34: Drawing of the Core

The plates are about 14,40 m long and alternate in height in between 2350 mm and 2900 mm, which coincides with the vertical floor spacing for each four levels. Openings in these plates are cut out coherent with the vertical floor spacing. This results in plate strips with a smaller cross section in the middle which will be seen as monolithically connected lintels.

3.12.1 Joint stiffness influence

Plates are connected to each other in the corners. The influence of these joints on the moment of inertia is determined here. This is done through calculation of the shear factor for the Steiner part of sections according to EN 1995-1-1, which is:

$$\gamma = \left[1 + \pi^2 \cdot \frac{E \cdot A \cdot s}{K \cdot l^2}\right]^{-1}$$

In which:

γ =	shear factor	
E =	modulus of elasticity	11800 N/mm^2
A =	cross section area of shearing part	
s =	spacing of fasteners	48 mm
K =	stiffness of fasteners	
l =	system length beam	

The modulus of elasticity is based on the value of nine layers thick cross laminated timber (§ 3.6.3.3). When the core section is imagined as a rectangular hollow section, each 'flange' plate is at least connected to two 'web' plates, which implies two shear planes. The flange plate is taken the shearing part for this calculation. The joint interface consists of two rows of screws with a spacing of 48 mm. The stiffness of the fasteners is based on § 3.10.2. For cantilever beams, the length l in equation must be taken twice the span according to appendix B of EN 1995-1-1.

The calculation for one plate on the perimeter of the core is

$$A = A_{net} = (14400 - 2000) \cdot 400 = 5{,}16 \cdot 10^6 \quad mm^2$$

$$K = 2 \cdot 2 \cdot 16200 = 64800 \quad N/_{mm}$$

$$l = 2 \cdot 112 \cdot 10^3 = 224 \cdot 10^3 \quad mm$$

This results in a shear factor of:

$$\gamma = \left[1 + \pi^2 \cdot \frac{11800 \cdot 5160 \cdot 10^3 \cdot 48}{64800 \cdot \left(224 \cdot 10^3\right)^2}\right]^{-1} = 0{,}991$$

This implies that the Steiner part of the largest section area that is shearing is reduced with less than 1% for the calculation of the second moment of inertia (I). For other plates and parts that are smaller and are connected with these fastener arrangements even less reduction takes place. It is therefore assumed that the influence of joints is negligible.

3.12.2 Section properties

The basic section properties of the core are evaluated by importing the geometry of the plan drawn in AutoCAD software with a DXF-format into GSA software as shown in figure 3.35. The software then automatically calculates the section properties of the imported geometry, in this case the core, which is applied to 1D elements within the software.

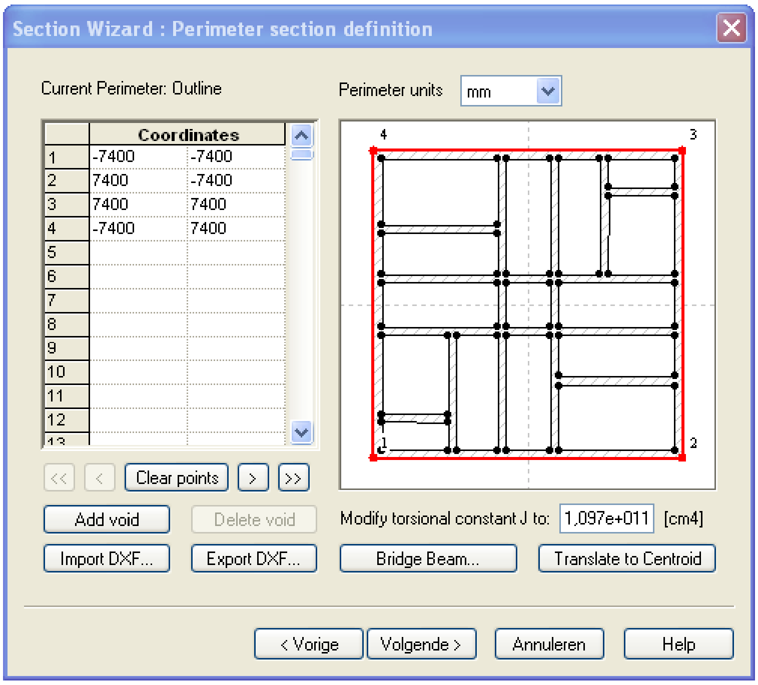

figure 3.35: Section wizard GSA Oasys

GSA software makes calculations of sections by calculating the properties of the sections outline and extracting voids, which is also done manually to verify this. The section area, the second moment of inertia in both local directions and the torsional moment of inertia calculated by GSA software are respectively:

A	$5{,}64 \cdot 10^7$	[mm^2]
I_{yy}	$1{,}23 \cdot 10^{15}$	[mm^4]
I_{zz}	$1{,}23 \cdot 10^{15}$	[mm^4]
J	$1{,}67 \cdot 10^{15}$	[mm^4]

The values of the second moment of inertia are not representative because the core contains several vertical openings in walls for access to lift shafts, staircases, wet rooms and technical shafts. When considered geometrically, the core consists of four quadrants that are coupled through lintels (couple-beams). Within these lintels proportionally large deformations will occur when loaded with shear forces associated with global bending behavior. The internal shear stiffness is therefore reduced.

In order to incorporate the influence of openings in calculation of the bending stiffness of the cross laminated timber core, two methods are used that verify each other, namely:

- Shear factor method
- Finite element method

In the shear factor method the shear stiffness of the lintels above openings is calculated and translated into a spring stiffness value. The core section basically consists of four quadrants. The section properties of these quadrants combined with spring stiffness value a shear factor is calculated. With this shear factor the second moment of inertia is calculated. The finite element model is produced with linear 2D elements and incorporates all openings.

3.12.3 Openings Shear-Factor Method

The layout and the dimensions of the building core is shown in figure 3.36. It can be observed from this figure that the section area is point symmetric coincident with the center of gravity. The following assumptions are made for the calculation:

- walls are 400 mm thick
- parallel in plane modulus of elasticity of CLT ($E_{||}$) is 11800 N/mm^2
- perpendicular in plane modulus of elasticity of CLT ($E_\perp$) is 9600 N/mm^2
- wall elements consist of one uninterrupted plate as shown in figure 3.38 and $E_{||}$ is directed along the vertical direction.
- Each level of plates overlaps the former level at the corner as shown in figure 3.38
- Shear connection between plates is assumed infinitely stiff

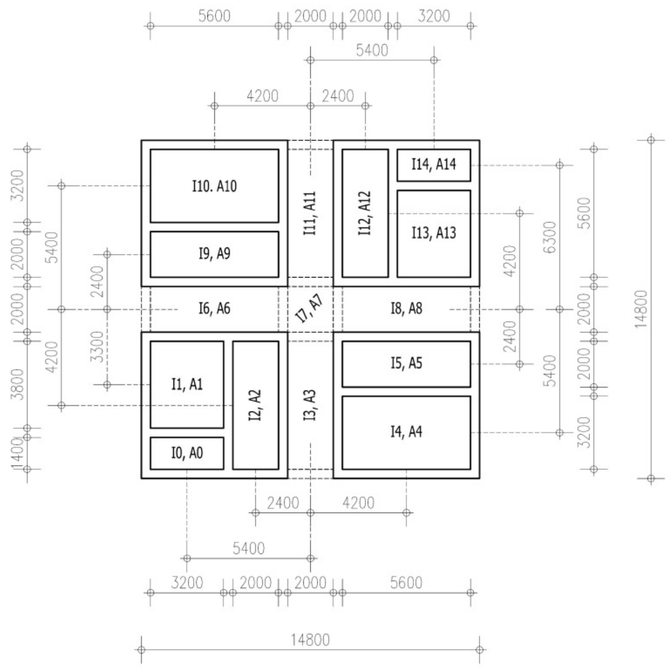

figure 3.36: Layout and Dimensions of the Core

In figure 3.36 the assignment of area-numbers of the so called voids is indicated. The section properties of the individual quadrants are calculated by subtraction of the voids from the "outline" with the equations (3.69) and (3.70) as shown in table 3.21.

$$I_i = \frac{b_i \cdot h_i^3}{12} \tag{3.69}$$

$$A_i = b_i \cdot h_i \tag{3.70}$$

The effective second moment of inertia (I_{eff}) of the quadrants is calculated with equation (3.71), in which the Steiner contribution is multiplied with a shear reduction factor shown in equation (3.72). Both equations are adopted from EN 1995-1-1 appendix B. The modulus of elasticity is equal for all parts and is therefore eliminated from the original equation of equation (3.71).

$$I_{eff} = \sum_{i=1}^{n} I_i + \gamma_i \cdot A_i \cdot a_i^2 \tag{3.71}$$

$$\gamma_i = \left[1 + \pi^2 \cdot \frac{E_i \cdot A_i \cdot s_i}{K_i \cdot l^2} \right]^{-1} \tag{3.72}$$

	i	b_i [m]	H_i [m]	A_i [m^2]	I_i [m^4]
equation:				(3.69)	(3.70)
Quadrant 1	Outline	6,00	6,00	36,00	108,00
	0	3,20	1,40	-4,48	-0,73
	1	3,20	3,80	-12,16	-14,63
	2	2,00	5,60	-11,20	-29,27
				8,16	63,37
Quadrant 2	Outline	6,00	6,00	36,00	108,00
	4	5,60	3,20	-17,92	-15,29
	5	5,60	2,00	-11,20	-3,73
				6,88	88,97
Quadrant 3	Outline	6,00	6,00	36,00	108,00
	9	5,60	2,00	-11,20	-3,73
	10	5,60	3,20	-17,92	-15,29
				6,88	88,97
Quadrant 4	Outline	6,00	6,00	36,00	108,00
	12	2,00	5,60	-11,20	-29,27
	13	3,20	3,80	-12,16	-14,63
	14	3,20	1,40	-4,48	-0,73
				8,16	63,37

table 3.21: Section properties Core with Shear Correction

The shear reduction originates from the deformation of the lintels as shown in figure 3.37. The stiffness value of the lintels can be deduced from the equation for a double sided clamped beam as shown in (3.73).

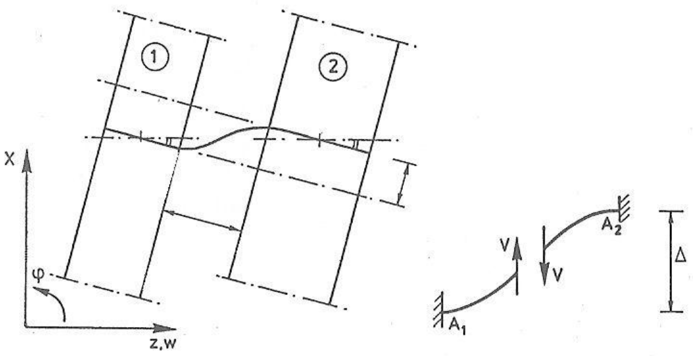

figure 3.37: Deformation of the lintels in the core [44]

$$V = \boxed{\frac{12 \cdot EI}{l^3}} \cdot \Delta$$

$$F = \boxed{K} \cdot u \qquad \textbf{(3.73)}$$

As can be observed in figure 3.38, are lintels 1200 mm deep and span a length of 2000 mm, thus for one lintel the following is valid:

$$I = \frac{400 \cdot 1200^3}{12} = 57,6 \cdot 10^9 mm^4$$

$$l = 2000mm$$

$$K = 2 \cdot \frac{12 \cdot EI}{l^3} = 2 \cdot \frac{12 \cdot 9600 \cdot 57,6 \cdot 10^9}{2000^3} = 1,66 \cdot 10^6 \, N/mm$$

Each quadrant is connected by two lintels per floor level in each direction, as can be observed from figure 3.36 and figure 3.38 this implies: s_i =*3500 mm*. For cantilever beams, the length l in equation (3.72) must be taken twice the span according to appendix B of EN 1995-1-1.

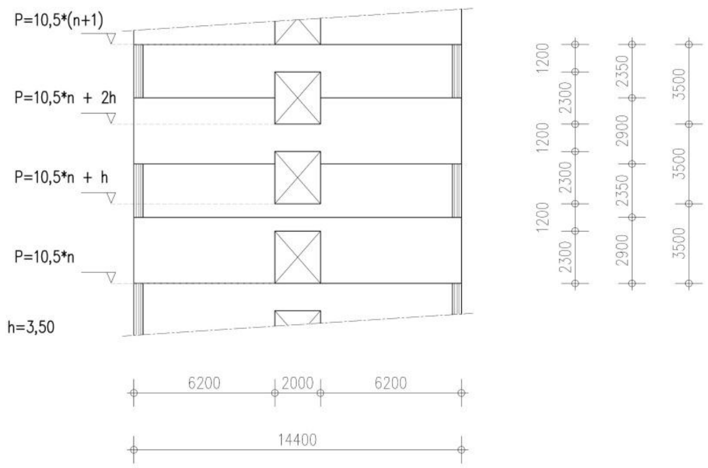

figure 3.38: Side View of the Core

The calculation of the effective second moment of inertia (I_{eff}) for is as follows:

$$A_{q1} = 8,16 \cdot 10^6 \quad mm^2 \qquad I_{q1} = 63,37 \cdot 10^{12} \quad mm^4 \qquad a_1 = a_2 = a_3 = a_4 = 4200 \quad mm$$

$$A_{q2} = 6,88 \cdot 10^6 \quad mm^2 \qquad I_{q2} = 88,97 \cdot 10^{12} \quad mm^4 \qquad K_1 = K_2 = K_3 = K_4 = 2,04 \cdot 10^6 \quad N/mm$$

$$A_{q3} = 6,88 \cdot 10^6 \quad mm^2 \qquad I_{q3} = 63,37 \cdot 10^{12} \quad mm^4$$

$$A_{q4} = 8,16 \cdot 10^6 \quad mm^2 \qquad I_{q4} = 88,97 \cdot 10^{12} \quad mm^4$$

$$\gamma_i = \left[1 + \pi^2 \cdot \frac{E_i \cdot A_i \cdot s_i}{K_i \cdot l^2}\right]^{-1} \rightarrow \gamma_1 = \gamma_4 = \left[1 + \pi^2 \cdot \frac{11800 \cdot 8,16 \cdot 10^6 \cdot 3500}{2,66 \cdot 10^6 \cdot \left(2 \cdot 112 \cdot 10^3\right)^2}\right]^{-1} = 0,961$$

$$\gamma_2 = \gamma_3 = \left[1 + \pi^2 \cdot \frac{11800 \cdot 6,88 \cdot 10^6 \cdot 3500}{2 \cdot 1,02 \cdot 10^6 \cdot \left(2 \cdot 112 \cdot 10^3\right)^2}\right]^{-1} = 0,967$$

$$I_{eff} = \sum_{i=1}^{n} I_i + \gamma_i \cdot A_i \cdot a_i^2 \begin{cases} I_{eff} = 2 \cdot \left(63 + 89\right) \cdot 10^{12} + 2 \cdot \left(0,961 \cdot 8,16 + 0,967 \cdot 6,88\right) \cdot 10^6 \cdot 4,20^2 \\ I_{eff} = 0,305 \cdot 10^{15} + 0,512 \cdot 10^{15} \\ \boxed{I_{eff} = 0,816 \cdot 10^{15}} \end{cases}$$

The second moment of inertia is also calculated assuming a shear factor (γ) equal to 1,00 as follows:

$$I_{eff} = \sum_{i=1}^{n} I_i + A_i \cdot a_i^2 \begin{cases} I_{eff} = 2 \cdot \left(63 + 89\right) \cdot 10^{12} + 2 \cdot \left(8,16 + 6,88\right) \cdot 10^6 \cdot 4200^2 \\ I_{eff} = 0,305 \cdot 10^{15} + 0,531 \cdot 10^{15} \\ I_{eff} = 0,835 \cdot 10^{15} mm^4 \end{cases}$$

3.12.4 Openings with FE-Model

In figure 3.39 and figure 3.40 pictures are shown of the core model over one floor height. It is intended to keep the number of elements as small as possible to reduce calculation time. On the contrary it is necessary to keep the aspect ratio (width over height) of single elements close to 1.0.

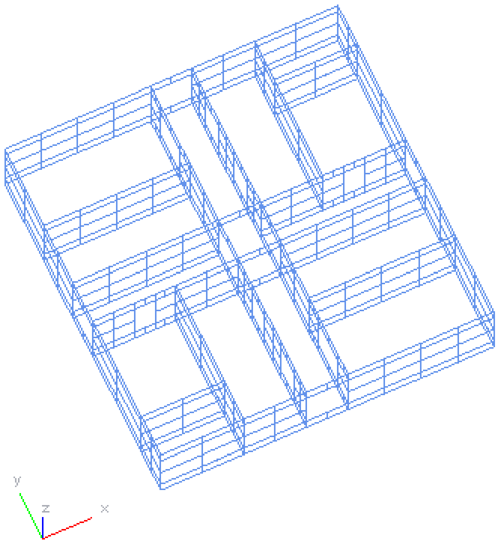

figure 3.39: Model over Single Floor Height

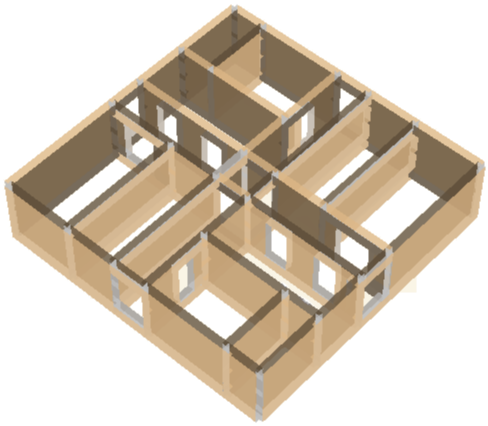

figure 3.40: Full Section

To model the behavior of the core correctly and for easy application of loads the displacement of the most important nodes are linked to a central node in the horizontal plane, to mimic the diaphragm action of the surrounding and internal floor elements which are assumed to be infinitely stiff by comparison as shown in figure 3.41. By copying the single floor to the building height of 32 levels, a model is created of 14487 linear 2-D elements, which is shown in figure 3.42 (section display is turned on).

Axis definition: The global axis for this model is defined as in figure 3.39. The local x-axis of elements coincides with the global z-axis, while the local z-axis is perpendicular to the plane of the element

Element Type: Elements used in this model are linear "Quad 4" elements as defined in ref. [29]. Linear elements are believed to model the global behavior sufficiently while keeping the calculation time at an expectable level.

Size of Elements: The thickness applied to all elements is 387 mm. The horizontally division of the mesh of outer walls in meters is 1,80-1,80-1,35-1,35-0,90-…(symmetric). The mesh is vertically divided over a per floor repeating grid 0,60-1,15-1,15-0,60 for all elements. All openings in this model are therefore 2,30 m high. The width of the openings are adopted from the floor plan. The horizontal grid of internal elements is incidentally adapted to the width of openings.

Interface conditions: All elements are fixed at intermediate nodes in all translational and rotational directions. This assumption is believed to be justified because joint seams are small in number and not assumed to have influence on the stiffness as shown in paragraph 3.11.3.

Material properties: The material stiffness properties applied to all elements are extracted from table 3.1 for nine layer thick cross laminated timber. The modulus of elasticity parallel to the grain ($E_{eff,||}$) coincides with the local x-axis for all elements.

Loading on the model: Because the objective of the finite element model calculation is to determine the stiffness of the core cross section, the magnitude of the loading is of less importance. It is chosen to load the core model with the full lateral wind load, of which the weighed mean value is 2,18 kN/m^2. The central nodes are spaced at 3,50 m and the width of the façade on the perimeter of the building is about 30 m. This results in a load of 228,9 kN per node, rounded down this results in a load of 200 kN per node.

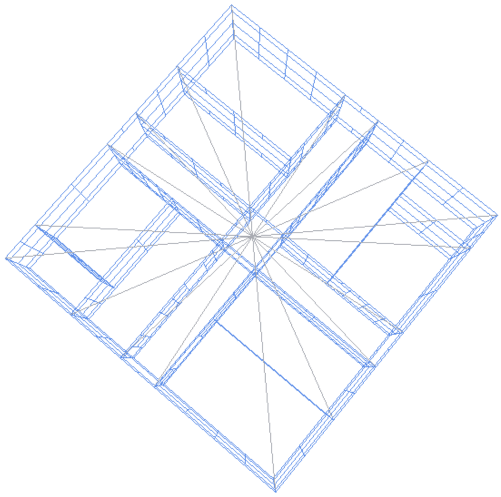

figure 3.41

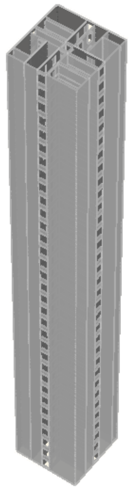

figure 3.42

Results

The computer system used (paragraph 4.1) needed 201 seconds to solve the system matrix associated with the finite element model. The maximum deflection at the top is 111,7 mm in the direction of the load.

Reduced Second Moment of Inertia (I)

To calculate the internal moment of inertia of the core section a simple relation is used from the field of elastic mechanics. The shear stiffness is incorporated in the deflection, therefore, the equation shown in (3.74) for a clamed beam loaded by a uniformly distributed load is used. The uniformly distributed load is calculated as in equation (3.75). This resulted in the calculation of the bending stiffness and the second moment of inertia as in equation (3.76) and (3.77) respectively.

$$\omega_{\max} = \frac{q \cdot l^4}{8 \cdot EI} \rightarrow EI = \frac{q \cdot l^4}{8 \cdot \omega_{\max}} \tag{3.74}$$

$$q = \frac{F}{h} \rightarrow q = \frac{200}{3,50} = 57 \cdot \left[\frac{kN}{m}\right] \tag{3.75}$$

$$EI_{FEM} = \frac{q \cdot l^4}{8 \cdot \omega_{\max}} = \frac{57 \cdot \left(112 \cdot 10^3\right)^4}{8 \cdot 111,7} = 10,04 \cdot 10^{18} \cdot \left[Nmm^2\right] \tag{3.76}$$

$$I_{FEM} = \frac{EI_{FEM}}{E} = \frac{9,46 \cdot 10^{18}}{11800} = 0,851 \cdot 10^{15} \cdot \left[mm^4\right] \tag{3.77}$$

3.12.5 Conclusion

It was assumed, based on the calculation of the shear factor of a decisively large plate part, the influence of the joint stiffness on the section properties is negligible. The influenced of openings was calculated with two different methods, namely the shear factor method and the finite element model. Both methods result in similar values for the moment of inertia, that only deviate 4% from each other. It is chosen to use the value calculated with the finite element model, because this includes more accurately all parameters.

3.13 Universal Support Stiffness

In this paragraph the stiffness of the foundation is determined to be used in the case study models.

3.13.1 Description of the Foundation

The foundation consist of bored piles located directly beneath each column of the tube structure, which results in equivalent spacing for the piles. The foundation beneath the core consists of bored piles as well. The piles are not connected together in the vertical direction, but share a ring beam to spread horizontal loading as shown in figure 3.43.

Bored piles are chosen because their dimensions are virtually unlimited and do not suffer from grouping effects as much as driven piles do. Bored piles can therefore also take the full load of one column. Virtually, other foundation systems could be used with similar load bearing capacity and stiffness, but this makes the assumption of the support stiffness easier.

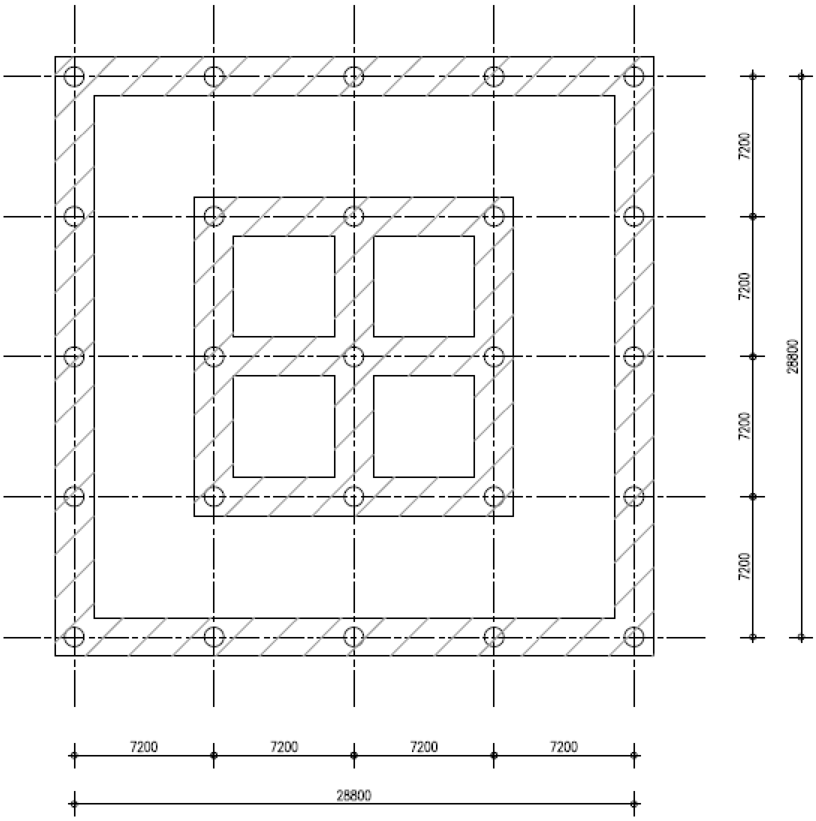

figure 3.43: Plan of the Foundation

3.13.2 Diameter of piles

Because the column spacing of the tube structure is different between variants, the load on the piles beneath these columns is also different. The column spacing of variant 1 to 3 are similar, therefore the diameter of the piles is assumed equal. The diameter of piles for the different variants is given below.

Variant 1 to 3: The diameter of all piles beneath the tube structures of variant 1 to 3 are 1,50 m.

Variant 4: All piles beneath the tube structures of variant 4 are 2,50 m in diameter.

Core foundation: The diameter of piles beneath the core are 2,00 m for all variants.

3.13.3 Soil assumption

To take account for unfavorable soil conditions, a soil profile is used that is common in the western part of the Netherlands in the vicinity of Rotterdam and Amsterdam. The top layer consists of clay and peat and the stronger, load bearing, soil configurations that consist of sand are at a depth of about 20 m beneath the surface which are about 13 m to 20 m thick. In figure 3.44 two profiles are given based on data available from recent subway excavation works in Amsterdam and information from the city of Rotterdam. The assumed pile depth herein is located 25,0 m beneath the surface, or at N.A.P.-22,0 m which will result in similar results for both soil profiles.

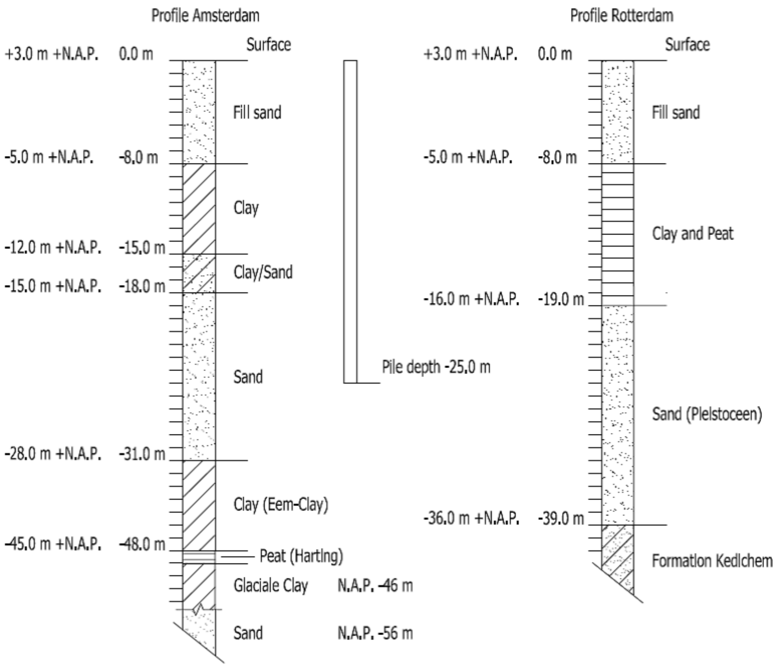

figure 3.44: Soil profiles

3.13.4 Stiffness of Individual Piles

It is assumed that only the elastic stiffness of the piles contributes to the stiffness of the foundation. This implies the estimation of the stiffness given in equation (3.78) for the individual piles beneath the structure.

$$k = \frac{EA}{l} \tag{3.78}$$

In which:
k = spring stiffness
l = length of the pile
E = modulus of elasticity of piles
A = cross section area of piles

In the assumed soil profile, load bearing soil configurations that consist of sand, start at a depth of about 20 m beneath the surface and are about 13 m to 20 m thick. The pile head is therefore assumed to be at a depth of 25,0 m beneath the surface, hence, length of piles is assumed to be 25 m. According to paragraph 6.2.2.3 of NEN 6743, the modulus of elasticity of concrete for piles is $20 \cdot 10^9$ N/m^2. The cross section area of the bored piles is given in equation (3.79).

$$A = \frac{1}{4} \cdot \pi \cdot D^2 \tag{3.79}$$

The calculation of the spring stiffness that is representative for piles, according to equation (3.78) combined with equation (3.79) is given in table 3.22.

Common Parameters: *l =25 m* and *E =20·10⁹ N/m²*.

D	A	k
equation:	(3.79)	(3.78)
[m]	[m²]	[N/m]
1,50	1,767	$1,41 \cdot 10^9$
2,00	3,142	$3,92 \cdot 10^9$
2,50	4,909	$3,92 \cdot 10^9$

table 3.22: Stiffness of Individual Piles

3.13.5 Unified Support Stiffness

The unified translational stiffness of the foundation beneath the core or the tube structure can be calculated by multiplying the number of piles beneath these structures with the individual stiffness of these piles as shown in equation (3.80) and in figure 3.45.

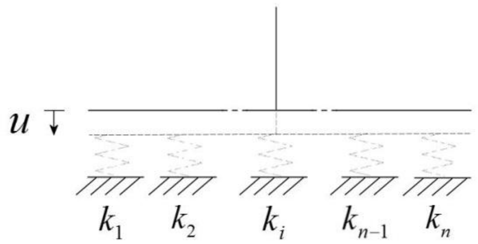

figure 3.45: Schematics Unified Translation

$$k_{uni} = n \cdot k \qquad \textbf{(3.80)}$$

In which:
k_{uni} = unified translational spring stiffness
n= number of piles involved
k = spring stiffness of piles

The unified rotational stiffness of the foundation beneath the core or tube structure (k_r) can be calculated with equation (3.81). This equation is derived from a simple kinematic relation between the rotation at the center of the structure and the translation of the piles involved and moment-force equilibrium over the lever-arm (b) as shown in figure 3.46 (next page). The algebraic deduction of equation (3.81) is:

$$\left.\begin{array}{l} \left.\begin{array}{l} u_i = \dfrac{\theta \cdot b_i}{2} \\ F_i = k_i \cdot u_i \end{array}\right\} F_i = k_i \cdot \dfrac{\theta \cdot b_i}{2} \\ \\ \left.\begin{array}{l} M = k_r \cdot \theta \\ M = \sum_{i=1}^{m} F_i \cdot b_i \end{array}\right\} k_r \cdot \theta = \sum_{i=1}^{m} F_i \cdot b_i \end{array}\right\} k_r \cdot \cancel{\theta} = \sum_{i=1}^{m} k_i \cdot \frac{\cancel{\theta} \cdot b_i}{2} \cdot b_i \rightarrow k_r = \sum_{i=1}^{m} \frac{k_i \cdot b_i^2}{2}$$

$$k_r = \sum_{i=1}^{m} \frac{k_i \cdot b_i^2}{2} \tag{3.81}$$

In which:

k_r = rotational spring stiffness
m= number of pile couples involved
k_i = spring stiffness of pile i
b_i = internal lever arm of pile couple i

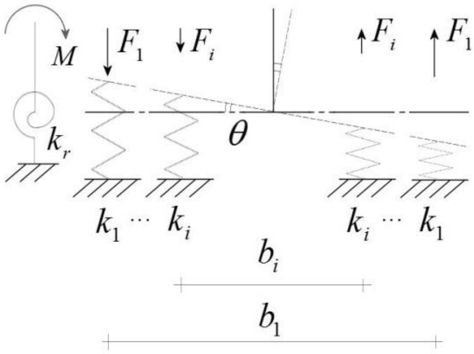

figure 3.46: Schematics Rotational Spring

The calculation of the spring stiffness that represents the foundation beneath the tube structure for variant 3 and the core according to equation (3.80) and (3.81) is given in table 3.23.

	n	m	k	b	k_{uni}	k_r
equation:	-	-	-	-	(3.80)	(3.81)
	[-]	[-]	[N/m]	[m]	[Nm/rad]	[N/m]
Tube foundation	16	7	$1{,}41 \cdot 10^9$	Var.	$2{,}26 \cdot 10^{10}$	$3{,}21 \cdot 10^{12}$
Core foundation	9	3	$2{,}03 \cdot 10^9$	14,40	$3{,}53 \cdot 10^{10}$	$1{,}22 \cdot 10^{12}$

table 3.23: Unified Spring Stiffness of the Foundation

3.13.6 Universal Support Stiffness

The stiffness for the categorized variants and individual structural components is given in table 3.24.

Support	Spring stiffness (k) N/m	Rotational stiffness (k_r) Nm/rad
Tube Support Variant 1 to 3	$1{,}41\ 10^9$	0,00
Tube Support Variant 4	$3{,}92\ 10^9$	0,00
Unified Support 1D-model	$2{,}26 \cdot 10^{10}$	$3{,}21 \cdot 10^{12}$
Unified Core Support all models	$3{,}53 \cdot 10^{10}$	$1{,}22\ 10^{12}$

table 3.24: Support Stiffness Values

The spring stiffness values in table 3.24 are representative for the stiffness of the foundation and are used in the framework calculation models of the case study.

3.13.7 Pile Load-Bearing Capacity

The representative load-bearing capacity of a single pile is determined by the capacity of the pile head and the friction along the shaft of the pile, as shown in equation (3.82).

$$F_{r,\max} = F_{r,\max,p} + F_{r,\max,f} \tag{3.82}$$

The load-bearing capacity of the pile head is determined by the pile head area and the soil resistance, and the shaft friction resistance is determined by the shaft friction and the average perimeter of the pile. Hence NEN 6773 suggests equations (3.83) and (3.84) in which the shaft friction and the pile head pressure are defined as in equations (3.85) and (3.86) respectively.

$$F_{r,\max,head} = A_{head} \cdot p_{r;\max;head} \tag{3.83}$$

$$F_{r,\max;shaft} = O_{s;\Delta L;gem} \cdot \int_{\Delta L} p_{r;\max;shaft} \tag{3.84}$$

$$p_{r;\max;head} = \alpha_p \times \beta_s \times s \times q_c \tag{3.85}$$

$$p_{r;\max;shaft} = \alpha_s \times q_c \tag{3.86}$$

In which (bored piles):

$\alpha_p = \quad 0,50$

$\beta_s = \quad 1,00$

$s = \quad 1,00$

$\alpha_s = \quad 0,006$

The soil assumption made in paragraph 3.13.3 gives rise to the use of the following parameters of which the cone resistance is based on the value of clean sand with a moderate consistency found in table 1 of NEN 6770:

$$\Delta L = \quad 5,00 \quad [m]$$
$$q_c = \quad 15 \quad [MPa]$$

The calculation of the load-bearing capacity of individual piles according to equations (3.82) to (3.86) combined with equation (3.79) is given in table 3.25.

D	A	$F_{r,max}$
equation:	(3.79)	(3.82)
[m]	[m^2]	[kN]
1,50	1,767	15374
2,00	3,142	28946
2,50	4,909	40351

table 3.25: Load Bearing Capacity of Individual Piles

The pile capacity values in table 3.25 are compared with the support reactions of framework calculation models and therefore, so, to verify the assumed support stiffness.

3.14 Load Cases

The structure and structural components of the building are loaded by the following load cases:

- Self Weight Main Structure LC1;
- Permanent Floor Loads LC2;
- Permanent Façade Loads LC3;
- Variable Floor Loads LC4;
- Wind load LC5;
- Equivalent Wind Load LC6;
- Dynamic Wind Load LC7.

3.14.1 Self Weight Main Structure (LC1)

The self weight of the main structure is calculated by Oasys-GSA software with the feature gravity loading.

3.14.2 Permanent Floor Load (LC2)

The permanent floor loads consist of:

- Self Weight Floor LC2a;
- Additional Floor Load LC2b;

Self Weight Floor

The self weight originating from the floor layup is shown in table 3.26. The assumption of the floor solution for sound insulation is based on the dry timber floor solution of 'Projekt 8+' documented in ref. [5].

Floor Layup Solution				
Thickness	Material	Weight		Floor load
200 mm	Raised floor system	80,0	kg/m^2	0,80 kN/m^2
25 mm	Dry screed elements	30,0	kg/m^2	0,30 kN/m^2
30 mm	Sound insulation layer	130,0	kg/m^3	0,03 kN/m^2
25 mm	Split gravel	16,0	kN/m^3	0,40 kN/m^2
301 mm	Cross Laminated Timber	900,0	kg/m^3	1,65 kN/m^2
30 mm	Gypsum fiber board	9,00	kg/m^3	0,27 kN/m^2
611 mm	Total floor load			3,45 kN/m^2

table 3.26: Self Weight originating from Floor Construction

Additional Floor Load

In order to take account for additional loads originating from commonly used light-weight partition walls, pipes and ducts for services the following loads are added. The additional permanent floor loads are shown in table 3.27.

Additional permanent floor load				
Thickness	Material	Weight		Floor load
-	Static partition walls	G < 1,0	kN/m^1	0,50 kN/m^2
-	Pipes and ducts	50	kg/m^2	0,50 kN/m^2
	Total floor load			1,00 kN/m^2

table 3.27: Permanent floor Loads

Total Permanent Floor Load

The sum of the permanent floor loads is shown in table 3.28.

Total permanent floor load				
Thickness	Material	Weight		Floor load
611 mm	Self weight floor layup	285	kg/m^2	3,45 kN/m^2
3089 mm	Additional loads	150	kg/m^2	1,00 kN/m^2
3500 mm	Total floor load			4,45 kN/m^2

table 3.28: Total Permanent Floor Load

3.14.3 Façade Loads (LC3)

The load originating from the façade is a product of the self-weight of the curtain wall. When the solid wall structure is used, additional cladding has to be accounted for, which is assumed to be of similar magnitude as a curtain wall solution. In table 3.29 the load of the façade is calculated.

Curtain wall				
Thickness	Material	Weight		Floor load
34 mm	Double glazing	63,0	kg/m^2	2,21 kN/m^1
190 mm	Alum. frame (190 x 50)	0,07	kN/m^2	0,24 kN/m^1
190 mm	Total load			2,45 kN/m^1

table 3.29: Permanent Façade Loads

3.14.4 Variable Floor Load (LC4)

The variable load originating from people and furniture is shown in table 3.30 and is based on table 6.1 and table 6.2 of EN 1991-1-1 in combination with the Dutch the national annex.

Variable floor load		
Load	Category	Floor load
Imposed	B Office Areas	2,50 kN/m^2

table 3.30: Variable Floor Load

3.14.5 Variable Wind Load (LC5)

The only significant horizontal load that acts on the structure is the wind load. The wind loads are based on the European standard EN 1991-1-4. The general equations to calculate the wind load are given in (3.87) and (3.88). To calculate the wind loads, a maple file is used for quick adjustments, which is shown in appendix B.1. The wind loading spectrum over the height for the universal tall building design is best displayed in the graph of figure 3.47.

$$Q_w = c_s c_d \cdot c_f \cdot q_p(z) \tag{3.87}$$

In which:

$c_s c_d = 1,00$

$c_f = 1,39$

$$q_p(z) = \left(1 + 7 \cdot l_v(z)\right) \cdot \tfrac{1}{2} \cdot \rho \cdot v^2{}_m(z) \tag{3.88}$$

In which:

$\rho = 1,25$

The largest wind load occurs between the top of the building at 112 m high and 30 m below the top at 82 m height. The smallest wind load occurs between the base of the building and 30 m above the base. The wind load values that result from the calculations in appendix B.1 are given in equation (3.89) and (3.90) for 30 m and 112 m high.

$$q_p\begin{pmatrix} b \\ h \end{pmatrix} = \left(1 + 7 \cdot \begin{bmatrix} 0.20 \\ 0.16 \end{bmatrix}\right) \cdot \tfrac{1}{2} \cdot 1,25 \cdot \begin{bmatrix} 28.4^2 \\ 35.9^2 \end{bmatrix} = \begin{bmatrix} 1210 \\ 1708 \end{bmatrix} \cdot \left[N/m^2 \right] \tag{3.89}$$

$$\overline{Q_w}\begin{pmatrix} b \\ h \end{pmatrix} = 1,00 \cdot 1,39 \cdot \begin{bmatrix} 1210 \\ 1708 \end{bmatrix} = \begin{bmatrix} 1682 \\ 2374 \end{bmatrix} \cdot \left[N/m^2 \right] \tag{3.90}$$

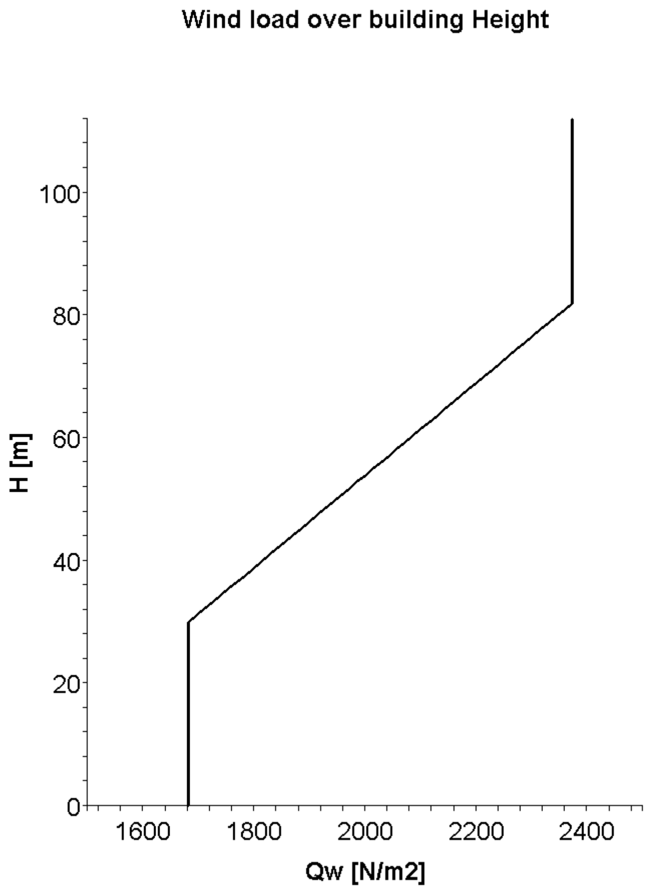

figure 3.47: Wind Load over the Building-height

Between 30 m and 82 m high, the wind load must be interpolated, which can be done with equation (3.91). Substitution of the known values gives the simplified equation (3.92).

$$Q_w(z) = \frac{Q_w(h) - Q_w(b)}{h - 2 \cdot b} \cdot (z - b) + Q_w(b) \qquad \textbf{(3.91)}$$

$$Q_w(z) = \frac{2374 - 1682}{112 - 2 \cdot 30} \cdot (z - 30) + 1682 \approx \frac{173}{13} \cdot z + 1283 \qquad \textbf{(3.92)}$$

The total variable lateral load originating from wind is shown in table 3.31.

Variable Wind Load Load Height	Value	Units
0m - 30m	1,68	kN/m^2
30 - 82	13,3·z+1,28	kN/m^2
82 - 112	2,37	kN/m^2

table 3.31: Variable Wind Load

3.14.6 Equivalent Wind Load (LC6)

For some calculations or quick global evaluations it is convenient to know the equivalent uniform distributed lateral wind load (q_{eq}) that effects in the same bending moment at the base. This is derived trough the calculation of the bending moment as in equation (3.93) combined with the values of table 3.31 and backward substitution in equation (3.94). The equivalent wind load is shown in table 3.32

$$M = \int_0^l q(x) \cdot x \cdot dx \tag{3.93}$$

$$M = \frac{1}{2} q_{eq} \cdot l^2 \rightarrow q_{eq} = \frac{2 \cdot M}{l^2} \tag{3.94}$$

Equivalent Wind Load	Value	Units
Uniform load	2,18	kN/m^2

table 3.32: Equivalent Wind Load

3.14.7 Dynamic Wind Load (LC7)

According to NEN 6702, the dynamic part of the wind load is described by equation (3.95) which results in the value given in table 3.33 for the height of the universal tall building. The dynamic wind load is taken as component or in other words part of the total wind load based on a literal interpretation of NEN 6702.

$$\tilde{p}_{w,1} = 100 \cdot \ln\left(\frac{h}{0,2}\right) \tag{3.95}$$

In which:
$\tilde{p}_{w,1}$ = dynamic part of the wind load
h = building height

Dynamic Wind Load	Value	Units
Uniform load	0,63	kN/m^2

table 3.33: Dynamic Wind Load

3.14.8 Summary Load Cases

The load cases are summarized in table 3.34.

Load Case	Name	Value	Units
LC 1	Self weight main structure	-	
LC 2	Permanent floor loads	4,45	kN/m^2
LC 3	Permanent façade loads	2,45	kN/m^1
LC 4	Variable floor load	2,50	kN/m^2
LC 5	Variable wind load	$1,68 < {}^{173}/_{13000} \cdot z + 1,28 < 2,37$	kN/m^2
LC 6	Equivalent wind load	2,18	kN/m^2
LC 7	Dynamic wind load	0,63	kN/m^2

table 3.34: Summary of Load Cases

3.15 Load Combinations

The load combinations are based on NEN 6702, safety classification 3 and consist of the following:

- ULS Combination 1 C1;
- ULS Combination 2 C2;
- SLS Combination C3;
- ULS Fire Combination C4;
- SLS Dynamic Combination C5;
- Quasi-Permanent Combination C6.

The load combinations are imposed onto the following models:

- Floor Structure;
- Main Structure.

3.15.1 Floor Structure

The load cases are imposed to the beam calculation model of the floor in following manor:

- LC 2 is multiplied with the floor strip width (1,00 m).
- LC 4 is applied equivalent to LC 2.
- LC 5 is multiplied with the floor height (3,50 m) in order to take into account the load transfer function of the floor between the main structural components.

The load combinations for the floor structure are determined according to table 3.35.

Load Combinations	LC 1	LC 2	LC 3	LC 4	LC 5	LC 6	LC 7
C1: ULS 1	-	1,20	-	1,50	-	1,50	-
C2: ULS 2	-	1,35	-	0,00	-	0,00	-
C3: SLS	-	1,00	-	1,00	-	1,00	-
C4: ULS Fire	-	-	-	-	-	-	-
C5: SLS Dynamic	-	-	-	-	-	-	-
C6: Quasi-Permanent	-	-	-	-	-	-	-

table 3.35: Load Combinations Floor-Structure

3.15.2 Main Structure

The ψ_0 factor for office buildings is 0,50. A Ψ-factor of 0,20 is taken into account for the wind load case in the fire combination (C4), in accordance with NEN 6702. The load combinations for the main load bearing structure with inclusion of these factors are defined as given in table 3.36.

For calculation of the main structure EN 1991-1-1 prescribes a facultative reduction factor (α_n) for the variable floor load according to equation (3.96) and results in α_n=0,53. This factor will be incorporated in the next chapter of this thesis were the loads are processed for the input of models.

$$\alpha_n = \frac{2+(n-2)\cdot\psi_0}{n} \tag{3.96}$$

In which:
n = the number of storey's (32)
Ψ_0 = 0,50

Load Combinations	LC 1	LC 2	LC 3	LC 4	LC 5	LC 6	LC 7
Description:	Self-Weight	Perm. Floor	Var. facade	Var. Floor	Var. Wind	Eq. Wind	Dynamic Wind
C0: ULS	1,20	1,20	1,20	1,50	1,50	-	-
C1: ULS	1,35	1,35	1,35	0,75	0,75		
C2: ULS	0,90	0,90	0,90	0,00	1,50	-	-
C3: SLS	1,00	1,00	1,00	1,00	1,00	-	-
C4: ULS Fire	1,00	1,00	1,00	1,00	0,20	-	-
C5: SLS Dynamic	1,00	1,00	1,00	1,00	0,73	-	0~1,00
C6: Quasi-Permanent	1,00	1,00	1,00	0,50	0,00	-	-

table 3.36: Load Combinations Tube-Structure

3.16 Floor Span Calculation

This paragraph concerns the structural analysis and verification calculation of the floor structure in order to prove feasibility. To make the design of the floor economical it is chosen to design cross laminated timber elements that span the distance of 7,20 m between the core and the tube structure without intervention of beam elements. This is possible for most of the floor area, except for the corners of the building which must consist of a floor and supporting beam layup. The floor consists of seven layer thick D70-CLT, in which each layer is 43 mm, thus resulting in a 301 mm thick plate. The corner beam is a 300x500 mm rectangular section of D70-LAM. This construction is representative for all the case study variants.

3.16.1 Floor Model Description

The Kreuzinger beam model is used to calculate the bending behavior of the floor as described in paragraph 3.8.1 on page 78. The model is created with GSA software.

Section Properties: The input for the beam sections are explicitly applied to the model as formulated in table 3.4 for a seven layer thick element and 7200 mm length.

Shear factor: For beam A the shear factor is set to zero, while for beam B the shear modifier is set to 1 and the appropriate section area as shown in table 3.4 is applied to beam B.

Loads on models: The loads are imposed on the beam model as described in paragraph 3.15.1.

3.16.2 Calculated Forces

The relevant results from the calculation of the GSA software are given in table 3.37.

Name	$F_{z,max}$ (ULS) [N]	$M_{yy,max}$ (ULS) [Nm]	w_{max} (SLS) [mm]	Θ_{max} (SLS) [rad]
Beam A	558	1016	7,54	0,0034
Beam B	28500	57110	7,54	0,0032

table 3.37: Results of GSA-Calculation

3.16.3 Verification Calculation

The bending moments and the shear-forces of table 3.37 are distributed proportionally to the stiffness of individual layers, according to equations (3.97) to (3.100) which originate from [28]. The stresses are then calculated using these forces taking into account the section properties of the individual layers according to equations (3.101) to (3.103) which also originate from [28]. This calculation procedure is done with a maple file shown in appendix B.3.

$$M_i = \frac{E_i \cdot I_i}{(EI)_A} \cdot M_A \tag{3.97}$$

$$N_i = \frac{E_i \cdot A_i \cdot z_i}{(EI)_B} \cdot M_B + \frac{E_i \cdot A_i}{\sum_{i=1}^{n} E_i \cdot A_i} \cdot N \tag{3.98}$$

$$\tau_{A,i} = \frac{E_i \cdot I_i}{(EI)_A} \cdot Q_A \cdot \frac{3}{2} \cdot \frac{1}{d_i \cdot b_i} \tag{3.99}$$

$$\tau_{B,i,i+1} = \frac{Q_B}{(EI)_B} \cdot \frac{\sum_{i=1}^{i} E_i \cdot A_i \cdot z_i}{\min\begin{cases} b_i \\ b_{i+1} \end{cases}} \qquad (3.100)$$

$$\sigma_{m,i} = \frac{M_i}{W_i} \qquad (3.101)$$

$$\sigma_{c,i} \text{ or } \sigma_{t,i} = \frac{N_i}{A_i} \qquad (3.102)$$

$$\begin{aligned} \tau_{max,i} &= \tau_{A,i} + \tau_{1,i} + \frac{\tau_{2,i}}{2} + \frac{\tau_{2,i}^2}{16 \cdot \tau_{A,i}} && \text{if } \tau_{A,i} > \frac{\tau_{2,i}}{4} \\ \tau_{max,i} &= \tau_{1,i} + \tau_{2,i} && \text{if } \tau_{A,i} \le \frac{\tau_{2,i}}{4} \end{aligned} \qquad (3.103)$$

The bending stress, normal stress and shear stress calculated in appendix B.3 are given below for the maximum stressed layers both parallel and perpendicular to the grain of the 7 layer thick floor element.

$$\sigma_{m,0} = 0.785 \quad \left[{}^{N}\!/_{mm^2}\right] \qquad \sigma_{n,0} = 4,558 \quad \left[{}^{N}\!/_{mm^2}\right] \qquad \tau_{\max,0} = 0.134 \quad \left[{}^{N}\!/_{mm^2}\right]$$

$$\sigma_{m,90} = 0.05 \quad \left[{}^{N}\!/_{mm^2}\right] \qquad \sigma_{n,90} = 0,203 \quad \left[{}^{N}\!/_{mm^2}\right] \qquad \tau_{\max,90} = 0.134 \quad \left[{}^{N}\!/_{mm^2}\right]$$

Ultimate limit state (ULS) verification

The base material used for D70-CLT is D70. The material factor is chosen to be 1,20 similar as for conventional laminated timber. The modification factor of 0,80 is based on a medium-long load duration and environment class 2 for laminated timber. Therefore the design values are calculated with equation (3.104). The design values of the applied material are given below.

$$f_{x,\alpha,d} = \frac{f_{x,\alpha,k}}{\gamma_M} \cdot k_{\text{mod}} = \frac{f_{x,\alpha,k}}{1,25} \cdot 0,80 = f_{x,\alpha,k} \cdot 0,64 \qquad (3.104)$$

$$f_{m,d} = 70 \cdot 0,64 = 44,80 \quad \left[{}^{N}\!/_{mm^2}\right] \qquad f_{c,0,d} = 34 \cdot 0,64 = 21,76 \quad \left[{}^{N}\!/_{mm^2}\right]$$

$$f_{t,0,d} = 42 \cdot 0,64 = 26,90 \quad \left[{}^{N}\!/_{mm^2}\right] \qquad f_{t,90,d} = 0,6 \cdot 0,64 = 0,38 \quad \left[{}^{N}\!/_{mm^2}\right]$$

$$f_{v,d} = 6 \cdot 0,64 = 3,84 \quad \left[{}^{N}\!/_{mm^2}\right] \qquad f_{R,d} = 1,0 \cdot 0,64 = 0,64 \quad \left[{}^{N}\!/_{mm^2}\right]$$

Equations (3.105) and (3.106) give the general formulation for the ULS check for the combination of bending and tension parallel to the grain. Because the bending in the orthogonal direction is absent under unidirectional bending the calculation is reduced to equations (3.107) and (3.108). The ULS verification for rolling shear is not stated in the Dutch standards nor the Euro codes, therefore the verification is based on the German code DIN 1052:2004, given in equation (3.109).

$$\frac{\sigma_{t,0,d}}{f_{t,0,d}}+\frac{\sigma_{m,y,d}}{f_{m,y,d}}+\frac{\sigma_{m,z,d}}{f_{m,z,d}}\leq 1 \quad and \quad \left(\frac{\tau_d}{f_{v,d}}\right)^2+\left(\frac{\tau_{drill,d}}{f_{v,d}}\right)^2\leq 1 \tag{3.105}$$

$$\frac{\sigma_{c,0,d}}{f_{c,0,d}}+\frac{\sigma_{m,y,d}}{f_{m,y,d}}+\frac{\sigma_{m,z,d}}{f_{m,z,d}}\leq 1 \tag{3.106}$$

$$\frac{\sigma_{t,0,d}}{f_{t,0,d}}+\frac{\sigma_{m,y,d}}{f_{m,y,d}}\leq 1 \quad and \quad \frac{\tau_d}{f_{v,d}}\leq 1 \tag{3.107}$$

$$\frac{\sigma_{c,0,d}}{f_{c,0,d}}+\frac{\sigma_{m,y,d}}{f_{m,y,d}}\leq 1 \tag{3.108}$$

$$\frac{\sigma_{t,90,d}}{f_{t,90,d}}+\frac{\tau_{R,d}}{f_{R,d}}\leq 1 \quad or \quad \frac{\sigma_{c,90,d}}{f_{c,90,d}}+\frac{\tau_{R,d}}{f_{R,d}}\leq 1 \tag{3.109}$$

It is suggested in the DIN 1052:2004 that when perpendicular layers are executed in cut lumber the modulus of elasticity for these layers go to zero, which results in zero stress. For the seven layer thick element this implies:

layers parallel to the grain:

$$\frac{\sigma_{t,0,d}}{f_{t,0,d}}+\frac{\sigma_{m,y,d}}{f_{m,y,d}}=\frac{4,56}{26,90}+\frac{0,79}{44,80}=0,17+0,02=0,19\leq 1$$

$$\frac{\tau_d}{f_{v,d}}=\frac{0,15}{3,84}\leq 1$$

$$\frac{\sigma_{t,0,d}}{f_{t,0,d}}+\frac{\sigma_{m,y,d}}{f_{m,y,d}}=\frac{4,56}{26,90}+\frac{0,79}{44,80}=0,17+0,02=0,19\leq 1$$

$$\frac{\tau_d}{f_{v,d}}=\frac{0,15}{3,84}\leq 1$$

layers perpendicular to the grain

$$\frac{\sigma_{t,90,d}}{f_{t,90,d}}+\frac{\tau_{R,d}}{f_{R,d}}=\frac{0,20}{0,38}+\frac{0,13}{0,64}=0,53+0,20=0,73\leq 1$$

The seven layer and thick floor element meets the ultimate limit state requirements. In the following, the serviceability limit state verification is executed.

Serviceability Limit State (SLS) verification
The largest theoretical span of the floor is 7200 mm. The final deflection and the additional deflection are checked according to NEN 6702. The deflection was 7,54 mm for the seven layer thick floor element. The instantaneous deflection under dead and live load are calculated linearly as in equations (3.110).

$$u_{inst,G} = u_{inst,G+Q} \cdot \frac{G}{G+Q} \qquad u_{inst,Q} = u_{inst,G+Q} \cdot \frac{Q}{G+Q} \tag{3.110}$$

In which:

$$G = 4,45 \qquad \left[{}^{kN}\!/\!{}_{m^2} \right]$$

$$Q = 2,50 \qquad \left[{}^{kN}\!/\!{}_{m^2} \right]$$

The load factor $\psi_{2,1}$ is 0,30 for office buildings according the Dutch national annex of EN-1995. The modification factor k_{def} is 0,80 for laminated timber according to EN-1995. The final and the additional deflection are calculated as in equations (3.111) to (3.113).

$$u_{fin} = u_{fin,G} + u_{fin,Q} \tag{3.111}$$

$$u_{fin,G} = u_{inst,G} \cdot \left(1 + k_{def}\right) \tag{3.112}$$

$$u_{fin,Q} = u_{inst,Q} \cdot \left(1 + \psi_{2,1} \cdot k_{def}\right) \tag{3.113}$$

The maximum allowable deflection according to the Dutch standard NEN 6702 is $^{4}/_{1000}$ of the span which results in 28,8 mm. The combination of equations (3.111) to (3.113) leads to a simple check for the final deflection in equation (3.114).

$$u_{fin} = u_{inst,G+Q} \cdot 1,60 \tag{3.114}$$

For the seven layer element the manual calculation with equation (3.114) resulted in a final deflection of 12,1 mm, which did meet the standard of 28,8 mm ($^{4}/_{1000} \cdot 7200$ mm).

3.16.4 Calculation of Corner Beams

There are several solution thinkable for the design of corner beams. The same problem was encountered in the steel frame of the Rembrandt Tower in Amsterdam the Netherlands. The optimal solution was believed to be found in a large floor beam that runs from the corner of the building perimeter to the corner of the building core, as shown in figure 3.48. The theoretical span of the floor beam is 10,18 m for this case.

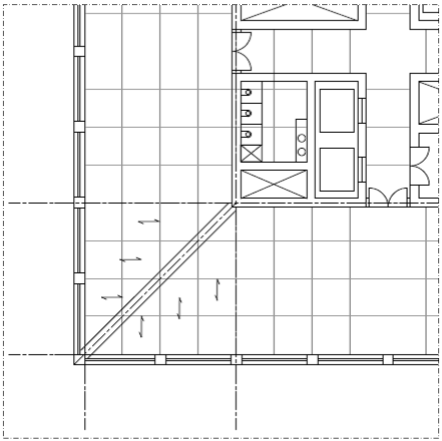

figure 3.48: Floor Beam Solution

figure 3.49: Shape Factor For Loading

3.16.4.1 Model Description

The calculations were executed with a GSA beam model with the following input:

Material properties: D70-LAM, as described in paragraph 3.6.2.
Section: 300 mm x 500 mm (Standard Rectangular Section).
Loading on the Model: The floor load as described in paragraph 3.15.1 is applied the beam model with incorporation of a shape factor. The shape factor is trapezium shaped and starts at 0,0 at the beginning running to 3,6 times at the end of the beam as shown in figure 3.49.

3.16.4.2 Calculated Forces

The result of the calculation by GSA are given in table 3.38.

Name	$F_{z,max}$ (ULS) [N]	$M_{yy,max}$ (ULS) [Nm]	w_{max} (SLS) [mm]	Θ_{max} (SLS) [rad]
300x500 mm, D70-LAM	109600	209200	24,26	0,008

table 3.38: Relevant Results of GSA-Model

3.16.4.3 Calculation of stresses

The calculation of stresses in the corner beams is a straight forward task. The stresses are generally low within the beam, which could be judged as uneconomic. The calculation is given below.

$$W = \frac{1}{6} b \cdot h^2 \rightarrow \frac{1}{6} \cdot 300 \cdot 500^2 = 12,5 \cdot 10^6 \cdot \left[mm^4 \right]$$

$$\sigma_m = \frac{M_y}{W_y} \rightarrow \frac{209,2 \cdot 10^6}{12,5 \cdot 10^6} = 16,7 \cdot \left[\frac{N}{mm^2} \right]$$

$$\tau_d = \frac{V \cdot S_y}{t \cdot I_y} = \frac{2 \cdot V}{3 \cdot b \cdot h} \rightarrow= \frac{3 \cdot 109600}{2 \cdot 300 \cdot 500} = 1,10 \cdot \left[\frac{N}{mm^2} \right]$$

3.16.4.4 Ultimate limit state (ULS) verification

Design values:

$$f_{m,d} = \frac{f_{m,k}}{\gamma_M} \cdot k_{mod} \rightarrow f_{m,d} = \frac{70}{1,25} \cdot 0,80 = 44,8$$

$$f_{v,d} = \frac{6,0}{1,25} \cdot 0,80 = 3,8$$

Unity check:

$$\frac{\sigma_{m,y,d}}{f_{m,y,d}} \leq 1 \rightarrow \frac{16,7}{44,8} = 0,37 \leq 1$$

$$\frac{\tau_d}{f_{v,d}} \leq 1 \rightarrow \frac{1,10}{3,8} = 0,29 \leq 1$$

3.16.4.5 Serviceability limit state (SLS) verification

The SLS deflection requirement for the floor beam with a span of 10180 mm results in 40,7 mm. The final deflection of the corner beam using equation (3.114) resulted in 38,8 mm which satisfies the standard requirement. The height of the floor layup is 410 mm, excluding the raised floor system. This implies that the corner-beam of 500 mm high beam has a 90 mm overlap which is either easily glossed under the raised floor or the suspended ceiling.

3.16.5 Summary

The absence of floor beams is believed to increase the building speed and therefore make the building design economically more feasible. In this paragraph it is shown that a timber floor could span the total building depth of 7200 mm of the case study design without intervention of additional floor beams, except in the corners of the building.

> The floor structure of 7 layer thick D70-CLT combined with a 300 x 500 mm rectangular section of D70-LAM in the corners of the building plan satisfies the requirements.

4 Universal Model Properties

4.1 Equipment

The software and the computer system that is used to conduct finite element analysis and create the associated finite element models are described below.

Software
GSA-OAYSIS 8.5 build 14

Computer system

The operation system:	Windows XP Home Edition SP3
CPU:	Intel Celeron D 3.20 GHz
Internal memory:	1,99 GB

4.2 Build-up Models

A general visualization of the models is given in figure 4.1 and shows that the model, like the building is build up around the core. The core elements are spaced between central nodes which are linked with 3D springs to the nodes of the tube. The tube elements are spaced between these last mentioned nodes. The tube elements are geometrically orientated in accordance with the systems geometry.

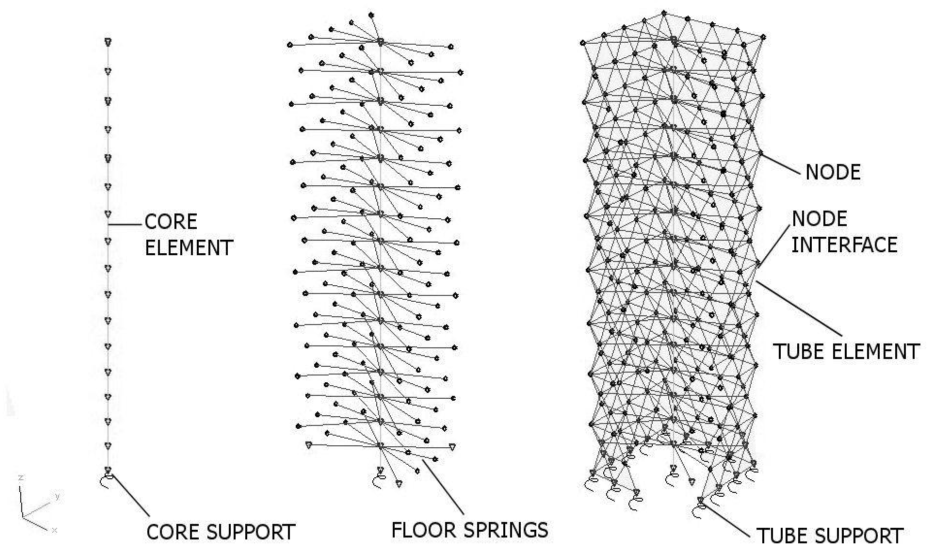

figure 4.1: General visualization of models

Per variant several models are created for analysis. This is necessary because different parameters are investigated. The differences in the models manifest in the following manor. The first model (BASE) is the template for all the other models of the same variant. Then the changes are made in:

- Support stiffness;
- Core stiffness and;
- Joint stiffness.

4.2.1 Axis definition

The definition of the local and the global axis sets is as given in figure 4.2. The global Z-axis is parallel to the vertical, in other words parallel to the core elements. The local x-axis of linear elements is parallel to the direction of that element. The local z-axis is equal to the positive global Z-axis, which is the software's default for horizontal elements. In models with vertical elements the orientation of linear elements is rotated around the local x-axis in order to orientate the local y-axis parallel to the inside of the building. This is done because the default local y-axis for vertical elements is parallel to the positive global Y-axis which gives problems with the assignment of beam-releases, hence joint stiffness assignment.

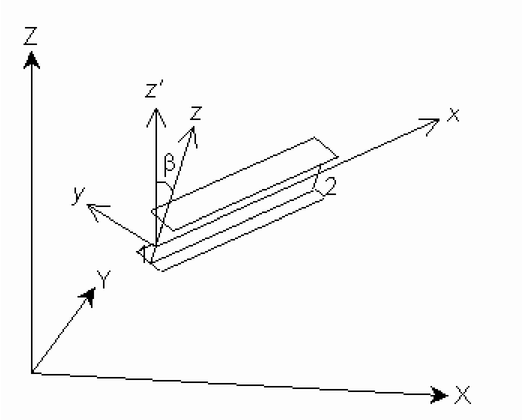

figure 4.2: Global Axis definition [29]

The rotations about the axes follow the right hand screw rule. The rotations are indicated as xx for the rotation around the x-axis and yy and zz respectively around the y-axis and z-axis.

4.2.2 Element Typology

The linear elements used in the models are called either BEAM, BAR or SPRING. The plate elements used in the models are called QUAD 8 indicating 2D isoparametric elements. The full definition of these elements is given in ref. [29].

BEAM: Beam elements have six degrees of freedom at nodes, include bending terms in the stiffness matrix and can either include or exclude shear deformations. The shear effects are ignored if the shear factor is set to zero for which the reduced element stiffness matrix is shown in figure 4.3. The default shear factor is 1 and is preserved unless specified otherwise. The element stiffness matrix in figure 4.3 is modified as shown in figure 4.4 to include shear deformation.

$$[k]=\begin{bmatrix}
\frac{AE}{l} & 0 & 0 & 0 & 0 & 0 & -\frac{AE}{l} & 0 & 0 & 0 & 0 & 0 \\
 & \frac{12EI_{xx}}{l^3} & 0 & 0 & 0 & \frac{6EI_{xx}}{l^2} & 0 & -\frac{12EI_{xx}}{l^3} & 0 & 0 & 0 & \frac{6EI_{xx}}{l^2} \\
 & & \frac{12EI_{yy}}{l^3} & 0 & -\frac{6EI_{yy}}{l^2} & 0 & 0 & 0 & -\frac{12EI_{yy}}{l^3} & 0 & -\frac{6EI_{yy}}{l^2} & 0 \\
 & & & \frac{GJ}{l} & 0 & 0 & 0 & 0 & 0 & -\frac{GJ}{l} & 0 & 0 \\
 & & & & \frac{4EI_{yy}}{l} & 0 & 0 & 0 & \frac{6EI_{yy}}{l^2} & 0 & \frac{2EI_{yy}}{l} & 0 \\
 & & & & & \frac{4EI_{xx}}{l} & 0 & -\frac{6EI_{xx}}{l^2} & 0 & 0 & 0 & \frac{2EI_{xx}}{l} \\
 & & & & & & \frac{AE}{l} & 0 & 0 & 0 & 0 & 0 \\
 & & & & & & & \frac{12EI_{xx}}{l^3} & 0 & 0 & 0 & -\frac{6EI_{xx}}{l^2} \\
 & & & & & & & & \frac{12EI_{yy}}{l^3} & 0 & \frac{6EI_{yy}}{l^2} & 0 \\
 & & & & & & & & & \frac{GJ}{l} & 0 & 0 \\
 & & & & & & & & & & \frac{4EI_{yy}}{l} & 0 \\
 & & & & & & & & & & & \frac{4EI_{xx}}{l}
\end{bmatrix}$$

figure 4.3: Stiffness Matrix excluding Shear Deformation [29]

$$\alpha = 12\frac{EI_{ii}}{l^2 GA_s} \qquad A_s = Ak_j$$

$$\frac{2EI}{l} \rightarrow \frac{2-\alpha}{1+\alpha}\frac{EI}{l} \qquad \frac{6EI}{l^2} \rightarrow \frac{6}{1+\alpha}\frac{EI}{l^2}$$
$$\frac{4EI}{l} \rightarrow \frac{4+\alpha}{1+\alpha}\frac{EI}{l} \qquad \frac{12EI}{l^3} \rightarrow \frac{12}{1+\alpha}\frac{EI}{l^3}$$

figure 4.4: Shear Stiffness Modification [29]

BAR: Bar elements have four degrees of freedom and are considered to transfer axial loads only. The terms in the element stiffness matrix are based on axial stiffness (EA) and the length of the element as shown in figure 4.5.

$$[k] = \begin{bmatrix} \frac{AE}{l} & 0 & 0 & -\frac{AE}{l} & 0 & 0 \\ & 0 & 0 & 0 & 0 & 0 \\ & & 0 & 0 & 0 & 0 \\ & & & \frac{AE}{l} & 0 & 0 \\ & & & & 0 & 0 \\ & & & & & 0 \end{bmatrix}$$

figure 4.5: Bar Stiffness Matrix [29]

SPRING: Spring elements used in the models include axial and shear terms in the stiffness matrix of which the general element stiffness matrix is shown in figure 4.6.

$$[k] = \begin{bmatrix} k_x & 0 & 0 & -k_x & 0 & 0 \\ & k_y & 0 & 0 & -k_y & 0 \\ & & k_z & 0 & 0 & -k_z \\ & & & k_x & 0 & 0 \\ & & & & k_y & 0 \\ & & & & & k_z \end{bmatrix}$$

figure 4.6: Spring Stiffness Matrix [29]

QUAD 8: Quad 8 elements used in the models have a Flat Shell typology as defined in ref. [29] which include in-plane and out-of-plane effects. The elements have 8 notes each with 6 degrees of freedom. The local z-axis of 2D elements is always orientated perpendicular to the plain of the element. The orientation of the local x-axis and y-axis can be customized within the plain of the element.

4.2.3 Support stiffness

Two possibilities for the support stiffness are investigated. For both cases the supports are fixed in the horizontal plane. The vertical support stiffness is either as described in paragraph 3.13 and be referred to as SPRING or infinitely stiff, which will be referred to as FIXED. FIXED implies that the translation of tube supports, as defined in figure 4.1, are restrained in all directions, and the core support is restrained both in translation and rotation of all global directions.

4.2.4 Core stiffness

The stiffness of the core is adjusted through the alteration of the core elements. The section properties of core elements are as described in paragraph 3.14. In the models the core elements are either assigned as a BEAM or a BAR as defined in ref. [29], to analyze the influence of the core stiffness.

4.2.5 Joint Stiffness

Four possibilities for the joint stiffness are investigated, namely: TUBE-F, DOWEL, PINNED, RIGID. In the models, translational and rotational stiffness are assigned between nodes and elements orientated to the local axis of the beam with the application of beam releases [29] as shown in figure 4.7.

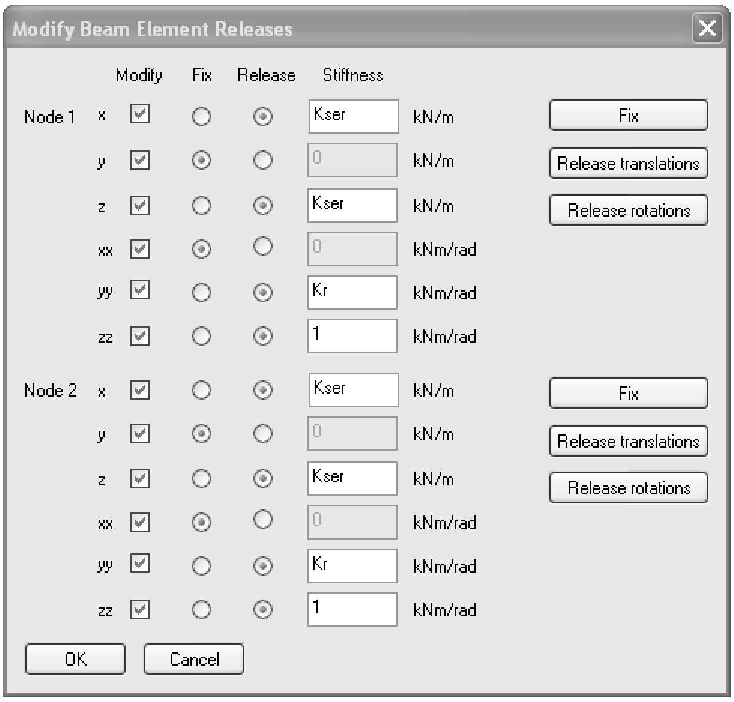

figure 4.7: Beam releases in GSA Software

In figure 4.7 the beam releases are figuratively modified to K_{ser} and K_r indicating the translational and rotational stiffness respectively. When in the following the rotational stiffness is described as free, then the rotational stiffness is set to 1 kNm/rad in the beam releases of the model, which is small by comparison. This is done because the value 0 can result in modeling errors (singularities).

TUBE-F: indicates that the joint stiffness is equal to the stiffness of tube fastener joints as described in paragraph 3.10. The values K_{ser} and K_r shown in figure 4.7 are replaced with joint stiffness values associated with the adjacent section and the tube fastener joint.

DOWEL: indicates that the joint stiffness is equal to the dowel fastener as described in paragraph 3.10. The values K_{ser} and K_r shown in figure 4.7 are replaced with joint stiffness values associated with the adjacent section and the doweled joint.

PINNED: indicates that all rotations (xx,yy,zz) are free and translations (x,y,z) are fixed .

RIGID: indicates that all rotations (xx,yy,zz) and translations (x,y,z) are fixed.

4.2.6 Floor Spring Stiffness

The floor elements function as in plane axial spacers and diaphragms between the tube structure and the core. To incorporate the influence of these finite stiffness's some geometrical assumptions are used to calculate the spring stiffness in the horizontal plane. The spring stiffness value in the axial direction is calculated by equation (4.1). The shear spring stiffness value of the floor is calculated by equation (4.3).

The net area per spring is calculated by equation (4.3) as a relation between the outer building width (w_{out}), the core width (w_{core}) and the average spacing of the tube nodes (a), in other words the spacing of the springs on the tube-frame side. The area spring stiffness value is multiplied a integer (n) because the vertical spacing of the tube-frame grid is equivalent to a number of floor heights. The modulus of elasticity (E) of the material (D70-CLT) and the thickness of the floor (t) are determined in paragraph 3.8.

$$k_x = \frac{EA}{l} \tag{4.1}$$

$$k_y = \frac{GA}{l} \tag{4.2}$$

$$A = n \cdot t \cdot a \cdot \frac{1}{2} \cdot \left(1 + \frac{w_{core}}{w_{tube}}\right) \tag{4.3}$$

In which:

k_x =	(local) axial spring stiffness	
E =	modulus of elasticity	12000 N/mm^2
A =	representative area	
l =	length of the floor section	7200 mm
G =	shear modulus	998 N/mm^2
t =	thickness floor	301 mm
a =	tube nodes spacing	
n =	number of floors involved	

The calculated floor spring stiffness's are given in table 4.1. Indices x and y associated with the spring stiffness k_i in this table are defined to the local axis of a spring. This implies that all springs represent a triangular portion (pie-section) of the floor of which the stiffness's orientates itself to the direction of the spring as shown in figure 4.8, resulting in a realistic way of modeling.

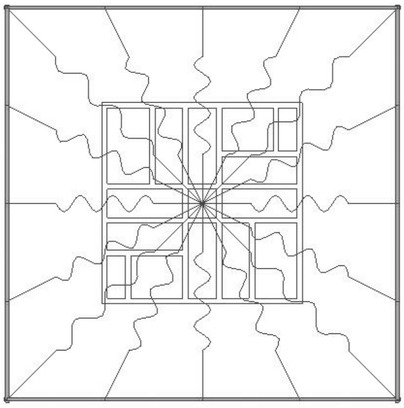

figure 4.8: Floor Spring Orientation

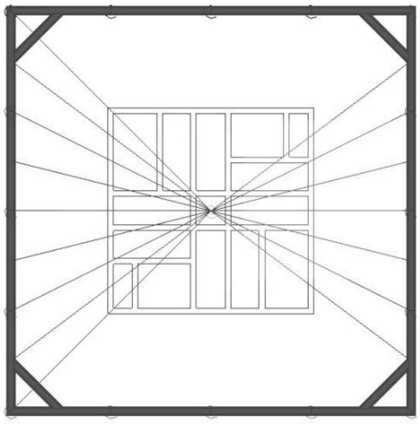

figure 4.9: Floor Springs

Variant	a mm	n -	axial stiffness (k_x) N/m	shear stiffness (k_y) N/m
1	8400	2	$6{,}32 \cdot 10^6$	$5{,}20 \cdot 10^5$
2 and 3	7200	2	$5{,}42 \cdot 10^6$	$4{,}46 \cdot 10^5$
4	3,500	1	$1{,}32 \cdot 10^6$	$1{,}09 \cdot 10^5$

table 4.1: Floor Spring Stiffness

The floor springs tend to take over the forces of the horizontal members of the tube elements. This behavior could be the case in reality, because the floors act as rigid diaphragms, and when properly connected in shear to the beams on the perimeter, composite action takes place. Here however this is assumed to be a modeling error. The wind load is imposed though forces on the tube nodes on the left side of the model and floor springs are cut out as shown in figure 4.9, to realize a conservative approach.

4.2.7 Loads

The uniform distributed load cases defined in paragraph 3.14 are converted into concentrated loads located at the nodes of the models. Herein a division of permanent an variable load is kept for load combinations purposes as defined in paragraph 3.15.

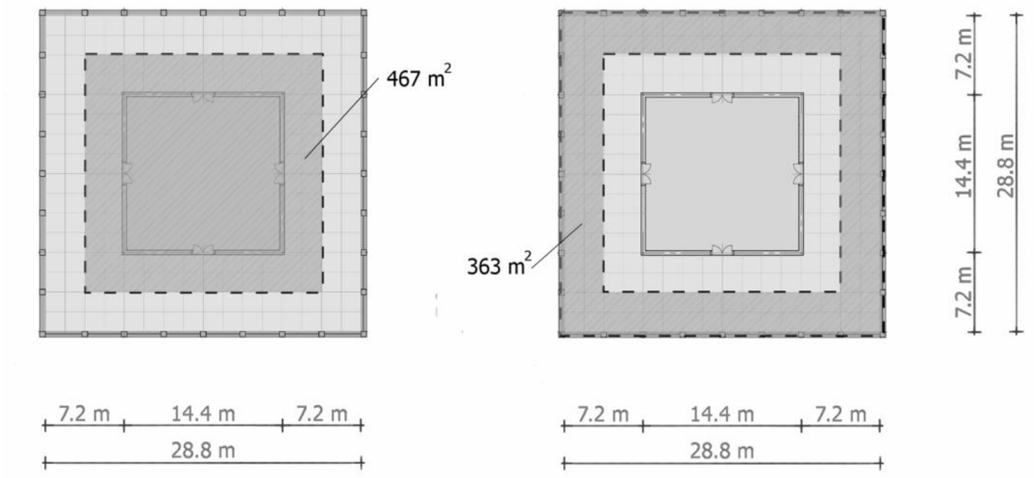

figure 4.10: Loaded Area Core and Tube Structure

4.2.7.1 Vertical loads

Because the floor is equally supported on both sides, the load on the floor span is equally divided between the core and the tube structure on the perimeter of the building as shown in figure 4.10. The vertical node spacing shown in figure 4.1 is a multiple of the floor spacing and is the same for the core nodes and tube structure nodes. The part of the vertical floor loads acting on the tube structure is equally distributed over the perimeter and therefore concentrated at the tube nodes. The vertical load on the core nodes is therefore calculated with (4.4) and the loads on the tube structure is calculated with (4.5) to (4.7). The index *i* can either be *p* for permanent or *q* for variable loading as suggested by equation (4.8).

$$F_{i;core,rep} = A_{corepart} \cdot Q_{i;rep} \cdot n_{floor} \tag{4.4}$$

$$F_{i;tube;rep} = q_{i;rep} \cdot l_{ctc} \cdot n_{floor} \tag{4.5}$$

$$q_{p;rep} = \frac{A_{tube}}{L_{tube}} \cdot Q_{p;rep} + q_{rep,facade} \tag{4.6}$$

$$q_{q,rep} = \frac{A_{tube}}{L_{tube}} \cdot Q_{q;rep} \cdot \alpha_n \tag{4.7}$$

$$i = \{q, p\} \tag{4.8}$$

In which:

$F_{i,core,rep}$ =	Vertical force acting on the core nodes	
$F_{i,tube,rep}$ =	Vertical force acting on the tube nodes	
$A_{corepart}$ =	Area of the floor load transferred to the core	467 m^2
$Q_{i,rep}$ =	Representative value of floor load with index i	
$q_{i,rep}$ =	Vertical distributed load on the tube structure with index i	
α_n =	Variable floor load reduction factor	0,53
A_{tube} =	Area of the floor load transferred to the tube structure	363 m^2
L_{tube} =	Length of the perimeter of the tube structure	155 m^1
l_{ctc} =	spacing of the tube nodes	
n_{floor} =	number of floors per node	

The calculations for the general case result in the following values:

$$F_{p;core,rep} = 467 \cdot 4,45 \cdot n_{floor} \rightarrow$$
$$F_{q;core,rep} = 467 \cdot (2,50 \cdot 0,53) \cdot n_{floor} \rightarrow$$
$$q_{p;rep} = \frac{363}{115} \cdot 3,45 + 2,45 \rightarrow$$
$$q_{q,rep} = \frac{363}{115} \cdot (2,50 \cdot 0,53) \rightarrow$$

$$F_{p;core,rep} = 2078 \cdot n_{floor} \qquad \cdot \left[{}^{kN}\!/_{node} \right]$$
$$F_{q;core,rep} = 619 \cdot n_{floor} \qquad \cdot \left[{}^{kN}\!/_{node} \right]$$
$$q_{p;rep} = 13,34 \qquad \cdot \left[{}^{kN}\!/_{m^1} \right]$$
$$q_{q,rep} = 4,18 \qquad \cdot \left[{}^{kN}\!/_{m^1} \right]$$

4.2.7.2 Static Wind loads

The static wind load case defined in paragraph 3.14 is imposed on the model through multiplication with the equivalent area as in equation (4.9) for the general case.

$$F_{w;node;rep}(z) = Q_{w;rep}(z) \cdot A_{eq;i} \tag{4.9}$$

In which:
$F_{w,node,rep}$ = Horizontal force acting on nodes
$Q_{w,rep}(z)$ = Representative value of wind load over height z
$A_{eq,i}(z)$ = Equivalent area

Because the wind load increases over the height as is described in paragraph 3.14, the wind load acting on nodes is calculated with equations (4.10) to (4.12) for the height *z* in meters.

$$F_{w;node;rep}(b) = Q_{w;rep}(0 < z < 30) \cdot A = \quad 1,68 \cdot A_{eq;i} \cdot kN / node \tag{4.10}$$

$$F_{w;node;rep}(z) = Q_{w;rep}(30 < z < 82) \cdot A = \quad \left(\frac{173}{13000} \cdot z + 1,28 \right) \cdot A_{eq;i} \cdot kN / node \tag{4.11}$$

$$F_{w;node;rep}(h) = Q_{w;rep}(82 < z < 112) \cdot A = \quad 2,37 \cdot A_{eq;i} \cdot kN / node \tag{4.12}$$

4.2.7.3 Dynamic wind loads

The dynamic response is determined through the use of an excitation of the static wind load case normalized to a time-load curve. The dynamic wind load case is defined in paragraph 3.14. The static wind load at the top of the building is defined in paragraph 4.2.7.2. A ratio of 0,27 can be established between the maximum static and the dynamic part of the wind load.

The wind load curve is shown in figure 4.11. It is reasonable to assume that the peak dynamic wind load only occurs when the static wind load is present, i.e. during a storm. This establishes a load factor running from 0,73 over some time (from 0 to 8 sec) to 1,00 during about half the eigen period (1-2 sec), for conservative results.

To make a fair analysis, the envelope of the results consists of the event after 9 seconds, because the structure starts from equilibrium at 0 seconds and will experience the event from 0 to 9 seconds as an excitation with a load factor of 0,73 of the static wind load, which is unrealistic.

The preference of a load curve that runs from 0,73 to 1,00 over a load curve that runs from 0,00 to 0,27 deserves some further explanation. First of all, it was experientially determined during this study that the structure can spring back to the other side of the equilibrium position when the wind load suddenly drops to zero, which resulted in unrealistically high accelerations. This was not the case with the chosen load curve.

Secondly, the behavior of the structure is different starting from the equilibrium position because, when not, some elements are in compression while others are in tension, which influences the local, hence the global stiffness.

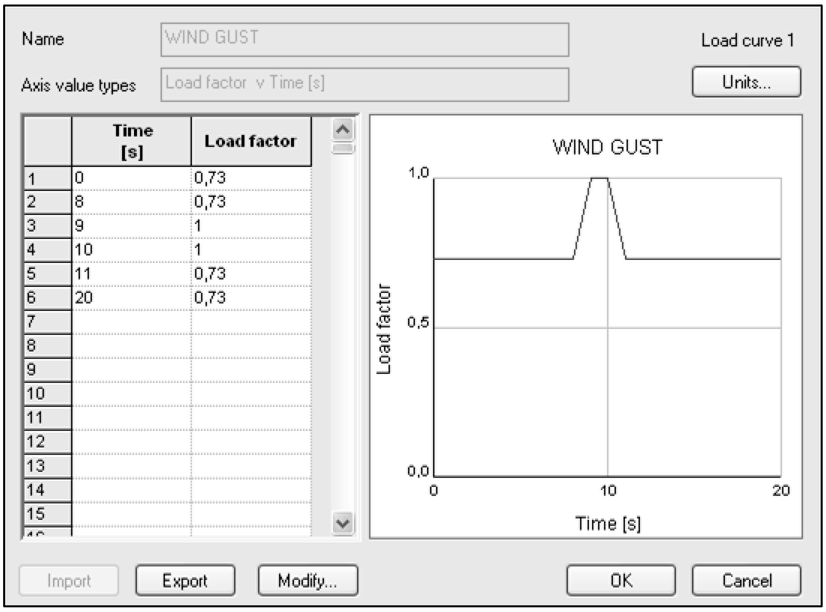

figure 4.11: Dynamic Wind Load Factor

Thereby the results seem to correlate best with the building code (NEN 6702) for the chosen load curve. Finally, as was previously mentioned, it is reasonable to assume that only during a storm these dynamic wind loads occur and not during windless periods of time.

4.2.8 Summery

The parameters as they are defined in the models are summarized in table 4.2 and will be referred to by the names stated in this table.

Parameter	Value according to
Support stiffness	
- SPRING	§ 3.13
- FIXED	§ 4.2.3
Core stiffness	
- BEAM	§ 3.14
- BAR	§ 4.2
Joint stiffness	
- TUBE-F	§ 3.10
- DOWEL	§ 3.10
- PINNED	§ 4.2.5
- RIGID	§ 4.2.5
Floor stiffness	§ 4.2.6
Loads	§ 4.2.7

table 4.2: Values of Parameters

4.3 Sub-Models

For all case study variants a base model and several sub-models are created. The parameters applied to these models are given in table 4.3. The base models of variant 3 and 4 are in concept similar to JOINT-R and JOINT-P respectively because the type of joints used in these variants where assumed to have no influence on the global stiffness earlier in this thesis.

Model name	Support stiffness	Core stiffness	Joint stiffness	Variant 1	2	3	4
BASE	SPRING	BEAM	TUBE-F	●	●	-	-
FOUND	FIXED	BEAM	TUBE-F	●	●	-	-
JOINT-D	SPRING	BEAM	DOWEL	●	●	-	-
JOINT-P	SPRING	BEAM	PINNED	●	●	-	-
JOINT-R	SPRING	BEAM	RIGID	●	●	-	-
NO-CORE	SPRING	BAR	TUBE-F	●	●	-	-
BASE-3	SPRING	BEAM	RIGID	-	-	●	-
FOUND-3	FIXED	BEAM	RIGID	-	-	●	-
NO-CORE-3	SPRING	BAR	RIGID	-	-	●	-
BASE-4	SPRING	BEAM	PINNED	-	-	-	●
FOUND-4	FIXED	BEAM	PINNED	-	-	-	●
NO-CORE-4	SPRING	10% BEAM	PINNED	-	-	-	●

table 4.3: Parameters of Base and Sub-Models

The optimization of the structure is done for both BASE-models and NO-CORE-models. The sections of the BASE-models that are applied after the optimization process, are assigned to the underling models, which are FOUND and JOINT-(D/P/R) models.

In the NO-CORE models the core elements are defined as BAR, except for those occasions in which this results in complications. For these the section modifiers are used to reduce the core stiffness to 10% BEAM.

5 Fire Analysis

In this chapter the different fire safety solutions are presented first. Then the parametric fire load and the fire exposure is established for those solutions. Subsequently, the charring depth is calculated which will establish the fire load and the associated fire curves. Finally an analysis is made on the features of the different fire safety solutions that where proposed. The calculations in this chapter are based on the informative annexes of the Eurocode. The results must therefore be treated with some skepticism.

5.1 Solutions

The fire safety solutions are influenced by a combination of three choices that are relevant to the fire behavior. The consecutive choices consist of:

- Stability system
- Fire safety concept
- Fire suppression measures

Stability system
For the fire safety solution the stability systems can be split up in two different groups, namely the shear wall option and the lattice structure option. The categorization, visualized in figure 5.1, is based on corresponding geometrical influence factors. The geometrical differences between categories are relevant because their associated window openings influence ventilation conditions and combustible surface.

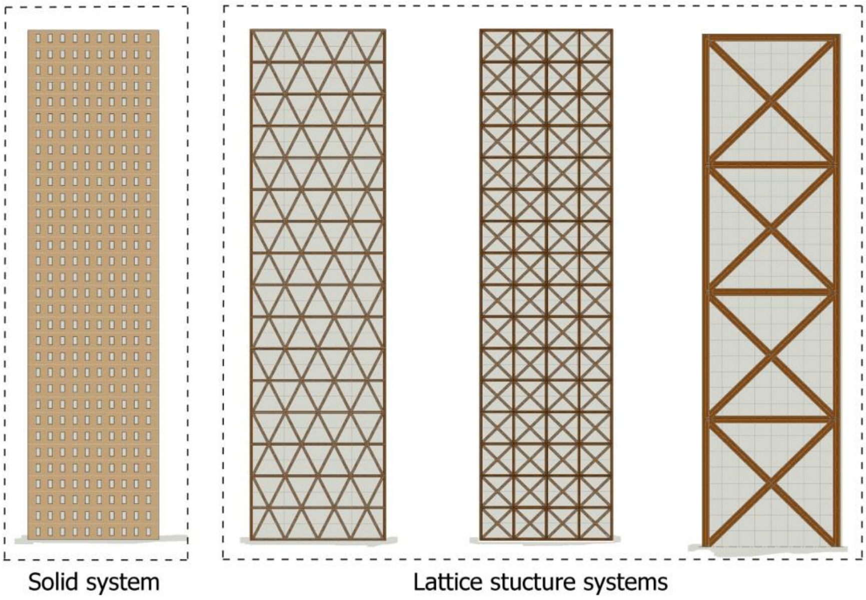

figure 5.1: Categorization of Stability Systems

The shear wall option has relatively small window openings and consequently a larger combustible area compared to lattice structures. These differences influence the ventilation conditions and the magnitude of the fire load respectively, which consequently have a large impact on the behavior of the fire.

Fire safety concept
The possible options for the fire safety concept consist of either the building encapsulation concept or the finite charring concept. The difference in combustible surface of these concepts have consequences for the behavior of the fire, and therefore also for the fire safety.

Fire suppression measures
The application of fire suppression measures like sprinkler and alarm systems have great effect on the duration of a fire. As was noted in the preliminary research, the presence of a sprinkler system can stop the fire before flashover occurs, at least for small compartments in full scale fire tests. For the analysis of this study the influence of sprinklers is quantified in the model through a reduction of the fire load.

Fire solutions
The combination of three times two choices results in two to the third, thus eight different solutions. These are analyzed further, later on in this chapter.

5.2 Parametric Fire Load

The fire load is determined with Appendix E of EC 1991-1-2 which is an informative annex. The design value of the fire load is given in equation (5.1) of which the parameters are defined in the following.

$$q_{f,d} = q_{f,k} \cdot m \cdot \delta_{q1} \cdot \delta_{q2} \cdot \delta_n \qquad \textbf{(5.1)}$$

Burning factor: (m) Since the structure is made out of timber and the majority of the combustible content of an office building consists of cellulose materials, the burning factor is assumed to be 0,8 in accordance with paragraph E.3 of EC 1991-1-2.

Size risk factor: (δ_{q1}) The size of each fire compartment is smaller then or equal to 622 m^2. A size risk factor of 1,57 results from interpolation of table E.1 of EC 1991-1-2.

Function risk factor: (δ_{q2}) Because the building is assumed to be used as office space the risk factor determined by the function of the compartments is 1,00 in accordance with table E.1 of EC 1991-1-2.

Fire suppression factor: (δ_n) Two extreme possibilities where proposed for application of fire suppression measures, subsequently with and without automatic fire suppression measures. For both possibilities the minimum required 'manual' fire measures are present. In table 5.1 the fire suppression factors ($\delta_{n,i}$) and their products (δ_n) are presented.

Active fire safety measure	Index	Automatic fire suppression Present	Automatic fire suppression Absent
Automatic fire suppression system	$\delta_{n,1}$	0,61	-
Independent water supply	$\delta_{n,2}$	1,00	-
Automatic fire detection trough smoke	$\delta_{n,3}$	0,87	-
Automatic fire detection trough heat	$\delta_{n,4}$	-	-
Automatic alarm at fire brigade	$\delta_{n,5}$	0,87	-
Private fire brigade	$\delta_{n,6}$	-	-
Public fire brigade	$\delta_{n,7}$	0,78	0,78
Safe approach for fire brigade	$\delta_{n,8}$	1,00	1,00
Fire extinguishers	$\delta_{n,9}$	1,00	1,00
Smoke ventilation system	$\delta_{n,10}$	1,00	1,00
Product of measures	δ_n	0,36	0,78

table 5.1: Fire Suppression Measure Factors

Characteristic fire load: ($q_{f,k}$) The magnitude of the fire load is dependent on the function of the space in which the fire compartment is located and the combustible material present in the fire compartment, including the structure and combustible linings. These are quantified respectively trough $q_{f,k}^{(1)}$ and $q_{f,k}^{(2)}$ as shown in equation (5.2). Because the building is used as office space the first fire load contribution is 420 MJ/m^2 in accordance with table E.4 of EC 1991-1-2.

$$q_{f,k} = q_{f,k}^{(1)} + q_{f,k}^{(2)} \tag{5.2}$$

$$q_{f,k}^{(1)} = 420\left[{MJ}/{m^2}\right] \tag{5.3}$$

The second contribution is dependent on the fire safety concept used and the area exposed to fire. For the building encapsulation concept it is assumed that the second contribution to the fire load does not take place. The chosen structural stability system has significant influence on the magnitude of the timber surface exposed to heat. The general description is given in equations (5.4) to (5.5).

$$q_{f,k}^{(2)} = \frac{Q_{f,k}^{(2)}}{A_f} \tag{5.4}$$

$$Q_{f,k}^{(2)} = \sum M_{k,i} \cdot H_{u,i} \cdot \psi_i \tag{5.5}$$

In which:

$Q_{f,k}^{(2)}$	= total fire load	MJ
A_f	= floor area	m^2
$M_{k,i}$	= mass of the material	kg
$H_{u,i}$	= net combustion value	MJ/kg
ψ_i	= factor for shielding of the fire load	-

The net combustion value of wood is 17,5 MJ/kg but is influenced by the moister content of the material. Most wood based material have a certified production quality control that guarantees a moister content of about 12% in most cases. The influence of the moister content is incorporated in appendix E of 1991-1-2 by equation (5.6). The combustion value of wood based products is therefore assumed to be 15,1 MJ/kg. Because no shielding of the combustible material is present, ψ is initially assumed to be 1,00.

$$H_u = H_{u0} \cdot \left(1 - 0,01 \cdot u\right) - 0,025 \cdot u \tag{5.6}$$

The mass of the material which is believed to contribute to the fire load is a product of the surface exposed to the initial fire in the compartment, the charring depth and the characteristic density. This is analytically summarized in equation (5.7).

$$\left.\begin{aligned} M_k &= V \cdot \rho_k \\ V &= A_{com} \cdot d_{char} \end{aligned}\right\} \rightarrow \qquad M_k = A_{com} \cdot d_{char} \cdot \rho_k \tag{5.7}$$

In which:

V	= the volume of the combustible material	m^3
ρ_k	= the characteristic density of the combustible material	kg/ m^3
A_{com}	= the area of the combustible material	m^2
d_{char}	= charring depth	mm

In this thesis it was chosen that the building structure is constructed out of wood based materials with a base material of at least strength class D70. The characteristic density for the fire load calculation is therefore assumed to be 900kg/m^3.

Total fire load: In summation, equations (5.2) to (5.7) combined, result in a general formula which is function of the charring depth and is shown in (5.8). This can be quantified by the values given below resulting in equation (5.9).

$$q_{f,k} = q_{f,k}^{(1)} + \frac{\sum A_{com} \cdot d_{char} \cdot 10^{-3} \cdot \rho_k \cdot H_{u,i} \cdot \psi_i}{A_f} \quad \textbf{(5.8)}$$

$q_{f,k}^{(1)}$	= 420	MJ/m^2
ρ_k	= 900	kg/m^3
H_u	= 15,1	MJ/kg
ψ_i	= 1,00	-
A_f	= 622	m^2

$$q_{f,k} = 420 + 21{,}85 \cdot \sum A_{com} \cdot d_{char} \cdot 10^{-3} \quad \textbf{(5.9)}$$

In reality the actual fire load can be dependent on the level of shielding which will increase when timber members start to develop a significant layer of charcoal which insulates and protects the wood. For reasons of simplicity and conservatism this is omitted.

The calculation of the combustible surface exposed to the fire is different for both stability system and fire safety concept. The exposed surface for the building encapsulation concept is assumed to be zero. The combustible surface for the finite charring concept is given in equation (5.10) and can be explained as the sum of the ceiling, the core wall and the façade wall minus the window area. The results of this calculation are given in table 5.2.

$$\sum A_{com} = A_f + 4 \cdot \left(c + w \cdot \left(1 - R_w\right)\right) \cdot h \quad \textbf{(5.10)}$$

In which:

A_{com}	= Area of combustible material	
A_f	= Ceiling (floor) area:	622 m^2
c	= width of the building core:	14,40 m
w	= width of the building:	28,80 m
R_w	= wall-to-window ratio:	variable
h	= height of the ceiling:	3,00 m

Stability System	R_w [-]	A_{com} [m^2]
Solid Shear wall	0,17	1082
Lattice structure	0,61	930

table 5.2: Combustible Area of Systems

Design value: The design value of the fire load can be broken down in the product of the risk factors and the magnitude of the total fire load as shown in equations (5.11) and (5.12) of which values of the parameters are given in table 5.3 for the presence and absence of active fire suppression systems.

$$q_{f,d} = q_{f,k} \cdot \prod \delta_i \tag{5.11}$$

$$\prod \delta_i = m \cdot \delta_{q1} \cdot \delta_{q2} \cdot \delta_n \tag{5.12}$$

Active fire suppression systems	$\prod \delta_i$
Present	0,45
Absent	0,98

table 5.3: Product of Risk Factors

The exposure to the fire load is calculated with equation (5.13) because the fire load acts on the total surface of the compartment, while its value is normalized to square unit length of the floor area.

$$q_{t,d} = \frac{q_{f,d} \cdot A_f}{A_t} \tag{5.13}$$

In which:

$q_{t,d}$ = Fire load over the total surface

$q_{f,d}$ = Fire load over the floor area

A_f = Floor area

A_t = Total area of compartment enclosures

Intermediate summery

The combination of equations (5.8), (5.11) and (5.13) results in the equation (5.A) which summarizes the parametric fire load for the general case.

$$q_{t,d} = \frac{A_f}{A_t} \cdot \left(q_{f,k}^{(1)} + \frac{\sum A_{com} \cdot d_{char} \cdot 10^{-3} \cdot \rho_k \cdot H_{u,i} \cdot \psi_i}{A_f} \right) \cdot \prod \delta_i \tag{5.A}$$

In which:

A_f	= Floor area	m^2
A_t	= Total area of compartment enclosures	m^2
$q_{f,k}^{(1)}$	= function dependant characteristic fire load	MJ/m^2
A_{com}	= Area of combustible material	m^2
d_{char}	= charring depth	mm
ρ_k	= the characteristic density of the combustible material	kg/m^3
$H_{u,i}$	= net combustion value	MJ/kg
ψ_i	= factor for shielding of the fire load	-
$\prod \delta_i$	= product the risk and burning factors	-

5.3 Parametric Fire Exposure

The parametric fire exposure is determined with Appendix A of EC 1995-1-2 which is also an informative annex. The design value of the parametric charring rate is given below in equation (5.14) of which the parameters are defined in the following.

$$\beta_{par} = 1,5 \cdot \beta_n \cdot \frac{0,2 \cdot \sqrt{\Gamma} - 0,04}{0,16 \cdot \sqrt{\Gamma} + 0,08} \tag{5.14}$$

Apparent charring rate: (β_n)The base material of the wood based composite used in building structure is a deciduous species with a charlatanistic density of at least 900 kg/m^3. The apparent charring rate is therefore 0,55 mm/min in accordance with table 3.1 of EC 1995-1-2. For the building encapsulation concept the gypsum board is used of type A,F or H with a minimum thickness of 14 mm. The apparent charring rate of gypsum board is 0,36 mm/min, which is derived from 3.4.3.3 of EC 1995-1-2 taking the reciprocal value.

Thermal factor: (Γ) The thermal factor is determined trough the opening factor and the thermal absorption coefficient. The general formulation is given in equations (5.15) to (5.17)

$$\Gamma = \frac{\left(\frac{O}{b}\right)^2}{\left(\frac{0,04}{1160}\right)^2} \tag{5.15}$$

$$O = \frac{A_v}{A_t}\sqrt{h_{eq}} \quad \text{(opening factor)} \tag{5.16}$$

$$b = \sqrt{\rho \cdot c \cdot \lambda} \quad \text{(absorption coefficient)} \tag{5.17}$$

Area vertical openings: (A_v) the area of vertical openings is dependant on the system used. The general equation to calculate the vertical openings is given in equation (5.18) which can be explained as the compartment side area of the façade multiplied by the wall-to-window ratio.

$$A_v = 4 \cdot w \cdot h \cdot R_w \tag{5.18}$$

In which:

w	= width of the building:	28,80 m
h	= height of the ceiling:	3,00 m
R_w	= wall-to-window ratio:	variable

The wall-to-window ratio is 0,17 for the variant with solid walls on the perimeter, while for other systems this ratio is approximately 0,61 dependant on the cross sectional dimensions of façade elements.

Total area of enclosures: (A_t) The total area of the enclosures of a single fire compartment is for all case study alternatives 1762 m^2 and consists of the floor, the ceiling and all walls.

Height vertical openings: (h_{eq}) the height of vertical openings is dependant on the applied stability system. For the solid walls system variant, this height is 1,80 m while for others the ceiling height of approximately 3,00 m is assumed.

Absorption coefficient: (b) The walls and ceilings of the fire safety concept 'building encapsulation' are covered by gypsum board. The surface of the finite charring fire concept is assumed to be unprotected wood. In table 5.4 values of relevant parameters adopted from ref. [30] are given for both materials.

Surface	ρ	c	λ	b
Gypsum board	800	840	0,23	393
Wood	900	1880	0,17	536

table 5.4: Values of Parameters for Absorption factor (b)

Parametric charring rate: (β_{par}) The parametric charring rate is dependent on the applied stability system and the fire concept used. The result of these combinations is given in table 5.5. The influence of the opening factor has large influence on the charring rate.

Stability System	Fire concept	R_w [-]	h_{eq} [m]	O [$m^{0,5}$]	b [$J/m^2s^{1/2}K$]	Γ [-]	β_n [mm/min]	β_{par} [mm/min]
Solid Shear wall	Encapsulation	0,17	1,80	0,04	393	8,7	0,36	0,54
	Finite charring	,,	,,	,,	536	4,7	0,55	0,76
Lattice structure	Encapsulation	0,61	3,00	0,20	393	217,8	0,36	0,64
	Finite charring	,,	,,	,,	536	117,1	0,55	0,97

table 5.5:Parametric Charring Rate Calculation

Charring depth: The charring depth is calculated trough integration of the charring rate over time. For paramedic fire exposure this is equal to the area beneath the curve shown in figure 5.2 which results in equation (5.B). The duration of time in which the charring rate is constant (t_0), is dependent on the fire load ($q_{f,d}$) as shown in equation (5.C).

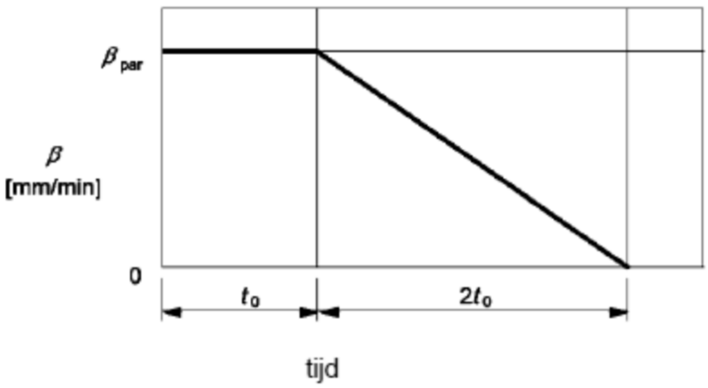

figure 5.2: Parametric Charring Rate Curve

$$d_{char}\Big|_0^{3\cdot t_0} = \int_0^{3\cdot t_0} \beta \cdot dt = 2 \cdot t_0 \cdot \beta_{par} \qquad \textbf{(5.B)}$$

$$t_0 = 0,009\frac{q_{t,d}}{O} \qquad \textbf{(5.C)}$$

5.4 Calculation Charring Depth

Substitution of equations (5.A) to (5.C) and solving for d_{char} gives equation (5.D) and represents the charring depth of a compartment burnout within certain conditions. Substitution of the constant values results in equation (5.19).

$$d_{char} = \frac{q_{f,k}^{(1)} \cdot A_f}{\left(\frac{O \cdot A_t}{0{,}018 \cdot \beta_{par} \cdot \prod \delta_i} - \sum A_{com} \cdot \rho_k \cdot H_{u,i} \cdot \psi_i \cdot 10^{-3} \right)} \quad \textbf{(5.D)}$$

$$d_{char} = \frac{261 \cdot 10^3}{\left(98 \cdot 10^3 \cdot \frac{O}{\beta_{par} \cdot \prod \delta_i} - 14 \cdot \sum A_{com} \right)} \quad \textbf{(5.19)}$$

The charring depth must be larger than zero, therefore the denominator has to be larger than zero. This results in the condition stated in equation (5.20) and (5.21) for substitution with constant values.

$$\sum A_{com} < \frac{O \cdot A_t}{0{,}018 \cdot \beta_{par} \cdot \prod \delta_i \cdot \rho_k \cdot H_{u,i} \cdot \psi_i} \quad \textbf{(5.20)}$$

$$\sum A_{com} < \frac{7221 \cdot O}{\beta_{par} \cdot \prod \delta_i} \quad \textbf{(5.21)}$$

It turns out that the solid shear wall stability system combined with the finite charring concept is not feasible primarily because of the small associated opening factor and the large combustible surface. The minimum condition for this concept reads: A_{com} < 844 m^2 or 388 m^2 which is not satisfied (A_{com} =1082 m^2). The calculation of the charring depth is given in table 5.6 for the remaining six principle solutions. The charring depth calculation could also be conducted in an irritative manor, which shows convergent behavior towards the values in table 5.6, demonstrating the validation of the analytical method.

Stability System	Fire concept	Active fire measures	O	β_{par}	$\prod \delta_i$	A_{com}	d_{char}
Solid Shear wall	Encapsulation	Present	0,04	0,54	0,45	0,00	16
		Absent	,,	,,	0,98	,,	35
	Finite charring	Present	,,	0,76	0,45	1082	N/A
		Absent	,,	,,	0,98	,,	N/A
Lattice structure	Encapsulation	Present	0,20	0,64	0,45	0,00	4
		Absent	,,	,,	0,98	,,	8
	Finite charring	Present	,,	0,97	0,45	930	8
		Absent	,,	,,	0,98	,,	34

table 5.6: Calculation of Charring Depth

5.5 Parametric Fire Curves

The parametric fire curves that were determined with Appendix A of EC 1991-1-2 are plotted in figure 5.3. The time-temperature- curves consist of two parts, the heating phase and the cooling phase. The heating phase is represented by the exponential part and the linear part represents the cooling phase. The curves give insight in the behavior of different solutions.

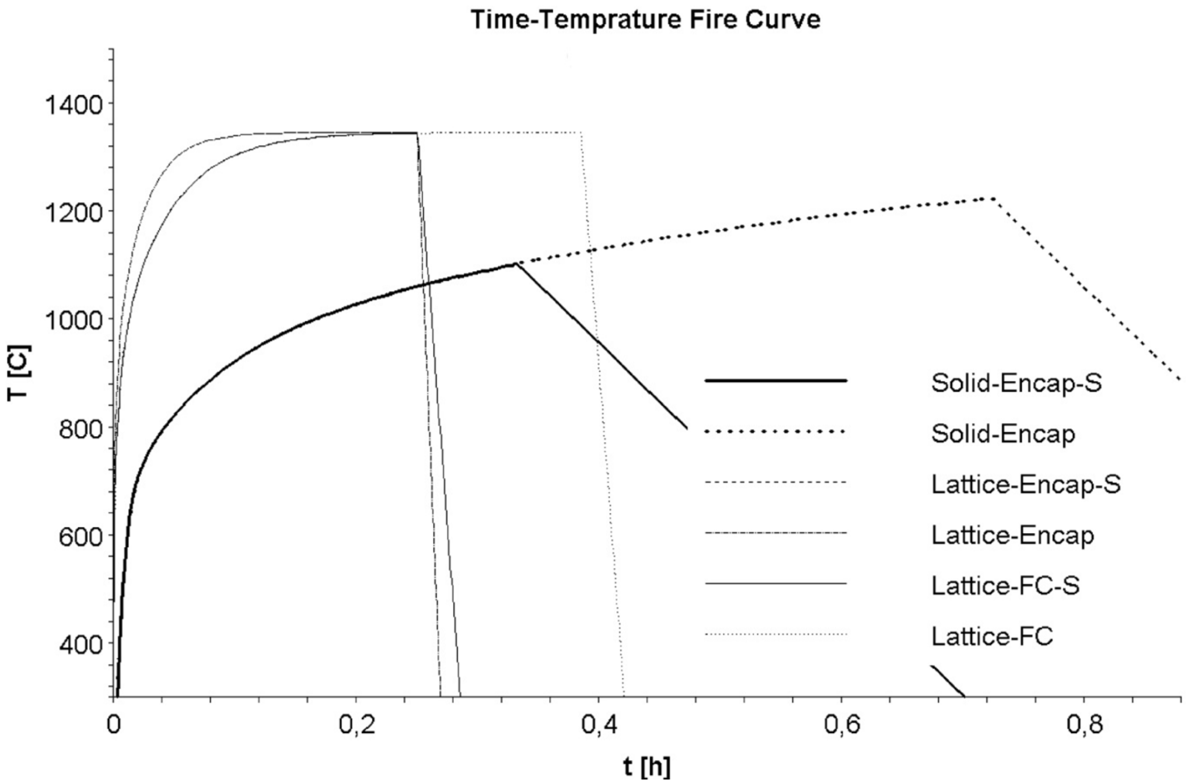

figure 5.3: Parametric Fire Curves

General
There is one basic principle that summarizes the fire behavior. This is the principle of heat energy and rate of energy dissipation. Fast growing fires release energy in a short period of time with relatively high peak temperatures, compared to fires with a medium and slow growth rate. There are three essential parameters that influence the behavior of a fire, which are: the opening factor, the thermal absorption coefficient and the magnitude of the fire load. The first two parameters determine the rate of dissipation, while the third indicates the amount of potential heat energy.

Opening factor
The area beneath the fire curves is an indication of the release of energy within the burning period. The dissipation of the heat is largely influenced by the size of window openings, i.e. the ventilation of the compartment. The fire load, i.e. the amount of potential heat energy, of encapsulated solutions with similar suppression measures is the same, while the area beneath their curves is not. A large opening factor results therefore in a fast growing but short lasting fire, with relatively small damage.

Absorption coefficient
Compared to the opening factor, the absorption coefficient results in an opposite effect. The heat energy can dissipate through the compartment enclosures resulting in lower gas temperature and a smaller growth rate. The absorptions coefficient does not influence the duration of the heating phase, but rather the peak temperature due to heat storage in the mass of enclosures.

Magnitude of the fire load
The fire load magnitude indicates the potential heat energy, which stored in the material and the building content. The influence of encapsulation and active fire suppression systems is clearly visible between solutions of similar structural systems and concepts.

5.6 Analysis of Solutions

The largest difference in fire behavior is observed in the choice of stability system because of associated opening factors. The analysis is therefore discussed here accordingly. First the

5.6.1 Effective charring depth

The effective charring dept can be calculated according to EC 1995-1-2 with equation (5.22) which represents the calculated charring rate including and the heat effected zone (HEZ). The factor k_0 is assumed conservative.

$$d_{ef} = d_{char,n} + k_0 \cdot d_0 \tag{5.22}$$

In which:

d_{ef} = effective charring depth

k_0 = 1,0

d_0 = 7 mm

This will conservatively result in an additional charring depth of 7 mm for wooden parts. The assumption of the apparent charring rate of gypsum board made earlier, requires a additional thickness of 14 mm.

5.6.2 Solid shear wall systems

The relatively small opening factor of solid shear wall systems results in a medium to slow growing and consequently long lasting fire. The finite charring concept is not feasible unless large parts are covered with non-combustible gypsum board. This suggest a combination between concepts, where for example only the ceiling, the façade adjacent walls or both are encapsulated.

Application of fire suppression systems result in a shorter duration and therefore lower peak temperature, as is expected. The difference in damage to the gypsum board is about 19 mm, which is equivalent to one or two layers of 15 mm. Because both solutions are possible, the choice between either additional layers of gypsum board or a suppression system is therefore economical.

The final thickness of the gypsum board encapsulation is shown in table 5.7. Furthermore, suggestions are made in this table to make the finite charring concept feasible.

Stability System	Fire concept	Active fire measures	d_{char}	d_{ef}	Solution and feasibility
Solid shear wall	Encapsulation	Present	16 mm	30 mm	2 layers of 15 mm gypsum board
		Absent	35 mm	49 mm	3 to 4 layers of 15 mm gypsum board
	Finite charring	Present	43 mm	50 mm	Feasible when 69% encapsulation is applied
		Absent	93 mm	100 mm	Not feasible, 100 mm charring at 86% encapsulation

table 5.7: Results and Fire Solutions for Solid Shear Wall System

5.6.3 Lattice structure systems

Large opening factor of lattice structures results in a fast growing and consequently short lasting fire. All proposed lattice structure solutions are feasible, oppose to the solid shear wall system.

Application of fire suppression systems do not effect encapsulation solutions much, but can be rather significant when the finite charring concept is used. The difference of wood charring is 26 mm when suppression systems are applied to the finite charring solutions. The choice of applying suppression systems will depend on the necessity to increase dimensions to resist the reduced mechanical loads under fire conditions or a cost assessment between options.

The final thickness of the gypsum board and the charring of the wood is shown in table 5.8. For finite charring concept solutions, the structural analysis must prove sufficient resistance against mechanical loading which is shown in the next chapter.

Stability System	Fire concept	Active fire measures	d_{char}	d_{ef}	Solution and feasibility
Lattice structure	Encapsulation	Present	4 mm	18 mm	2 layers of 15 mm gypsum board
		Absent	8 mm	22 mm	2 layers of 15 mm gypsum board
	Finite charring	Present	8 mm	15 mm	Pending on structural analysis
		Absent	34 mm	41 mm	Pending on structural analysis

table 5.8: Results and Fire Solutions for Lattice Structure Systems

5.6.4 Reduction of sections

The cross sections of structural components must be reduced by twice the effective charring depth for ultimate limit state verifications, because the sections are assumed to char on all sides. In order to proof the feasibility for all structural lattice systems, the sections will be reduced by the largest effective charring depth, hence the total reduction is 82 mm .

5.7 Summery

It was found that not all proposed solutions are feasible from the perspective of fire safety. In terms of fire concepts, building encapsulation is feasible for all stability systems without application of fire suppression. Additional fire suppression systems are relevant when a cost assessment is conducted between options. Finite charring is only feasible for systems with a large opening factor, i.e. lattice structures with a curtain wall façade, or in combination with partial encapsulation and fire suppression for solid shear wall structures.

Fire safety can be guaranteed for all structural solutions provided that the appropriate combination of fire concept and fire suppression is applied, which result in compartment burn-out. The economic feasibility however can depend on this combination.

The structural feasibility of finite charring concept solutions has to be proven through structural analysis of the systems by checking the resistance of the reduced cross section after charring.

6 3D-Models

6.1 Introduction

For the structural analysis three dimensional models are used that are created of 1D-elements. Three dimensional models are used because these models can incorporate shear lag of the tube structure better than two dimensional frame analyses. This does not only influence the stiffness of the tube structure but also includes the effect of the spring supports.

6.1.1 General Model Input

The input description of the models is build op in the following manner:

Geometry: The elements of models are orientated coherent with the geometry of the variant concerned. This is achieved by placing elements that are used in GSA models between nodes which coordinates follow the geometry. An example of this is shown in figure 6.1.

Sections: Because the forces in members on the first floor of a building are larger, the sections of elements change with each level. In this thesis the sections of elements are the same for one level and (can) change the next level. The section assignment to elements is indicated by making use of these levels in this thesis.

Beam-Releases: To incorporate the influence of the joint stiffness, Beam-Releases are applied. Beam-Releases are the interface stiffness properties between the endpoints of elements and the nodes. As has been mentioned earlier, these can be assigned as springs for all local rotations and translations.

Support Stiffness: The stiffness values of the supports are assigned to the tube supports coherent with the variant concerned and to the core support based on earlier calculations. The definition of tube supports and core supports is given in figure 6.1.

Material Properties: The material properties are assigned to the section within the used software. The material properties consist of moduli of elasticity and density (specific gravity). The moduli of elasticity are based on earlier calculations and vary between models and materials.

Load Cases: The loads are imposed on the nodes of the models and are categorized in load cases that are used in load combinations within the software used.

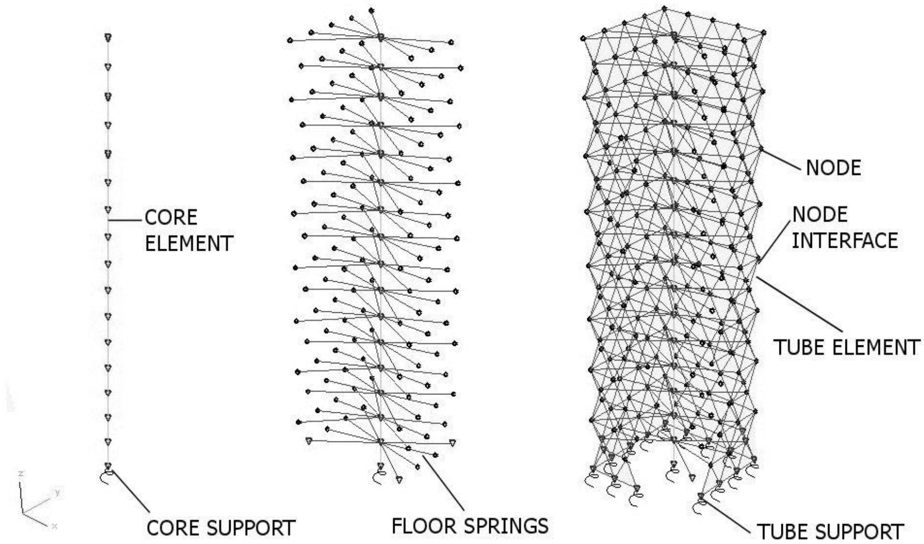

figure 6.1: Build-up Principle of Models

6.1.2 Model Modifications

A BASE-model is created for all variants. The input for these models is defined in the individual model descriptions. In order to investigate the influence of the timber building core and the influence of the foundation on the structure, the following modifications are made to all models:

NO-CORE-model: In this modified model the typology of the core elements (figure 6.1) is changed, with the result that the bending stiffness of these elements becomes zero. However, the core elements are still stiff in the axial direction.

FOUND: The foundation is altered to a fixed support in order to observe the influence to the deflection at the top of the building (model). This modification is only done to the BASE model.

6.1.3 General Model Output

The output of the models consists of the following:

Element forces: Forces that occur in elements after the calculation done by the software (linear elastic analysis) are grouped into level to which their affiliated sections belong to. The buckling resistance and the tension capacity of elements is verified with these forces.

Lateral deflection: The lateral deflection at the top of models is verified against the Dutch building code after calculation done by the software (linear elastic analysis).

Dynamic Results: The combination of Eigen-frequencies and the maximum occurring acceleration are verified against the Dutch building code.

Support reactions: The support reactions of the linear elastic analysis are compared to the capacity of the piles to verify the support stiffness assumption.

6.1.4 Data handling

The elements are assigned to element list in the software in order to keep the handling of data manageable. Results can be sorted with these element lists. There is also the possibility to sort the data in accordance with the assigned section properties and associated numbers, which was used plenty. The most important issue when handling data of these amounts is to build the data processing tool (in this case a spreadsheet) around the format and structure of the finite element software output, and being consistent therein. This allows one to adjust the data rapidly when something changes in the model and its parameters.

6.2 Variant 1: Diagrid Geometry

6.2.1 Model Description

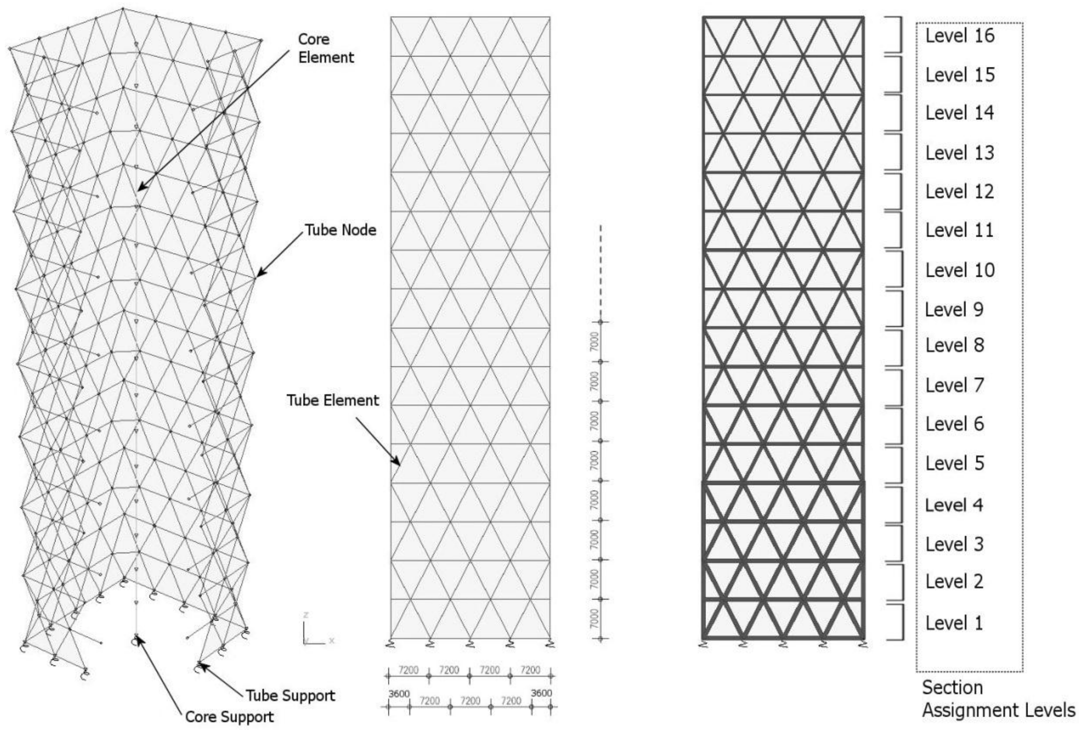

figure 6.2: Geometry and Section Assignment of 3D-model of Variant 1

6.2.1.1 Geometry

The elements of the model are orientated coherent with the geometry of the variant. The geometry and the dimensions of the geometry for this model are shown in figure 6.2 and is the same for all faces of the tube structure. In addition to this figure a textual description is given here of the geometry.

The 1D elements used in GSA models are orientated by placing them between nodes. The tube nodes in one plane of the geometry are spaced with the following dimensions:
Horizontal node spacing = 7200 mm
Vertical node spacing = 7000 mm

When one face of the tube structure is considered as is shown in the middle of figure 6.2, the first row of nodes is at the height of the supports and consists of five nodes. The second row of nodes is shifted 3600 mm horizontally in comparison to the first row of nodes and consists of four nodes.

6.2.1.2 Model Material Properties

The material properties assigned to the sections applied in the model are defined as in table 6.1

Material Name	GSA Material model	Modulus of elasticity	Poisson's Ratio	Shear modules	Density
Symbol:		E	μ		ρ
Unit:		[N/mm^2]	[-]	[N/mm^2]	[kg/m^3]
D70-LAM	Elastic Isotropic	20000	0	1250	900
D70-CLT	Elastic Isotropic	11800	0	998	900

table 6.1: Material Properties Applied to Diagrid Models

6.2.1.3 Section Core Elements

The material assigned to the section of the core elements is D70-CLT as defined in table 6.1. The section properties of the core elements are:

$A = 5{,}64 \cdot 10^{7}$ [mm^2]
$I_{yy} = 1{,}23 \cdot 10^{15} \cdot 0{,}69 = 0{,}848 \cdot 10^{15}$ [mm^4]
$I_{zz} = 1{,}23 \cdot 10^{15} \cdot 0{,}69 = 0{,}848 \cdot 10^{15}$ [mm^4]
$J = 1{,}67 \cdot 10^{15}$ [mm^4]

6.2.1.4 Sections Tube Elements

The timber sections of tube elements are indicated with Section Assignment Levels as shown in figure 6.2 (right-hand side). For this variant this applies to both diagonal and horizontal tube structure elements. The material assigned to the sections of the tube elements is D70-LAM as defined in table 6.1.

The timber sections of the tube elements of the BASE-model are assigned according to table 6.2. The timber sections of the tube elements of the NO-CORE-model are assigned according to table 6.3.

BASE-model					
Section Assignment Level	Section	Beam Releases DOWEL		Beam Releases TUBE-F	
Units:	b x h [mm]	K_{ser} [MN/mm]	K_r [kNm/rad]	K_{ser} [MN/mm]	K_r [kNm/rad]
1-2	700 x 700	10,57	5626	10,89	7316
3-4	650 x 650	8,45	2250	9,33	3919
5-6	550 x 550	7,61	3376	6,22	1866
7-5	500 x 500	4,75	2250	4,67	1866
9-10	450 x 450	3,80	1283	3,89	684
11-12	400 x 400	2,54	405	3,11	709
13-14	350 x 350	1,17	787	2,33	709
15-16	300 x 300	0,65	0	1,17	709

table 6.2: Sections applied to Elements

NO-CORE-model			
Section Assignment Level	Sections	Beam Releases TUBE-F	
Units:	b x h [mm]	K_{ser} [MN/mm]	K_r [kNm/rad]
1-2	700 x 700	10,57	5626
3-4	700 x 700	10,57	5626
5-6	650 x 650	8,45	2250
7-5	550 x 550	7,61	3376
9-10	500 x 500	4,75	2250
11-12	450 x 450	3,80	1283
13-14	400 x 400	2,54	405
15-16	300 x 300	0,65	0

table 6.3: Sections of the Diagrid Model

6.2.1.5 Beam Releases

To incorporate the stiffness of joints into the model, beam releases are used. The beam releases are assigned coincident with the timber sections as these are indicated in table 6.2 and table 6.3. The default beam releases for the BASE-model of this variant are the joint stiffness values of the tube faster (TUBE-F). For the BASE-model the values of the beam releases are varied between:

TUBE-F: beam releases are equal to the stiffness of tube fastener joints.

DOWEL: beam releases are equal to the stiffness dowel fastener joints.

PINNED: indicates that the local node rotations (yy,zz) are free and local node translations (x,y,z) are fixed to the element. The local node rotation (xx) is always fixed to the element.

RIGID: indicates that all local node rotations (xx,yy,zz) and local translations (x,y,z) are fixed.

The values of K_{ser} are translation stiffness values in the local x-axis and z-axis direction and K_r are rotation stiffness values around the local y-axis. Rotation around the local z-axis is always free while the remaining translation (y) and rotation (xx) are fixed.

6.2.1.6 Support Stiffness

The support stiffness values of this variant are indicated in table 6.4 below.

	Spring stiffness (k) N/m	Rotational stiffness (k_r) Nm/rad
Tube Supports	$1,41\ 10^{9}$	0,00
Core Support	$3,53{\cdot}10^{10}$	$1,22\ 10^{12}$

table 6.4: Support Stiffness Values of the Diagrid Model

6.2.1.7 Load Cases

Self-Weight Main Structure (LC1)
The self-weight of the main structure is calculated automatically by gravity loading feature of the software.

Permanent Vertical Loads (LC2 + LC3)
The vertical loads are concentrated at the tube nodes and the core nodes as shown in figure 6.4 (left-hand side). The vertical node spacing of both tube nodes and core nodes coincides with two storey heights (vertical floor spacing). The following values are therefore valid: n_{floor} = 2 and l_{ctc} = 7,20m. The permanent vertical loads result therefore in the values given in table 6.5 based on § 4.2.7.1 as shown below:

$$F_{p;core,rep} = 2078 \cdot 2 = \quad 4156 \quad \left[{}^{kN}\!/_{node} \right]$$

$$F_{p;tube;rep} = 13,34 \cdot 7,20 \cdot 2 = \quad 193 \quad \left[{}^{kN}\!/_{node} \right]$$

Load case	Nodes	Direction	Value	Units
Permanent loading	Core nodes	z	-4156	kN
Permanent loading	Tube nodes	z	-193	kN

table 6.5: Loads on the Models of Variant 1

Variable Vertical Loads (LC4)
In a similar manner as the permanent vertical loads are the values of variable vertical loads given in table 6.6 based on § 4.2.7.1 as shown below:

$$F_{q;core,rep} = 619 \cdot 2 = \quad 1238 \cdot \left[{}^{kN}\!/_{node} \right]$$

$$F_{q;tube;rep} = 4,18 \cdot 7,20 \cdot 2 = \quad 60 \cdot \left[{}^{kN}\!/_{node} \right]$$

Load case	Nodes	Direction (Global)	Value	Units
Variable loading	Core nodes	z	-1238	kN
Variable loading	Tube nodes	z	-60	kN

table 6.6: Loads on the Models of Variant 1

Variable wind load (LC5)

Geometrically, the tube elements of variant 1 create triangles as can be observed in figure 6.2. All tube nodes of variant 1, except for the nodes at the base and the top of the building, are adjacent to 6 of these triangles as shown in figure 6.3. Each tube node takes part of $^1/_3$ of the wind load on these triangles, which results in the following equivalent area calculation for the wind load.

$$A_{eq} = 6 \cdot \frac{1}{3} \cdot A_{\Delta} = 6 \cdot \frac{1}{3} \cdot \frac{1}{2} \cdot 7,2 \cdot 7,0$$

$$A_{eq} = 50,4 \cdot m^2$$

This results in the following values for the wind load for one representative node, based on earlier calculations in § 4.2.7.2:

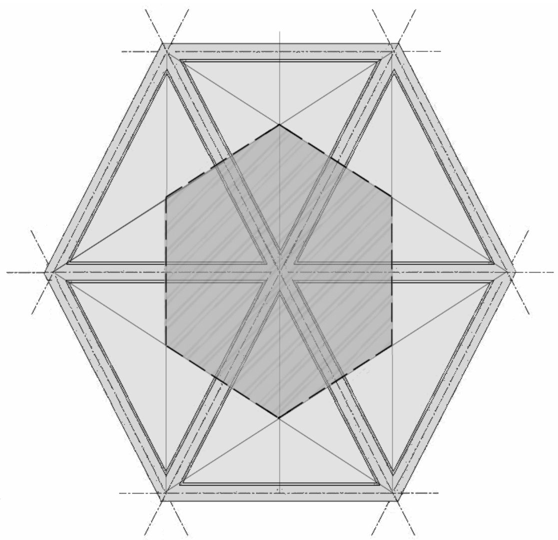

figure 6.3: Loaded Node Area Variant 1

$$F_{w;node;rep}(b) = Q_{w;rep}(0 < z < 30) \cdot A = \quad 1,68 \cdot 50,40 \quad = 84,7 \quad kN/node$$

$$F_{w;node;rep}(z) = Q_{w;rep}(30 < z < 82) \cdot A = \quad \left(\frac{173}{13000} \cdot z + 1,28\right) \cdot 50,4 \quad kN/node$$

$$F_{w;node;rep}(h) = Q_{w;rep}(82 < z < 112) \cdot A = \quad 2,37 \cdot 50,4 \quad = 119,4 \quad kN/node$$

Wind loads are imposed on the tube nodes of one face of tube structure of the model and results in the horizontal loads as these are shown in figure 6.4.

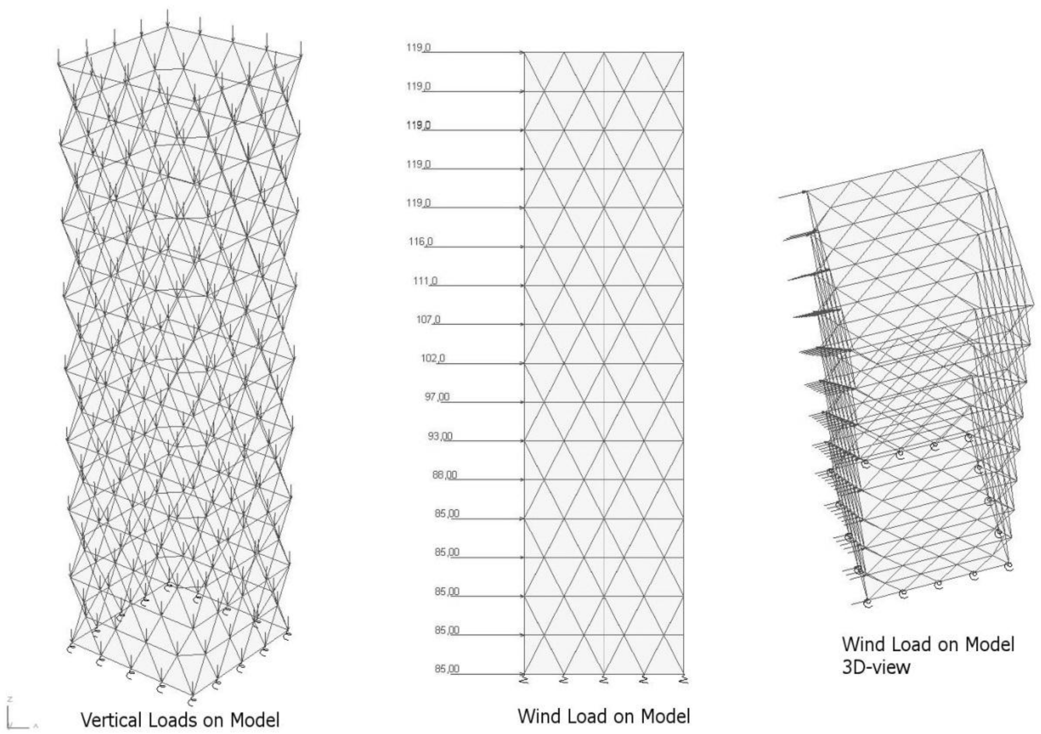

figure 6.4: Load on Nodes of Model

The wind loaded area for nodes on the corner of the building is smaller. Nonetheless, is the full wind load applied to the wind loaded nodes. The sum of the wind load is therefore verified with the expected value. The sum imposed of the wind load is:

$$\bar{n}_y = [5 \quad 4 \quad 5 \quad 4 \quad 5 \quad 4 \quad 5 \quad 4 \quad 5 \quad 4 \quad 5 \quad 4 \quad 5 \quad 4 \quad 5 \quad 4]$$
$$\bar{F} = [119 \quad 119 \quad 119 \quad 119 \quad 119 \quad 116 \quad 111 \quad 107 \quad 102 \quad 97 \quad 93 \quad 88 \quad 85 \quad 85 \quad 85 \quad 85]^T \; kN$$
$$\sum F = \bar{n}_y \cdot \bar{F} = 7429\,kN$$

The expected value is:

$$A_{tot} = 28,80 \cdot 112,00 = 3226 \; m^2$$
$$q_{w,gem} = 2,19 \; kN/m^2$$
$$\sum F = q_{eq} \cdot A_{tot} = 7064 \; kN$$

In which:

$\bar{n}_y$ = The vector of the number of nodes in the direction

$\bar{F}$ = The forces corresponding to the nodes

A_{tot} = The total area of the loaded face.

q_{eq} = The equivalent wind load

This implies that the total wind load becomes about 5% to high, which is conservative thus justified.

6.2.1.8 Load Combinations

The load combinations of load cases are applied in the model as defined in table 6.7.

Load Combinations	LC 1	LC 2	LC 3	LC 4	LC 5	LC 6	LC 7
C0: ULS	1,20	1,20	1,20	1,50	1,50	-	-
C1: ULS	1,35	1,35	1,35	0,75	0,75		
C2: ULS	0,90	0,90	0,90	0,00	1,50	-	-
C3: SLS	1,00	1,00	1,00	1,00	1,00	-	-
C4: ULS Fire	1,00	1,00	1,00	1,00	0,20	-	-
C5: SLS Dynamic	1,00	1,00	1,00	1,00	0,73	-	0~1,00
C6: Quasi-Permanent	1,00	1,00	1,00	0,50	0,00	-	-

table 6.7: Load Combinations

6.2.2 Results

The magnitude of the bending moments compared to the axial forces is small and does not result in significant stress changes (less than 1%). It is therefore that all members are only verified on axial forces, in particular critical buckling compression stresses. The element force results that were calculated with finite element model for the ultimate limit state combinations are discussed here.

The forces on the elements ($F_{d,i}$) are extracted from the models by handling the data. The buckling resistance ($R_{d,buc}$) of members is described in paragraph 3.9. The tension capacity ($F_{d,t}$) is calculated by multiplying the cross section by the design value of the used material as is shown in equation (6.1).

$$R_{d,t} = A \cdot \frac{f_{c,0,k}}{\gamma_M} \cdot k_{\text{mod}} = A \cdot \frac{19,0}{1,25} \cdot 0,70 \qquad \textbf{(6.1)}$$

Fundamental Combinations

ULS verification on maximum occurring element forces calculated with the BASE-model and the NO-CORE-model for ULS load combinations C0 and C1 was satisfied for the applied sections, in which C0 was decisive. The ULS load combination C2 did not result in tension forces in the tube supports for both models.

Charring and Fire Combinations

The reduced sections due to charring in a fire are 82 mm smaller than their original. The axial element verifications of the fire combination (C4) are given for the BASE-model in graph 6.1 in which results are sorted by section allocation level. It can be observed that the ULS verification is not satisfied for the smaller (higher level) sections. In the graphs below the following definitions of symbols are used:

$R_{d,buc}$ = Buckling resistance of a section
$R_{d,t}$ = Tension capacity of a section
$F_{d,c}$ = compression force on the elements
$F_{d,t}$ = Tension force on the elements

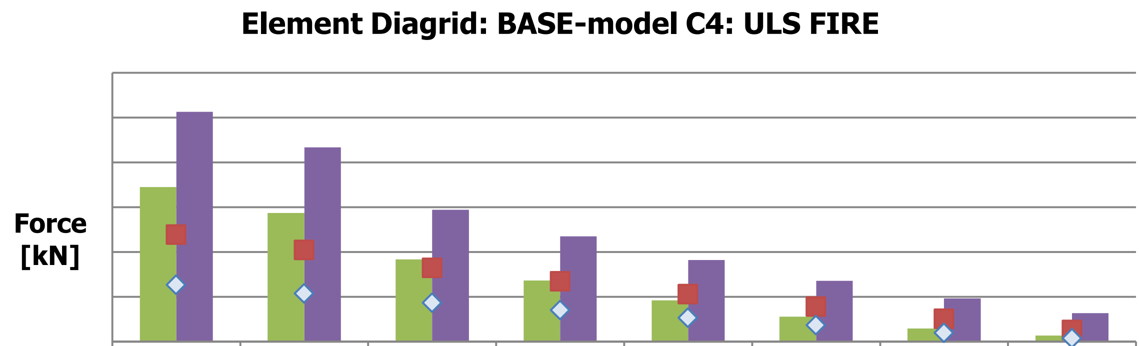

Level:	618 (1-2)	568 (3-4)	468 (5-6)	418 (7-8)	368 (9-10)	318 (11-12)	268 (13-14)	218 (15-16)
Rd,buc	6903	5744	3666	2723	1849	1114	588	265
Rd,t	10266	8672	5887	4697	3640	2718	1931	1277
Fd,c	4776	4092	3288	2698	2122	1571	1027	526
Fd,t	2541	2154	1741	1402	1065	733	399	143
UC	0,69	0,71	0,90	0,99	1,15	1,41	1,75	1,99

graph 6.1: Forces in Members, Fire Combination C4

Within graphs, for example graph 6.1, compression forces are indicated with squares and tension forces are indicated with diamonds. In this same graph the buckling resistance is given for sections indicated by a green bar (left of a group results). The tension capacity is respectively indicated by a purple bar (right of a group results). The tension capacity of a section is always larger than its buckling resistance. The decisive unity check is stated in the lower row of the table beneath the graph.

The axial element force results of the NO-CORE-model for the fire combination (C4) are given in graph 6.2 also sorted by section allocation level. Here it also can be observed that the ULS verification is not satisfied for the smaller (higher) sections.

Elements Diagrid: NO-CORE-model, C4: ULS FIRE

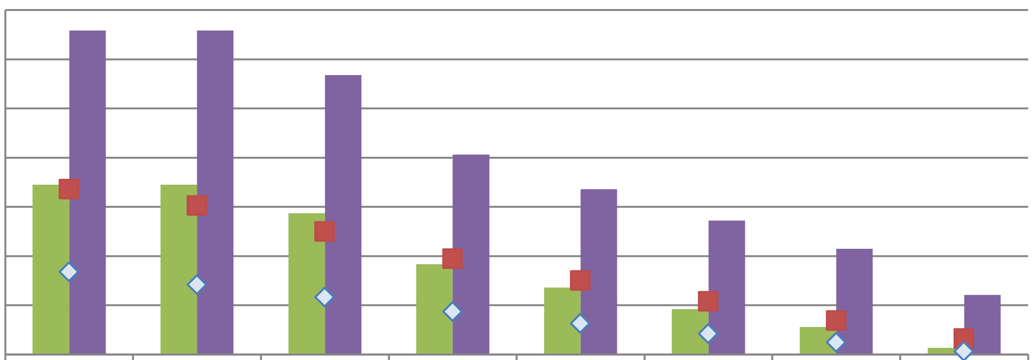

	659	659	609	509	459	409	359	259
Level:	(1-2)	(3-4)	(5-6)	(7-8)	(9-10)	(11-12)	(13-14)	(15-16)
Rd,buc	6903	6903	5744	3666	2723	1849	1114	265
Rd,t	13171	13171	11357	8131	6720	5443	4301	2419
Fd,c	6717	6054	4998	3882	3004	2147	1371	637
Fd,t	3351	2826	2317	1733	1258	834	482	122
UC	0,97	0,88	0,87	1,06	1,10	1,16	1,23	2,41

graph 6.2: Forces in Members, Fire Combination C4

6.2.3 Conclusion

In the first step of the optimization, all element sections where chosen to be 500 x 500 mm, which satisfied the serviceability requirements. Thereafter, the optimization to satisfy the ultimate limit state requirements of the fundamental combinations (C0 and C1) resulted in the timber sections shown in table 6.2 and table 6.3 for the tube elements of this variant. Those section dimensions must become larger in case the core is not lateral stiff or absent. However, increasing tube elements is more efficient, because these sections did not increase much in that case.

Thereafter the sections are verified for the load combination in fire conditions. The cross section of the members was therefore reduced with 82 mm which resulted in particularly small sections to fail. One could repeat this experiment with sections that are slightly larger than are given here. This is intentionally not done in this thesis because the method that was used proofs that large timbers are protected by their inherent massiveness in a fire which is a conformation of at least one scientific opinion.

6.3 Variant 2: Diagonal Braced Frame

6.3.1 Model Description

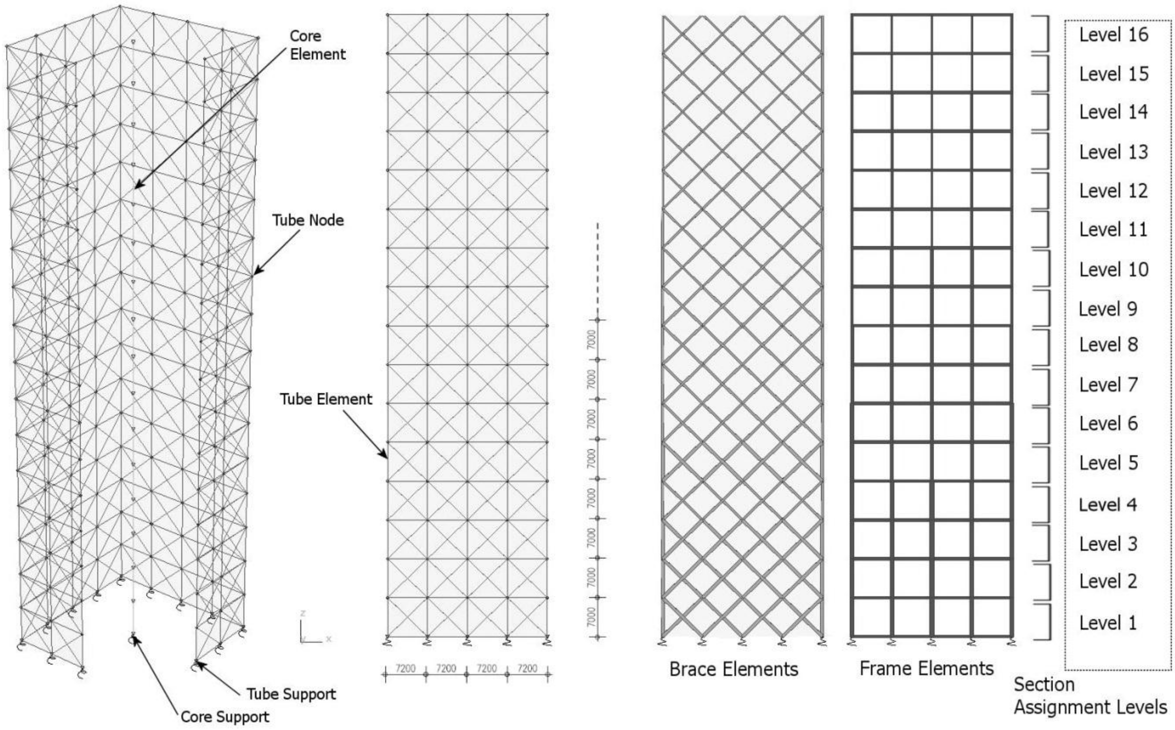

figure 6.5: Geometry and Section Assignment of 3D-model of Variant 2

6.3.1.1 Geometry

The elements of the model are orientated coherent with the geometry of the variant. The geometry and the dimensions of the geometry for this model are shown in figure 6.5 and is the same for all faces of the tube structure. In addition to this figure a textual description is given here of the geometry.

The 1D elements used in GSA models are orientated by placing them between nodes. The tube nodes in one plane of the geometry are spaced with the following dimensions:
Horizontal node spacing = 7200 mm
Vertical node spacing = 7000 mm
Elements can consist of braces or of frame elements like columns as shown in figure 6.5.

6.3.1.2 Model Material Properties

The material properties assigned to the sections applied in the model are defined as shown in table 6.1

Material Name	GSA Material model	Modulus of elasticity	Poisson's Ratio	Shear modules	Density
Symbol:		E	μ		ρ
Unit:		[N/mm^2]	[-]	[N/mm^2]	[kg/m^3]
D70-LAM	Elastic Isotropic	20000	0	1250	900
D70-CLT	Elastic Isotropic	11800	0	998	900

table 6.8: Material Properties Applied to Braced Frame Models

6.3.1.3 Section Core Elements

The material assigned to the section of the core elements is D70-CLT as defined in table 6.8. The section properties of the core elements are:

$$A = 5{,}64 \cdot 10^{7} \quad [mm^2]$$
$$I_{yy} = 1{,}23 \cdot 10^{15} \cdot 0{,}69 = 0{,}848 \cdot 10^{15} \quad [mm^4]$$
$$I_{zz} = 1{,}23 \cdot 10^{15} \cdot 0{,}69 = 0{,}848 \cdot 10^{15} \quad [mm^4]$$
$$J = 1{,}67 \cdot 10^{15} \quad [mm^4]$$

6.3.1.4 Sections Tube Elements

The timber sections of tube elements are indicated with Section Assignment Levels as shown in figure 6.5 (right-hand side). A differentiation is made between brace elements and frame elements. The material assigned to the sections of the tube elements is D70-LAM as defined in table 6.8.

The timber sections of the tube elements of the BASE-model are assigned according to table 6.9. The timber sections of the tube elements of the NO-CORE-model are assigned according to table 6.10. The sections of horizontal elements (beams) are equal to the adjacent columns of that section level.

BASE-model					
Section Assignment Level	Section	Beam Releases DOWEL		Beam Releases TUBE-F	
Units:	b x h [mm]	K_{ser} [MN/mm]	K_r [kNm/rad]	K_{ser} [MN/mm]	K_r [kNm/rad]
Frame Elements 1	750 x 750	13,61	12193	7,78	4370
Frame Elements 2	700 x 700	10,89	7316	6,48	4152
Frame Elements 3-4	700 x 700	10,89	7316	6,48	4152
Frame Elements 5-6	600 x 600	7,78	3919	4,67	2491
Frame Elements 7-8	550 x 550	6,22	1866	3,89	4152
Frame El. 9-10	500 x 500	5,18	684	3,24	4152
Frame El. 11-12	400 x 400	3,11	709	1,95	1311
Frame El. 13-14	350 x 350	2,33	709	1,30	219
Frame El. 15-16	300 x 300	1,56	709	0,78	131
Braces 1-5	550 x 550	6,22	1866	3,89	11144
Braces 6-9	400 x 400	3,89	1182	2,33	2491
Braces 10-13	350 x 350	3,11	709	1,56	787
Braces 14-16	300 x 300	3,89	980	1,58	675

table 6.9: Sections applied to Elements

NO-CORE-model			
Section Assignment Level	Section	Beam Releases TUBE-F	
Units:	b x h [mm]	K_{ser} [MN/mm]	K_r [kNm/rad]
Columns 1	800 x 800	7,78	4370
Columns 2	750 x 750	7,78	4370
Columns 3-4	750 x 750	7,78	4370
Columns 5-6	650 x 650	8,45	2250
Columns 7-8	600 x 600	4,67	2491
Columns 9-10	500 x 500	3,24	4152
Columns 11-12	400 x 400	1,95	1311
Columns 13-14	350 x 350	1,30	219
Columns 15-16	300 x 300	0,78	131
Braces 1-5	600 x 600	5,19	13110
Braces 6-9	450 x 450	2,72	5769
Braces 10-13	400 x 400	2,33	2491
Braces 14-16	350 x 350	1,56	787

table 6.10: Sections applied to Elements

6.3.1.5 Beam Releases

To incorporate the stiffness of joints into the model, beam releases are used. The beam releases are assigned coincident with the timber sections as these are indicated in table 6.9 and table 6.10. The default beam releases for the BASE-model of this variant are the joint stiffness values of the tube faster (TUBE-F). For the BASE-model the values of the beam releases are varied between:

TUBE-F: beam releases are equal to the stiffness of tube fastener joints.

DOWEL: beam releases are equal to the stiffness dowel fastener joints.

PINNED: indicates that the local node rotations (yy,zz) are free and local node translations (x,y,z) are fixed to the element. The local node rotation (xx) is always fixed to the element.

RIGID: indicates that all local node rotations (xx,yy,zz) and local translations (x,y,z) are fixed.

The values of K_{ser} are translation stiffness values in the local x-axis and z-axis direction and K_r are rotation stiffness values around the local y-axis. Rotation around the local z-axis is always free while the remaining translation (y) and rotation (xx) are fixed.

6.3.1.6 Support Stiffness

The support stiffness values of this variant are indicated in table 6.4 below.

	Spring stiffness (k) N/m	Rotational stiffness (k_r) Nm/rad
Tube Supports	$1{,}41\ 10^{9}$	0,00
Core Support	$3{,}53 \cdot 10^{10}$	$1{,}22\ 10^{12}$

table 6.11: Support Stiffness Values of the Diagrid Model

6.3.1.7 Loading Cases

Self-Weight Main Structure (LC1)

The self-weight of the main structure is calculated automatically by gravity loading feature of the software.

Permanent Vertical Loads (LC2 + LC3)

The vertical loads are concentrated at the tube nodes and the core nodes as shown in figure 6.6 (left-hand side). The vertical node spacing of both tube nodes and core nodes coincides with two storey heights (vertical floor spacing). The following values are therefore valid: n_{floor} = 2 and l_{ctc} = 7,20m. The permanent vertical loads result therefore in the values given in table 6.12 based on § 4.2.7.1 as shown below:

$$F_{p;core,rep} = 2078 \cdot 2 = \quad 4156 \quad \left[{kN}/{node}\right]$$

$$F_{p;tube;rep} = 13{,}34 \cdot 7{,}20 \cdot 2 = \quad 193 \quad \left[{kN}/{node}\right]$$

Load case	Nodes	Direction	Value	Units
Permanent loading	Core nodes	z	-4156	kN
Permanent loading	Tube nodes	z	-193	kN

table 6.12: Loads on the Models of Variant 2

Variable Vertical Loads (LC4)

In a similar manner as the permanent vertical loads are the values of variable vertical loads given in table 6.13 based on § 4.2.7.1 as shown below:

$$F_{q;core,rep} = 619 \cdot 2 = \quad 1238 \cdot \left[{kN}/{node}\right]$$

$$F_{q;tube;rep} = 4{,}18 \cdot 7{,}20 \cdot 2 = \quad 60 \cdot \left[{kN}/{node}\right]$$

Load case	Nodes	Direction (Global)	Value	Units
Variable loading	Core nodes	z	-1238	kN
Variable loading	Tube nodes	z	-60	kN

table 6.13: Loads on the Models of Variant 2

Variable Wind load (LC5)
Geometrically, the tube elements of variant 2 create rectangles as can be observed in figure 6.5. Each tube node is loaded with the wind load of one such rectangle, which results in the following equivalent area calculation for the wind load:

$$A_{eq} = 7,2 \cdot 7,0 = 50,4 \cdot m^2$$

This results in the following values for the wind load for one representative node, based on earlier calculations in in § 4.2.7.2:

$$F_{w;node;rep}(b) = Q_{w;rep}(0 < z < 30) \cdot A = \quad 1,68 \cdot 50,40 \quad = 84,7 \quad kN/node$$

$$F_{w;node;rep}(z) = Q_{w;rep}(30 < z < 82) \cdot A = \quad \left(\frac{173}{13000} \cdot z + 1,28\right) \cdot 50,4 \quad kN/node$$

$$F_{w;node;rep}(h) = Q_{w;rep}(82 < z < 112) \cdot A = \quad 2,37 \cdot 50,4 \quad = 119,4 \quad kN/node$$

Wind loads are imposed on the tube nodes of one face of tube structure of the model and results in the horizontal loads as these are shown in figure 6.6.

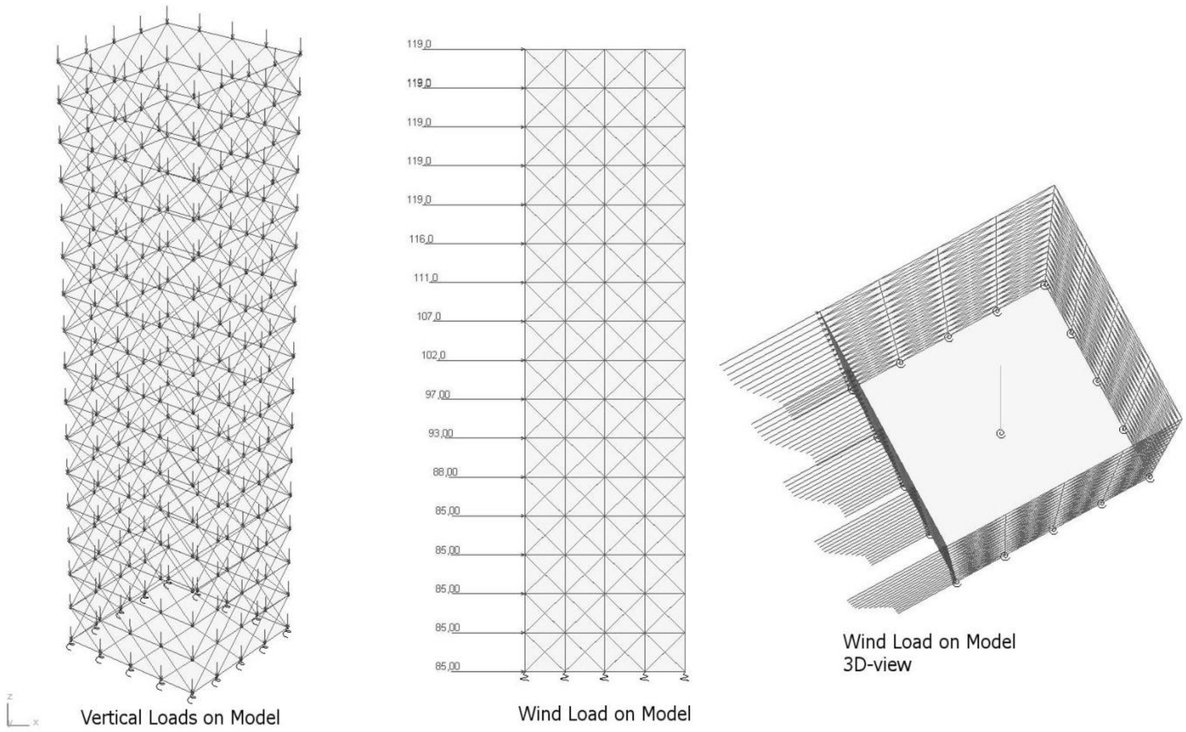

figure 6.6: Load on Nodes of Model

6.3.1.8 Load Combinations

The load combinations of load cases are applied in the model as defined in table 6.14.

Load Combinations	LC 1	LC 2	LC 3	LC 4	LC 5	LC 6	LC 7
C0: ULS	1,20	1,20	1,20	1,50	1,50	-	-
C1: ULS	1,35	1,35	1,35	0,75	0,75		
C2: ULS	0,90	0,90	0,90	0,00	1,50	-	-
C3: SLS	1,00	1,00	1,00	1,00	1,00	-	-
C4: ULS Fire	1,00	1,00	1,00	1,00	0,20	-	-
C5: SLS Dynamic	1,00	1,00	1,00	1,00	0,73	-	0~1,00
C6: Quasi-Permanent	1,00	1,00	1,00	0,50	0,00	-	-

table 6.14: Load Combinations

6.3.2 Results

The magnitude of the bending moments compared to the axial forces is small and does not result in significant stress changes (less than 1%). Tension forces do not occur in braces or columns. It is therefore that all members are only verified on critical buckling compression stresses. The element force results that were calculated with finite element model for the ultimate limit state combinations are discussed here.

The forces on the elements ($F_{d,i}$) are extracted from the models by handling the data. The buckling resistance ($R_{d,buc}$) of members is described in paragraph 3.9

Fundamental Combinations

ULS verification on maximum occurring element forces calculated with the BASE-model and the NO-CORE-model for ULS load combinations C0 to C2 was satisfied for the applied sections, in which C0 was decisive. The ULS load combination C2 did not result in tension forces in the tube supports for both models.

Charring and Fire Combinations

The reduced sections due to charring in a fire are 82 mm smaller than their original. The verifications of the columns for the fire combination (C4) are given in graph 6.3 for the BASE-model in which results are sorted by section allocation level. It can be observed that the ULS verification is not satisfied for the smaller (higher level) column sections. The same can be observed for the NO-CORE-model in graph 6.4.

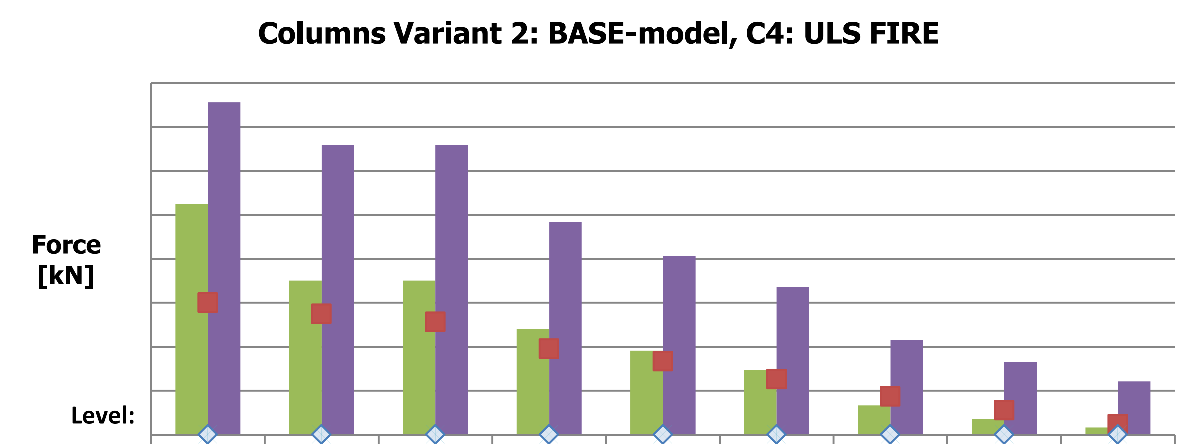

Level:	668 (1)	618 (2)	618 (3-4)	518 (5-6)	468 (7-8)	418 (9-10)	318 (11-12)	268 (13-14)	218 (15-16)
Rd,buc	10494	7008	7008	4801	3828	2930	1330	724	330
Rd,t	15120	13171	13171	9677	8131	6720	4301	3293	2419
Fc,d	6003	5493	5120	3902	3335	2518	1728	1106	472
Fd,t	0	0	0	0	0	0	0	0	0
UC	0,57	0,78	0,73	0,81	0,87	0,86	1,30	1,53	1,43

graph 6.3: Forces in Columns, Fire Combination C4

The verification of the braces shows a different picture. Where the buckling verification of elements for small members is not satisfied for the BASE-model as shown in graph 6.5 it is for the NO-CORE-model as shown in graph 6.6.

Columns Braced Frame: NO-CORE-model, C4: ULS FIRE

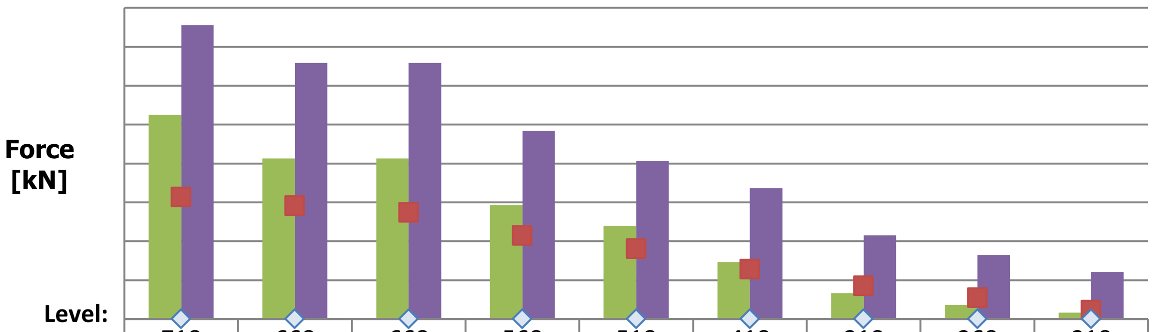

Level:	718 (1)	668 (2)	668 (3-4)	568 (5-6)	518 (7-8)	418 (9-10)	318 (11-12)	268 (13-14)	218 (15-16)
Rd,buc	10494	8250	8250	5859	4801	2930	1330	724	330
Rd,t	15120	13171	13171	9677	8131	6720	4301	3293	2419
Fc,d	6270	5831	5484	4286	3615	2553	1705	1091	448
Fd,t	0	0	0	0	0	0	0	0	0
UC	0,60	0,71	0,66	0,73	0,75	0,87	1,28	1,51	1,36

graph 6.4: Forces in Columns, Fire Combination C4

Braces Variant 2: BASE-model, C4: ULS FIRE

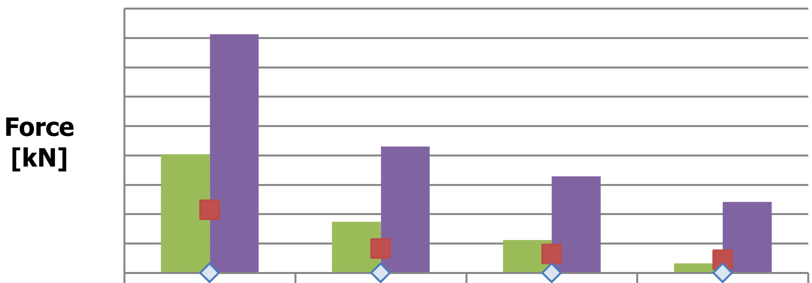

Level:	468 (1-4)	318 (5-9)	268 (10-13)	218 (15-16)
Rd,buc	4041	1737	1124	330
Rd,t	8131	4301	3293	2419
Fd,c	2151	829	646	455
Fd,t	0	0	0	0
UC	0,53	0,48	0,57	1,38

graph 6.5: Forces in Braces, Fire Combination C4

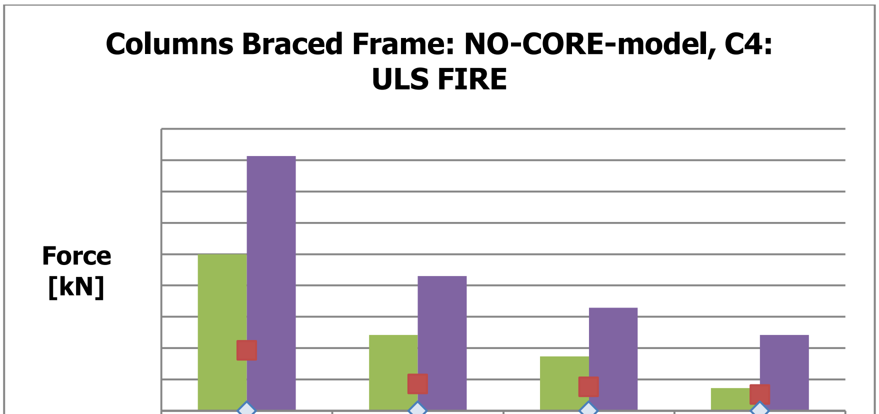

	518 (1-4)	368 (5-9)	318 (10-13)	268 (15-16)
Rd,buc	4992	2419	1737	724
Rd,t	8131	4301	3293	2419
Fc,d	1927	859	763	522
Fd,t	0	0	0	0
UC	0,39	0,36	0,44	0,72

graph 6.6: Forces in Braces, Fire Combination C4

6.3.3 Conclusion

In the first design the braces where chosen as steel rods with a small cross section. It was observed that this design did not fulfill the serviceability requirements with initially chosen cross-sections of 500 x 500 mm for the columns and beams. In the second run the rods where replaced by timber braces which delivered more promising results, because brace elements can also transfer compression forces in this configuration.

Thereafter, the optimization to satisfy the ultimate limit state requirements of the fundamental combinations (C0 and C1) resulted in the timber column sections shown in table 6.9 and the brace sections shown in table 6.10.

The sections are verified for the load combination in fire conditions. The cross section of the members was therefore reduced with 82 mm which resulted in particularly small sections to fail. A similar conclusion can be drawn from these results as was done for the previous variant. However, in addition to this it could be concluded that: when a timber building is designed, the absence of a lateral stiff core could result in section dimensions of a tube structure that are simultaneously protected against fire by their massiveness.

6.4 Variant 3: 1D-Closed

Most of the structural analysis of variant 3 is conducted with 2D element models. This model however, consists of 1D beam elements, and is included in the analysis because the used software cannot process dynamical analysis on 2D elements. This 1D beam model is chosen to include shear through use of the modification K_y=K_z=1 which makes the deflection similar to the 2D element models of variant 3.

6.4.1 Model Description

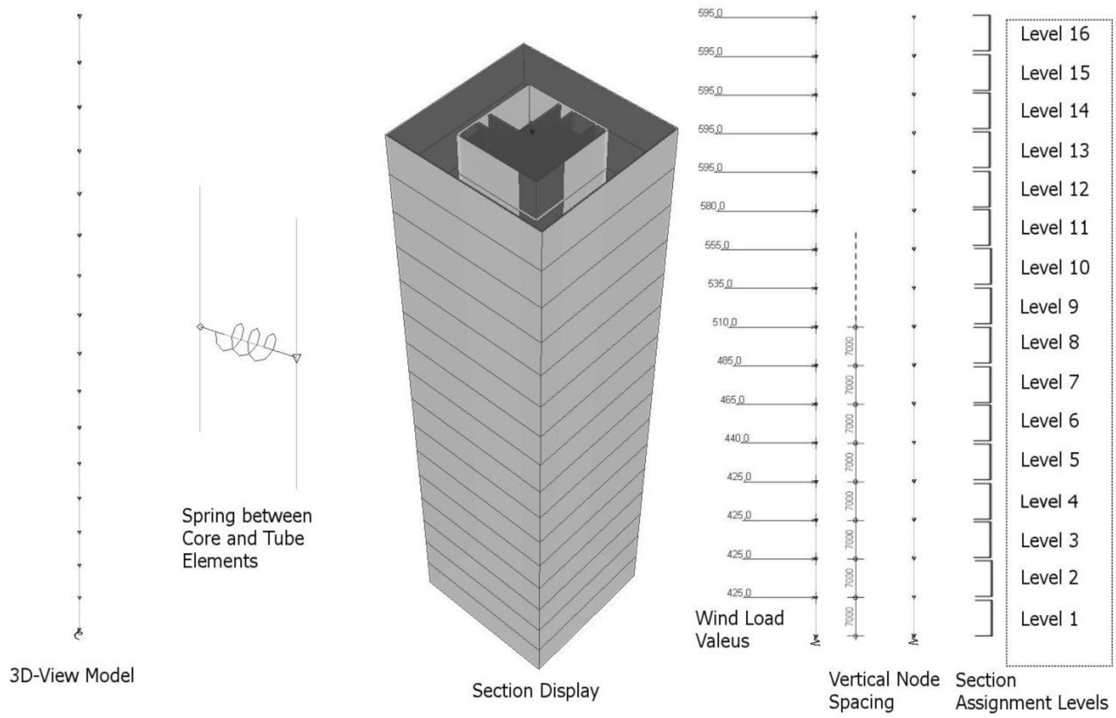

figure 6.7: Geometry and Section Assignment of 1D-model of Variant 3

6.4.1.1 Geometry

The geometry and the dimensions of the geometry for this model are shown in figure 6.7. In addition to this figure a textual description is given here of the geometry. The 1D elements used in GSA models are orientated by placing them between nodes. These nodes are spaced with the following dimensions:

Horizontal node spacing = 100 mm
Vertical node spacing = 7000 mm

The core nodes are very close to the tube nodes (0,10 m), to avoid problems with eccentricity.

6.4.1.2 Model Material Properties

The material properties assigned to the elements applied in the model are defined as shown in table 6.15. These model material properties of D70-CLT-OPEN are created through correction with the openings factor defined in paragraph 3.6.3.5. The density is modified with straight forward reduction of volume.

Material Name	GSA Material model	Modulus of elasticity	Poisson's Ratio	Shear modules	Density
Symbol:		E	μ		ρ
Unit:		[N/mm^2]	[-]	[N/mm^2]	[kg/m^3]
D70-CLT	Elastic Isotropic	11800	0	998	900
D70-CLT-OPEN	Elastic Isotropic	8732	0	519	746

table 6.15: Material Properties applied to 1D Solid Shear Frame Model

6.4.1.3 Section Core Elements

The material properties assigned to the section of the core elements is D70-CLT as defined in table 6.15. The section properties of the core elements are:

A		$= 5{,}64\cdot10^{7}$	[mm^2]
I_{yy}	$= 1{,}23\cdot10^{15}\cdot0{,}69$	$= 0{,}848\cdot10^{15}$	[mm^4]
I_{zz}	$= 1{,}23\cdot10^{15}\cdot0{,}69$	$= 0{,}848\cdot10^{15}$	[mm^4]
J		$= 1{,}67\cdot10^{15}$	[mm^4]

6.4.1.4 Sections Tube Elements

The sections that are assigned to the tube elements of the 1D model are rectangular hollow sections of 28800 mm squared with a certain thickness. The thicknesses of these sections of both 1D BASE-model and the NO-CORE-model are assigned according to table 6.16. The material assigned to the sections of the tube elements is D70-CLT-OPEN as defined in table 6.15.

	BASE-model	NO-CORE-model
Section Assignment Level	Section	Section
Units:	t [mm]	t [mm]
0-2	301	301
3-6	215	301
7-16	215	215

table 6.16: Sections applied to Elements

6.4.1.5 Beam Releases

In this model element releases are not applied to the nodes of elements. All elements are therefore fixed to the system nodes in all translational and rotational directions.

6.4.1.6 Support Stiffness

The support stiffness values of this model are indicated in table 6.17 below.

	Spring stiffness (k) N/m	Rotational stiffness (k_r) Nm/rad
Tube Support	$2{,}26\cdot10^{10}$	$3{,}21\cdot10^{12}$
Core Support	$3{,}53\cdot10^{10}$	$1{,}22\ 10^{12}$

table 6.17: Support Stiffness Values of the 1D-Model

6.4.1.7 Load Cases

Self-Weight Main Structure (LC1)

The self-weight of the main structure is calculated automatically by gravity loading feature of the software.

Permanent Vertical Loads (LC2 + LC3)

The vertical loads are concentrated at the tube nodes and the core nodes. The vertical node spacing of both tube nodes and core nodes coincides with two storey heights (vertical floor spacing). The tube nodes represent the full perimeter of the tube structure. The following values are therefore valid: n_{floor} =2 and l_{ctc} = 115,2. The permanent vertical loads result therefore in the values given in table 6.21 based on § 4.2.7.1 as shown below:

$$F_{p;core,rep} = 2078 \cdot 2 = \quad 4156 \quad \left[{}^{kN}\!/_{node}\right]$$

$$F_{p;tube;rep} = 13,34 \cdot 115,2 \cdot 2 = \quad 3074 \quad \left[{}^{kN}\!/_{node}\right]$$

Load case	Nodes	Direction	Value	Units
Permanent loading	Core nodes	z	-4156	kN
Permanent loading	Tube nodes	z	-3074	kN

table 6.18: Loads on the Models of Variant 1

Variable Vertical Loads (LC4)
In a similar manner as the permanent vertical loads are the values of variable vertical loads given in table 6.19 based on § 4.2.7.1 as shown below:

$$F_{q;core,rep} = 619 \cdot 2 = \quad 1238 \quad \left[{}^{kN}\!/_{node}\right]$$

$$F_{q;tube;rep} = 4,18 \cdot 115,2 \cdot 2 = \quad 963 \quad \left[{}^{kN}\!/_{node}\right]$$

Load case	Nodes	Direction (Global)	Value	Units
(LC4)	Core nodes	z	-1238	kN
(LC4)	Tube nodes	z	-963	kN

table 6.19: Loads on the Models of Variant 1

Variable wind load (LC5)
The equivalent area for the wind load of one node is calculated as:

$$A_{eq} = 28,80 \cdot 7,0 = 201,6 \cdot m^2$$

This results in the following values for the wind load for one representative node, based on earlier calculations in § 4.2.7.2:

$$F_{w;node;rep}(b) = Q_{w;rep}(0 < z < 30) \cdot A = \quad 1,68 \cdot 201,6 \quad = 338,7 \quad kN / node$$

$$F_{w;node;rep}(z) = Q_{w;rep}(30 < z < 82) \cdot A = \quad \left(\frac{173}{13000} \cdot z + 1,28\right) \cdot 201,6 \quad kN / node$$

$$F_{w;node;rep}(h) = Q_{w;rep}(82 < z < 112) \cdot A = \quad 2,37 \cdot 201,6 \quad = 477,8 \quad kN / node$$

These wind load values are unequal (relatively low) in comparison to the wind load on the models of variant 1 and 2. Therefore the values of the wind forces of those models are multiplied by 5 and imposed on the tube nodes of this model, because the loaded nodes ratio is 1:5. The variable wind loads result therefore in the values shown in figure 6.7.

6.4.1.8 Load Combinations

The load combinations of load cases are applied in the model as defined in table 6.20.

Load Combinations	LC 1	LC 2	LC 3	LC 4	LC 5	LC 6	LC 7
C0: ULS	1,20	1,20	1,20	1,50	1,50	-	-
C1: ULS	1,35	1,35	1,35	0,75	0,75		
C2: ULS	0,90	0,90	0,90	0,00	1,50	-	-
C3: SLS	1,00	1,00	1,00	1,00	1,00	-	-
C4: ULS Fire	1,00	1,00	1,00	1,00	0,20	-	-
C5: SLS Dynamic	1,00	1,00	1,00	1,00	0,73	-	0~1,00
C6: Quasi-Permanent	1,00	1,00	1,00	0,50	0,00	-	-

table 6.20: Load Combinations

6.5 Variant 3: 2D-Open

6.5.1 Model Description

For the solid shear wall frame two models were created with 2D-ellements (QUAD 8), in order to get realistic verification concerning the global stiffness and element stresses. In this 2D element model, tube elements are arranged around openings in order to take into account and verify the influence of openings.

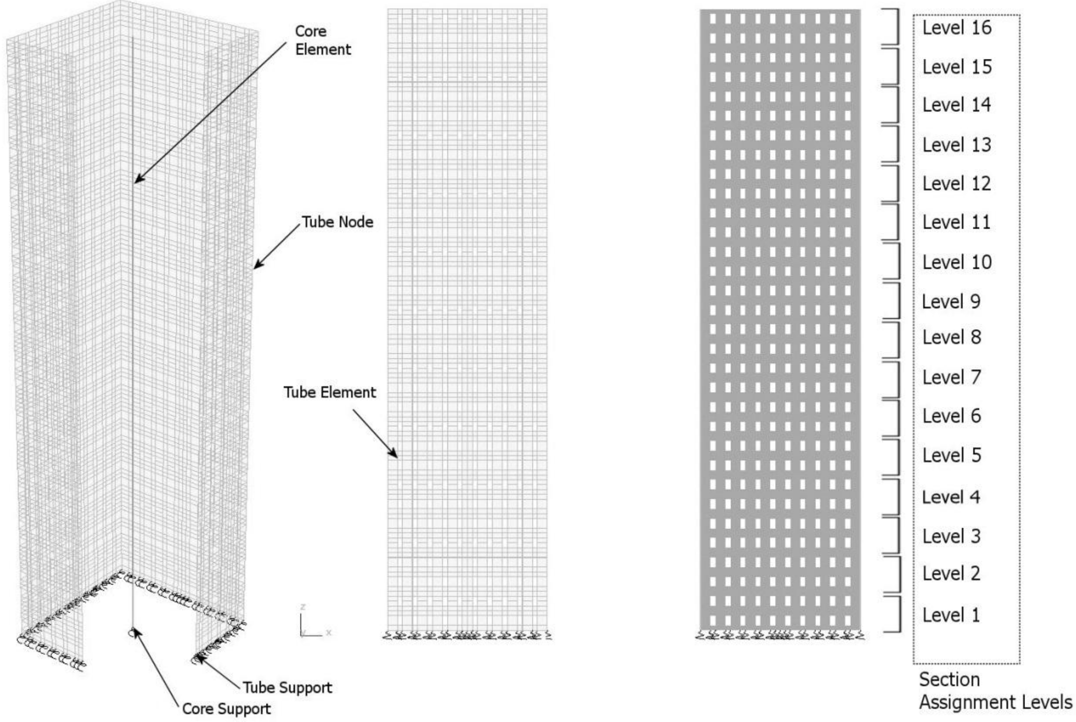

figure 6.8: Geometry and Section Assignment of 3D-model of Variant 3

6.5.1.1 Geometry

The elements of the model are orientated coherent with the geometry of the variant. The geometry for this model is shown in figure 6.8 and is the same for all faces of the tube structure. In addition to this figure a textual description is given below of the geometry.

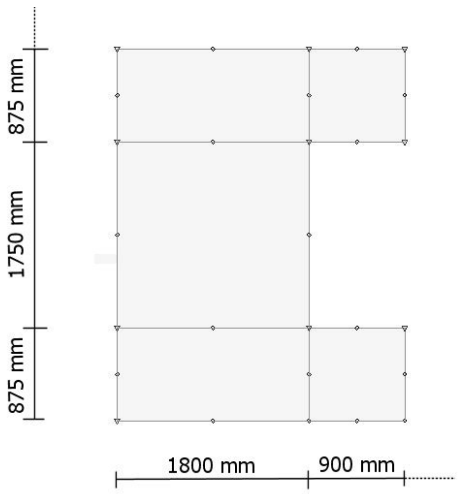

figure 6.9: Node spacing 2D-Open Model

The 2D elements used in GSA models are orientated by placing them between nodes. Nodes are spaced in such a manner that a tube structure with openings can be created with 2D elements. This implies that nodes are spaced with the following sequences which are also shown in figure 6.9:
Vertical: {875 mm, 1750 mm, 875 mm, … , 875 mm, 1750 mm, 875 mm}.
Horizontal: {1800 mm, 900 mm, …(x5), 900 mm, (symmetrical)}

The local x-axis of 2D elements is orientated parallel to the global Z-axis. Because 2D models consist of many nodes, the floor springs and the core nodes, are spaced on a vertical grid of 7000 mm and a horizontal grid of 7200 mm.

6.5.1.2 Model Material Properties

The material properties assigned to the elements applied in the model are defined as shown in table 6.21. The properties of material D70-CLT-ORT are defined orthotropic in the used software.

Material Name:	Symbol	D70-CLT-ORT	D70-CLT	Units
GSA Material model		Elastic Orthotropic	Elastic Isotropic	
Young's Modulus-x	E_x	11800	11800	[N/mm^2]
Young's Modulus-y	E_y	9600	N/A	[N/mm^2]
Young's Modulus-z	E_z	1330	N/A	[N/mm^2]
Poisson's Ratio xy	μ	0	0	[-]
Poisson's Ratio yz	μ	0	N/A	[-]
Poisson's Ratio zx	μ	0	N/A	[-]
Density	ρ	900	900	[kg/m^3]
Shear modulus-xy	G_{xy}	998	988	[N/mm^2]
Shear modulus-yz	G_{yz}	998	N/A	[N/mm^2]
Shear modulus-zx	G_{zx}	100	N/A	[N/mm^2]

table 6.21: Material Properties applied to 2D Solid Shear Frame Model

6.5.1.3 Section Core Elements

The material properties assigned to the section of the core elements is D70-CLT as the material is defined in table 6.21. The section properties of the core elements are:

$A = 5{,}64\cdot10^{7}$ [mm^2]
$I_{yy} = 1{,}23\cdot10^{15}\cdot0{,}69 = 0{,}848\cdot10^{15}$ [mm^4]
$I_{zz} = 1{,}23\cdot10^{15}\cdot0{,}69 = 0{,}848\cdot10^{15}$ [mm^4]
$J = 1{,}67\cdot10^{15}$ [mm^4]

6.5.1.4 Sections Tube Elements

The sections of the tube elements of the BASE-model and the NO-CORE-model are assigned according to table 6.22. The material assigned to the sections of the tube elements is D70-CLT-ORT as the material is defined in table 6.21.

	BASE-model	NO-CORE-model
Section Assignment Level	2D-ellement thickness	2D-ellement thickness
Units:	t [mm]	t [mm]
0-2	301	301
3-6	215	301
7-16	215	215

table 6.22: Sections applied to Elements

6.5.1.5 Element Releases

In this model element releases are not applied to the nodes of elements. All elements are therefore fixed to the system nodes in all translational and rotational directions. This implies that all local node rotations (xx,yy,zz) and local node translations (x,y,z) are fixed to the element.

6.5.1.6 Support stiffness

Unlike the 1D element models of variants 1 and 2, are the bottom nodes of this 2D element model spaced as shown in figure 6.9. The support stiffness is therefore averaged in accordance with this node spacing. The support stiffness values of this variant are given in table 6.23 below.

	Spring stiffness (k) N/m	Rotational stiffness (k_r) Nm/rad
Tube Supports	$0{,}32\ 10^{9}$	0,00
Core Support	$3{,}53\cdot10^{10}$	$1{,}22\ 10^{12}$

table 6.23: Support Stiffness Values of the Diagrid Model

6.5.1.7 Load Cases

Because the 2D models consist of many nodes, the loaded nodes are chosen coherent with variant 1 and 2, which implies that loads are applied as given in table 6.24, table 6.25 and figure 6.6.

Load case	Nodes	Direction	Value	Units
Permanent loading	Core nodes	z	-4156	kN
Permanent loading	Tube nodes	z	-193	kN

table 6.24: Loads on the Models

Load case	Nodes	Direction (Global)	Value	Units
Variable loading	Core nodes	z	-1238	kN
Variable loading	Tube nodes	z	-60	kN

table 6.25: Loads on the Models

6.5.1.8 Load Combinations

The load combinations of load cases are applied in the model as defined in table 6.26.

Load Combinations	LC 1	LC 2	LC 3	LC 4	LC 5	LC 6	LC 7
C0: ULS	1,20	1,20	1,20	1,50	1,50	-	-
C1: ULS	1,35	1,35	1,35	0,75	0,75		
C2: ULS	0,90	0,90	0,90	0,00	1,50	-	-
C3: SLS	1,00	1,00	1,00	1,00	1,00	-	-
C4: ULS Fire	1,00	1,00	1,00	1,00	0,20	-	-
C5: SLS Dynamic	1,00	1,00	1,00	1,00	0,73	-	0~1,00
C6: Quasi-Permanent	1,00	1,00	1,00	0,50	0,00	-	-

table 6.26: Load Combinations

6.6 Variant 3: 2D-Closed

6.6.1 Model Description

In this 2-D element model, no openings are created with 2D-elements. The influence of openings on the stiffness is accounted for by modification of the moduli of elasticity.

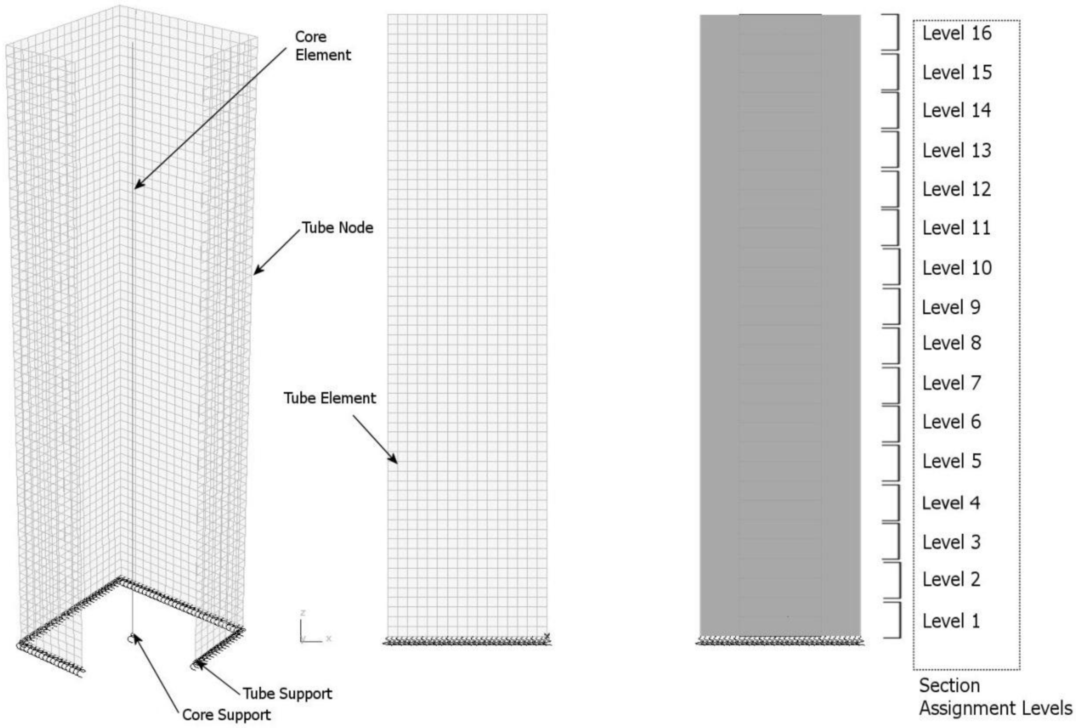

figure 6.10: Impression of the Solid 2D-Closed Model

6.6.1.1 Geometry

The 2D-closed model serves as a verification of the modified modulus of elasticity approach, therefore only the BASE-model is created. Tube nodes are spaced with 1800 mm, in the horizontal direction and 1,75 m in the vertical direction as shown in figure 6.11. The local x-axis of 2D elements is orientated parallel to the global Z-axis, which is important to note because the 2D material properties are orientated coincident with the local element axis's.

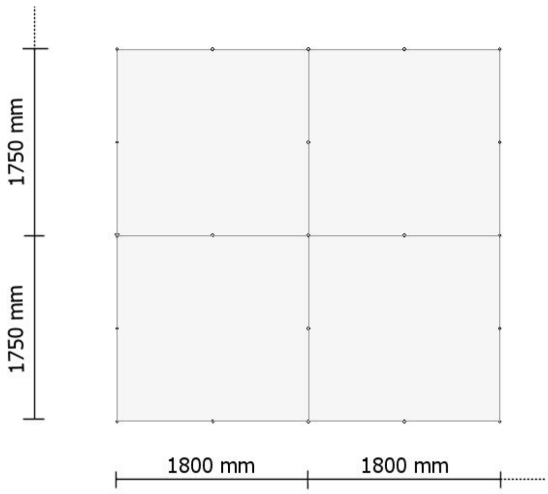

figure 6.11: Node spacing 2D-Closed Model

6.6.1.2 Model Material Properties

The material properties assigned to the elements applied in the 2D-Closed model are defined as shown in table 6.27. The properties of material D70-CLT-ORT-2 in this table are defined orthotropic and modified according to § 3.6.3.5 to take into account the effect of openings.

Material Name:		D70-CLT-ORT-2	D70-CLT	
	Symbol			Unit
Material model		Elastic Orthotropic	Elastic Isotropic	
Young's Modulus-x	E_x	8732	11800	[N/mm^2]
Young's Modulus-y	E_y	7100	N/A	[N/mm^2]
Young's Modulus-z	E_z	1330	N/A	[N/mm^2]
Poisson's Ratio xy	μ	0	0	[-]
Poisson's Ratio yz	μ	0	N/A	[-]
Poisson's Ratio zx	μ	0	N/A	[-]
Density	ρ	746	900	[kg/m^3]
Shear modulus-xy	G_{xy}	519	988	[N/mm^2]
Shear modulus-yz	G_{yz}	519	N/A	[N/mm^2]
Shear modulus-zx	G_{zx}	100	N/A	[N/mm^2]

table 6.27: Material Properties applied to 2D Element Solid Shear Frame Model

6.6.1.3 Section Core Elements

The material properties assigned to the section of the core elements is D70-CLT as defined in table 6.27. The section properties of the core elements are:

A		$= 5{,}64 \cdot 10^{7}$	[mm^2]
I_{yy}	$= 1{,}23 \cdot 10^{15} \cdot 0{,}69$	$= 0{,}848 \cdot 10^{15}$	[mm^4]
I_{zz}	$= 1{,}23 \cdot 10^{15} \cdot 0{,}69$	$= 0{,}848 \cdot 10^{15}$	[mm^4]
J		$= 1{,}67 \cdot 10^{15}$	[mm^4]

6.6.1.4 Sections Tube Elements

The sections of the tube elements in the models BASE-model are assigned according to table 6.28. The material assigned to the sections of the tube elements is D70-CLT-ORT-2 as defined in table 6.27.

	BASE-model
Section Assignment Level	2D-ellement thickness
Units:	t [mm]
0-2	301
3-6	215
7-16	215

table 6.28: Sections of Model

6.6.1.5 Element Releases

In this model element releases are not applied to the nodes of elements. All elements are therefore fixed to the system nodes in all translational and rotational directions. This implies that all local node rotations (xx,yy,zz) and local node translations (x,y,z) are fixed to the element.

6.6.1.6 Support stiffness

Unlike the 1D element models of variants 1 and 2, are the bottom nodes of this 2D element model spaced as shown in figure 6.11. The support stiffness is therefore averaged in accordance with this node spacing The support stiffness values of this variant are given in table 6.29 below.

	Spring stiffness (k) N/m	Rotational stiffness (k_r) Nm/rad
Tube Supports	$0{,}22\ 10^9$	0,00
Core Support	$3{,}53 \cdot 10^{10}$	$1{,}22\ 10^{12}$

table 6.29: Support Stiffness Values of the Model

6.6.1.7 Load Cases

Because the 2D models consist of many nodes, the loaded nodes are chosen coherent with variant 1 and 2 which implies that loads are applied as given in table 6.30, table 6.31 and figure 6.6.

Load case	Nodes	Direction	Value	Units
Permanent loading	Core nodes	z	-4156	kN
Permanent loading	Tube nodes	z	-193	kN

table 6.30: Loads on the Models

Load case	Nodes	Direction (Global)	Value	Units
Variable loading	Core nodes	z	-1238	kN
Variable loading	Tube nodes	z	-60	kN

table 6.31: Loads on the Models

6.6.1.8 Load Combinations

The load combinations of load cases are applied in the model as defined in table 6.7.

Load Combinations	LC 1	LC 2	LC 3	LC 4	LC 5	LC 6	LC 7
C0: ULS	1,20	1,20	1,20	1,50	1,50	-	-
C1: ULS	1,35	1,35	1,35	0,75	0,75		
C2: ULS	0,90	0,90	0,90	0,00	1,50	-	-
C3: SLS	1,00	1,00	1,00	1,00	1,00	-	-
C4: ULS Fire	1,00	1,00	1,00	1,00	0,20	-	-
C5: SLS Dynamic	1,00	1,00	1,00	1,00	0,73	-	0~1,00
C6: Quasi-Permanent	1,00	1,00	1,00	0,50	0,00	-	-

table 6.32: Load Combinations

6.6.2 Results

The calculated stresses of the 2D element models of variant 3 can be projected into forces over a unit length inside the element. The critical buckling of plate elements are verified with these forces. The stresses derived from the models can be either presented as averaged stresses in the center of 2D elements or as peak stresses near nodes connected to floor springs and other hot spots. These peak stresses are assumed not to be realistic representations of the stress flow because the mesh is rather coarse and the corners near openings are sharp (hot spot). Therefore the averaged stresses in the center are used to for ultimate limit state verifications. Because the material properties of cross laminated timber elements are orthotropic, the projected forces of these stresses are used to verify the cross section area of the plates, rather than the stresses.

The results in graph 6.7 deserve some explanation. The 2D-closed model which is shown is corrected with a stress concentration factor. The stress concentration factor of equation (6.2) is used.

$$SCF = \frac{w_{full}}{w_{open}} \qquad \textbf{(6.2)}$$

In which:
w_{full} = representative width: 1800 mm
w_{open} = width of the opening: 900 mm

The values of these parameters are derived from figure 5.6 and results in a SCF of 2,0 which was used to plot the values of $F_{d,c}$ (CLOSED, COR) implying the corrected values of the closed model. These values correspond rather well with the forces of the 2D-open model. However, there is still ongoing research concerning the stress distribution of cross laminated timber with openings [15].

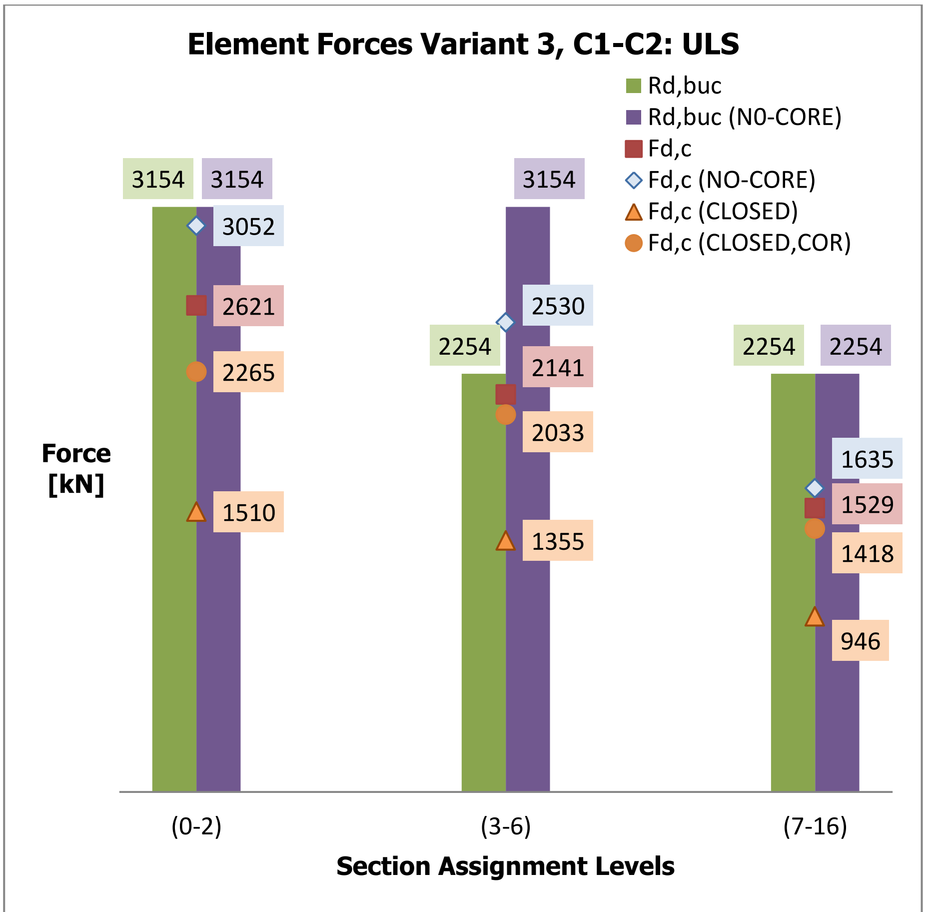

graph 6.7: Forces in Wall Plate

Significant tension forces do not occur in the elements of the model except at the bottom nodes, because these are supported by stiff springs as shown in figure 6.12, which corrupt some of the data. These elements are therefore excluded from the data. This implies furthermore, because tension forces are absent, that the joints only have to resist the shear forces which are also small by comparison as shown in graph 6.8. In this graph, forces are indicated according the definition given in figure 6.13, and only the absolute shear force (N_{xy} ABS) is presented independent of its sign. It can be observed that all maximum occurring forces are smaller than the maximum capacity of CLT-joints which is indicated with $R_{v,j}$ (MAX).

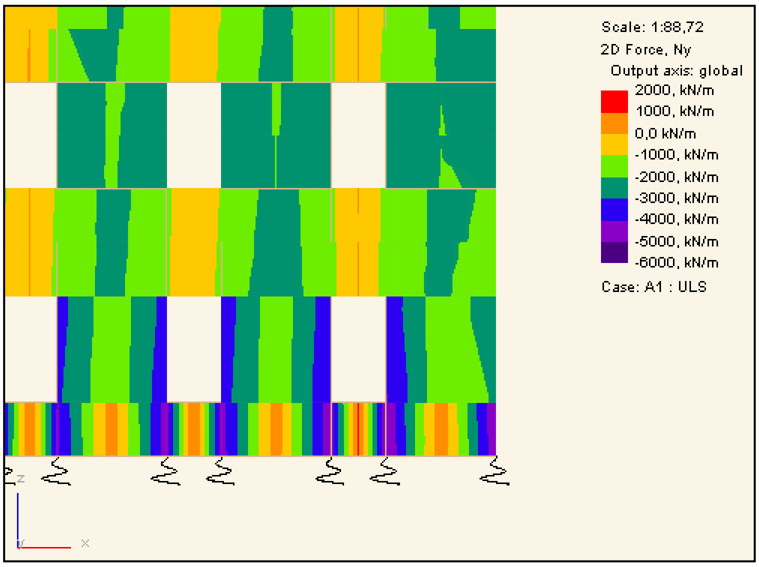

figure 6.12: 2D force at Bottom Elements

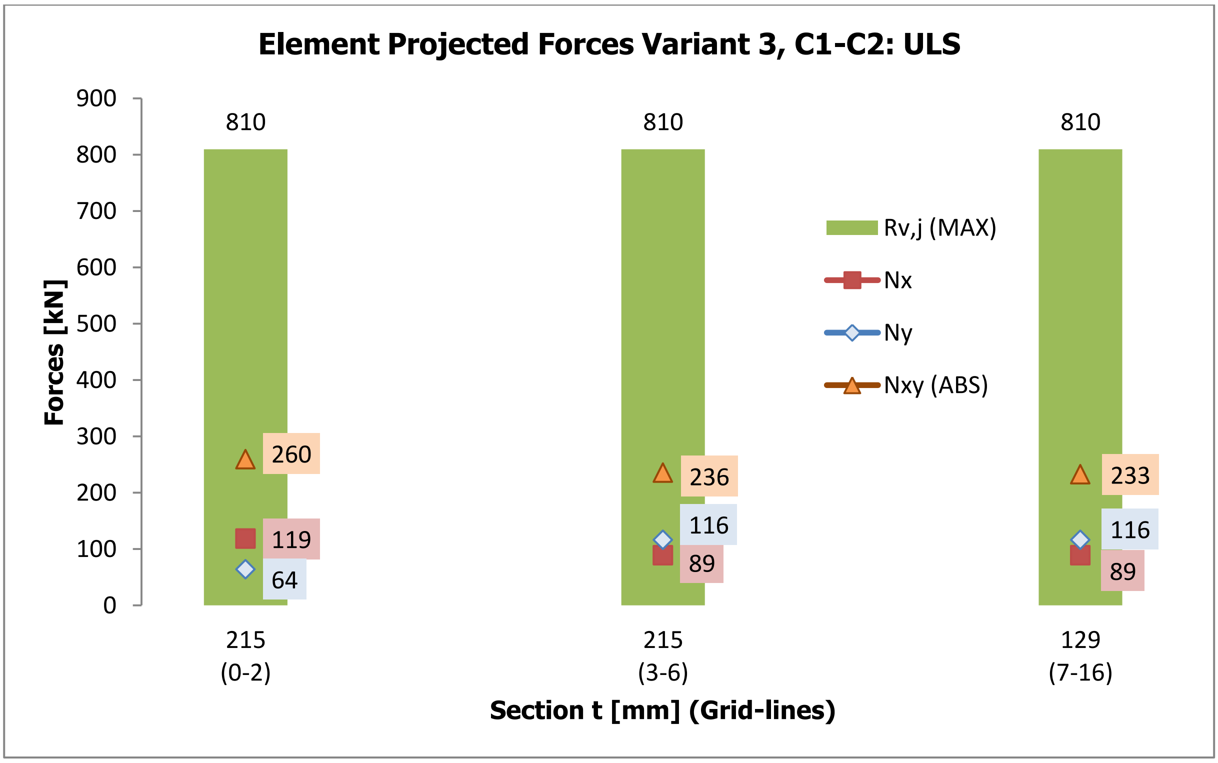

graph 6.8: Shear and Tension Forces in Elements

The effective cross sections given in paragraph 3.6.3.4 are used to calculate the stresses shown in graph 6.9. The index of these stresses (x,y) are consistent with the global axis set as shown in figure 6.13 and rotate with the orientation of the element. This implies that the local element x-axis coincides with the force output in the y-direction which is parallel to the global z-axis. This can be rather confusing, it is best observe S_y as stress in the vertical direction and S_x as stress in the horizontal direction of the world.

The shear stress is also given which is calculated with the full section area per meter length. It can be observed that maximum stresses are smaller than the corresponding strength, within an acceptable range.

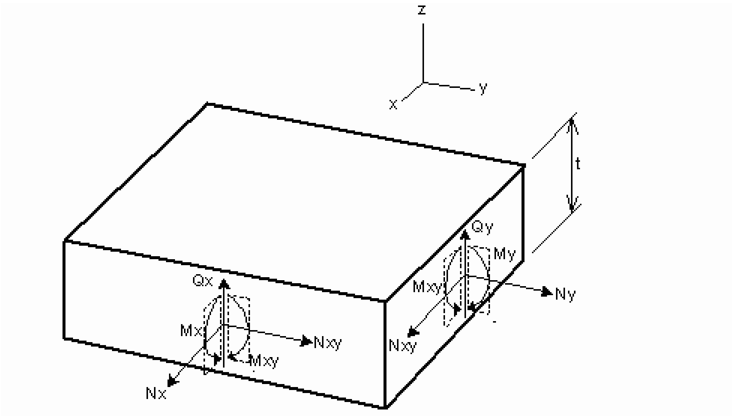

figure 6.13: Output Force Orientation 2D-elements

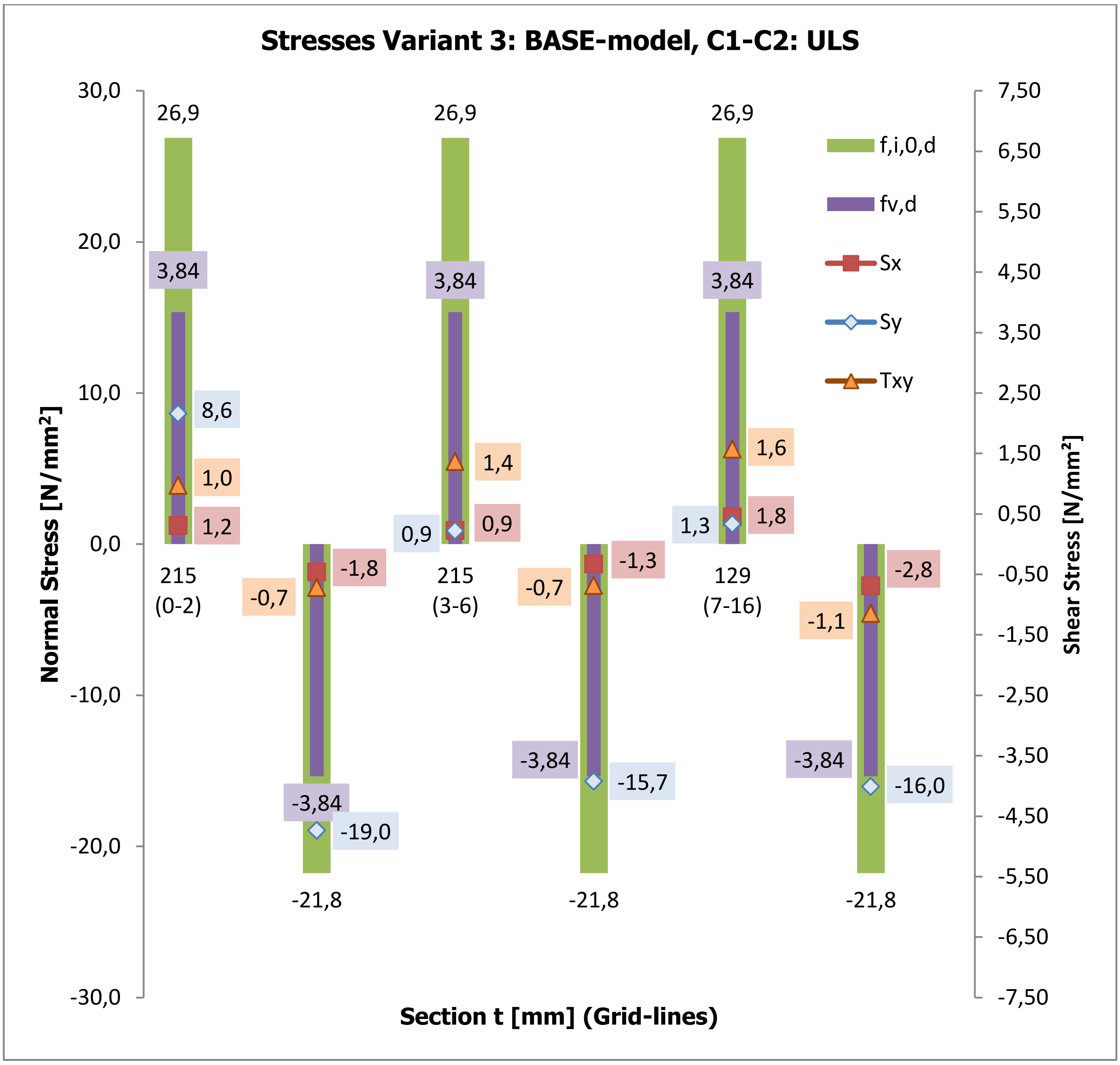

graph 6.9: Maximum Stresses in Wall Plate

6.6.3 Conclusion

In the first design the plate thicknesses where chosen 400 mm thick, which satisfied the serviceability requirements. Thereafter, the optimization to satisfy the ultimate limit state requirements of the ULS load combinations (C0 and C1) resulted in the timber sections shown in table 6.22. The thickness also increases when a core is not lateral stiff or absent but increasing tube elements is also more efficient, because these sections did not increase much.

Load combination C2 resulted in relatively small tension forces in the tube supports in the corner of the building model, while other windward supports remain in compression. This could be a sign of wind push over, but is also shows that the tube structure redevised the load to surrounding supports. However it is odd to realize that an equally supported tube structure as this results in tension forces, while other discrete supported structures (variant 1 and 2) do not, under the same load conditions.

A closed 2D-element model can be used without much compromise in stress results when a simple stress concentration factor is used. Using a closed model with the material modification, as was done, can be more efficient because creating a model with openings is more labor intensive and can result in stress peak errors in corners.

The sections are not verified for the load combination in fire conditions because this type of structure is not suitable for the finite charring concept as it is proposed, because of the small opening factor.

6.7 Variant 4: Mega Frame

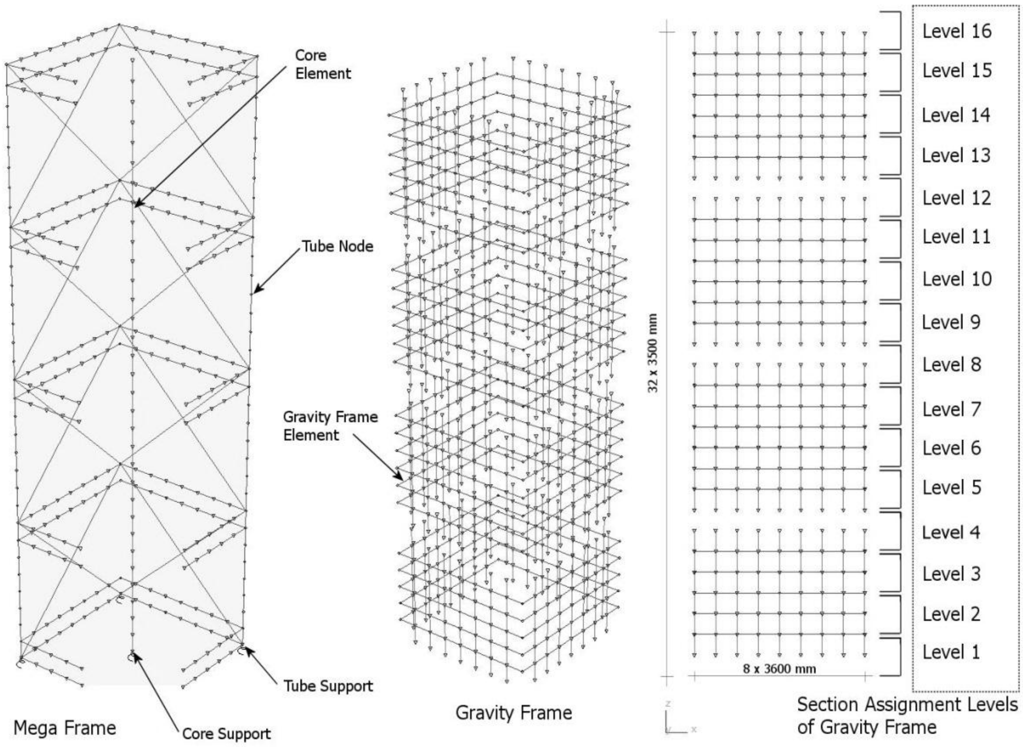

figure 6.14: Geometry of Mega Frame and Section Assignment of Gravity Frame

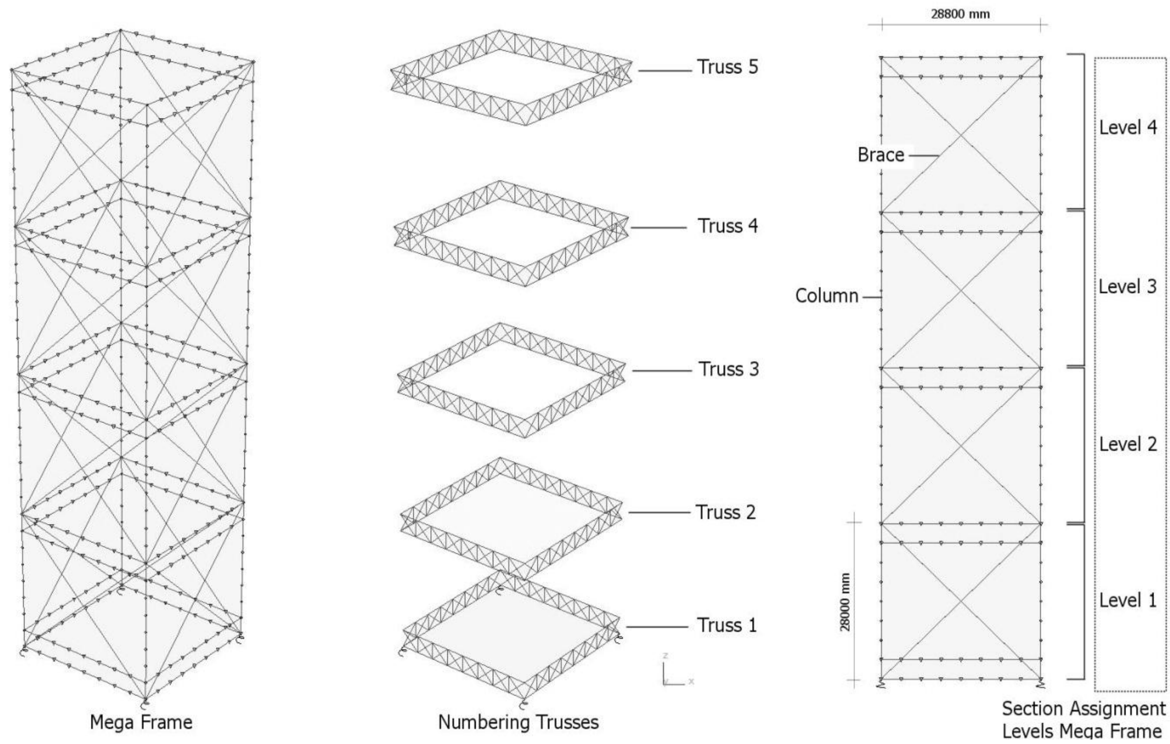

figure 6.15: Section Assignment of the Mega Frame and numbering of Trusses

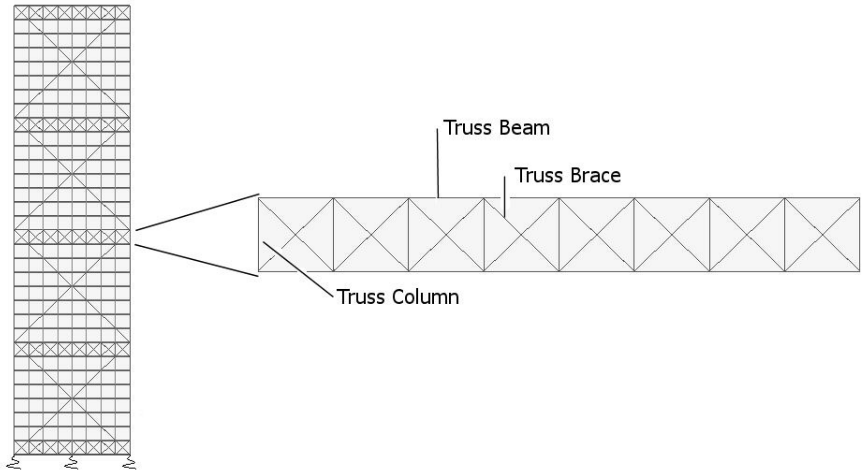

figure 6.16: Assignment of Truss Elements

6.7.1 Model Description

The mega frame model consists of three major parts: the Mega-frame, the Gravity-frame and trusses as shown in figure 6.14, figure 6.15 and figure 6.16. Elements of the Mega frame consists of columns and braces that are combined with truss beams. These elements can be referred to with the mega-prefix.

The gravity frame by itself is a sway-frame and must transfer the vertical loads to the trusses. The trusses transfer the vertical loads to the mega-columns. There are no supports present under the columns at the base of the Gravity-frame, because if there where, tension forces occur in the support of the mega-columns which is not allowed (wind push-over).

6.7.1.1 Geometry

The elements of the model are orientated coherent with the geometry of the variant. The geometry and the dimensions of this model are shown in figure 6.14, figure 6.15 and figure 6.16 and is the same for all faces of the tube structure. In addition to this figure a textual description is given here of the geometry.

The 1D elements used in GSA models are orientated by placing them between nodes. The tube nodes in one plane of the geometry are spaced with the following dimensions:
Horizontal node spacing = 3600 mm
Vertical node spacing = 3500 mm

Mega-frame elements are placed between nodes that are spaced 28800 mm in the horizontal direction. The mega-column elements are spaced 3500 mm in the vertical direction. Mega-Braces are placed between a grid of nodes spaced 28000 mm vertically as are the trusses.

The grid of the gravity frame is spaced 3,60 m in the horizontal direction and 3,50 m in the vertical direction coherent with the secondary grid of the variant.

6.7.1.2 Model Material Properties

The material properties assigned to the elements applied in the model are defined as shown in table 6.33.

Material Name	GSA Material model	Modulus of elasticity	Poisson's Ratio	Shear modules	Density
Symbol:		E	μ		ρ
Unit:		[N/mm^2]	[-]	[N/mm^2]	[kg/m^3]
D70-LAM	Elastic Isotropic	20000	0	1250	900
D70-CLT	Elastic Isotropic	11800	0	998	900

table 6.33: Material Properties applied to Mega Frame Models

6.7.1.3 Section Core Elements

The material properties assigned to the section of the core elements is D70-CLT as defined in table 6.33 The section properties of the core elements are:

A		$= 5{,}64 \cdot 10^{7}$	[mm^2]
I_{yy}	$= 1{,}23 \cdot 10^{15} \cdot 0{,}69$	$= 0{,}848 \cdot 10^{15}$	[mm^4]
I_{zz}	$= 1{,}23 \cdot 10^{15} \cdot 0{,}69$	$= 0{,}848 \cdot 10^{15}$	[mm^4]
J		$= 1{,}67 \cdot 10^{15}$	[mm^4]

The second moments of inertia (I_{yy} and I_{zz}) are 10% of the values given above for the NO-CORE-model.

6.7.1.4 Sections Tube Elements

The profile sections of the gravity-frame are indicated according to the definitions of the section assignment levels given in figure 6.14. Similarly are the profiles sections of the mega-frame indicated in figure 6.15. The trusses elements are named in figure 6.16. The sections of the tube elements in the BASE-model and the NO-CORE-model are assigned according to table 6.34, table 6.35 and table 6.36 respectively for the mega-frame, the trusses and the gravity frame of the model. The material assigned to all the sections of the tube elements is D70-LAM as defined in table 6.33.

	BASE-model	NO-CORE-model
Section Assignment Level	Section	Section
Units:	b x h [mm]	b x h [mm]
Mega-Columns 1	1300 x 1300	1350 x 1350
Mega-Columns 2	1150 x 1150	1200 x 1200
Mega-Columns 3	1000 x 1000	1000 x 1000
Mega-Columns 4	1000 x 1000	1000 x 1000
Mega-Brace 1	750 x 750	800 x 800
Mega-Brace 2	700 x 700	750 x 750
Mega-Brace 3	650 x 650	700 x 700
Mega-Brace 4	650 x 650	650 x 650
Truss beams 1	900 x 900	900 x 900
Truss beams 2	600 x 600	600 x 600
Truss beams 3	350 x 350	350 x 350
Truss beams 4	350 x 350	350 x 350
Truss beams 5	350 x 350	350 x 350

table 6.34: Sections of Mega Frame Elements

	BASE-model	NO-CORE-model
Section Assignment Level	Section	Section
Units:	b x h [mm]	b x h [mm]
Truss Columns 1	100 x 100	100 x 100
Truss Columns 2	200 x 200	200 x 200
Truss Columns 3	200 x 200	200 x 200
Truss Columns 4	150 x 150	150 x 150
Truss Columns 5	100 x 100	100 x 100
Truss Brace 1	550 x 550	550 x 550
Truss Brace 2	400 x 400	400 x 400
Truss Brace 3	350 x 350	350 x 350
Truss Brace 4	300 x 300	350 x 350
Truss Brace 5	300 x 300	300 x 300

table 6.35: Sections of Truss Elements

	BASE-model	NO-CORE-model
Section Assignment Level	Section	Section
Units:	b x h [mm]	b x h [mm]
1-2	300 x 300	300 x 300
3-4	300 x 300	300 x 300
5-6	400 x 400	400 x 400
7-8	250 x 250	250 x 250
9-10	250 x 250	250 x 250
11-12	200 x 200	200 x 200
13-14	200 x 200	200 x 200
15-16	100 x 100	200 x 200

table 6.36: Sections of the Gravity Frame Elements

6.7.1.5 Beam Releases

The following definitions apply to beam releases:

PINNED: indicates that the local node rotations (yy,zz) are free and local node translations (x,y,z) are fixed to the element. The local node rotation (xx) is always fixed to the element.

RIGID: indicates that all local node rotations (xx,yy,zz) and local translations (x,y,z) are fixed.

The beam releases of the Gravity-frame elements are pinned. Brace and columns elements of trusses shown in figure 6.16 are also connected pinned to the nodes. Truss-beam elements are rigid to intermediate nodes but pinned at the end nodes, where they intersect with mega-elements.

Mega-elements placed between nodes that are spaced coherent with the primary grid are connected RIGID to intermediate nodes and PINNED at the ends where they coincide with another type of mega-elements, i.e. the beam releases of mega-columns are pinned at nodes that also connect mega braces.

6.7.1.6 Support Stiffness

The support stiffness values of this variant are indicated in table 6.37 below.

	Spring stiffness (k) N/m	Rotational stiffness (k_r) Nm/rad
Tube Supports	$3{,}92\ 10^{9}$	0,00
Core Support	$3{,}53 \cdot 10^{10}$	$1{,}22\ 10^{12}$

table 6.37: Support Stiffness Values of the Model

6.7.1.7 Load Cases

Self-Weight Main Structure (LC1)
The self-weight of the main structure is calculated automatically by gravity loading feature of the software.

Permanent Vertical Loads (LC2 + LC3)
The vertical loads are concentrated at the tube nodes and the core nodes as shown in figure 6.17 (left-hand side). The vertical node spacing of both tube nodes and core nodes coincides with the vertical floor spacing. The following values are therefore valid: n_{floor} = 1 and l_{ctc} = 3,60m. The permanent vertical loads result therefore in the values given in table 6.38 based on § 4.2.7.1 as shown below:

$$F_{p;core,rep} = 2078 \cdot 1 = \quad 2078 \quad \left[{kN}/{node} \right]$$

$$F_{p;tube;rep} = 13{,}34 \cdot 3{,}60 \cdot 1 = \quad 48 \quad \left[{kN}/{node} \right]$$

Load case	Nodes	Direction	Value	Units
Permanent loading	Core nodes	z	-2078	kN
Permanent loading	Tube nodes	z	-48	kN

table 6.38: Permanent loads on the Model

Variable Vertical Loads (LC4)

In a similar manner as the permanent vertical loads are the values of variable vertical loads given in table 6.39 based on § 4.2.7.1 as shown below:

$$F_{q;core,rep} = 619 \cdot 2 = \qquad 1238 \cdot \left[{}^{kN}\!/_{node} \right]$$

$$F_{q;tube;rep} = 4,18 \cdot 7,20 \cdot 2 = \qquad 60 \cdot \left[{}^{kN}\!/_{node} \right]$$

Load case	Nodes	Direction (Global)	Value	Units
Variable loading	Core nodes	z	-619	kN
Variable loading	Tube nodes	z	-15	kN

table 6.39: Variable loads on the Model

Variable Wind load (LC5)

The horizontal loads are imposed on the nodes in line with the mega-columns of one (left) face. These loads are spaced vertically with 7000 mm because it is coherent with the other models. This results in the calculation of the equivalent wind loaded area.

$$A_{eq} = 14,40 \cdot 7,0 = 100,8 \cdot m^2$$

This results in the following values for the wind load for one representative node, based on earlier calculations in § 4.2.7.2:

$$F_{w;node;rep}(b) = Q_{w;rep}(0 < z < 30) \cdot A = \quad 1,68 \cdot 100,80 \quad = 169 \qquad kN / node$$

$$F_{w;node;rep}(z) = Q_{w;rep}(30 < z < 82) \cdot A = \quad \left(\frac{173}{13000} \cdot z + 1,28 \right) \cdot 100,80 \; kN / node$$

$$F_{w;node;rep}(h) = Q_{w;rep}(82 < z < 112) \cdot A = \quad 2,37 \cdot 100,80 \quad = 211 \qquad kN / node$$

These wind load values are unequal (relatively low) in comparison to the wind load on the models of the other variants. Therefore the magnitude of the wind load of those models are multiplied by ${}^{5}/_{2}$ and imposed on this model, because the loaded nodes ratio is 2:5. The variable wind loads result therefore in the values shown in figure 6.17.

6.7.1.8 Load Combinations

The load combinations of load cases are applied in the model as defined in table 6.7.

Load Combinations	LC 1	LC 2	LC 3	LC 4	LC 5	LC 6	LC 7
C0: ULS	1,20	1,20	1,20	1,50	1,50	-	-
C1: ULS	1,35	1,35	1,35	0,75	0,75		
C2: ULS	0,90	0,90	0,90	0,00	1,50	-	-
C3: SLS	1,00	1,00	1,00	1,00	1,00	-	-
C4: ULS Fire	1,00	1,00	1,00	1,00	0,20	-	-
C5: SLS Dynamic	1,00	1,00	1,00	1,00	0,73	-	0~1,00
C6: Quasi-Permanent	1,00	1,00	1,00	0,50	0,00	-	-

table 6.40: Load Combinations Tube-Structure

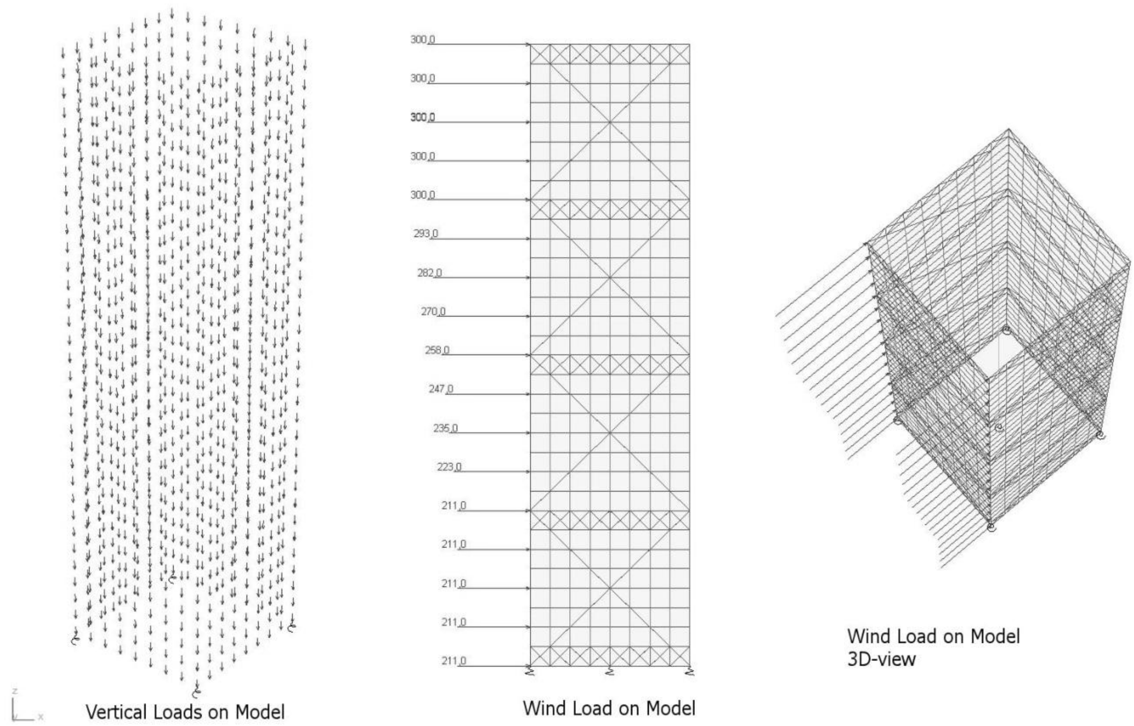

figure 6.17: Load on Nodes of Model

6.7.2 Results

The bending moments in the mega beams are relatively large in comparison to other members. Mega beams are laterally supported by floors and can therefore be verified as shown in equation (6.3). This equation represents this unity verification of which an example of a yield contour is shown in graph 6.10. A vertical log scale is applied because bending moments are still small in comparison to the resistance. The ultimate limit state verification for mega beams is not decisive for the dimensions, but are oversized to counteract the sag in the middle.

$$\left(\frac{M_d}{M_u}\right)^2 + \left(\frac{F_d}{F_{buc}}\right) \leq 1 \qquad \textbf{(6.3)}$$

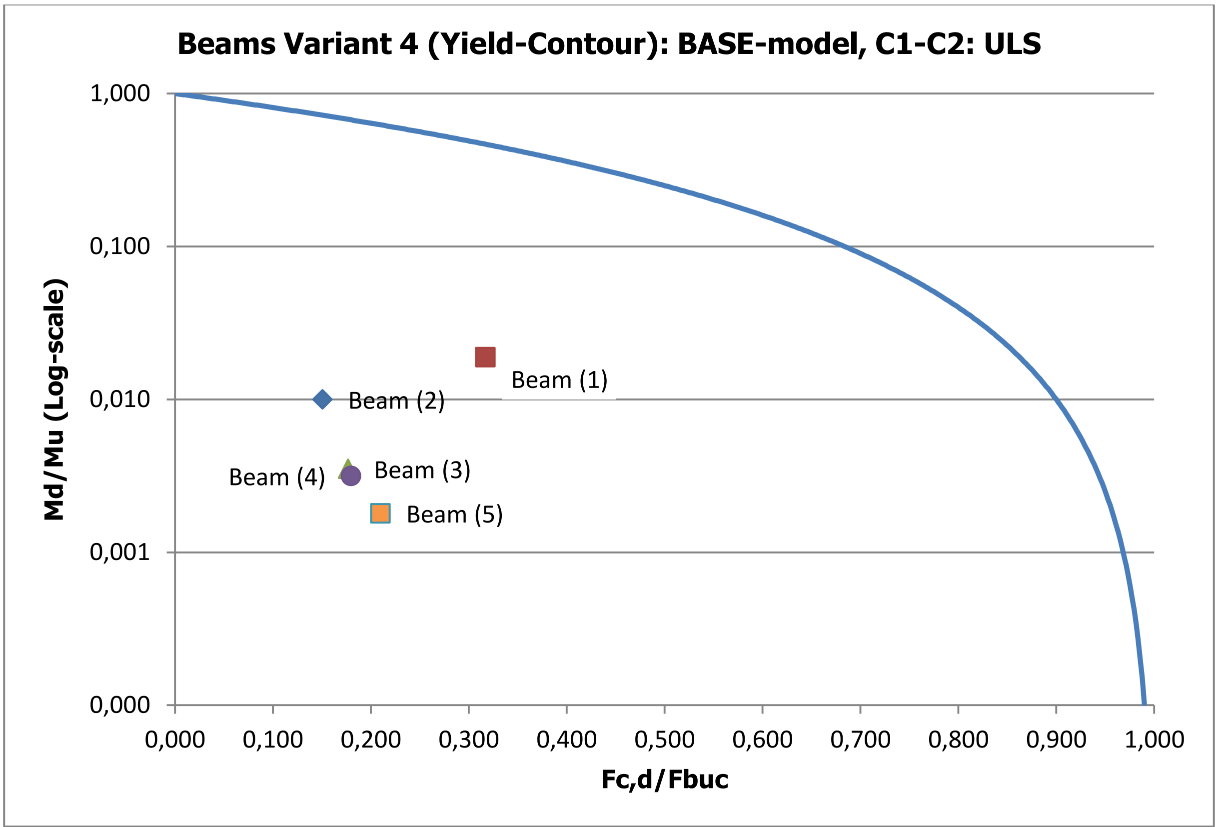

graph 6.10: Forces and Moments in Mega-Beams, ULS Combinations C1-C2

All members are only verified on axial forces, in particular critical buckling compression stresses. The forces on the elements ($F_{d,i}$) are extracted from the models by handling the data. The buckling resistance ($R_{d,buc}$) of members is described in paragraph 3.9.

Fundamental Combinations

ULS verification on maximum occurring element forces calculated with the BASE-model and the NO-CORE-model for ULS load combinations C0 to C2 was satisfied for the applied sections, in which C0 was decisive. The ULS load combination C2 did not result in tension forces in the tube supports for the BASE-model. For the NO-CORE-model however the ULS load combination C2 resulted in small tension forces in one of the windward tube supports of about 77,3 kN.

Charring and Fire Combinations

The reduced sections due to charring in a fire are 82 mm smaller than their original. The results for the gravity frame of the BASE-model and the NO-CORE-model are not different. The fire combination (C4) verifications of the gravity frame of both models is therefore given in graph 6.11. The results in this graph are sorted by section allocation level. It can be observed that the ULS verification is not satisfied for the most of the sections.

Gravity Frame Columns Variant 4: All models, C4: ULS FIRE

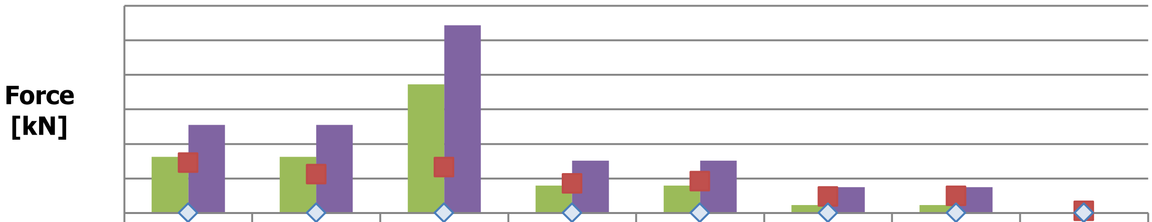

Level:	218 Col. 2-4	218 Col. 5-7	318 Col. 9-12	168 Col. 13-15	168 Col. 17-20	118 Col. 21-23	118 Col. 25-28	18 Col. 29-31
Rd,buc	811	811	1861	398	398	112	112	0
Rd,t	1277	1277	2718	759	759	374	374	9
Fd,c	729	559	663	427	459	236	248	27
Ft,d	0	0	0	0	0	0	0	0
UC	0,90	0,69	0,36	1,07	1,15	2,10	2,21	404,31

graph 6.11: Forces in Gravity Frame Columns, Fire Combination C4

6.7.3 Conclusion

In the first model that was generated, the internal gravity frame was only coupled to the mega frame in the horizontal direction, which resulted in tension on windward side mega columns and supports. A solution was found for this problem. The mega columns were loaded by all the gravity forces to avoid tension forces. This had two reasons. First of all to avoid tension forces acting on the foundation and, secondly to counteract against overturning wind forces and possible uplift. This modification is visualized in figure 6.18.

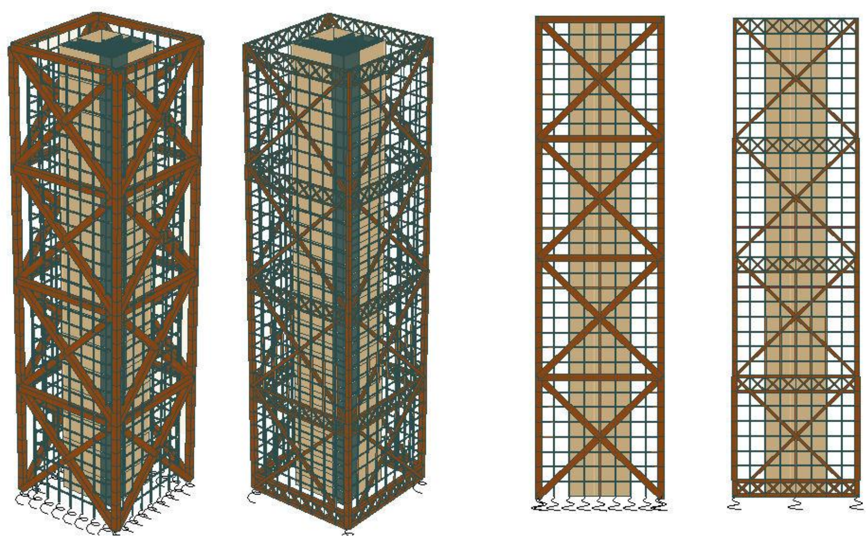

figure 6.18: Impression and Modification of Mega-Frame Model

In the second design stiff trusses where added located at the horizontal members of the mega frame. The foundation supports of the gravity frame were removed and the columns of the gravity frame where coupled on the mega trusses in order to transfer all the vertical loads to the mega columns. It was found that no tension forces occurred on the supports.

The mega braces have to span 28,8 m in length along the horizontal and 28,0 m along the vertical. This large span could invoke unwanted buckling of the brace element and loss in stiffness and stability. The diagonal braces are therefore assumed supported at least in the middle in order to reduce the buckling length and avoid stability problems. This local lateral brace support can only be accommodated by the building core. The NO-CORE model verifications are therefore pending on the real stiffness of a building core replacement.

The optimization to satisfy the ultimate limit state requirements of the fundamental combinations (C0 and C1) resulted in the timber sections shown in table 6.34, table 6.35 and table 6.36. The difference between the dimensions of sections of the BASE-model and the NO-CORE is small, which implies that the mega-frame is especially capable of transferring loads without additional bracing of a core. However, sections are large in comparison to other solutions.

The tension force in the tube support of the NO-CORE-model that occurred in the unfavorable load combination C2 is insignificant in the relative sense. The tension force of 77 kN is small compared to the weight of the supposed foundation, especially when a concrete basement is considered. However, push-over in wind conditions is a point of concern for a timber mega frame.

The verification of the gravity frame in fire conditions showed that the sections of the gravity frame are not large enough for those conditions by default.

7 General Results

7.1 Lateral Deflection

The maximum lateral displacement at the top of the different models for the load combination C3:SLS as defined in paragraph 3.15 is given in graph 7.1. The relative displacement to the BASE models of their eponymous models is given in graph 7.2, in order to assess the influence of the different parameters on the deflection, hence the lateral stiffness.
The dimensions of the members are bound by the ultimate limit state requirement of individual elements. Serviceability limit state requirements of the deflection at the top are therefore satisfied by default. The requirement according to the Dutch standard NEN 6702 for the lateral deflection at the top is $^{1}/_{500}$ of the height which results in 224 mm.

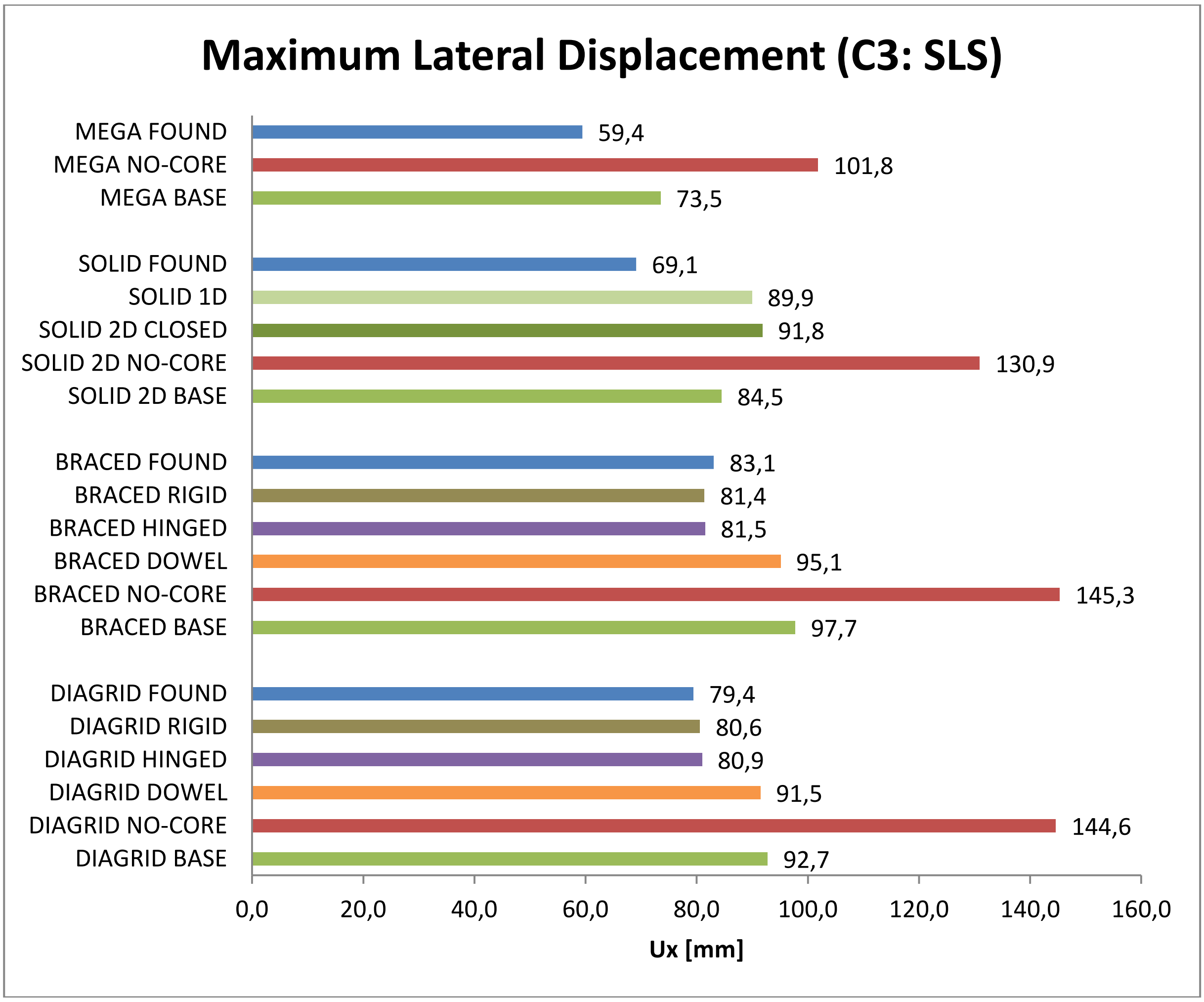

graph 7.1: Maximum Lateral Displacement

From these results several observations can be made. The joint stiffness is responsible for 14% to 20% of the deflection. This conclusion is based on the comparison of deflections between the rigid joint models and the base model. The stiffness of the systems is not significantly influenced by the choice of fastener type, which is expected when one observes the joint stiffness in paragraph 1.10. This is because the joints for both fastener types are designed to resist the same forces and the material density is high.

The core is responsible for 28% to 36% of the stiffness contribution to the structure because the relative deflections between BASE and NO-CORE models range between 39% and 56 % (index calculation). The influence of the support stiffness on the deflection ranges from 16% to 23% dependent on the system used. Obviously, variant 4, the mega frame, is affected the most by changes on the stiffness of the supports hence, the foundation. To get insight into the global stiffness of variants the simplification of equation (3.74) is used to calculate the lateral stiffness shown in graph 7.3.

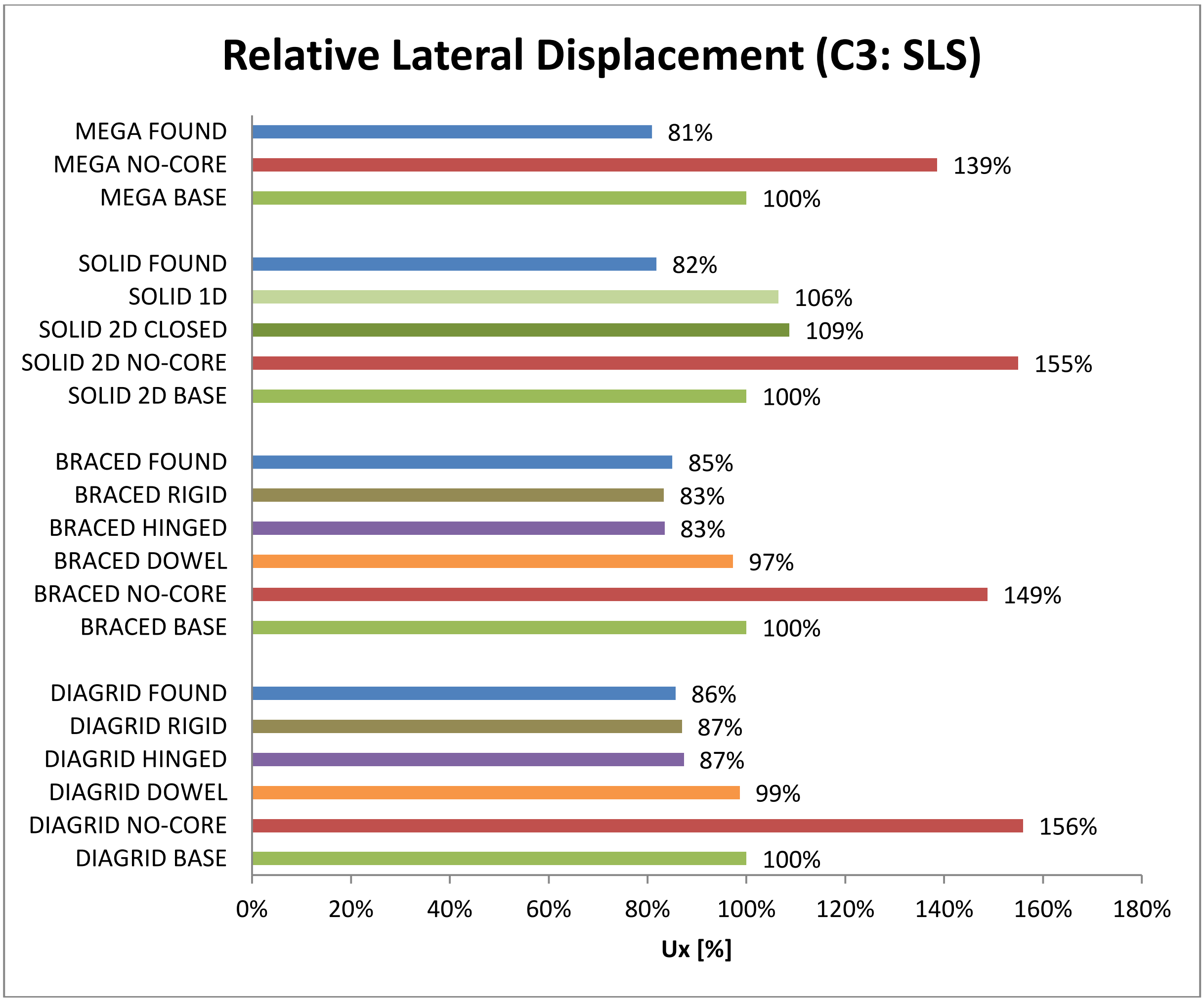

graph 7.2: Relative Lateral Displacement normalized to BASE models

$$EI = \frac{q \cdot l^4}{8 \cdot \omega_{\max}} \tag{7.1}$$

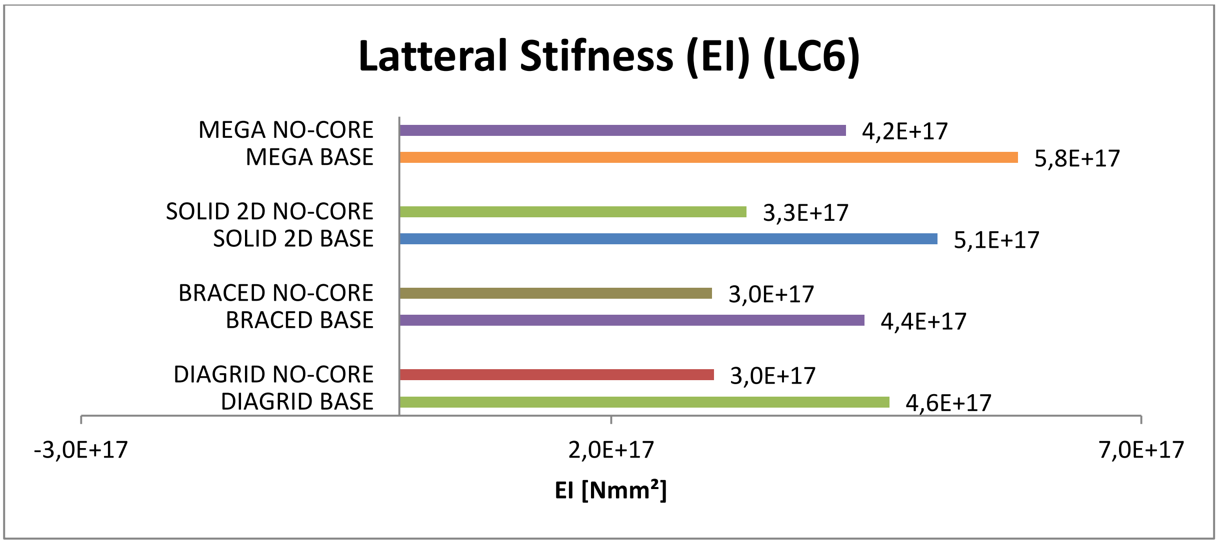

graph 7.3: Lateral System Stiffness (indication)

7.2 Force-Moment Ratio

The results shown in graph 7.4 give the maximum axial forces and moment in the structural components. From these results it becomes clear that the bending moments due to rotational stiffness of the joints as they are designed do not develop in a significant manner.

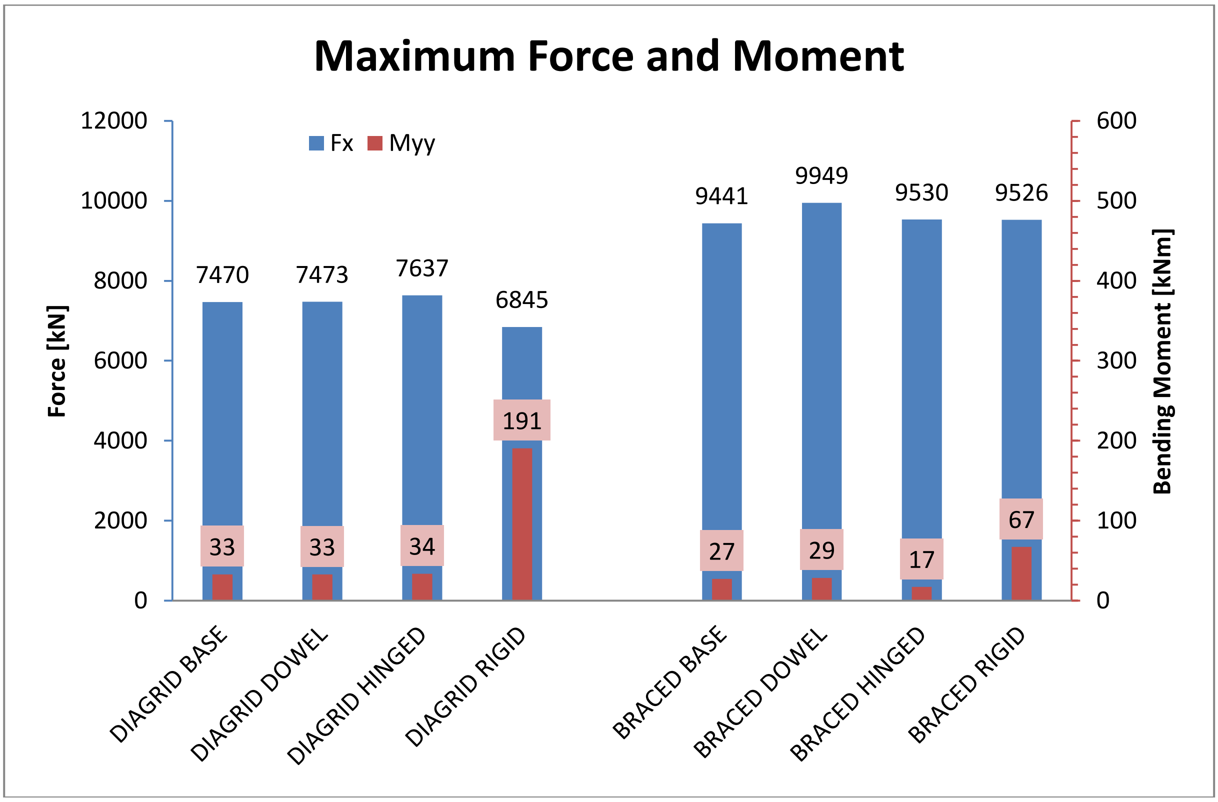

graph 7.4: Maximum Forces and Moments in Models of different Joint Stiffness

The relative forces to the RIGID model of eponymous models are given in graph 7.5, in order to assess the influence of the joint stiffness on the forces. The joints stiffness as designed (BASE and DOWEL) result in similar axial forces and moments as a hinged connection, especially for the Diagrid structure, but the bending moments are not equal to zero. This is because the bending moments in elements develop under influence of the self weight (LC 1) of the structure which is not lumped at the nodes in the models like other load cases, as can be observed in figure 7.1.

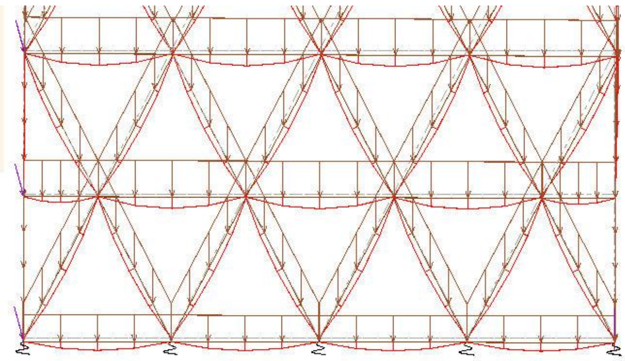

figure 7.1: Gravity Loading in GSA

Rigid connections translate itself in relative high bending moments but do not reduce deflection significantly or at all when compared to hinged connections (graph 7.2). The rotational stiffness of joints as designed, combined with the geometry of the both structures addresses the axial stiffness of elements much more than their bending stiffness.

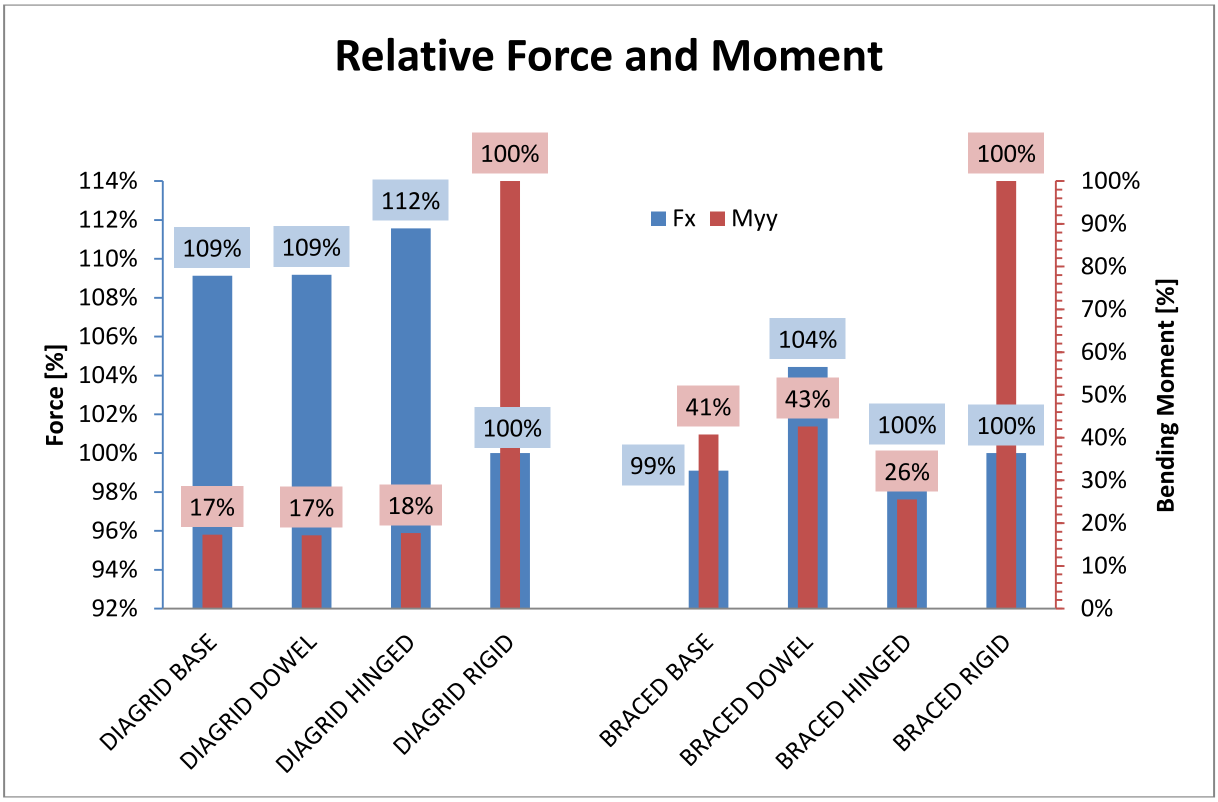

graph 7.5: Normalized Maximum Forces and Moments in Models of different Joint Stiffness

7.3 Dynamic Analysis

The wind induced vibrations that occur in the structure can be determined either by finite element response calculations or through the use of the Dutch building code NEN 6702. Both methods first determine the characteristic frequency and then calculation of the response acceleration.

7.3.1 Vibrations according to NEN 6702

To determine the characteristic frequencies manually, the NEN 6702 prescribes the calculation of the deflection under loads by the quasi-permanent load combination directed in the direction of the wind load, in order to establish a value that is representative for the stiffness-mass ratio. The deflection is then used in equation (7.2) to determine the eigen frequency. The wind induced response acceleration is then determined with equation (7.4). The general definition of parameters and procedure is given below.

$$f_e = \sqrt{\frac{a}{\delta}} \qquad \textbf{(7.2)}$$

Specific acceleration: (a) The value "a" in equation (7.2) is equal to 0,384 m/s^2 for buildings and structures in which the mass is equally distributed over the height.

Quasi permanent lateral deflection: (δ) The deflection of the structure under the quasi-permanent load combination C6 as defined in paragraph 3.15 is imposed on the model in the lateral (global-x) direction.

$$\phi_2 = \sqrt{\frac{0{,}0344\, f_e^{-\frac{2}{3}}}{D\times(1+0{,}12\, f_e\, h)\times(1+0{,}20\, f_e\, b_m)}} \qquad \textbf{(7.3)}$$

Dynamical factor: (φ_2) The dynamical factor used in equation (7.4) is calculated with equation (7.3).

Damping-factor: (D) The damping factor is set to 0,01 for frequencies below 1 Hz.

Building structure height: (h) The height of the building structure is 112 m.

Averaged building width: (b_m) The averaged width of the building is 30 m.

$$1{,}6\times\left(\frac{\varphi_2\times\tilde{p}_{w;1}\times C_t\times b_m}{\rho_l}\right)<a \qquad \textbf{(7.4)}$$

Dynamical wind pressure: (p_w) The dynamic part of the wind pressure which was determined earlier in paragraph 3.14 is 663 N/m^2 for a building of 112 m.

Wind shape factor: (C_t) The sum of the wind shape factors which is assumed equal to 1,20 based on the a square shaped building plan.

Mass of the building (ρ_l) The mass per unit length of the building was determined using the output feature total loads and reactions for the quasi permanent load combination (C6). This saves time concerning load case 1, because the software uses shape functions of elements that determine the volume and mass of the structure by multiplication of the entered material density. The total loads are divided by the gravitational acceleration and the building height in order to obtain the mass per unit length.

The results of the manual calculation are summarized in table 7.1, in which 'δ' is the lateral deflection of the lateral quasi permanent load combination, 'ρ_l' is the calculated mass of the structure per meter height, 'f_e' is the eigen frequency according to equation (7.2), 'φ_2' is the dynamical factor according to equation (7.3) and 'a' is the acceleration according to equation (7.4). The relevant results are also plotted in graph 7.6.

Common parameters: $a=0{,}384\ m/s^2$, $D=0{,}01$, $h=112\ m$, $b_m=30\ m$, $p_{w,1}= 663\ N/m^2$, $C_t=1{,}20$

Model	δ [mm]	ρ_L [kg/m^1]	f_e [Hz]	φ_2 [-]	a [m/s^2]
equation:	N/A	N/A	(7.2)	(7.3)	(7.4)
DIAGRID	2338	216980	0,405	0,53	0,090
DIAGRID NO-CORE	3619	220711	0,326	0,68	0,112
BRACED	2244	219892	0,414	0,52	0,086
BRACED NO-CORE	3444	222077	0,334	0,66	0,108
SOLID	2160	215433	0,422	0,51	0,086
SOLID NO-CORE	3377	217253	0,337	0,65	0,109
MEGA	1742	216434	0,470	0,45	0,076
MEGA NO-CORE	3619	220711	0,326	0,68	0,112

table 7.1: Manual Calculated Structural Response

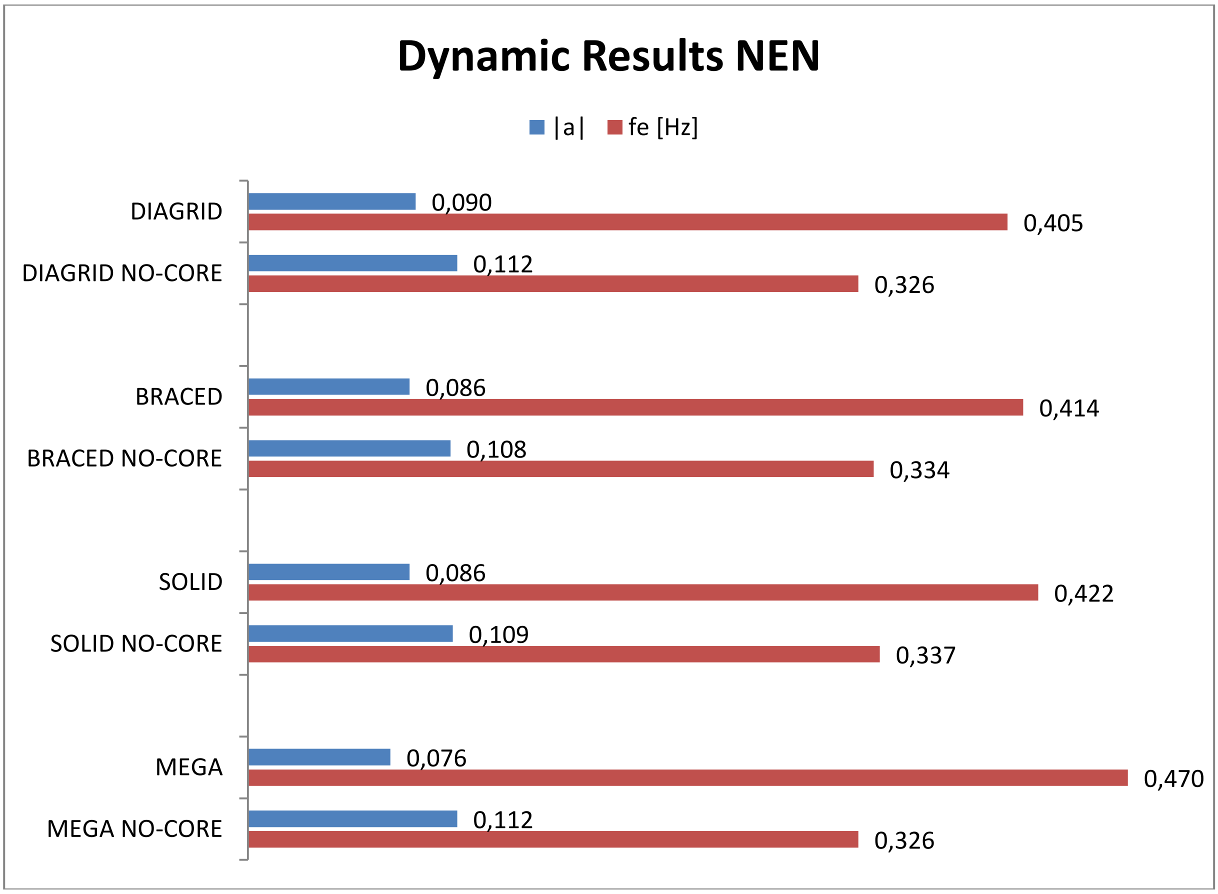

graph 7.6: Dynamic Results Manual Calculation Method

The results of the manual calculation according to NEN 6702 that are presented above serve as a verification of the results in the next paragraph.

7.3.2 Dynamics with software

The characteristic (eigen) frequencies were determined by the computer software GSA with the dynamic modal analysis option for several modes and where verified visually. Only the first mode is relevant for wind induced vibrations, because the velocity coincides with the wind forces. The maximum occurring acceleration corresponding to those frequencies is determined with the software using a dynamic response linear time history of the a wind force excitation of the dynamic wind load. The dynamic wind loads as described in paragraph 1.2.7 resulted for this analysis in peak acceleration shown in graph 7.7.

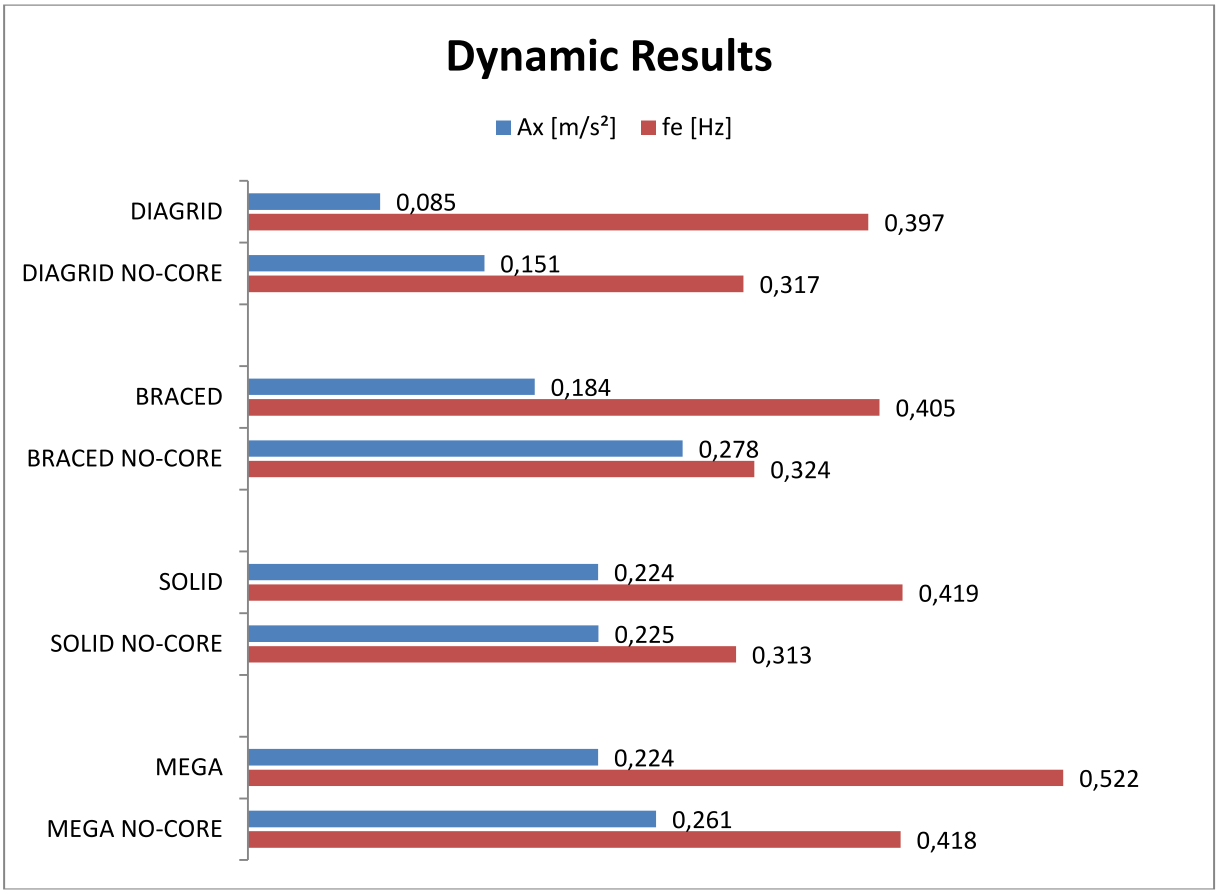

graph 7.7: Dynamic Results Finite Element Calculation Method

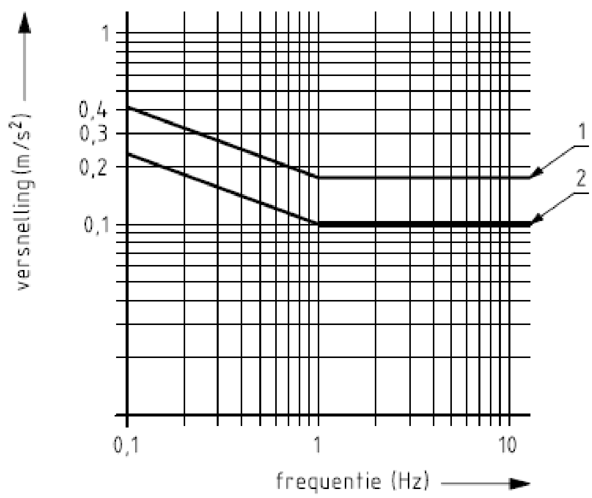

figure 7.2: Frequency–Acceleration Curve NEN 6702

7.3.3 Verification of results

The results of both calculations are verified with the frequency-acceleration curve stated in NEN 6702 shown in figure 7.2, in which curve (1) is to be used for office buildings and places of industry and curve (2) for residential buildings, hospitals, etc. The values resulting from the finite element models are plotted together with the verification curves in graph 7.8 and of the manual verification according to NEN 6702 respectively in graph 7.9.

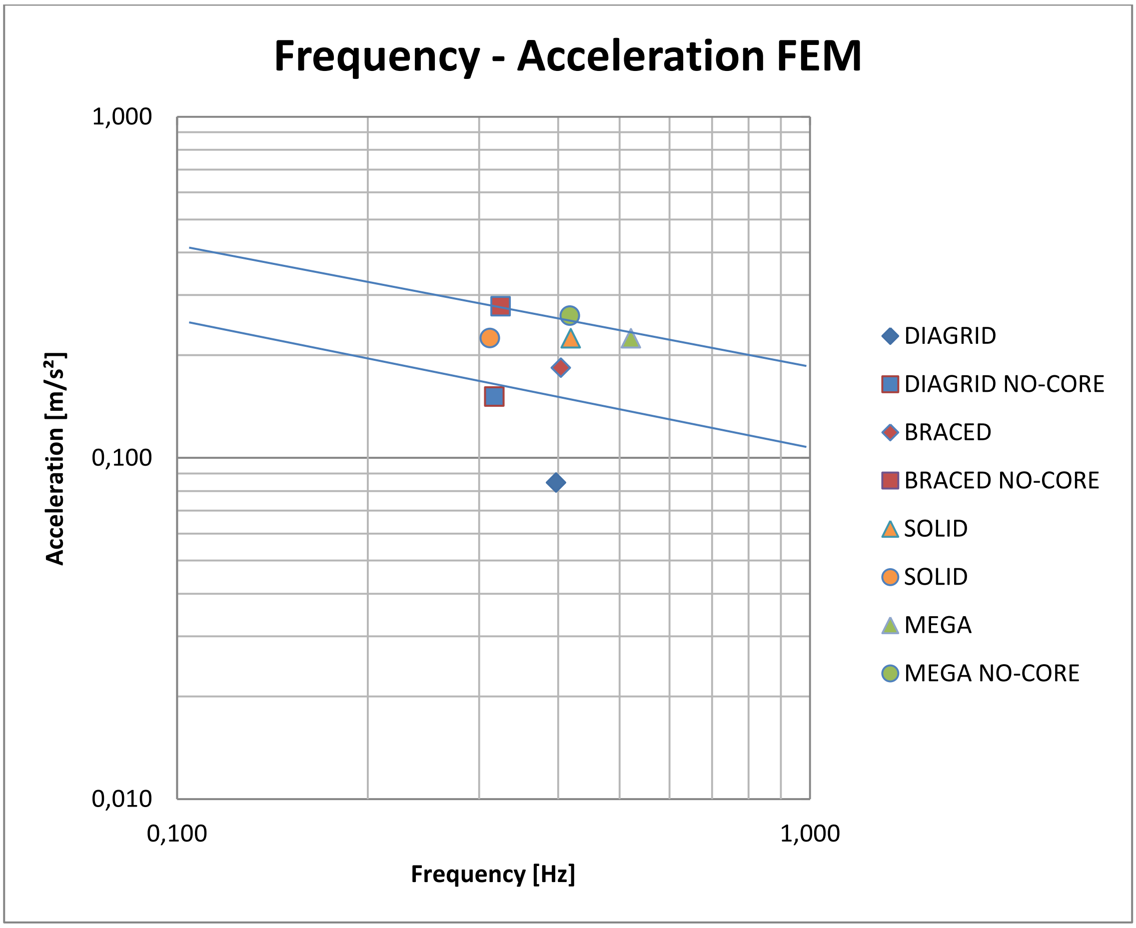

graph 7.8: Scatter plot of FEM Dynamic Results

Mathematical functions where derived algebraically from the curves shown in figure 7.2 which were used to compare the calculated acceleration against the requirement with a spreadsheet. The results of this comparison are presented in table 7.2. In the sixth and eighth column the limits of curve (1) and (2) are given respectively for the associated frequencies given in the fourth column. In column seven and nine the ratio is given between the calculated accelerations and the limit for both curves respectively.

What can be observed in general from graph 7.8, graph 7.9 and table 7.2 is that the calculations with finite element software is conservative relative to the manual calculations according to NEN 6702. While the dynamic behavior of all building structures is within the limits the regulations when the manual calculation method is applied, different conclusions emerge when software is used to determine the eigen-frequencies and acceleration.

Variant	Model	Method	f_e [Hz]	|a| [m/s²]	limit a_1 [m/s²]	|a|/a_1 [-]	limit a_2 [m/s²]	|a|/a_2 [-]
DIAGRID	BASE	FEM	0,40	0,08	0,25	34%	0,17	50%
		NEN 6702	0,41	0,09	0,25	36%	0,17	53%
	NO-CORE	FEM	0,32	0,15	0,27	56%	0,16	93%
		NEN 6703	0,33	0,11	0,27	42%	0,16	68%
BRACED	BASE	FEM	0,40	0,18	0,25	75%	0,17	109%
		NEN 6702	0,41	0,09	0,24	35%	0,17	51%
	NO-CORE	FEM	0,32	0,28	0,27	105%	0,16	170%
		NEN 6703	0,33	0,11	0,26	41%	0,16	66%
SOLID	BASE	FEM	0,42	0,22	0,24	92%	0,17	133%
		NEN 6702	0,42	0,09	0,24	36%	0,17	51%
	NO-CORE	FEM	0,31	0,22	0,27	83%	0,16	138%
		NEN 6703	0,34	0,11	0,26	42%	0,16	67%
MEGA	BASE	FEM	0,52	0,22	0,23	99%	0,17	129%
		NEN 6702	0,47	0,08	0,23	33%	0,17	44%
	NO-CORE	FEM	0,42	0,26	0,24	107%	0,17	155%
		NEN 6703	0,33	0,11	0,27	42%	0,16	68%

table 7.2: Verification of Acceleration to NEN 6702 for both Calculation Methods

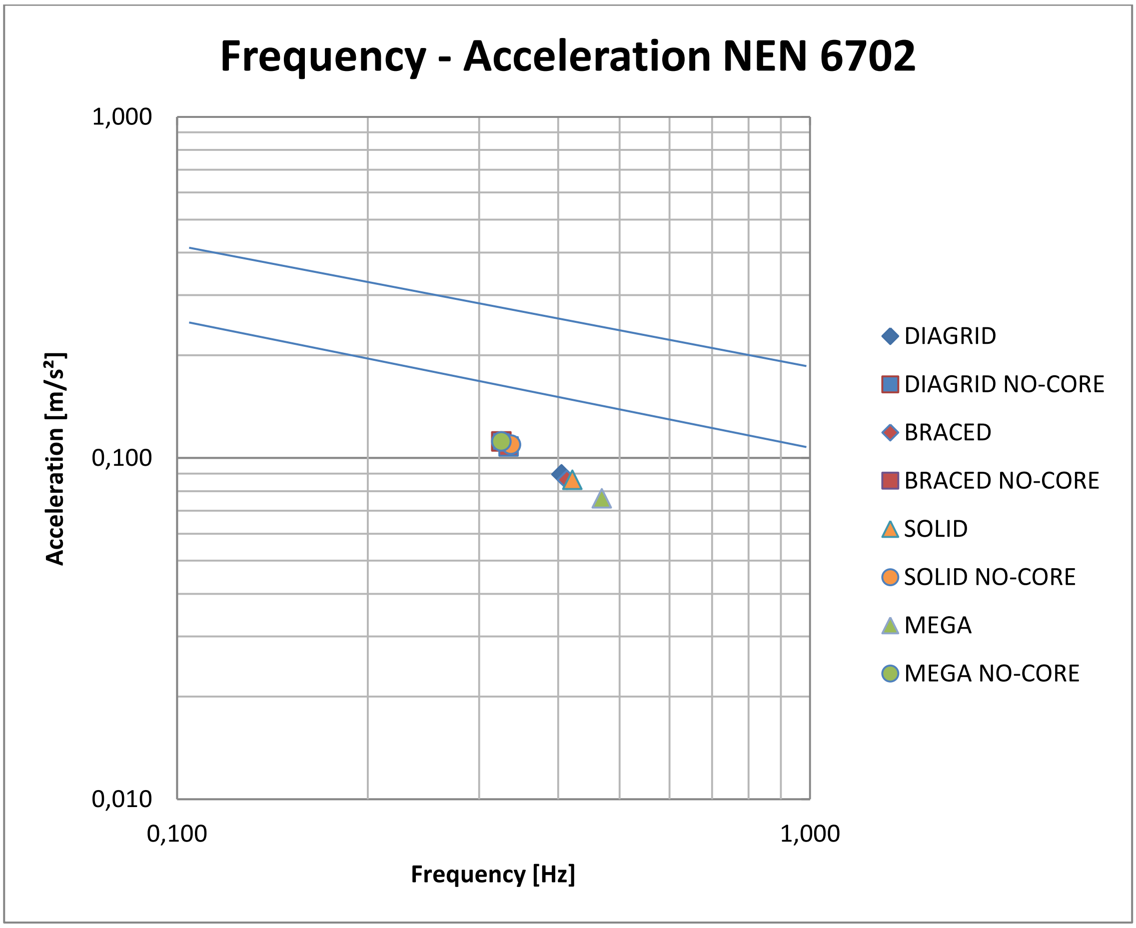

graph 7.9: Scatter Plot of Manual Verification Dynamic Results

7.4 Forces Building Core

The forces in the core elements for BASE-models of all variants and their collective maximum are given in graph 7.10. The maximum bending moment is used to derive equivalent lateral loading to impose on the 2D-elements model of the core as it is described in paragraph 3.12. This is done in order to verify the load bearing capacity of the walls of the core. The equivalent lateral loading is calculated with equation (7.5) which is deduced from a cantilever beam and results in 61 kN/m[1].

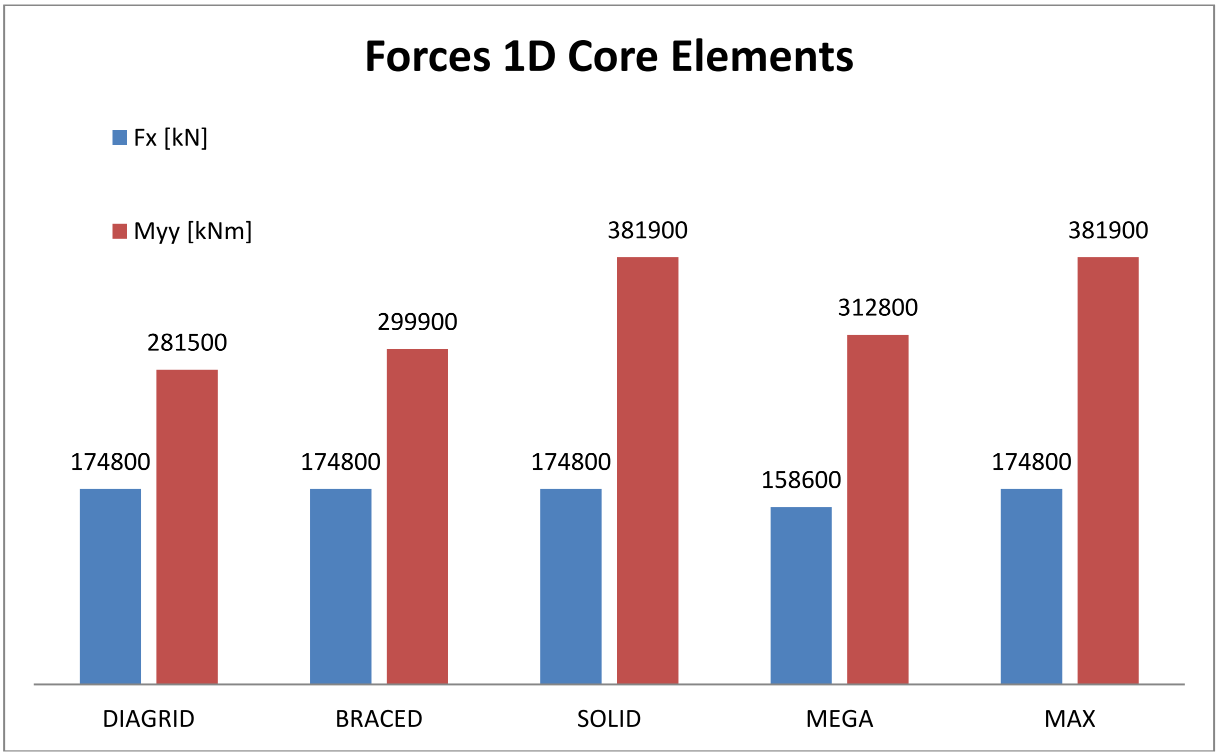

graph 7.10: Core Element Forces

$$M = \frac{1}{2} \cdot q \cdot l^2 \rightarrow q_{eq} = \frac{2 \cdot M}{l^2} \qquad \textbf{(7.5)}$$

In which:
M = maximum bending core moment
l = building height
q_{eq} = equivalent lateral loading

CORE Loading
The total vertical loading on the 2D core model is equivalent to any arbitrary core loading of other models and is divided over the principle nodes. The equivalent lateral load is multiplied by the floor height (3,50 m), divided over 1,5 to create a representative load and imposed on the central nodes. The load combinations C1 and C2 are used on the 2D core model.

Results
The results of the 2D model calculation are given in graph 7.11 and graph 7.12 and deserve some additional explanation. The forces are given for the local peak and the centre stress output, as explained earlier in this chapter.

The centre stress forces are used to verify the buckling forces as shown in graph 7.11 and thus include compression forces. The forces shown in graph 7.12 only contain shear and tension forces and are used to verify the stresses in cross laminated timber elements (D70-CLT) and the joint resistance ($R_{v,j}$ (MAX)).

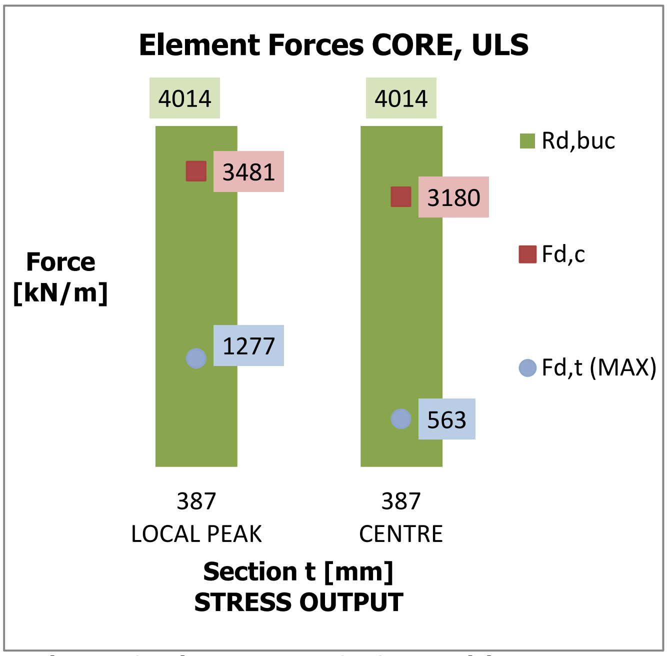

graph 7.11: 2D element Forces 2D Core Model

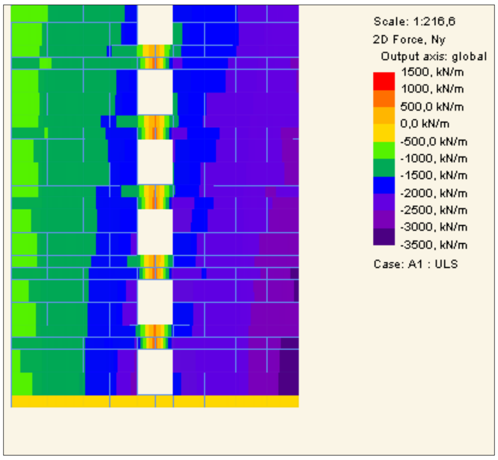

figure 7.3: Peak Stress in Core

The peak tension stresses are shown in figure 7.3 and occur in the lintels above openings as expected. The local peak stress forces shown in graph 7.12 are used to verify the magnitude of the stress as shown in graph 7.13 in which also the centre stress is given. The effective cross sections given in paragraph 3.5.3.4 are used to calculate the stresses similar to variant 3. The shear stress is also given which is calculated with the full section area per meter length. The material strength is equal to the base material D70. The design values are calculated with material factors given in paragraph 3.9.2.

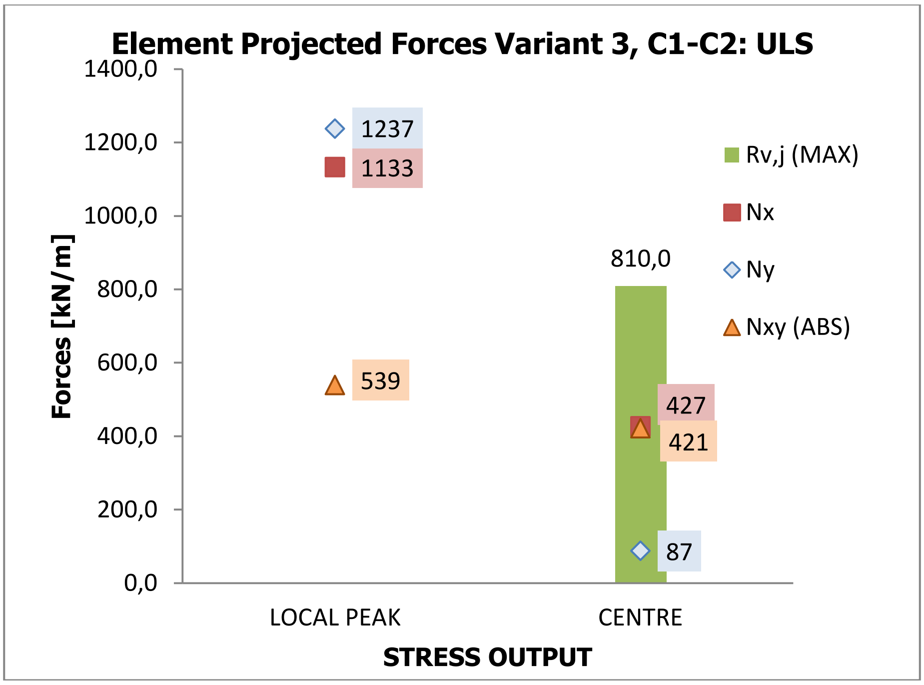

graph 7.12: Projected Element Forces

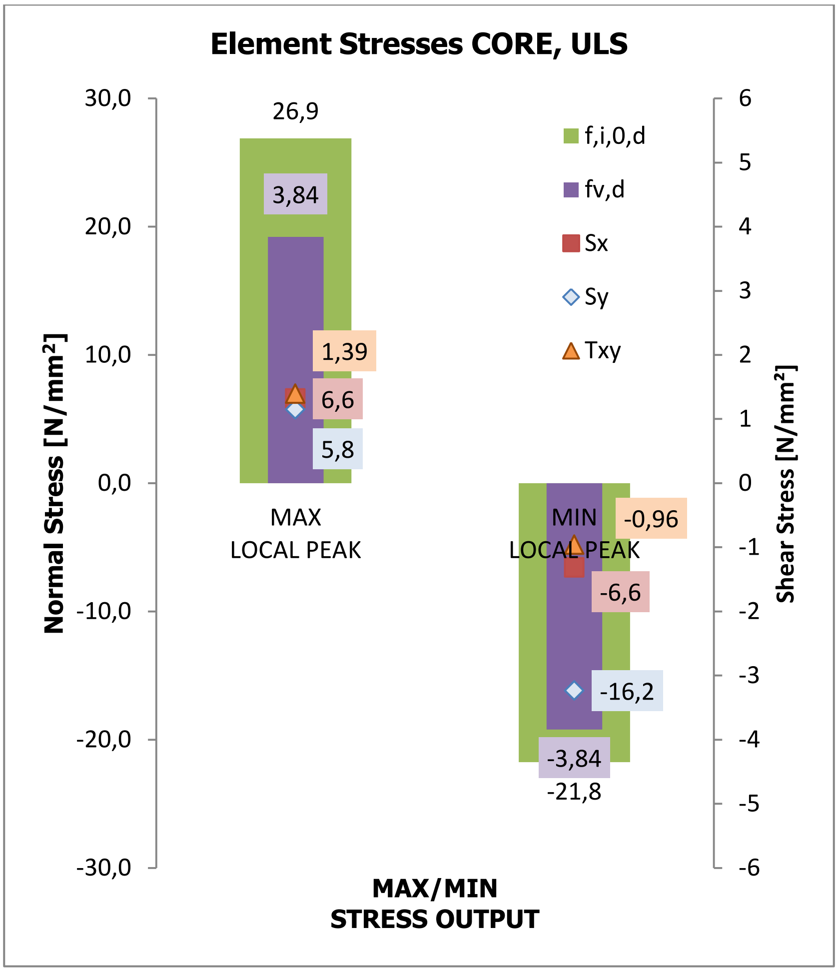

graph 7.13: Calculated Stresses and Verification

NO-CORE models

The core elements for the NO-CORE models can be dimensions to only carry the vertical loads. It was found that the building core has to consist of at least five layer thick D70-CLT in order to resist the buckling forces as shown in the following calculation:

$$F_{c,d} = \frac{F_{x,\max}}{A_{core}} \cdot t \cdot b$$

$$F_{c,d} = \frac{174800}{56,7 \cdot 10^6} \cdot 387 \cdot 1000 \approx 1200 \quad \frac{kN}{m^1}$$

$$F_{buc} = 2254 \quad \frac{kN}{m^1}$$

In which:

$F_{c,d}$ =	Design value of the compression force	[kN/m^1]
$F_{x,max}$ =	Maximum axial load building core elements	[kN]
A_{core} =	Cross section area of the core (paragraph 3.12)	[mm^2]
t =	Thickness of the plate elements	[mm]
b =	Unit length (1 meter)	[mm]
F_{buc} =	Buckling resistance of a five layer thick D70-CLT	[kN/m^1]

7.5 Support reactions

It is noted that no tension forces occur on the supports, despite the low material density. The maximum vertical reactions on the tube supports are given in graph 7.14. The reactions on the core support are given in graph 7.15 and consist of a vertical force combined with a bending moment.

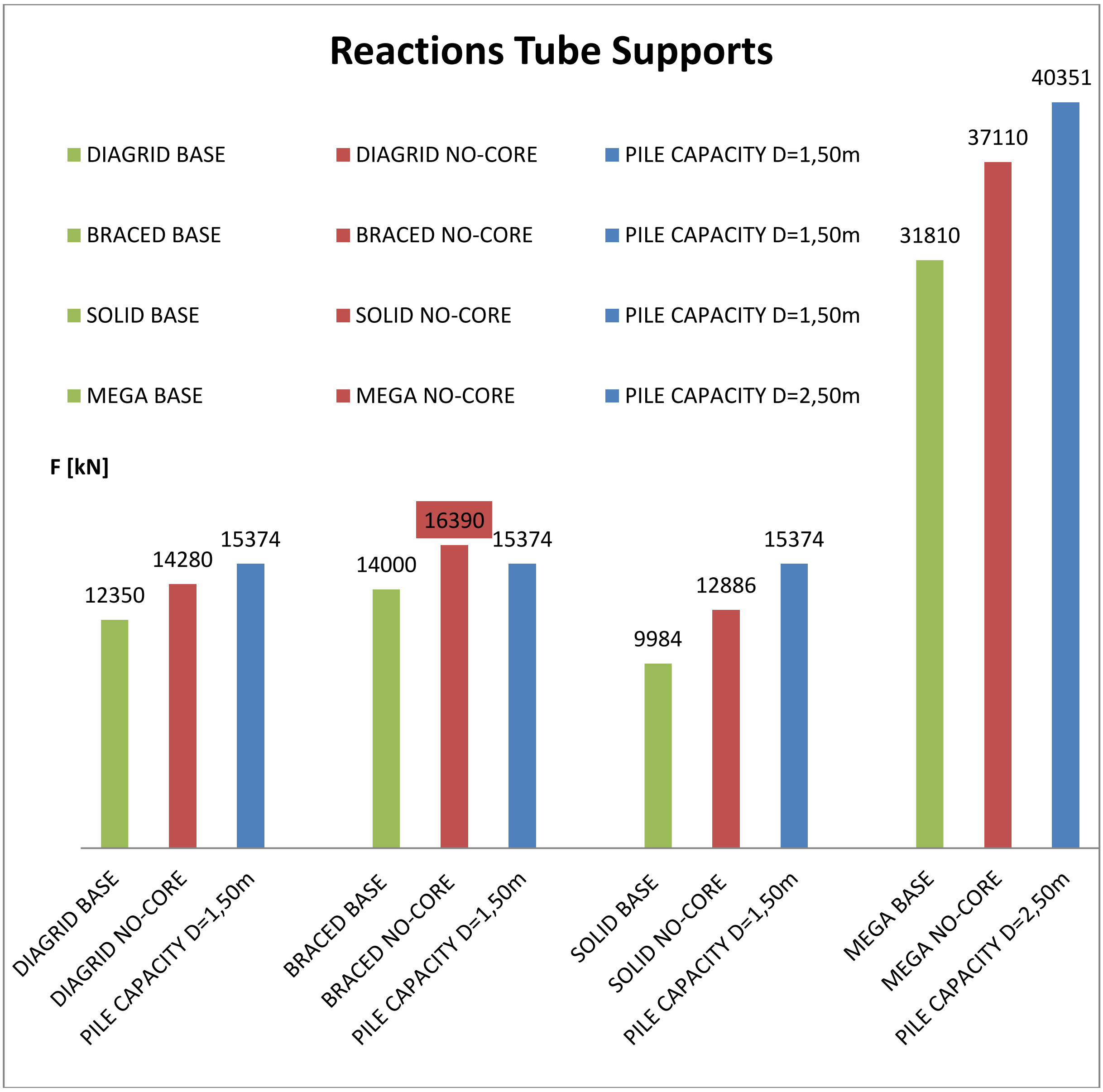

graph 7.14: Support Reactions Tube Supports

The support reactions shown in graph 7.14 can be assumed equal to the forces in the pile as was explained earlier in paragraph 3.13. These forces are smaller then but close to the load bearing capacity of the piles, with exception of variant 2, the braced frame. This justifies the assumed pile diameter, hence the assumed support stiffness, because dimensions are economically chosen, i.e. not oversized.

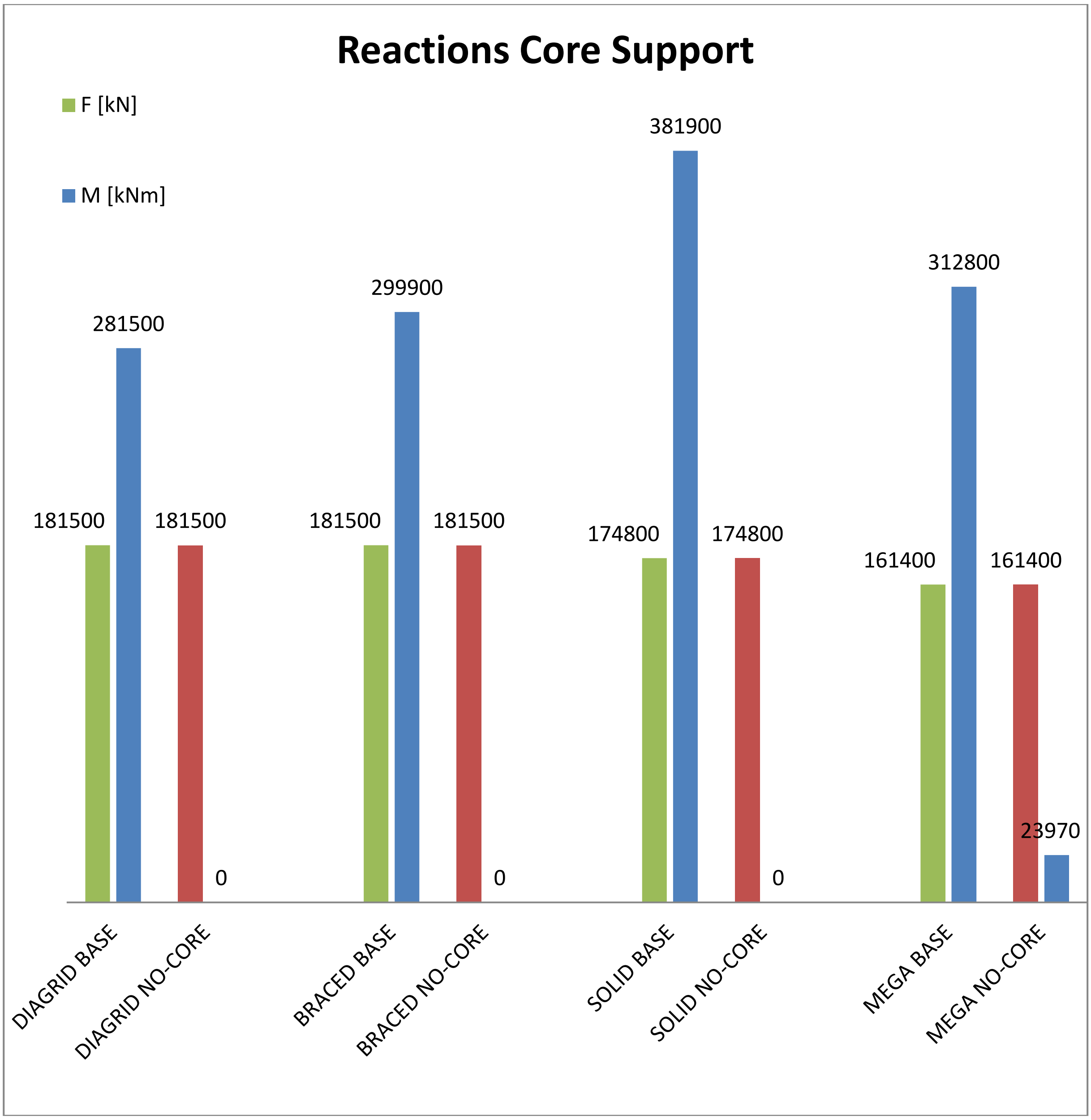

graph 7.15: Support Reactions Core Support

Based on the support reaction of the core support the foundation beneath the core is loaded by a total vertical load combined with a bending moment. To derive the load on the piles of the core foundation equation (7.6) is used .

$$\sum F = \frac{M}{b \cdot m} + \frac{F_z}{n} \qquad \textbf{(7.6)}$$

In which:
$\sum F$ = derived force on the pile
M = bending moment support reaction
b = internal lever arm of pile couple
m = number of pile couples involved
F_z = vertical support reaction
n = number of piles involved

There are nine piles that support the foundation of the core, with a internal lever arm of 14,40 m in each direction, which will result in the flowing vertical load per pile shown in graph 7.16.

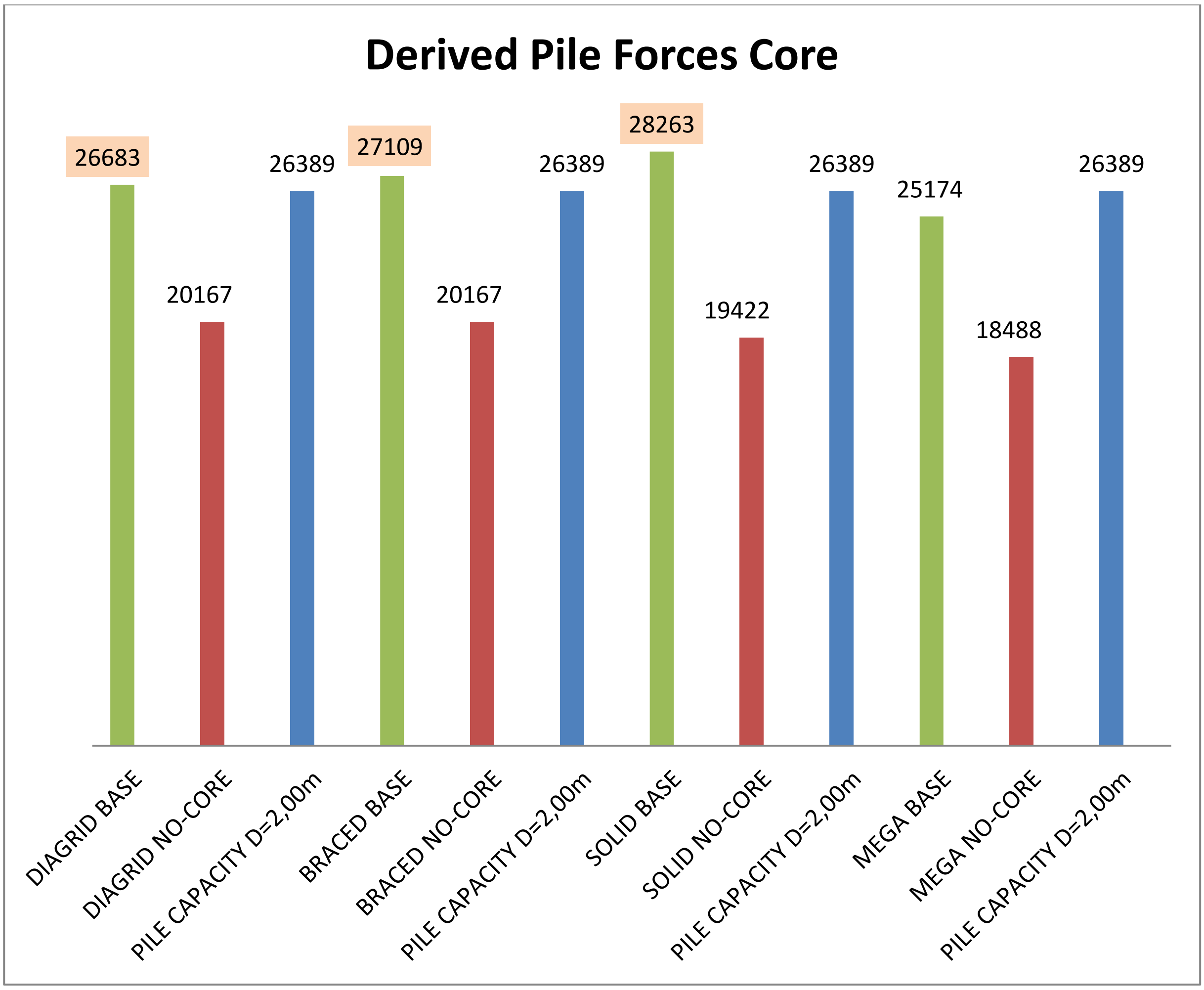

graph 7.16: Pile Forces derived from Core Support Reactions

The derived pile forces shown in graph 7.16 are close or equal to the load bearing capacity of the piles, which justifies the assumed pile diameter, hence the assumed support stiffness. In reality, the foundation will be designed have some additional capacity to omit uncertainties.

7.6 Summary of Results

All members of all variants meet the ultimate limit state requirements under load combinations C1 and C2. The larger reduced members do also meet the requirements under the fire load combination C4 while the smaller cross sections are relatively more compromised by the charring depth and are therefore prone to buckle under the load. This implies that smaller members have to be oversized a little.

The lateral deflection of all variants are within limits of the requirements. Models without core stiffness show an additional relative deflection of 39% to 56%. The models with a fixed foundation show a reduction of the deflection of 16% to 23%. Joints are responsible for 14% to 20% of the deflection but behave more hinged then rigid within the investigated systems, because no significant bending moments occur, which do develop when joints are assumed rigid.

The outcome of the dynamic behavior analysis is scattered for the finite element method. The results of two different methods do not match, except from the Diagrid geometry which are close to equal. The manual verification method is less conservative then the dynamic analysis with finite element software, contrary to expectations.

The dynamic behavior of the NO-CORE models of variant 2 and 4 did not meet the requirements according to the finite element method. The Diagrid geometry shows on average the best dynamical behavior for all models and methods.

The building core was verified to carry the maximum occurring buckling force and stresses. For the model concepts NO-CORE the section thickness can be reduced with a factor of $^5/_9$ to carry the vertical loads.

The support reactions are quite similar to the load bearing capacity of the foundation, which justifies the assumed support stiffness used in the models.

From these results the technical feasibility of a tall timber building is basically proven. The economic feasibility is analyzed further in the next chapter based on these results.

8 Feasibility Analysis

8.1 Mass raw material

The mass of the raw material necessary to create the building is a first indication of the cost. The mass of the raw material was partially determined with the environmental impact feature of the used software. The mass of the building core for the NO-CORE concept is modified with a factor $^{5}/_{9}$ in order to take account for the necessary cross section to resist vertical loads as indicated in paragraph 8.11. The mass of the total number of floors was calculated manually based on a seven layer thick member of D70-CLT over the floor plan area excluding part of the building core. In graph 8.1 the mass of raw material is given for all variants and their components differentiated over the concept of the models BASE and NO-CORE and the type of material.

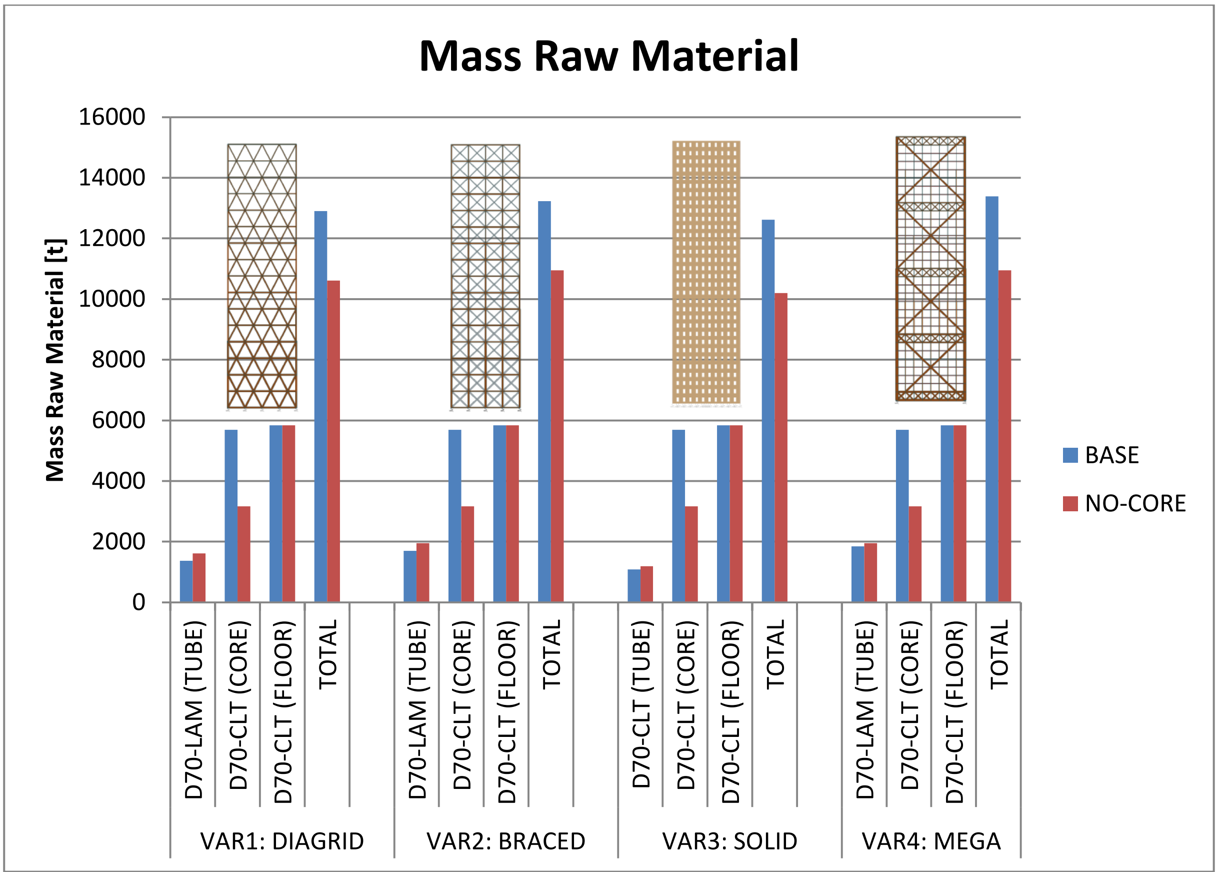

graph 8.1: Total Mass of Raw Material per Variant and Component

It can be observed that the contribution of the building core and the floors is large compared to the tube structure. While the mass of the floors is similar for both model concepts, the mass of the building core has some significant influence on the total. There is not much difference in the use of material between variants, because the biggest difference takes place between the mass of the tube structures, which relative contribution to the total is small.

From graph 8.1 it is tempting to conclude that the global strength and stiffness contribution of tube structure is much more material efficient than the building core, which is obvious when comparing their internal lever arm. Other conclusions emerge when the building stiffness derived in paragraph 7.8 is divided over the total mass of the structure as shown in graph 8.2. The stiffness of the NO-CORE concept is less material efficient, which is also misleading because the model did not include the core stiffness at all. However, when NO-CORE is used as a concept, some other characteristics like dynamical behavior are compromised.

Another important observation made based on graph 8.2 is the difference between variants the context of stiffness mass ratio, which is not affected by the noise of core stiffness. The relative economic advantages between variants is complemented by comparison of the number of actions involved combined with their production complexity in the next paragraph.

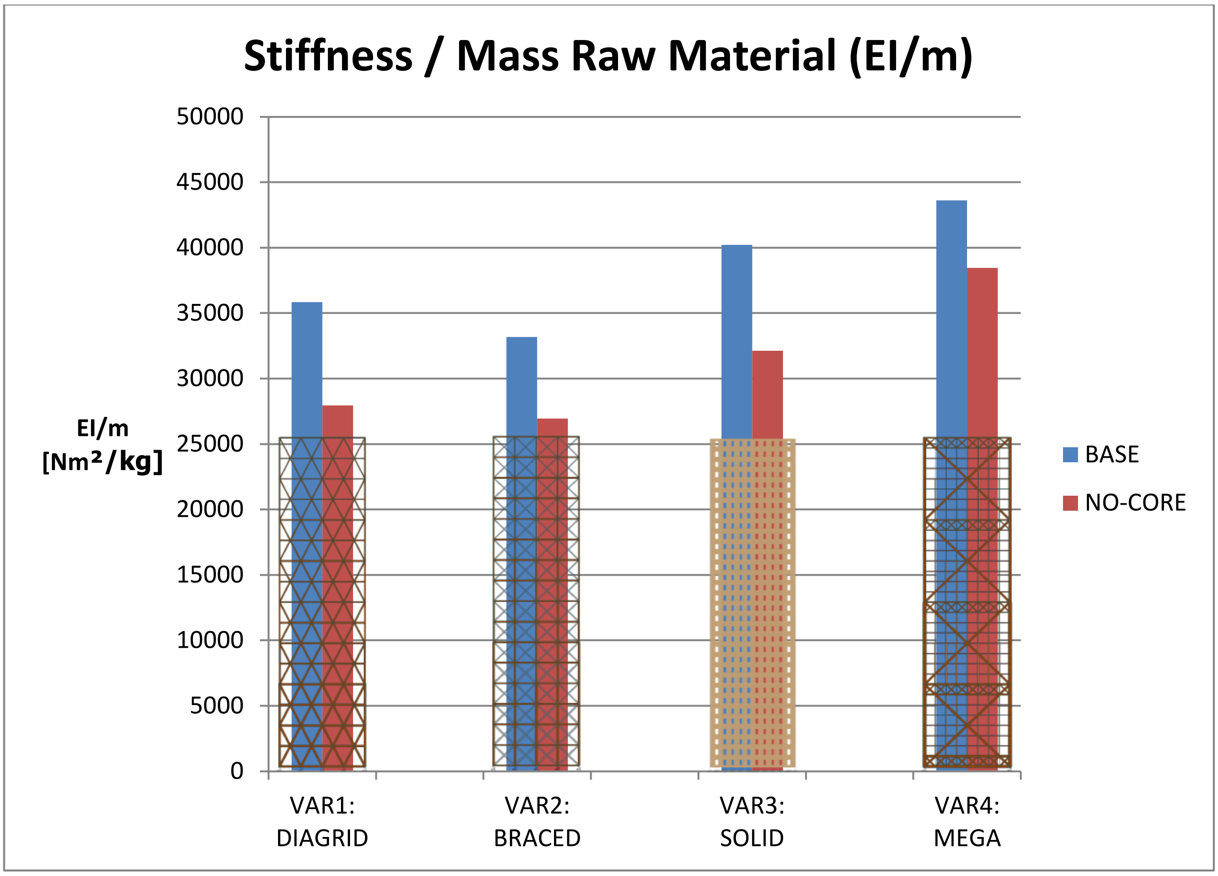

graph 8.2: Stiffness over Mass Ratio of Variants

8.2 Production Analysis

By counting the number of components like members, structural nodes and joints used in the building the variants can be compared to each other economically. In graph 8.3 to graph 8.7 the total number of components per variant are given. These can be used in the economic analysis on production complexity.

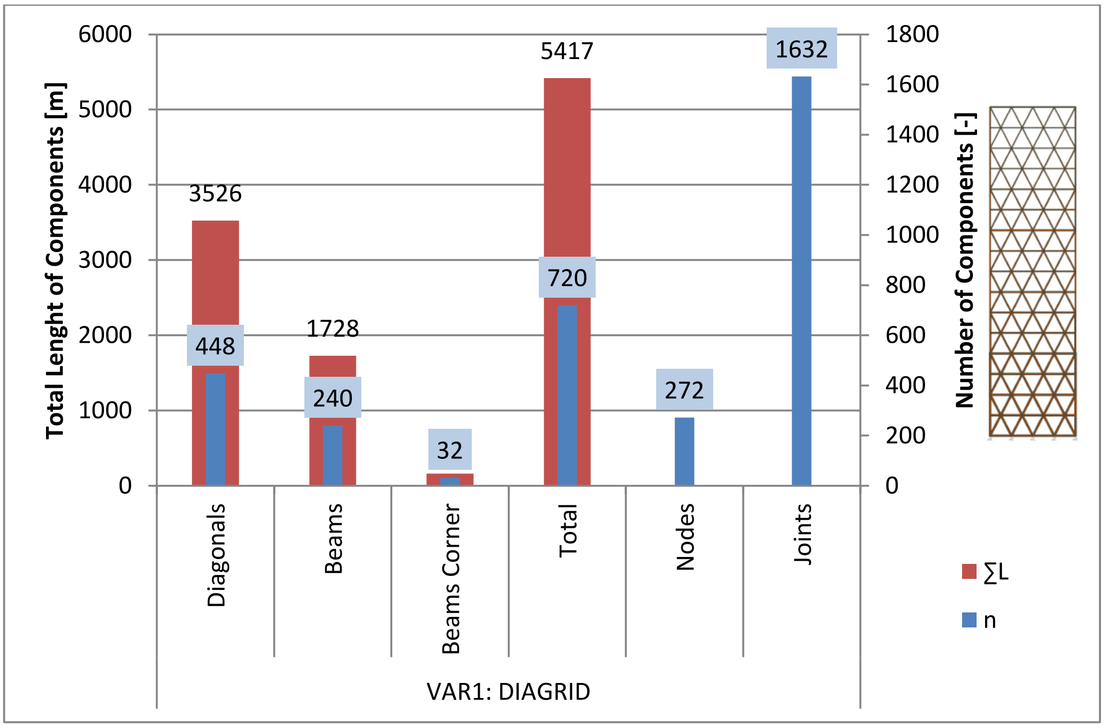

graph 8.3: Material per Component for Variant 1

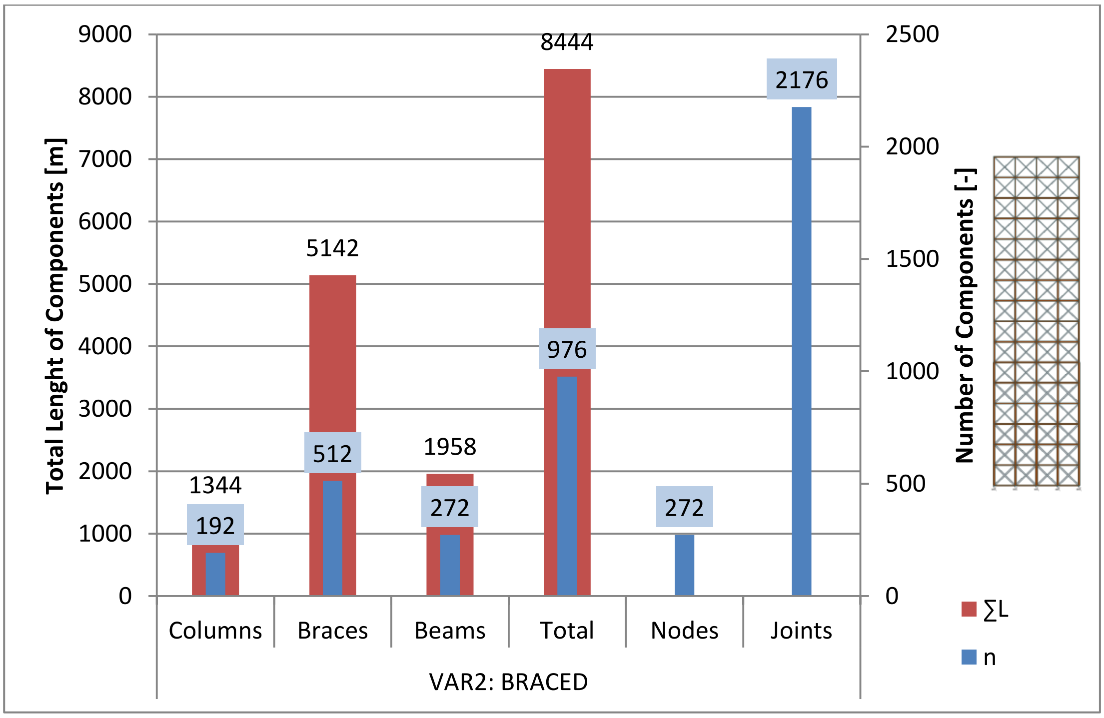

graph 8.4: Material per Component for Variant 2

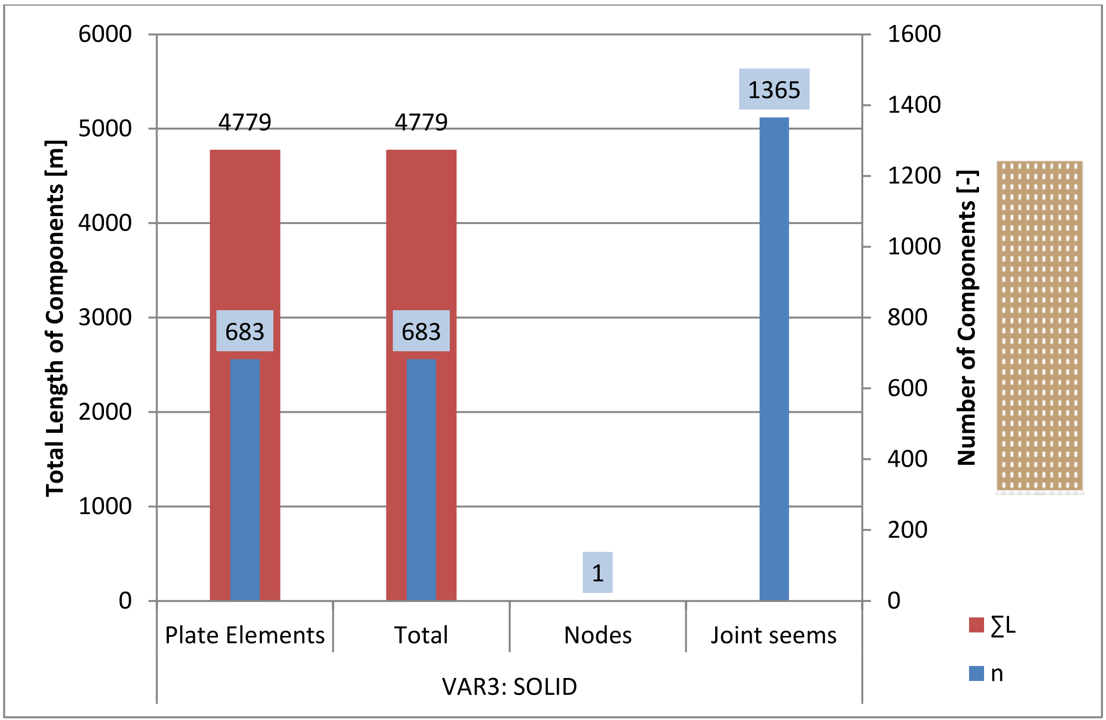

graph 8.5: Material per Component for Variant 3

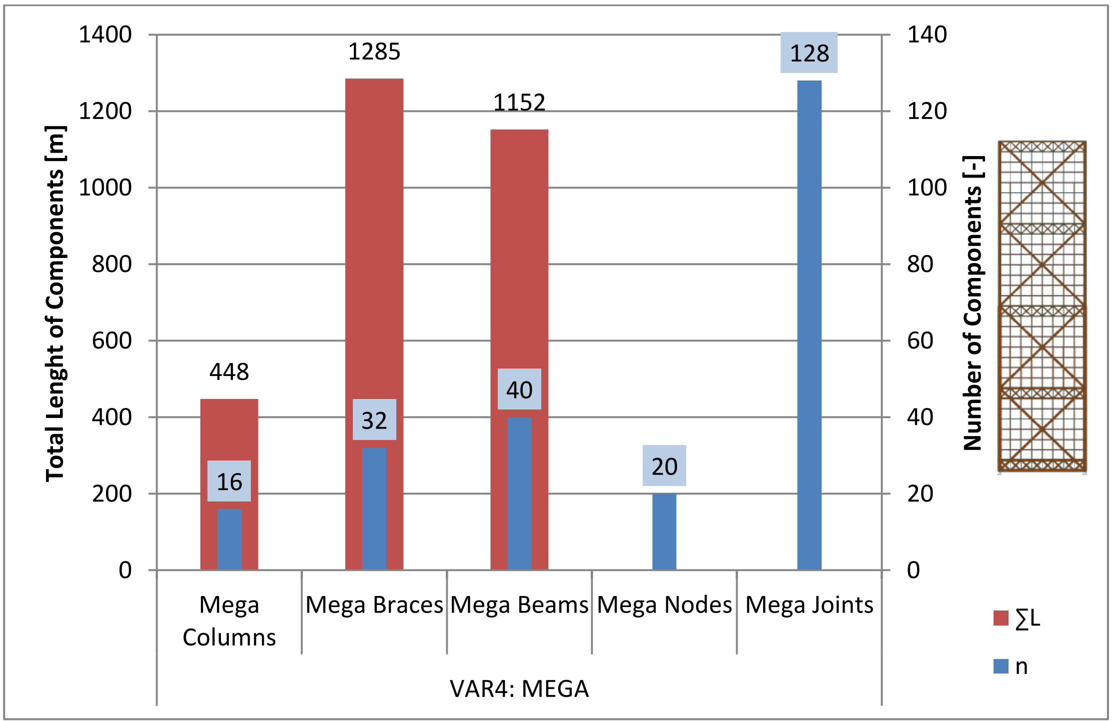

graph 8.6: Material per Component for the Mega Frame of Variant 4

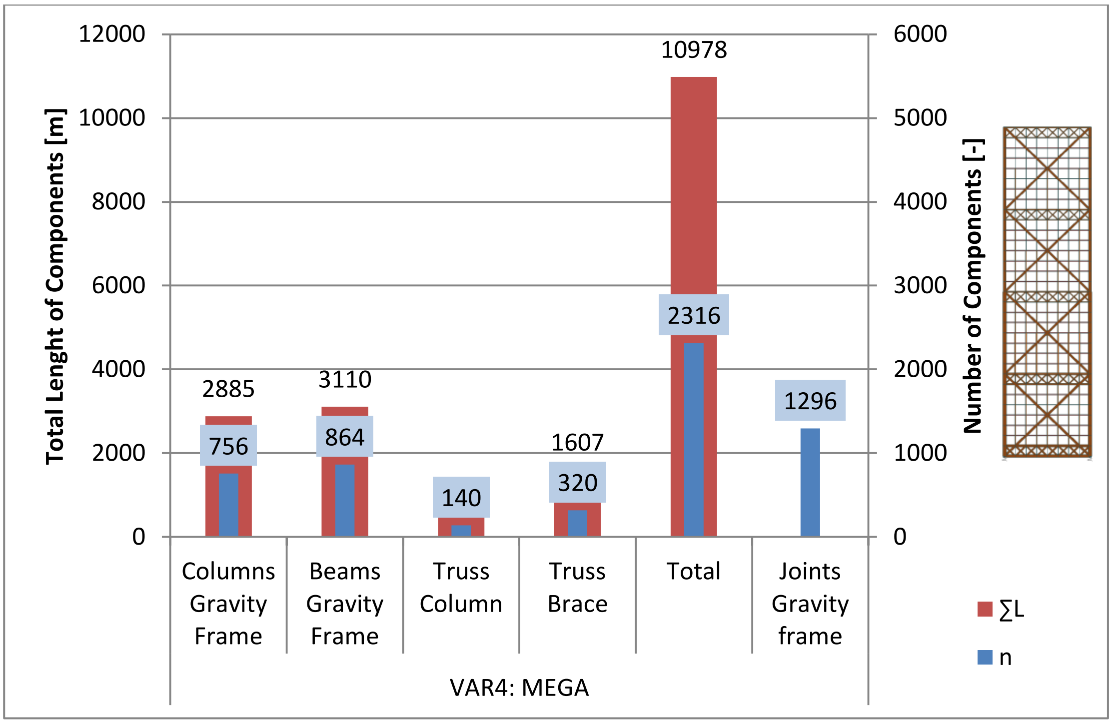

graph 8.7: Material per Component for the Gravity Frame of Variant 4

The total number of members gives an indication of the number of handlings like hoisting action and positioning on site as well as in transport. Five criteria are used in an opportunity cost analysis. Opportunity cost is defined as the value of the next best alternative. In this analysis this cost is the loss of points rather than value of currency. Grades from 1 to 10 are given to the different components per criteria. A higher grade implies a better a solution. The criteria used in the opportunity cost analysis are:

- hoisting action - size
- hoisting action - positioning
- Assembly (site)
- Production (factory or workshop)

Hoisting action - size

The size of members is an indication of their mass and their ability to be handled, because this reflects the necessary lifting capacity of the crane on site and the ease of transport. Nodes of the first two variant are given grade 10 because they are relatively small compared to laminated members. The grade for laminated members is correlated with the volume according to equation (8.1).

$$10 \cdot \left(1 - 0{,}9\frac{V_i}{\max(\{V\}_{i=1}^{N})}\right)^2 \qquad \textbf{(8.1)}$$

In which:
V_i = The volume of the member
N = total number of different components of all variants

Hoisting action - positioning

The positioning of members is also correlated with the size of components, but also based on the estimation of necessary temporary bracing and the number of points influencing the positioning.

Assembly

The assembly on site is an estimation of the number and complexity of actions on the building site that has to be taken to complete a component in the final structure. This is largely correlated with the joint type, because laminated members usually do not need any modifications on site. Joints that are assembled simple and fast like bolted joints, resembling a steel structure execution, are given grade 10.

Assembly of secondary elements of the first two variants are given grade 9 because they are simply placed between primary grid elements and held in place with coach screws without intervention of steel nodes. The gravity frame of variant four is connected with dowel type joints on site, which is a more time consuming procedure. The assembly of the gravity frame members are therefore given the grade 7.

Production

The size and simplicity of production of components are a measure for the cost of production. The simplicity of components is an estimation of the amount of labor and capital invested in their production. The size of components is measured by the volume to be processed in production and therefore given a grade according to equation (8.2).

$$10 \cdot \left(1 - 0{,}9 \frac{V_i}{\max(\{V\}_{i=1}^{N})}\right)^3 \qquad \textbf{(8.2)}$$

In which:

V_i = The volume of the member

N = total number of different components of all variants

Opportunity cost

The opportunity cost of components is calculated with equation (8.3). This equation can be explained as the points lost per criteria on the best alternative (10), times the number this occurs, consistent with the definition of opportunity cost.

$$n \cdot \big((10 - G_1) + (10 - G_2) + \cdots + (10 - G_5)\big) \qquad \textbf{(8.3)}$$

In which:

G_i = The opportunity cost grade

n = number of occurrence

The grading, the opportunity cost per component type and the sum of the opportunity cost per variant is shown in table 8.1. The grade given to a variant in the last column of this table is normalized to the minimum of total opportunity costs of all variants. In graph 8.8 the totals are given per variant which are used as a verification on table 8.1.

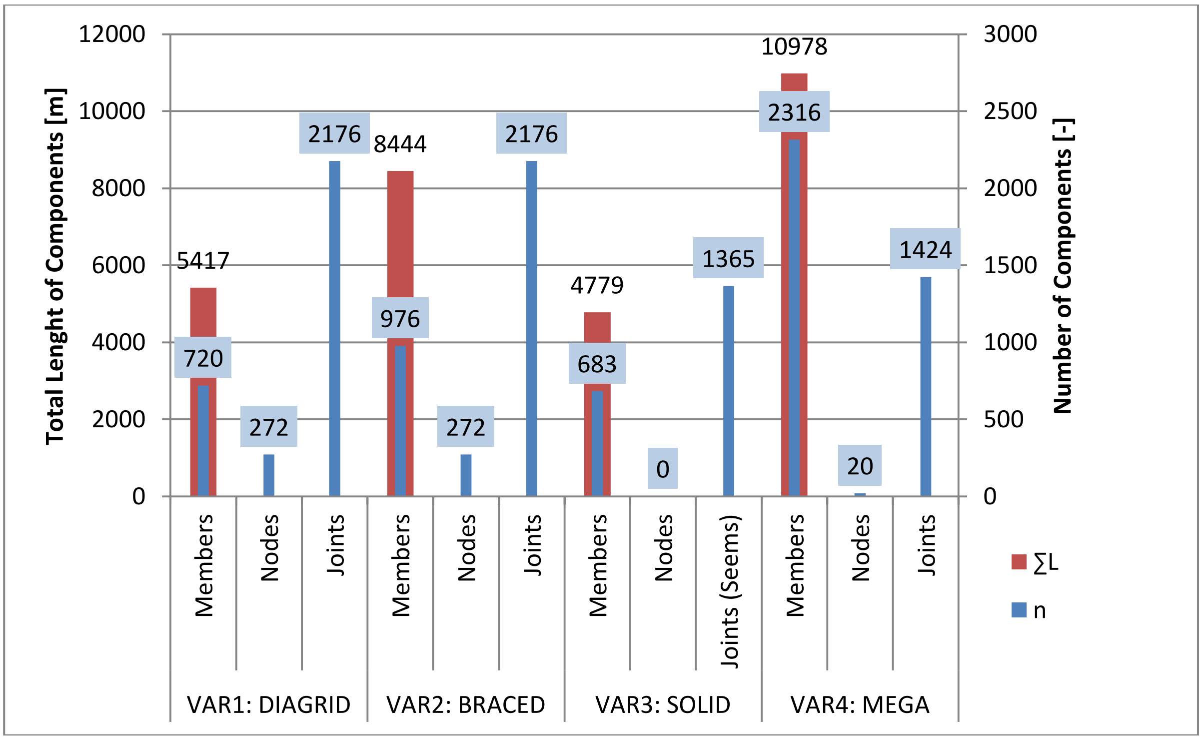

graph 8.8: Total of Components per Variant

	Number of occurrence (n)	width (b)	Length (L)	Volume (V)	Hoisting action - Size	Hoisting action - Positioning	Assembly (site)	Production - Size	Production - Simplicity	Opportunity Cost (OC)	Grade (Normalized)
	[-]	[m]	[m]	[m3]							
VAR1: DIAGRID											
Diagonals	448	0,49	7,87	1,87	9,1	8,0	10,0	8,6	8,0	2838	
Beams	240	0,49	7,20	1,71	9,1	8,0	10,0	8,7	8,0	1475	
Beams Corner	32	0,49	5,09	1,21	9,4	8,0	10,0	9,1	8,0	177	
Nodes	272	-	-	-	10,0	10,0	10,0	9,5	1,0	2584	
Joints	1632	-	-	-	10,0	10,0	10,0	9,5	7,0	5712	
Secondary Members	1344	0,18	3,50	0,11	9,9	9,0	9,0	9,9	10,0	2875	
Secondary Joints	1344	-	-	-	10,0	10,0	9,0	10,0	10,0	1344	
Sum of OC										17005	8,5
VAR2: BRACED											
Columns	192	0,54	7,00	2,03	9,0	8,0	10,0	8,5	8,0	1254	
Braces	512	0,40	10,04	1,61	9,2	7,0	10,0	8,8	8,0	3593	
Beams	272	0,54	7,20	2,09	8,9	8,0	10,0	8,5	8,0	1795	
Nodes	272	-	-	-	10,0	10,0	10,0	9,5	1,0	2584	
Joints	2176	-	-	-	10,0	10,0	10,0	9,5	7,0	7616	
Secondary Members	1792	0,18	3,50	0,11	9,9	10,0	9,0	9,9	10,0	2041	
Secondary Joints	2240	-	-	-	10,0	10,0	9,0	10,0	10,0	2240	
Sum of OC										21122	6,8
VAR3: SOLID											
Plate Elements	683	0,23	18,90	4,27	7,9	6,0	10,0	7,0	8,0	7552	
Joint	1365	-	-	-	10,0	10,0	6,0	10,0	9,0	6827	
Sum of OC										14379	10,0
VAR4: MEGA											
Mega Columns	16	1,11	28,00	34,65	0,1	1,0	1,0	0,0	1,0	750	
Mega Braces	32	0,69	40,17	18,99	2,6	1,0	1,0	1,3	1,0	1380	
Mega Beams	40	0,51	28,80	7,49	6,5	1,0	1,0	5,2	1,0	1411	
Mega Joints	128	-	-	-	10,0	9,0	1,0	10,0	1,0	2432	
Truss Column	140	0,14	3,50	0,07	10,0	6,0	7,0	9,9	10,0	992	
Truss Brace	320	0,38	5,02	0,73	9,6	6,0	7,0	9,4	10,0	2537	
Gravity Frame											
-Columns	756	0,25	3,50	0,22	9,9	8,0	7,0	9,8	10,0	3994	
-Beams	864	0,18	3,60	0,11	9,9	8,0	7,0	9,9	10,0	4443	
-Joints	1296	-	-	-	10,0	9,0	8,0	10,0	10,0	3888	
Sum of OC										21828	6,6

table 8.1: Economic Grading and Opportunity Cost Calculation

8.3 Daylight availability

Based on the philosophy that buildings with daylight availability are more attractive on the market is the wall-to-window ratio incorporated into the feasibility analysis. Each variant is graded with respect to this criteria. The benchmark grade 6 is set on the minimum requirement and the best alternative on grade 10. Other solutions are linearly interpolated between these two points.

8.4 Fire safety

The variants are assessed on their ability to survive a fire. Additional encapsulation measures are necessary for variant 3 in order to become fire safe and is therefore awarded grade 7. The fire safety feasibility of other variants is assessed on redundancy and the consequences of failure of single components in a fire. This assessment has correlations with the amount of material that either has to be encapsulated or oversized to comply with the requirements.

8.5 Comfort

The level of comfort is measured on the criteria of dynamic acceleration behavior. The finite element results of table 8.2 are used to estimate the comfort experienced by occupants. The value of the frequency–acceleration weighted against the requirement is transformed into a grade, in which the smallest value is assessed as grade 10 and the values on curve 1 of figure 8.4 are awarded grade 6.

8.6 Combined Results

When the stiffness over mass ratio shown in graph 8.2 is normalized to the highest value a grade emerges for this criteria. Together with grades for opportunity cost shown in table 8.1 and the grades awarded to daylight availability, fire safety and comfort a combined grade per variant can be produced as shown in graph 8.9. It is assumed that the fire safety and the comfort are more important. Daylight availability is considered less important because this can be compensated with artificial lighting and technical solutions.
The combined grade is therefore produced by factoring the fire safety grade with 2.0, the comfort grade with 1.5 and the daylight availability with 0.5 and remaining grades with 1.0. From graph 8.9 it becomes clear that variant 1 is the most feasible alternative based on these assumptions.

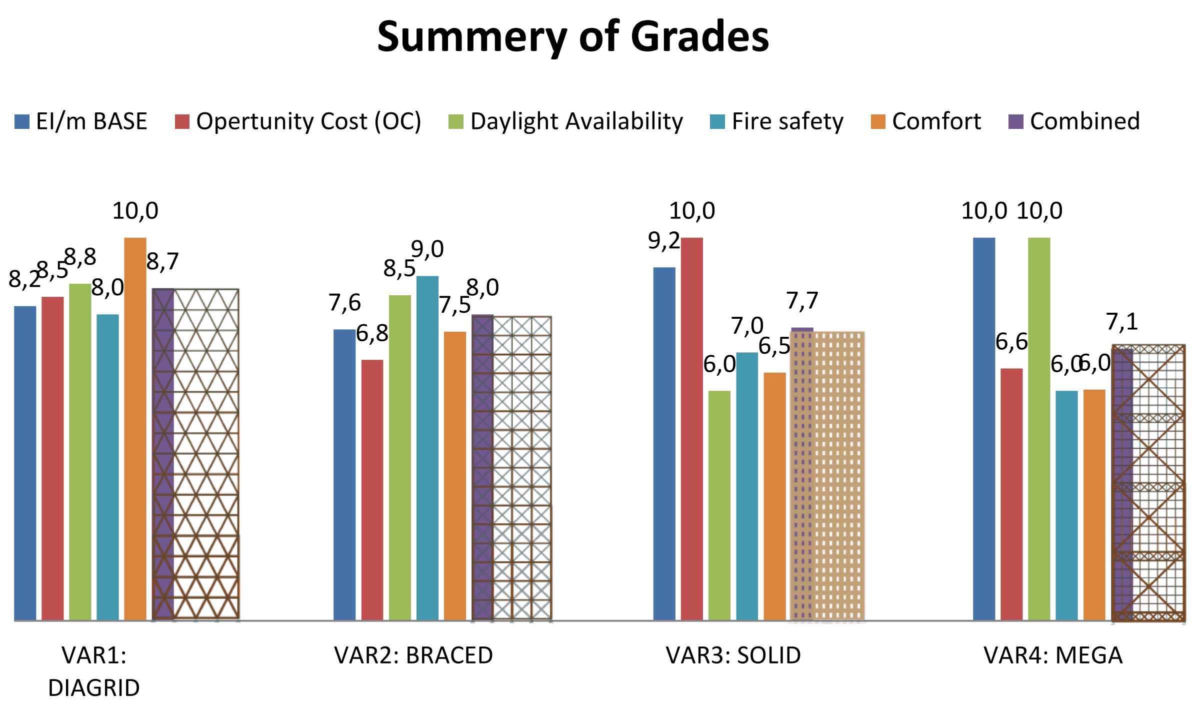

graph 8.9: Combined Grade for Variants

8.7 General Economic Issues

Remaining questions unanswered by the economic analysis is the market position of tall timber buildings. In ref. [5] a comparison shows that a tall timber building is only 12% more expensive than a steel-concrete alternative when all costs are included. It is furthermore important to realize that the choice of building material can be independent of cost within this 12% margin, when a client and architect already have decided on the preferred material on other grounds.

The market price of hardwood of strength class D70 and transportation cost of this material can however influence the feasibility. These are questions which are lie outside the scope of this thesis.

Some footnotes have to be placed at the use of hardwood as a building material. Because hardwood usually grows best within tropical climates there is always a risk of deforestation within these regions which will destroy the whole ecological advantage of using wood as a base material for tall buildings. Another issue not discussed is the impact on the environment and CO_2 emissions of shipping this material from tropical climates to Europe or elsewhere.
The first issue can be tackled with certification system of hardwood which is already in place. It is the opinion of the author of this thesis that these systems always should be approached with some skepticism because they operate on trust which can be vulnerable to corruption. The second issue cannot be answered within the scope of this thesis.

9 Conclusion and recommendation

In this master thesis the feasibility of tall timber buildings is investigated. The objective of this thesis was twofold, namely to find the influence factors on the height of a timber building and to establish the structural feasibility of a 100 m high timber building.

The first part of this thesis consisted of a preliminary study and was in some cases abstract and theoretical of nature, but was necessary to gain insight into the first part of the objective. In the second part of the thesis a case study was conducted on two fundamental issues concerning tall timber buildings, namely, the fire safety and the structural behavior. This part of the thesis was in essence more practical. The findings of the research are condensed in the first paragraph of this chapter, which will conclude with a final statement on the feasibility of tall timber buildings. Because a number parameters used in this investigation are based on several assumptions, recommendations on the continuation of this research are proposed. Finally some notes are given on the limitations of this research.

9.1 Conclusions

The conclusions can be categorized in two parts; the first part contains conclusions regarding the determination of influence factors. And the second part will contain the results of the structural analysis, structural feasibility and economic feasibility.

9.1.1 Determination of influence factors

The main influence factors on the height of a tall timber building are part of architectural requirements, structural problems, fire safety and building physics.

Architectural requirements can change between different projects, dependent on the clients demands and the collective character of the design team. The set of minimum of architectural requirements are in perspective of this thesis:

- Gross-Net floor ratio of 75%.
- Floor depth 7,20 m.
- Wall to window ratio of 15%.
- Building slenderness of 1:4.

Structural problems are tension in the foundation, comfort experienced by occupants of the building and concern the load bearing structure in general, which are mostly mass-stiffness ratio or strength-stiffness ratio related. Other material associated problems are hydroscopic, creep and anisotropic behavior and brittleness of wood based materials. The low density relative to the stiffness of wood based materials results in:

- Relative light structures that generate low permanent loading at the base in comparison to a conventional alternative and therefore evokes the building to be pushed over under lateral wind loads. This did not occur in the investigated structural systems, with exception of a mega frame.
- The stiffness-mass ratio of timber structures result in low natural frequencies of the system that are susceptible to uncomfortable wind induced dynamic responses. This is demonstrated for some of the investigated structural systems, dependent on the method used.

The low stiffness relative to the strength of wood based materials is the main reason for high lateral deflection of a timber buildings, which was not the case for any of the investigated structural systems.

Fire safety problems for tall timber buildings originate from the combustibility of wood based materials relative to conventional building materials. The material related problems of timber buildings are:

- Contribution to the fire load, hence therefore the inability of fire compartment burn out before building collapse occurs, resulting in a burn down of the entire building.
- Contribution to the production of smoke.

Fire safety problems of tall buildings in general are caused by the impossibility to evacuate the building. This problem increases when wood is applied as the main building material. Building physical influence factors are acoustic vibrations in vertical partitions, which are also caused by the inherent mass-stiffness ratio of wood based materials.

9.1.2 Proposed solutions

The main influence factors on the height of a tall timber building are addressed by integrated solutions. Architectural requirements combined with fire safety associated evacuation problems, congregate in a universal floor plan layout. Structural problems in general can be intergraded with daylight availability issues by a choice of stability system. Appling a high quality material of a strength class D70 compensates for material stiffness associated problems and simultaneously limits the production of fire and smoke. Fire safety related problems can furthermore be solved by establishing compartment burn out through application of an appropriate fire safety concept combined with fire suppression measures when necessary. Three types of structural bracing can be applied to a tube structure with or without a structural core (tube-in-tube structure) in association with three different joint types, to solve stiffness associated problems. Material inherent properties of wood based materials are addressed through the joint solutions. Acoustic vibrations problem in vertical partitions, is solved by using a suitable floor lay-up solution.

9.1.3 Results of Feasibility Study

The second objective of this thesis is satisfies by the calculation of a 112 m high timber building. Not all investigated solutions are structurally feasible. Sections of members can be rather large, but do not exceed the maximum producible dimensions by today's wood industry. The lateral displacement of the building at the top was not decisive, contrary to expectations. The dynamic behavior of most solutions was satisfactory within the limits of the regulations except the solutions of variant 1 and 4, combined with a flexible building core (NO-CORE) concept.

Influence on Stiffness

The largest contribution to the lateral stiffness is dedicated to the building core (28% to 36%), based on the values of lateral deflection. Dependent on the variant and therefore the stability system the contribution to the lateral deflection is:

- (-) 56% to 39% for a building core of high quality cross laminated timber (D70-CLT);
- (+) 16% to 23% for the assumed bored pile foundation;
- (+) 14% to 17% for the steel-timber joint stiffness.

The stiffness of the system was not significantly influenced by the type of fastener applied to the joints a Diagrid and braced frame tube structure (variants 1 and 2). This leads to believe there is no motivation to prefer tube-fasters over dowels based on this superficial observation. In more depth, the tube fastener joint configurations consist of a smaller number of fasteners and shorter embedded steel plates then doweled joints. This is an economic advantage, because the investigated structures consist of a large amount of joints, namely about 1632 to 2176 dependent on the chosen solution.

It must be noted that for structural systems that do not include the bending stiffness of a building core, i.e. a pending core as was assumed in NO-CORE models, the results are virtual. When a building core is applied these always have to at least carry vertical loads and is sized accordingly. When a cross laminated timber core is applied it is expected that in reality the building core will contribute to the stiffness because it is transversally coupled. When a flexible core is desired a sway frame with flexible nodes could be used.

The first three variants are approximately equally stiff, because they show similar lateral deflections at the top of the building. The fourth variant, the mega-frame, is much stiffer in terms of lateral deflection. The total mass of raw material for these solutions does not change significantly between variants. It is probable that the unfavorable dynamical behavior of a mega frame analyzed with a finite element method, originates from the high stiffness to mass ratio for which timber buildings are famous.

Fire Safety
The suggested fire safety solutions are not suitable for all structural systems as they were proposed. Based on calculations it was found that buildings with a large opening factor resulted in relatively high peak temperatures but shorter lasting fires. The dissipation of heat energy released in a fire is higher for fire compartments in buildings with large windows, which is more favorable in terms of charring depth.

The fire safety concept 'building encapsulation' is feasible for all structural systems without taking additional measures into account. The fire safety concept 'finite charring' is only suitable for structural systems with large openings in the façade, implying a curtain wall. Building systems with small window openings, i.e. the solid shear wall solution, within the configuration it was proposed, result in fires that do not burn out, or, result in a unfeasibly high charring depth for the concept of finite charring.

A structural system with an average wall to window ratio of 61%, in absentia of automatic fire suppression measures and a floor to ceiling height of 3,00 m results in an effective charring depth of 41 mm when the finite charring concept is applied. The reduction of square sections is therefore 82 mm accordingly. Forces in members under load combination in fire conditions showed that timber members are protected by the massiveness themselves, because the reduced sections of relatively small members fail.

Financial Economics
The economic feasibility of the proposed solutions in terms of money has not been investigated. Based on other studies a 75 m high timber building is feasible with 12% increase of the cost compared to the alternative. The increase of opportunity cost cannot be disproportionately higher in case the building height increases from 75 m to 112 m within this comparison. Based on this assumption a tall timber building of 112 m high is therefore economically feasible. The choice of material is furthermore set by the architect and client at the initiation of a design process, which is therefore independent of financial cost within sensible reasons.

9.1.4 Final statement

There is no reason thinkable why the structure of tall buildings cannot be build out of wood based materials. The structural feasibility in terms of ultimate limit state requirements was proven for several structural systems. The fire safety could also be satisfied through application of an appropriate fire concept with or without additional automatic fire suppression measures. Wood based materials also possess good thermal characteristics. The proposed solutions omit most of these material related problems.

To enable the possibility of a higher timber building several modification can be applied to the design. The feasibility of these modifications are not investigated. Possible modifications are:

- Increase of the section dimensions of members to a maximum of 1500 mm.
- Decrease of column spacing to reduce buckling lengths of members in compression.
- Application of outriggers for additional global strength and stiffness.
- Application of tuned mass dampers or mass tuning to regulate dynamical behavior.

The choice of structural system is one to make by a design team with emphasis on the architect and structural engineer, and can therefore be different from case to case. The best structural system does therefore not exist. But when an choice must be made between systems, the first to be eliminated from the list is a mega frame when such a structure is not necessary.

During investigations of this thesis it was found that a number of problems emerge when a mega frame is used. First of all additional trusses had to be applied to transfer gravity forces of the intermediate gravity frame into the mega columns to counteract uplift under wind loading. The deflection in the middle of these trusses must be controlled and members dimensions have to be increased disproportionally resulting in an uneconomic design. It was expected that a solid shear wall structure behaves much stiffer than the first two solutions, but the results where a little disappointing.

Of the investigated solution the solid shear wall is most cost effective, but the entry of daylight is low. The structural behavior of the Diagrid geometry tube structure is in some aspects superior to the braced frame tube structure. The Diagrid geometry tube structure is also aesthetically more appealing to the author of this thesis and is partially for this reason the preferred structural system.

9.2 Recommendations

A number of assumptions is made on the use of hardwood as a solution for tall timber buildings. In order to validate some of the results and conclusions the problem has to be seen in a larger perspective. Some issues are not worked out or even discussed in this thesis, for reasons of manageability, limited time and resources. The recommendations in this paragraph are clarified and considered in a broader sense.

Laminations of Hardwood
Material properties of laminated hardwood where assumed on a strength class D70 of a deciduous species according to NEN 338. It should be investigated if laminating hardwood is possible, if problems emerge with gluing, handling or otherwise on a production level and if the properties of the lamination change considerably compared to the base material.

Hardwood and Fasteners
In this thesis several assumptions have been made on the stiffness and embedment strength of fasteners in a high density deciduous species. It should be investigated if densified veneer wood reinforcement of tube fastener joints is still necessary when used in combination with a hardwood species. Similarly, it should be investigated if stout and solid dowels still behave ductile in hardwood laminations.

Finite charring Concept
It was found in this thesis that fire compartments in buildings with large openings for windows, burn faster and shorter because the ventilation of the space supplies oxygen en dissipates energy, resulting in compartment burn out. It is impossible to verify this entirely without conducting a proper experiment. Therefore a fire test should be performed similar to the experiments documented in ref. [18]. The fire test should be conducted on a fire compartment of a combustible structure with a high opening factor, build with large members of a high density wood, without intervention of an automatic sprinkler system with the objective to establish burnout of such a compartment.

Pre-stressing of Timber
The beams of the investigated mega frame in this thesis were sized uneconomically in order to counteract the deflection in the middle. This problem could be solved by compensating the permanent loads on the truss-beam through application of a pre-stressing cable. This solution should be investigated for the lower cord of common timber trusses loaded by high permanent loads in general, like road bridges.

Hardwood and Economy
It is uncertain if hardwood is disproportionally more expensive in terms of money and carbon foot-print because hard wood producing threes grow for the largest part in tropical climates. When hardwood should be used in a project like is discussed in this thesis, the influence of transportation cost must be investigated. In some cases, subsidies are granted to sustainable building projects like the “Murray Grove Tower” which was decisive for the feasibility of the project. On a social-macroeconomic level, therefore, these subsidies could not be allocated when this affects the European market negatively in terms of jobs and revenue for the European economy. On the other hand this could be explained as development aid to economies abroad. A macroeconomic cost analysis should be done before embarking on a similar solution as presented in this thesis.

9.3 Research Limitations

In short some limitations of this thesis will be stated here. The following aspects are not investigated and verified and analyzed to establish the structural feasibility of tall timber buildings:

- Disk action strength capacity of cross laminated timber floors in the tall buildings.
- Tension capacity in joints of doweled fasteners.
- The individual parts of tube-fastener joints in detail.
- Influence of the environment in terms of humidity, temperature and sunlight.
- Creep and shrinkage of the material and influence on the building structure

Bibliography

[1] **Mit Holz in luftige Höhen**
- Hochhäuser aus Holz beflügelt die Fantasie -
Article from the magazine: Mikado Nr 7, 2007
Dipl.–Ing. ETH/SIA Hermann Blumer;
Waldstatt, Switzerland

[2] **Building Tall with Timber**
- A Paean to Wood Construction -
Article from: Structural Engineering International Vol.18. nr.2, May 2008
Randolph Langenbach;
Consercationtech Consulting, California, United States of America

[3] **Overview of Design Issues for Tall Timber Buildings**
Article from: Structural Engineering International Vol.18. nr.2, May 2008
Prof. Dr. Ian Smith;
University of New Brunswick, Fredericton, Canada
Dr. Andrea Frangi;
Institute of Structural Engineering, ETH Zurich, Switzerland

[4] **Performance of Drift Levels of Tall Timber Frame Buildings under Seismic and Wind load**
Article from: Structural Engineering International Vol.18. nr.2, May 2008
Ph.D. Andreas Heiduschke;
Department of Civil Eng., Technische Universität Dresden, Germany
Prof. Bo Kasal;
Department of Civil and Environmental Eng., Pennsylvania State University, USA
Prof. Peer Haller
Department of Civil Eng., Technische Universität Dresden, Germany

[5] **Viergeschossiger Holzbau im urbanen Raum**
Dokumentation Forschungsprojekt 8+
Att. Zuschnitt – proHolz Austria

[6] **Urban Timber Houses in Vienna**
Article from: Structural Engineering International Vol.18. nr.2, May 2008
Dr. Eng. Martin Teilbinger;
Holzforschung Wien, Vienna, Austria

[7] **Case Studies of Multiple-Story Wood-Frame Construction in USA**
Article from: Structural Engineering International Vol.18. nr.2, May 2008
Dr. PE. Kevin C.K. Cheung
Director of Technical Services, western Wood Products Association,Portland, USA

[8] **Zum aktuellen Stand von Forschung und Entwicklung im Holzbau**
Bauingenieur, Band 78, Mai 2003
Prof. Dr.-Ing Wolfgang Rug
Fachhochschule Eberswalde, Germany
Dr.-Ing Karin Lißner
Ingenieursbüro Dr. Lißner, Dresden, Germany

[9] **Structural Engineering Handbook 1999**
Prof. Dr. PE. Wai-Fai Chen

[10] **Tall Timber Buildings in the Netherlands**
Article from: Structural Engineering International Vol.18. nr.2, May 2008
Prof. A.J.M. Jorissen
Eindhoven University of Technology, the Netherlands
Dr. A.J.M. Leijten
Eindhoven University of Technology, the Netherlands

[11] **High-Rise - Exploring the Ultimate Limits**
Master Graduation Thesis, September 2008
BSc. A.J. Dijkstra,
Faculty of Civil Engineering and Geosciences, Delft University of Technology, the Netherlands

[12] **Electricity Benefits of Daylighting and Photovoltaics for Various Solar Facade Layouts in Office Buildings**
Eero Vartiainen
Laboratory of Advanced Energy Systems, Helsinki University of Technology, Finland

[13] **Experimental Study on Flexural Behavior of Glulam and Laminated Veneer Lumber Beams**
W.Q. Liu & H.F. Yang
Nanjing University of Technology, Nanjing, China
F.Q. Dong
Chengxian College of Southeast University, Nanjing, China
D.M. Jiang
Sanjiang University, Nanjing, China

[14] **Accoya Verkeersbrug Sneek - Over een Wereld Wonder**
Article from: Het Houtblad, Februari 2009
Hoegina de Boer

[15] **Forschung an der TU Graz – Steifigkeitsuntersuchungen an BPS – Scheiben Elementen Cross-Laminated Timber Wall Segments under homogeneous Shear - with and without openings**
DDI Thomas Moosbrugger
Institut für Holzbau und Holztechnologie, Technische Universität Graz, Austria
Ao.Prof. DI Dr. techn. Werner Guggenberger
Institut für Stahlbau und Flächentragwerke, Technische Universität Graz, Austria
DI Dr. techn. Thomas Bogensperger
Institut für Holzbau und Holztechnologie, Technische Universität Graz, Austria

[16] **Timber Engineering STEP 1**
Lecture Notes, First Edition, Centrum Hout, The Netherlands

[17] **Densified veneer wood reinforced timber joints with expanded tube fasteners The development of a new timber joint**
Ir. A.J.M. Leijten
Faculty of Civil Engineering and Geosciences, Delft University of Technology, the Netherlands

[18] **Fire Design Concepts for Tall Timber Buildings**
Article from: Structural Engineering International Vol.18. nr.2, May 2008
Dr. Andrea Frangi
Institute of Structural Engineering, ETH Zurich, Switzerland
Prof. Dr. Mario Fontana
Institute of Structural Engineering, ETH Zurich, Switzerland
Dr. Markus Knobloch
Institute of Structural Engineering, ETH Zurich, Switzerland

[19] **Bouwbesluit 2003 - Dutch Building Regulations**
Ministerie van Infrastructuur en Milieu – Department of Infrastructure and Environment

[20] **Hout en Brand – Wood and Fire**
HoutWijzer, Artikelnummer 100012, Centrum Hout, the Netherlands

[21] **Forschung an der TU Graz – Bauphysikalische Aspekte für den Holz-Massivbau mit BSP**
DI Heinz Ferk
Bauphysik im Bautechnikzentrum, Technische Universität Graz, Austria

[22] **Brettsperrholz – Berechnungsgrundlagen**
Univ.-Prof. Dr.-Ing. Hans Joachim Blaß
Engineering and Building Constructions, Karlsruhe Institute of Technology, Germany
Dr.-Ing R. Görlacher
Engineering and Building Constructions, Karlsruhe Institute of Technology, Germany

[23] **Forschung an der Universität Karlsruhe – Stiftförmige Verbindungsmittel in Brettsperrholz**
Univ.-Prof. Dr.-Ing. Hans Joachim Blaß
Engineering and Building Constructions, Karlsruhe Institute of Technology, Germany
DI Thomas Uibel
Engineering and Building Constructions, Karlsruhe Institute of Technology, Germany

[24] **Forschung an der TU Graz - Anwendung der Johansen-Theorie für gekreuzt geschichtete Strukturen**
DI Gernot Pirnbacher,
holz.bau forschungs gmbh, Graz, Austria
DI Gianluigi Traetta
holz.bau forschungs gmbh, Graz, Austria
Univ.-Prof. DI Dr. techn. Gerhard Schickhofer
Institut für Holzbau und Holztechnologie, Technische Universität Graz, Austria

[25] **Influence of Rolling Shear Modulus on Strength and Stiffness of Structural Bonded Timber Elements**
International Council For Research and Innovation in Building and Construction
Univ.-Prof. Dr.-Ing. Hans Joachim Blaß
Engineering and Building Constructions, Karlsruhe Institute of Technology, Germany
Dipl.-Ing. Peter Fellmoser
Engineering and Building Constructions, Karlsruhe Institute of Technology, Germany

[26] **Mechanics of Cross-Laminated Timber Plates under Uniaxial Bending**
Ao.Prof. DI Dr. techn. Werner Guggenberger
Institut für Stahlbau und Flächentragwerke, Technische Universität Graz, Austria
DDI Thomas Moosbrugger
Institut für Holzbau und Holztechnologie, Technische Universität Graz, Austria

[27] **Plates and Shells – An analysis model for standard civil engineering software**
Bauen mit Holz, Vol. 1, p. 34-39, 1999
Univ.-Prof.i.R. Dr.-Ing. Heinirch Kreuzinger
Faculty of Civil Engineering and Surveying, Technische Universität München, Munich, Germany

[28] **Calculation models for prefabricated wood-based Load bearing stressed skin panels for use in roofs**
European Organization for Technical Approvals, TR 019, Edition February, 2005

[29] **User Manual GSA 8.5**
Oasys Ltd, Londen, Englend April 2011

[30] **Example of Traditional Tall Timber Buildings in China – the Yingxian Pagoda**
Ph.D. PE. Prof. Frank Lam
University of British Colombia, Canada
Ph.D. Prof. Minjuan He
Tongji University, China
Ph.D. PE. Principle. Chichao Yao
Read Jones Christoffersen Ltd, Canada

[31] **Dowel Type Timber Connections – Strength modeling (BYG-DTU R-039)**
Martin Uhre Pedersen

Sources Figures

[31] **Picture of Mühlacker Radio Transmission Tower**
http://www.skyscrapercity.com

[32] **Picture of Gliwice Radio Tower**
http://www.wikipedia.org, Photographer: Andrzej Jarczewski

[33] **Picture of E3 Berlin**
http://kaden-klingbeil.de

[34] **Picture of Murray Grove Tower**
Photographer: Smoothe

[35] **Picture of Yingxian Pagoda**
http://www.flickr.com

[36] **Artist impression of Forschungsprojekt 8+**
http://www.rhombergbau.at

[37] **Drawings of Tall Timber building**
Ing. H.Kuipers
Faculty of Civil Engineering and Geosciences, Delft University of Technology, Delft, the Netherlands

[38] **Picture of diagonal bracing**
Eingeklebte Gewindestangen in der Praxis Neubau Hochregallager der Salinen AG in Ebensee
DI Markus Schimpf

[39] **Picture of the Hearst Tower**
http://www.wikipedia.org

[40] **Picture of the 30 St Mary Axe, Re Swiss Headquarters**
http://news.thomasnet.com

[41] **Graphs of feasibility study**
Tall Timber Buildings, The Stadthaus, Hoxten, Londen, Techniker

[42] **Pictures of Blumer System Binder**
http://www.blumer-bsb.ch

[43] **Drawing of a floor lay-up solution**
http://www.dataholz.de/

[44] **Picture of Deformation in Lintels (modified)**
Mechanica van constructies – Elastostatica van Slanke Structuren - A.L.Bouma, figuur 20.4

A Preliminary research Appendix

A.1 Historical and recent examples

A.1.1 Reference Projects

The solutions of the reference projects, E3 Berlin, the Murray Grove Tower and the Yingxian Pagoda are systematically addressed in that order throughout this paragraph.

A.1.1.1 E3 Berlin

The structure is designed as a framework of columns and beams of glue laminated timber. The timber members are interconnected by steel nodes, which are connected to the timber with bolts. On top of the beams the floor of timber lamella is stacked and concrete is poured on top. In between the columns the walls are placed also made of timber lamella. The advantages of timber construction realizes its full potential mainly because of absence of glued connections by using dowels and bolts. […]

figure A.1: Pictures of bracing [32]

figure A.2: Pictures of connection details [32]

Structural bracing: The structural bracing for this project is realized trough diagonal steel plates (figure A.1). In combination with the diaphragm action of the composite floor slabs a stiff structure is realized. Two small concrete shafts are placed in the middle of the plan to combine ventilation and structural supports for a squat concrete girder intergraded with the floor slab.

Connections: The Glue laminated timber columns and beams are connected by steel nodes. The nodes are prefabricated in shop. They consist of steel plates that are placed inside pre sawn slots in the timber members and secured by steel dowels. The narrow sides of these plates are welded together by another plate that is perpendicular to the direction of the former. This plate is bolted to the centre of the node which also consists of steel plates. By doing so the connections can be made fast and stresses perpendicular to the grain in timber members are omitted. In figure A.2 some pictures of typical connection details are shown.

Floors: The structural flooring consists of a timber-concrete composite. The first layer is made of stacked timber lamella (Brettstapel) with a structural height of 160 mm. On top of that a 100 mm concrete layer is placed with a net of practical reinforcement as shown in figure A.3.

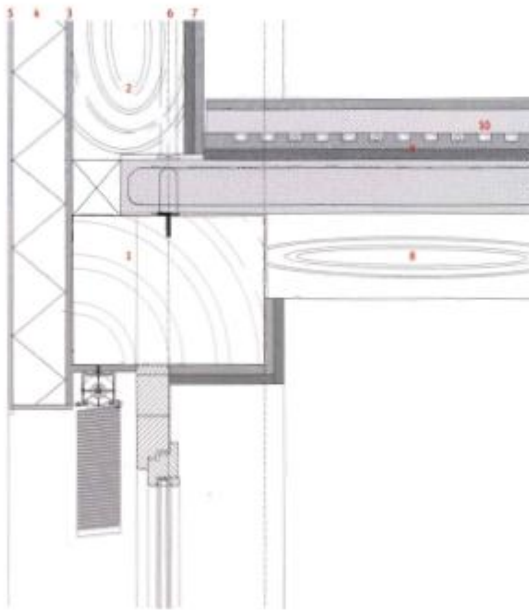

figure A.3: Detail of wall - floor connection

For the project E3 Berlin a fire safety strategy was developed in collaboration with fire safety engineers to proof that, with a combination of technical systems and structural solutions a security level could be reach that is equal to solid concrete construction. The following measures were taken.

Fire compartments: Every living unit is one fire compartment with sub compartments. On each floor only one unit is present, which results in that each floor has one area for vertical circulation and one living unit.

Structural Members: all timber members are have at least a fire resistance of 30 minutes. Two small RC-shaft cores are placed in the middle of the building to convince the authorities. The location is shown in figure A.4, marked in red. On these cores an floor integrated RC-squat girder was poured in situ.

Encapsulation: From the inside, all structural timber members and walls are encapsulated with two layers of gypsum board, resulting in capsulation class K 60, which is equivalent to 60 minutes of fire resistance. On the outside 12,5 mm planking is placed which is covered with 100 mm thick mineral wool insulation plates covered with gypsum board, which serves as thermal as well as fire insulation.

figure A.4: Fire safety floor plan

Layout: Escape routes flow to an exterior staircase, separated from the building, erected out of steel and concrete within a maximum proximity of 20 m from each compartment, which is shown in figure A.4 marked in yellow. A secondary escape route is provided through the use of al ladder between the 1st to the 3rd floor from which a spiral staircase continuous upward to the 7th floor.

Technical systems: In every living unit smoke detectors and fire alarms are placed that are equipped with automatic warning system communicating with the fire department in case of a fire.

Thermal insulation: The thermal insulation of the façade was not a problem, trough application of mineral insulation and solid timber members covered by two layers of gypsum board. The design of the building is categorized in the most energy efficient housing standard. This is also due to additional heat recovery and solar heating installations.

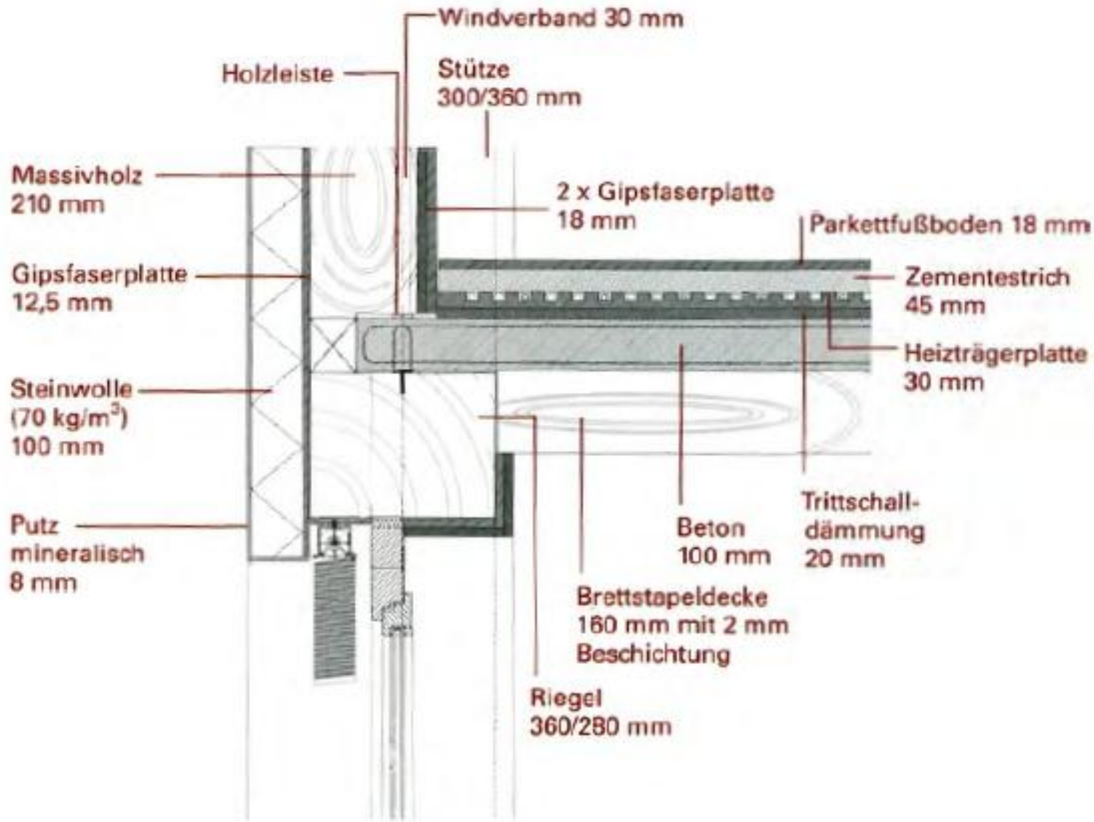

figure A.5: Floor-wall detail

Acoustics: The acoustic insulation between storey's was realized through the use of a floating cement screed cover. The buildup was based on the principles of a floor on a resilient/elastic foundation. The mass of the floating screed is coupled to the structural composite timber-concrete floor with a 20 mm thick sound insulation material figure A.5.

A.1.1.2 Murray Grove Tower

The design team of the Murray Grove Tower met some quite serious challenges early on and the design procedure had to readdress. A quote of the architect Mr. Waugh: "With a concrete frame building of this size, you simply look at a grid add a core and fill it out with studwork or block work. With timber, every wall is integral to the structure…,".

Material Strength
The building is constructed with cross laminated timber (CLT). Floor plates are made of five layer thick CLT and most walls of 3-layer thick CLT. The cross-laminated timber panels are made from Austrian spruce. Stresses are generally very low throughout the structure. The connection of wall, floor and wall below is the systems 'weak link'. The strength parallel to the grain of the wall panels is 24 N/mm^2, while the cross-grain crushing capacity of the floor plate is only 2.7 N/mm^2. Screw or nail arrays at highly loaded points alleviate these concentrations trough spreading out the forces over a larger area.

Stability and Stiffness
The internal structure creates a honeycomb, where every wall is integral to the building. The cross laminated timber panels have high in plain stiffness and form a cellular structure of timber load bearing walls, including all stair and lift cores, and floor slabs.

Robustness
Panelized buildings are susceptible to progressive collapse. A considerable part of the design work undertaken by structural engineering company Techniker on the this project was in the assessment of options to ensure the robustness of tall timber structures.

These requirements lead to alternative design approaches. Ties between units can be strengthened to a sufficient level. The preferred route has been to exploit the over-structuring typical in residential layouts by conjecturing alternative load-paths should any element be compromised.

The design team have therefore pursued a policy of 'efficient redundancy'. Wherever possible floor panels are designed to span in two directions or to cantilever if a support is removed. Effective ties are provided between floors and walls using simple 'off-the-shelf' brackets and screws. The inherently high in-plane stiffness of the cross-laminating process provides 'built-in' redundancy in the form of wall elements which can span laterally if support beneath is removed.

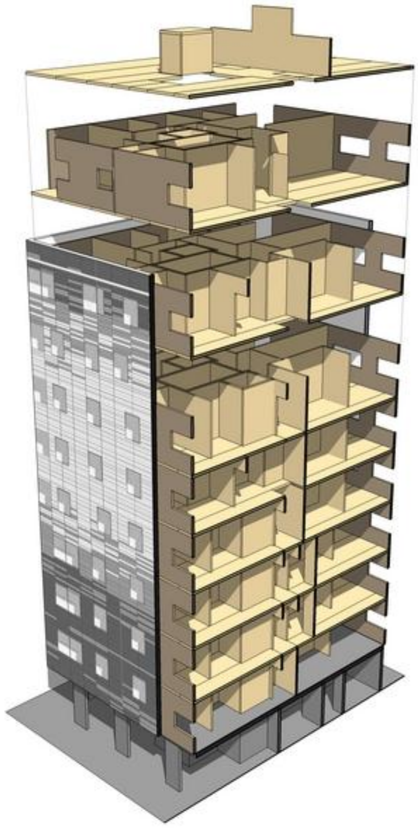

figure A.6: Cellular buildup of the building [5]

For this apartment building, four different scenarios of structural damage were considered. Adequate alternative load paths were demonstrated following the removal of various panels.

Connections: The connections are made simply by placing a wall (plate) element on to the floor (slab) element and screwing them together by means of angled steel plates and large screws.

Movement: The long-term creep movement of cross-laminated timber is negligible along the face of the panel and less than 1% across the grain. Similarly, moisture movement is neglectable over the panel surface and less than 2% cross-grain. The thermal coefficient of linear expansion is 34 $x10^{-6}$; about three times that of steel. Design research continues into the movement characteristics of these forms.

General Fire safety: For this project standard charring rates where set and tests have established the specific behavior of cross laminated timber from various sources.

Compartments: On each floor, there are four compartments appointed as living units and one as vertical circulation. Within and between living units 30 minutes and respectively 60 minutes integrity is reached. The fire resistance between living units and the principle vertical circulation (shaft) is 120 minutes.

Structural members: Close grain timber specified on the faces of panels significantly improves the fire resistance of members. Based on charring rates, the fire resistance is dependent on the number of layers, hence thickness, of the cross laminated timber panels. All wall elements have a build-up of three layers with a total thickness of 128 mm which results in a fire resistance of 30 minutes. All floor elements are 146 mm thick and have a fire resistance of 60 minutes. Between the living units and the shaft two elements are used divided trough mineral insulation which adds to the thermal and fire generated heat insulation.

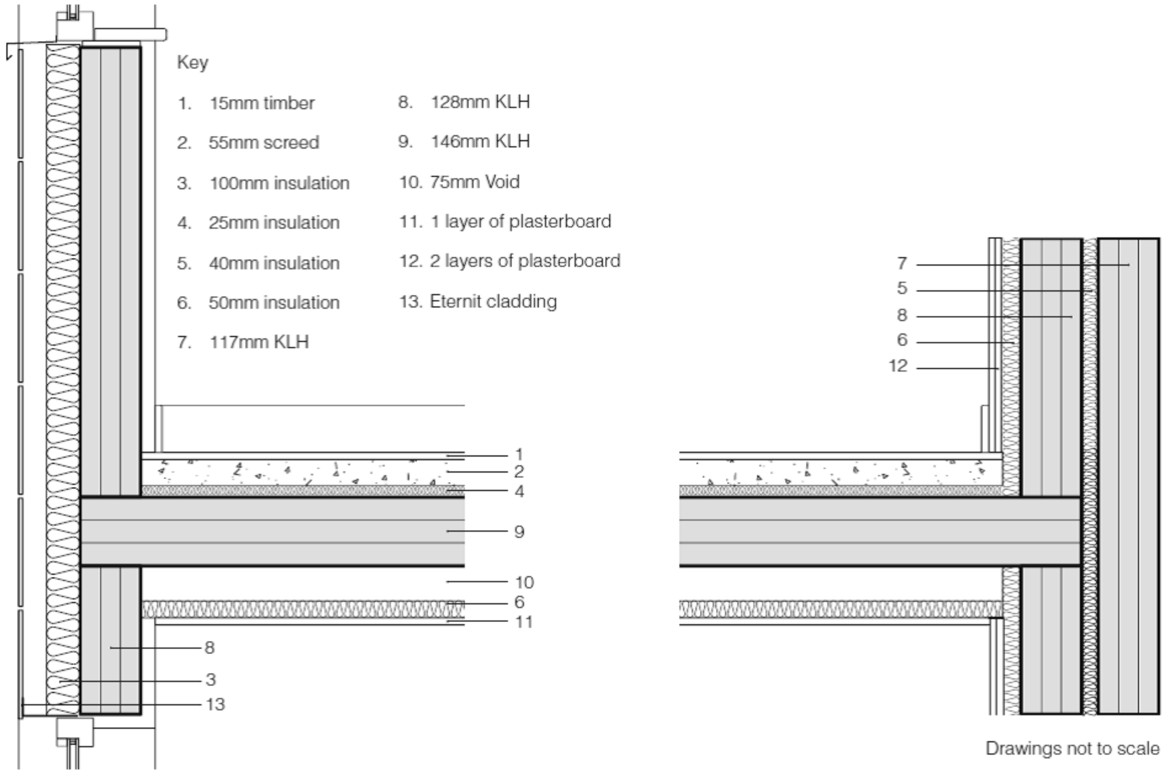

figure A.7: Floor-wall detail

Layout (Escape Routing): The only escape route is provided through a centralized staircase with a fire resistance of at least 120 minutes.

Encapsulation: Walls are covered with two layers of plasterboard which adds 60 minutes to the fire resistance. The floors are covered with a cement screed of 55 mm thick, which is incombustible. The suspended ceiling build-up consists of one layer of plasterboard, with a fire resistance of 30 minutes, and 50 mm thick mineral wool and a 75 mm airspace which provides additional fire-generated heat barrier.

Technical systems: for this project no additional technical measures had to be taken to satisfy the fire safety requirements stated by the authorities.

Building physical insulation measures are combined with fire safety measures, which is an observation of practical symbiotic solution finding in the shared field of fire safety and building physical engineering.

Thermal insulation: Cross laminated timber wall elements of 128 mm thickness met the thermal resistance requirement of 0.13 W/m²/K with just 100mm of insulation, without any additions.

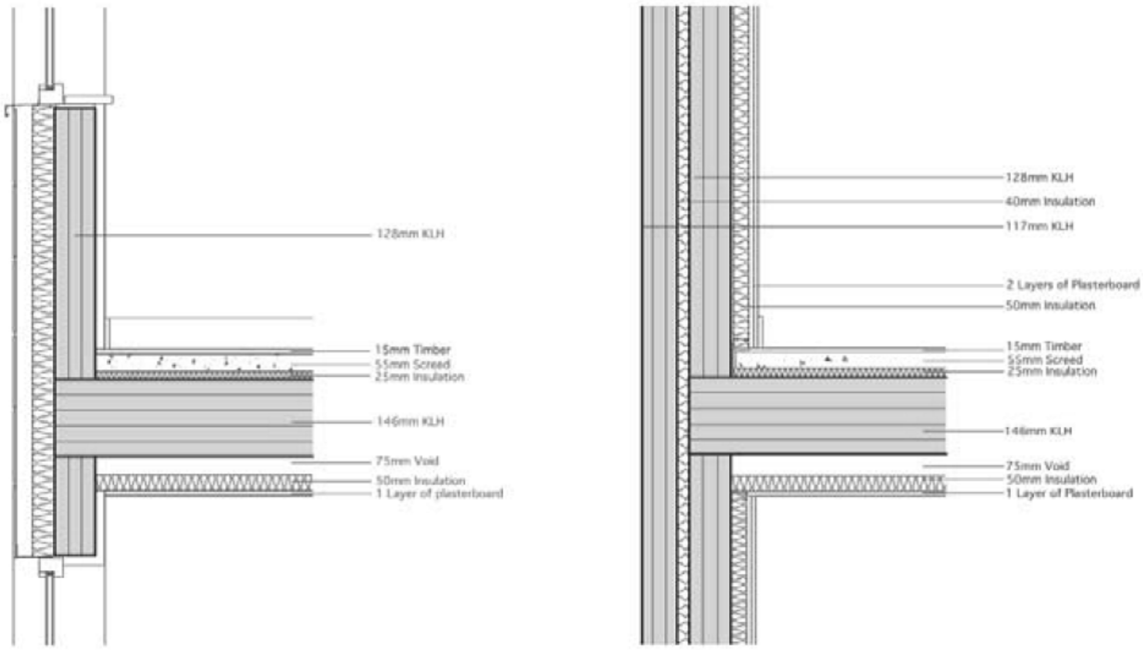

figure A.8: Floor-wall detail

Acoustics: The cross laminated timber structure is massive and partly takes account for the acoustic separation barrier. Across separation walls, two layers of 9 mm thick plasterboard on each side met requirements of the building regulations, externally a 10 mm air gap was necessary. For stairs and lift cores double wall construction is desirable with a 40 mm air gap. Similarly to E3, the Murray grove tower relies on a floating cement screed cover. In addition, the floors are provided with an acoustic ceiling which in total are adequate to prevent annoying impact sound transmission. (figure A.8)

Economic design: The speed of construction with cross laminated timber plate elements was very high as was experienced in this project. The nine storey Murray Grove tower was assembled within nine weeks, in which the structure was erected within three days per storey, all done with mobile cranes. The plate elements on the perimeter where thereby the full width of the building, which is approximately 17 m. This leads to believe that external conditions are not limiting the construction speed, especially because the erection process is very flexible within one week i.e. using mobile cranes and a three day working schedule.

A.1.1.3 Yingxian Pagoda

The construction method for Yingxian Wooden Pagoda followed the principle of an official building code (Yingzao Fashi), published by Li Jie in 1103 A.D. This method strives to take advantage of the compressive strength of wood. Most of what is discussed in this chapter is based on ref. [30]

Material Strength: The Yingxian Pagoda was built with Xing'an larch from Northern China, which is rarely available now. In the 1970s, a material test was conducted by taking specimens from secondary timber members [30]. Based on test results, the members easily reach values consistent with strength class D70 according to EN 338.

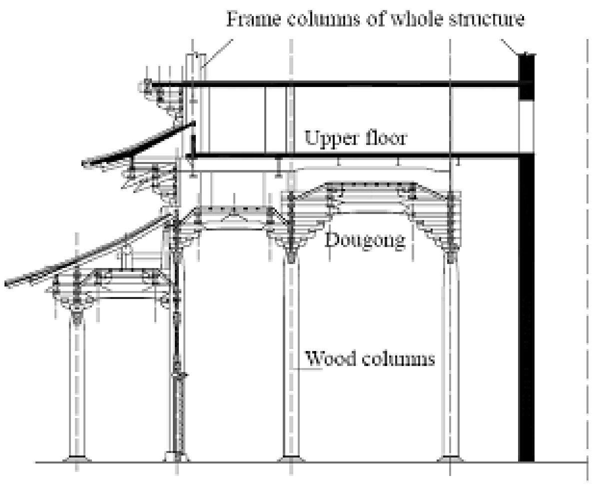

figure A.9: Basic principle Pagoda

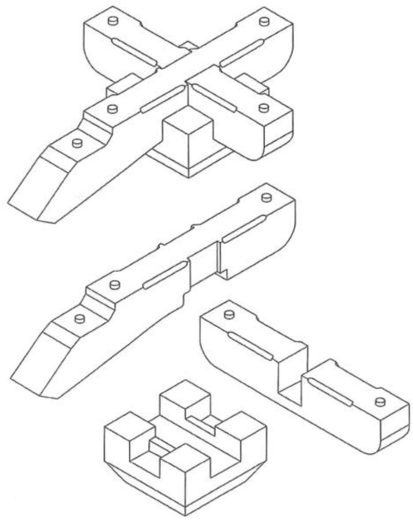

figure A.10: Basic principle Pagoda

Stability system: In terms of wind load, the heavy dead load of the structure help to resist the overturning forces induced by heavy wind while the ring of columns provide compression resistant elements to counter the overturning moment. It was also found that the compressive stress perpendicular to grain of Pu bai fang in the bottom three floors ranges from 2,02 to 7,19 N/mm^2. The relatively short column contributes to the overall stability of the building during wind action. The columns have a slight incline toward the apex of the pagoda, which are intended as stated in Yingzao Fashi.

Robustness: Historical records show that the Yingxian Wooden Pagoda survived major seismic events. By studying how the Yingxian Wooden Pagoda was built as a tall structure, one may be able to ascertain some of the reasons behind the well documented excellent seismic-resistant capabilities of pagodas.

- Wooden Pagoda is a flexible structure and unlikely to experience resonance
- The structure vibrates in a high mode with therefore small drifts, hence further reducing the chance of collapse due to second-order P-delta effects.
- Dou gong brackets are capable of dissipating energy via friction, damping of pagoda structures are believed to be well above 15% based on Japanese studies.
- Inclined columns could have increased the seismic resistance.

Connections: The building method used in ancient pagoda structures depends mainly on the heavy columns and the dou gong devices which are shown in figure A.10. The dou gong is intended to convert bending forces from beams and girders into vertical forces which go into the columns. The cross-arm and lever-arm members reduce the clear span of the main beam and girder. They in turn undergo short span bending until the forces are transferred to the column via the bracket in bearing. Depending on the span and load, multilayer dou gong brackets can be made to transfer high loads.

A.1.2 Solutions Previous studies

A.1.2.1 Projekt 8+

The structural design of the project 8+ makes use of a tube structure. The tube stucture combined with the floors take over the stiffening and stabilizing function of core shafts which appear in traditional concrete buildings, so that elevators shafts and staircases can be arranged freely in the plan. The capacity of the tube structure on the perimeter is much greater than that of traditional cores. Four different stability systems for the tube structure, each with a distinctive character, have been investigated: Diagonal braced, Portal frame grid structure, Cranked quadrangle and Auerman principle (Diagrid geometry).

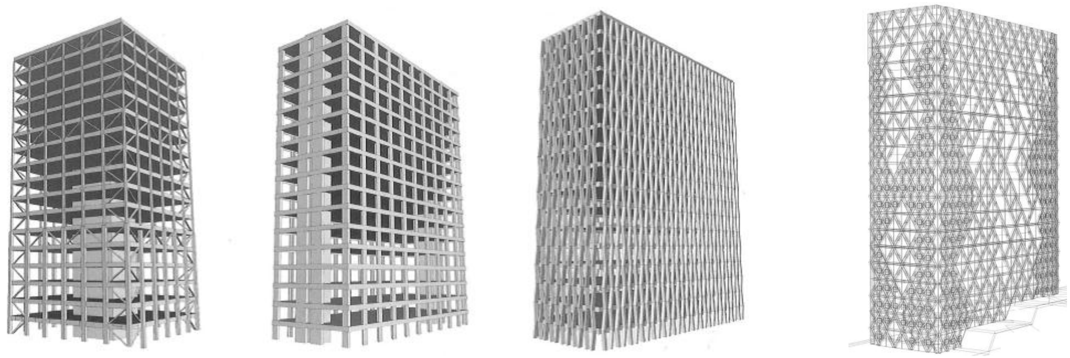

figure A.11: Different stability systems of office building Project 8+ [10]

Every system has a high degree of prefabrication with as little elements as possible. This is not just a natural feature of the modern timber but it is also tradition.

Structural floor

Several different type of floor solutions where investigated. The project team found that the advantages of timber construction are most effective when a dry principle is applied. This excluded both timber-concrete composite floors with a wet cover. The choice of the floor system, cross laminated timber floor with dry cement panel cover, is based on the combination of building physical properties and structural properties.

The research project 8+ differs particularly from existing tall buildings trough the use of timber for the load bearing structure, walls and floors. The goal is to prevent the risk for loss of life and to protect health of persons in case of fire. Also to limit the propagation of a fire in a way that effective fire fighting is possible and to limit the consequences of a fire at the property and neighboring buildings. The solutions for fire protection are manifold:

- Wood quality
- Treatment of the wood
- Timber cross section
- Smoke Detectors
- Sprinkler installation
- Evacuation Levels
- Short escape routes
- Evacuation measures in the various floors

Structural fire protection

The rules in the ONR 22000 are generally observed during a part of the project. The fire resistance of the supporting structure, the walls and floors, is achieved without taking the sprinkler system into account, in accordance with ONR 22000. A fire spread is among others limited by a full sprinkler system with additional redundancy in the form of a so called "Façade protection".

Operational fire protection
The entire building will be fire protected by the following operational facilities:

- Fire Alarm System with alarm to fire brigade
- Alerting facility – electrical audible alarm system
- Full sprinkler system with additional redundancy and "Facade protection"
- Fire lock compartments and in any case available secured escape routes which are equipped with a smoke dilution systems with a thirty times air renewal.
- Local smoke extraction systems to support the deployment of a fire department.
- Firefighters elevators.
- Wet pipes and wall hydrants and portable extinguishers.
- Security lighting according to ÖVE / ÖNORM E 800.
- Radio facility according to TRVB S 159th

Fire resistance floor system
The fire resistance of the floors in high-rise building must be consistent with REI 90, in accordance with the requirements. And the materials must at least be of the class A2 of Euro class scale. Since the structure consists of combustible materials, it was included in the fire protection concept, that no voids are present and the visible timber structure is executed without any additional planking or suspended ceilings.

The requirements for Noise Control in Austria are given in ÖNORM B 8115-2. For isolating components this leads to the following requirements: Regarding the noise transfer of separating floors in buildings between spaces of different units, a minimal sound level difference of 55 dB is required. This requirement, including the required for impact sound insulation, is easily met with the timber floor systems. The impact sound insulation is determined by the maximum rated standard impact sound. For spaces of transportation adjacent to spaces of different units this may amount to a maximum of 48dB. These requirements can be met by timber frame construction as well as with solid timber floor elements. The build-up of this floor system consists, from top to bottom, of the following layers:

- 200 mm Computer floor (Nortec)
- 25 mm Gypsum fiber panals (Rigidur)
- 29 mm Insulation layer (Floorrock HP30-1)
- 50 mm Gravel 4/8
- 162 mm Cross laminated timber

A.1.2.2 MSc Thesis E.C. Woudenberg

Diagonal bracing was proposed for stability purposes. Girders are placed between the columns in the parallel and perpendicular direction to the main axis of the building. The actions applied on behalf of the structural analyses comprise wind, snow, dead and life load and considers aspects like buckling and lateral torsional stability of the timber elements.

Because the floor plan of the building has a rectangular shape the total wind action on the long façade is larger than the other direction. The design of the stabilizing element in the short direction are therefore decisive. Four shear planes are placed in the short direction of the building, two in the façade and the other two are combined with separation walls. Trough the disc action of the floors the wind load is transferred to the shear planes. Glued-Laminated elements of strength grade GL28 were used for columns, beams and diagonals with cross-sectional dimensions of 440x400 mm^2, 200x500 mm^2 and 300x400 mm^2, respectively for these shear planes. The remaining columns have dimensions of 300x300 mm^2.The LIGNATUR floor has a hollow structure with a depth of 220 mm. The floors are considered rigid and transfer the in-plane loads to the diagonal braced vertical frames.

Fire compartments: In the thesis of E.C. Woudenberg all relevant checks were conducted with respect to fire safety, i.e. the limitation and the limitation of smoke and fire propagation trough use of proper compartment walls.

Structural measures: From the study done on fire safety is was concluded that a minimum fire resistance of 120 minutes was required for load baring structure. The maximum loaded column of 440x440 mm complied with the demand of 120 minutes by the charring of the section without any additional fire protection. The LIGNATUR floors have a maximum fire resistance of 90 minutes with addition of a concrete top layer and Fermacell plate ceiling the fire resistance is stretched with 30 minutes.

Encapsulation: Almost all internal separation walls, all ceilings and floors are covered with a gypsum fiber board (Fermacell) to comply with the building code regulations.

Layout: Two main staircases are located in the center of the building. The distance between a fire compartment of a single living unit and the staircase is in compliance with the regulations. All relevant checks were carried out with respect to layout.

Acoustics: Regarding acoustic transmission and floor vibrations, special software was used to evaluate various types of acoustic transmission. It appeared to be very difficult to design a timber floor that satisfies all the acoustic transmission requirements, especially the one dealing with impact sound. Since timber floors are by definition light in self-weight, very large cavities between the floor and ceiling are required to obtain an acceptable result. Ultimately, all acoustic-related problems could be solved except for impact sound, which require laboratory tests to find acceptable solutions. Some solutions suggest increasing the cavity height between floor and the ceiling or adding more insulation materials between the ceiling and floor. Acoustic transmission requirements for the internal walls could be satisfied without much problem. Regarding vibrations it was concluded that all the design requirements could be satisfied.

A.1.2.3 MSc Thesis H. Kuipers

For his project H. Kuipers chose to use a framework with rotational stiff connections, the so called moment frames. This moment frame is stiffened with additional braced shear planes. For the building design, three different alternatives are worked out with different column spacing, namely: 3600mm, 4800 mm and 6000 mm. Obviously the smallest column spacing results in the highest building design of 15 storey's. Horizontal displacement was the decisive factor for the design. A relatively simple differential equation is used to check the dynamic behavior of the building.

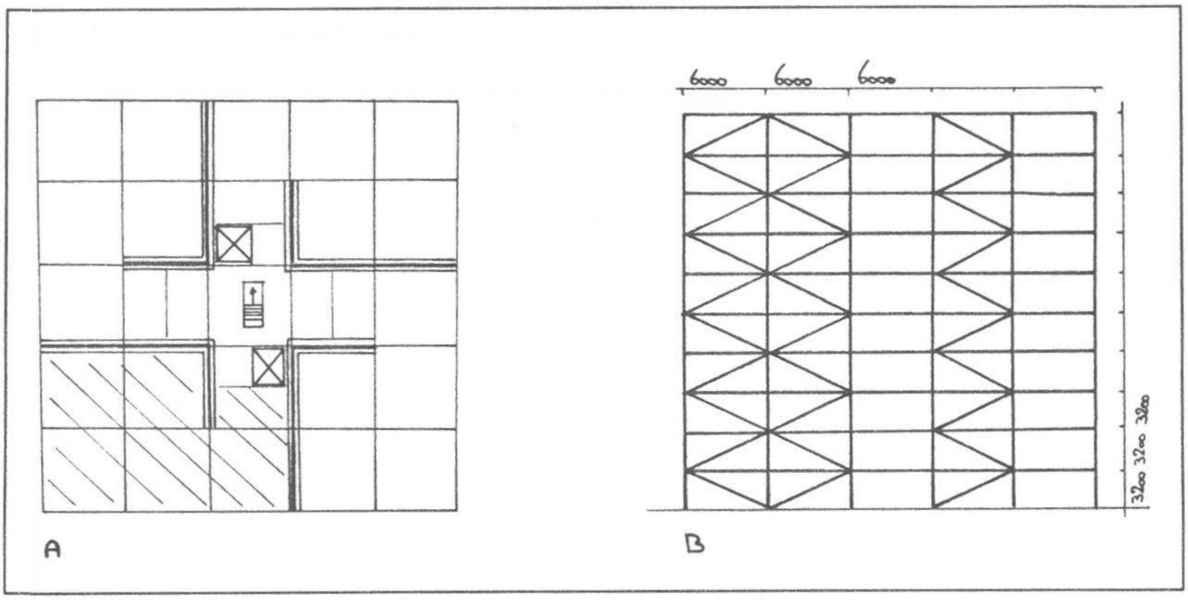

figure A.11: Drawing of timber building [36]

The design was checked in accordance with the Dutch standards (NEN). The lateral deflection of a building of twenty floors under wind loading, according to the NEN standards for the calculation of timber frames, was neatly within the allowable deflection. The NEN standards for the calculation of timber structures gave dubious results. As a consequence the standard was reviewed.

Horizontal stiffness of the building was assumed to be the decisive factor for the height of the design. The dynamic behavior of the building contributed to the height limitation.

A.1.2.4 Feasibility study Dock Tower

The result of the study was a tall timber building with a hybrid construction with a concrete stabilizing core and primary fire compartments of concrete and secondary compartments of timber. Four external staircases in reinforced concrete on the outside of the building caring a projecting concrete slabs after every three storey's.

Fire compartments: The residential apartments are divided into secondary fire compartments made of timber-concrete composite slabs and timber walls that are designed according to the requirement of burn-out. The building has five staircases placed as far away from each other as possible. The projecting concrete slabs shall effectively prevent the fire propagation on the building façade.

Layout: Four of the staircases are designed as escape routes and each apartment has direct access to two escape routes. Two of the staircases are open to the outside; two are pressurized to avoid smoke to enter.

Technical systems: In order to control and extinguish the fire in an early stage, the building rooms are equipped with a high-pressure water mist system. The activation of the water mist system is temperature-actuating or controlled by a fire alarm system. The high-pressure and special nozzles break the water down into very small drops leading to a cooling and smothering water fog in a way that the fire cannot persist. Further, the building has two high-pressure water mist fire hydrants placed on each floor of the central core. The fire hydrants can be used to extinguish the fire on the facade.

A.1.2.5 Urban Timber housing in Vienna

The timber housing project in Vienna [6] consisted of tree sites, namely A, B and C. Regulatory Vienna demands require a 60 minute of fire resistance for the supporting elements. Elements that are part of fire-compartments need to have a minimum fire resistance of 90 minutes. Building regulations of Vienna demands that facades are build of materials with at least combustibility class B1. The following solutions were applied in this project:

- Walls: encapsulation with plasterboard
- Floors: cement screed, non-combustible
- Ceilings, site A: Cross Laminated Timber Elements
- Ceilings, sites B + C: Suspended plasterboard ceiling
- Allied building core for wet rooms and staircases. (site B + C)
- Application of a 1,5 mm thick plate steel fire stop projecting 150 mm outward on the facade, combined with a Larch facade (B2). (site A) Solution was accepted on research of Holzforschugung Austria.

B Case Study Appendix

B.1 Wind loads

Maple worksheet: Programmed calculation of the wind load.

```
> restart;
```

Peak velocity pressure

```
> Q[w]:=c[s]*c[d]*c[f]*q[p];
```

$$Q_w := c_s\, c_d\, c_f\, q_p$$

```
> q[p]:=(1+7*l[v])*1/2*rho*v[m]^2;
```

$$q_p := \frac{1}{2}\,(1+7\,l_v)\,\rho\, v_m^{\,2}$$

Mean wind velocity

```
> restart;
```

General formula

```
> v[m]:=c[r]*c[o]*v[b];
```

$$v_m := c_r\, c_o\, v_b$$

Roughtness factor

```
> c[r]:=k[r]*ln(z[i]/z[0]);
```

$$c_r := k_r \ln\left(\frac{z_i}{z_0}\right)$$

```
> k[r]:=0.19*(z[0]/a)^0.07;
  a:=0.05;
```

$$k_r := 0.19\left(\frac{z_0}{a}\right)^{0.07}$$

$$a := 0.05$$

Basic wind velocity

```
> v[b]:=c[dir]*c[season]*v[b,0];
```

$$v_b := c_{dir}\, c_{season}\, v_{b,\,0}$$

Parameters

```
> v[b,0]:=27;k[l]:=1.0;c[o]:=1.0;z[0]:=0.20;
  c[dir]:=1.0;c[season]:=1.0;rho:=1.25;
  Z:=table([1=B,2=0.6*H,3=H]):B:=30:H:=112:
```

$$v_{b,\,0} := 27$$

$$k_l := 1.0$$

$$c_o := 1.0$$

$$z_0 := 0.20$$

$$c_{dir} := 1.0$$

$$c_{season} := 1.0$$

$$\rho := 1.25$$

```
> v[b]:=evalf[2](v[b]);
```

$$v_b := 27.$$

```
> k[r]:=evalf[2](k[r]);
```

$$k_r := 0.21$$

```
> for i from 1 to 3 do
  z[i]:=Z[i]:
  v[m,i]:=evalf[3](v[m]);
  end do;
```

$$z_1 := 30$$
$$v_{m,\,1} := 28.4$$
$$z_2 := 67.2$$
$$v_{m,\,2} := 32.9$$
$$z_3 := 112$$
$$v_{m,\,3} := 35.9$$

Turbulance intencity (lv)

```
> restart;
```

General formula

```
> l[v]:=k[l]/(c[o]*ln(z[i]/z[0]));
```

$$l_v := \frac{k_l}{c_o \ln\left(\frac{z_i}{z_0}\right)}$$

Parameters

```
> Z:=table([1=B,2=0.6*H,3=H]):B:=30:H:=112:z[0]:=0.2;k[l]:=1.0;c[o]
  =1.0;
```

$$z_0 := 0.2$$
$$k_l := 1.0$$
$$c_o := 1.0$$

```
> for i from 1 to 3 do
  z[i]:=Z[i]:
  l[v,i]:=evalf[2](l[v]);
  end do;
```

$$z_1 := 30$$
$$l_{v,\,1} := 0.20$$
$$z_2 := 67.2$$
$$l_{v,\,2} := 0.17$$
$$z_3 := 112$$
$$l_{v,\,3} := 0.16$$

Background factor B

```
> restart;
```

General formula

```
> B2:=(1+3/2*sqrt((b/L[zs])^2+(h/L[zs])^2+(b/L[zs]*h/L[zs])^2))^(-(:
  /2));
```

$$B2 := \frac{1}{\sqrt{1+\frac{3}{2}\sqrt{\frac{b^2}{L_{zs}^2}+\frac{h^2}{L_{zs}^2}+\frac{b^2 h^2}{L_{zs}^4}}}}$$

Turbulent lenght scale

```
> L[zs]:=L[t]*(z[s]/z[t])^alpha;
```

$$L_{zs} := L_t\left(\frac{z_s}{z_t}\right)^{\alpha}$$

```
> alpha:=0.67+0.05*ln(z[0]);
```

$$\alpha := 0.67 + 0.05\ln(z_0)$$

Parameters

```
> L[t]:=300;z[s]:=0.6*h;z[0]:=0.2;z[t]:=200;b:=30;h:=112;
```

$$L_t := 300$$
$$z_s := 0.6\,h$$
$$z_0 := 0.2$$
$$z_t := 200$$
$$b := 30$$
$$h := 112$$

```
> L[zs]:=evalf[3](L[zs]);
```

$$L_{zs} := 158.$$

```
> B:=evalf[2](sqrt(B2));
```

$$B := 0.84$$

Resonance Responce factor R

```
> restart;
```

General formula

```
> R2:=Pi^2/(2*delta)*S[L]*K[s];
```

$$R2 := \frac{\pi^2 S_L K_s}{2\,\delta}$$

Asuption: Timber bridges = Timber buildings

Stuctural damping

```
> delta:=0.06;
```

$$\delta := 0.06$$

Wind power spectral dencity function

```
> S[L]:=6.8*f[L]/(1+10.2*f[L])^(5/3);
```

$$S_L := \frac{6.8\, f_L}{(1 + 10.2\, f_L)^{(5/3)}}$$

```
> f[L]:=n[1]*L[zs]/v[m,zs];
```

$$f_L := \frac{n_1\, L_{zs}}{v_{m,\, zs}}$$

Size reduction factor

```
> K[s]:=(1+sqrt((G[y]*phi[y])^2+(G[z]*phi[z])^2+(2/Pi*G[y]*phi[y]*G[z]
  phi[z])^2))^(-1);
```

$$K_s := \frac{1}{1 + \sqrt{G_y^2\, \varphi_y^2 + G_z^2\, \varphi_z^2 + \frac{4\, G_y^2\, \varphi_y^2\, G_z^2\, \varphi_z^2}{\pi^2}}}$$

```
> phi[y]:=c[y]*b*n[1]/v[m,zs];
```

$$\varphi_y := \frac{c_y\, b\, n_1}{v_{m,\, zs}}$$

```
> phi[z]:=c[z]*h*n[1]/v[m,zs];
```

$$\varphi_z := \frac{c_z\, h\, n_1}{v_{m,\, zs}}$$

Parameters

```
> h:=112:b:=30:
```

```
> L[zs]:=158;v[m,zs]:=32.9;h:=112;n[1]:=46/h;
  c[y]:=11.5;c[z]:=11.5;G[y]:=1/2;G[z]:=3/8;
```

$$L_{zs} := 158$$

$$v_{m,\, zs} := 32.9$$

$$h := 112$$

$$n_1 := \frac{23}{56}$$

$$c_y := 11.5$$

$$c_z := 11.5$$

$$G_y := \frac{1}{2}$$

$$G_z := \frac{3}{8}$$

```
> f[L]:=evalf[3](n[1]*L[zs]/v[m,zs]);
  K[s]:=evalf[2](K[s]);S[L]:=evalf[2](S[L]);
```

$$f_L := 1.97$$

$$K_s := 0.091$$

$$S_L := 0.088$$

```
> R:=evalf[2](sqrt(R2));
```

$$R := 0.81$$

Structural factor cscd

```
> restart;
```

General formula

```
> cscd:=(1+2*k[p]*l[v,zs]*sqrt(B^2+R^2))/(1+7*l[v,zs]);
```

$$cscd := \frac{1 + 2\,k_p\,l_{v,\,zs}\,\sqrt{B^2 + R^2}}{1 + 7\,l_{v,\,zs}}$$

Peak factor

```
> k[p]:=max(3.0,k[p,1]);
```

$$k_p := \max(k_{p,\,1},\,3.0)$$

```
> k[p,1]:=sqrt(2*ln(2+ln(upsilon*T)))+0.6/sqrt(ln(2+ln(upsilon*T)))
```

$$k_{p,\,1} := \sqrt{2}\,\sqrt{\ln(2 + \ln(\upsilon\,T))} + \frac{0.6}{\sqrt{\ln(2 + \ln(\upsilon\,T))}}$$

```
> upsilon:=n[1]*sqrt(R^2/(B^2+R^2));
```

$$\upsilon := n_1\,\sqrt{\frac{R^2}{B^2 + R^2}}$$

Parameters

```
> B:=0.84;R:=0.81;l[v,zs]:=0.17;
  h:=112:
```

$$B := 0.84$$

$$R := 0.81$$

$$l_{v,\,zs} := 0.17$$

```
> n[1]:=46/h;T:=600;
```

$$n_1 := \frac{23}{56}$$

$$T := 600$$

```
> upsilon:=evalf[2](upsilon);
  k[p,1]:=evalf[2](k[p,1]);
  k[p]:=k[p];
```

$$\upsilon := 0.28$$

$$k_{p,\,1} := 2.4$$

$$k_p := 3.0$$

```
> cscd:=evalf[3](cscd);
```

$$cscd := 1.00$$

Qw Equation

```
> restart;
  with(plots):with(plottools):
Warning, the name changecoords has been redefined
Warning, the assigned name arrow now has a global binding
```

```
> Qz:=(Q[w,3]-Q[w,1])/(h-2*b)*(z-b)+Q[w,1];
```

$$Qz := \frac{(Q_{w,\,3} - Q_{w,\,1})\,(z - b)}{h - 2\,b} + Q_{w,\,1}$$

```
> b:=30:h:=112:
```

Parameters

Force coeficientcf

```
> c[f]:=c[f,0]*psi[r]*psi[lambda];
```

$$c_f := c_{f,\,0}\,\psi_r\,\psi_\lambda$$

```
> c[f,0]:=2.10;
  psi[r]:=1.00;
  psi[lambda]:=0.66;
```

$$c_{f,\,0} := 2.10$$
$$\psi_r := 1.00$$
$$\psi_\lambda := 0.66$$

```
> c[f]:=evalf[3](c[f]);
```

$$c_f := 1.39$$

```
> c[s]:=1.00;c[d]:=1.00;rho:=1.25;
```

$$c_s := 1.00$$
$$c_d := 1.00$$
$$\rho := 1.25$$

```
> Vm:=table([28.4,32.9,35.9]);
```

$$Vm := table([1 = 28.4,\ 2 = 32.9,\ 3 = 35.9])$$

```
> Lv:=table([0.20,0.17,0.16]);
```

$$Lv := table([1 = 0.20,\ 2 = 0.17,\ 3 = 0.16])$$

```
> for i from 1 to 3 do;
  l[v]:=Lv[i];
  v[m]:=Vm[i];
  q[p]:=evalf[4]((1+7*l[v])*1/2*rho*v[m]^2);
  Q[w,i]:=evalf[4](c[s]*c[d]*c[f]*q[p]);
  end do;
```

$$l_v := 0.20$$
$$v_m := 28.4$$
$$q_p := 1210.$$
$$Q_{w,\,1} := 1682.$$
$$l_v := 0.17$$
$$v_m := 32.9$$
$$q_p := 1482.$$
$$Q_{w,\,2} := 2060.$$
$$l_v := 0.16$$
$$v_m := 35.9$$
$$q_p := 1708.$$
$$Q_{w,\,3} := 2374.$$

```
> P1:=plot(-Q[w,1],z=0..30,color=black,thickness=2):
  P2:=plot(-Qz,z=30..82,color=black,thickness=2):
  P3:=plot(-Q[w,3],z=82..112,color=black,thickness=2):
> P4:=rotate(P1,Pi/2):P5:=rotate(P2,Pi/2):P6:=rotate(P3,Pi/2):
> display([P4,P5,P6],
  view=[1.5e3..2.5e3,0..112],
  font=[Thomaha,roman,19],
  labels=['"Qw [N/m2]"','"H [m]"'],
  labelfont=[Thomaha,bold,19],
  labeldirections=[HORIZONTAL,VERTICAL],
  title='"Wind load over building Height"',
  titlefont=[Thomaha,bold,19]);
```

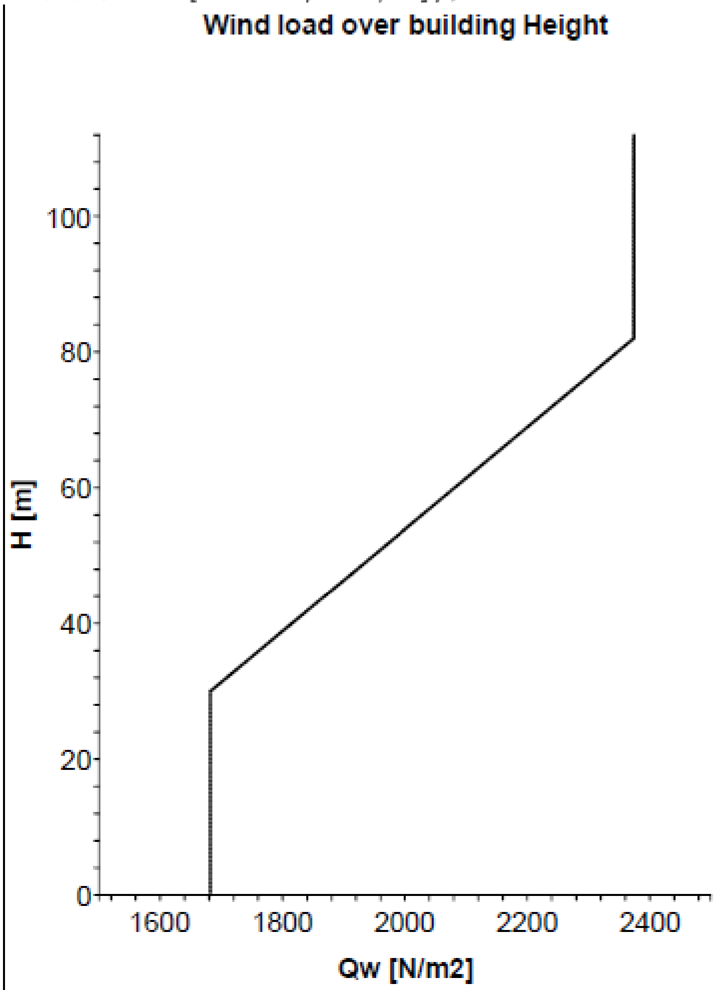

B.2 CLT Section Properties

Maple worksheet: Programmed calculation of section properties of a *m* number thick cross laminated timber element.

```
> restart;
> EI[eff,i]:=5/384*q*l^4/w[i];
```

$$EI_{eff,\,i} := \frac{5\,q\,l^4}{384\,w_i}$$

Own Bending Stiffness

```
> EI[A]:=sum(E[i]*Iy[i],i=1..m);
```

$$EI_A := \sum_{i=1}^{m} E_i\,Iy_i$$

```
> EI[A]:=n[0]*EI[0]+n[90]*EI[90];
```

$$EI_A := n_0\,EI_0 + n_{90}\,EI_{90}$$

```
> EI[0]:=E[0]*Iy;
  EI[90]:=E[90]*Iy;
```

$$EI_0 := E_0\,Iy$$

$$EI_{90} := E_{90}\,Iy$$

```
> Iy:=1/12*b*t^3;
  W:=1/6*b*t^2;
```

$$Iy := \frac{1}{12}\,b\,t^3$$

$$W := \frac{1}{6}\,b\,t^2$$

Steiner Bending Stiffness

```
> EI[B]:=sum(E[i]*A[i]*z[i]^2,i=1..m);
```

$$EI_B := \sum_{i=1}^{m} E_i\,A_i\,z_i^2$$

```
>
```

Shear Stiffness (finite)

```
> rS:=1/a^2*t/(2*G[1]*b)+sum(t/(2*G[1]*b),i=2..(m-1))+t/(2*G[m]*b);
```

$$rS := \frac{t}{2\,a^2\,G_1\,b} + \frac{(m-2)\,t}{2\,G_1\,b} + \frac{t}{2\,G_m\,b}$$

```
> rS:=1/a^2*t/(2*b)*((n[0]-1)/G[0]+(n[90])/G[90]);
```

$$rS := \frac{t\left(\frac{n_0-1}{G_0} + \frac{n_{90}}{G_{90}}\right)}{2\,a^2\,b}$$

```
> S:=1/rS;
```

$$S := \frac{2\,a^2\,b}{t\left(\frac{n_0-1}{G_0} + \frac{n_{90}}{G_{90}}\right)}$$

INPUT: Number of Layers

```
> m:=9:
> for i from 1 to m do;
   z[i]:=t*m/2-t*(1/2+i-1);
  end do:
> a:=(m-1)*t;
```

$$a := 8\,t$$

```
> for i from 1 to m do;
   A[i]:=b*t;
   E[i]:=`if`((-1)^i<0,E[0],E[90]):
  end do:
> n[0]:=(m+1)/2;
  n[90]:=(m-1)/2;
```

$$n_0 := 5$$

$$n_{90} := 4$$

```
> unassign('i');
>
```

INPUT: Parameters

```
> E[0]:=20000;
  E[90]:=1330;
  G[0]:=1250;
  G[90]:=125;
  t:=43;
  b:=1000;
```

$$E_0 := 20000$$

$$E_{90} := 1330$$

$$G_0 := 1250$$

$$G_{90} := 125$$

$$t := 43$$

$$b := 1000$$

OUTPUT: Section Properties to GSA Beam-Model

```
> EI[A]:=evalf[3](EI[A]);
  Iy[A]:=evalf[3](EI[A]/E[0]);
```

$$EI_A := 6.98\ 10^{11}$$

$$Iy_A := 3.49\ 10^{7}$$

```
> EI[B]:=evalf[4](EI[B]);
  Iy[B]:=evalf[4](EI[B]/E[0]);
```

$$EI_B := 6.572\ 10^{13}$$

$$Iy_B := 3.286\ 10^{9}$$

```
> GAs:=evalf[4](S);
  As:=evalf[5](S/G[0]);
```

$$GAs := 1.564\ 10^{8}$$

$$As := 1.2509\ 10^{5}$$

```
>
```

B.3 CLT Floor Element

```
> restart;
```

Own bending stiffness

```
> EI[A]:=sum(E[i]*Iy[i],i=1..m);
```

$$EI_A := \sum_{i=1}^{m} E_i\, Iy_i$$

```
> EI[A]:=n[0]*EI[0]+n[90]*EI[90];
```

$$EI_A := n_0\, EI_0 + n_{90}\, EI_{90}$$

```
> EI[0]:=E[0]*Iy;
  EI[90]:=E[90]*Iy;
```

$$EI_0 := E_0\, Iy$$

$$EI_{90} := E_{90}\, Iy$$

```
> Iy:=1/12*b*t^3;
  W:=1/6*b*t^2;
```

$$Iy := \frac{1}{12}\, b\, t^3$$

$$W := \frac{1}{6}\, b\, t^2$$

Steiner bending stiffness

```
> EI[B]:=sum(E[i]*A[i]*z[i]^2,i=1..m);
```

$$EI_B := \sum_{i=1}^{m} E_i\, A_i\, z_i^2$$

```
>
```

Shear stiffness (finite)

```
> rS:=1/a^2*t/(2*G[1]*b)+sum(t/(2*G[1]*b),i=2..(m-1))+t/(2*G[m]*b);
```

$$rS := \frac{t}{2\, a^2\, G_1\, b} + \frac{(m-2)\, t}{2\, G_1\, b} + \frac{t}{2\, G_m\, b}$$

```
> rS:=1/a^2*t/(2*b)*((n[0]-1)/G[0]+(n[90])/G[90]);
```

$$rS := \frac{t\left(\frac{n_0 - 1}{G_0} + \frac{n_{90}}{G_{90}}\right)}{2\, a^2\, b}$$

```
> S:=1/rS;
```

$$S := \frac{2\, a^2\, b}{t\left(\frac{n_0 - 1}{G_0} + \frac{n_{90}}{G_{90}}\right)}$$

INPUT number of layers

```
> m:=7:
> for i from 1 to m do;
   z[i]:=t*m/2-t*(1/2+i-1);
  end do:
> a:=(m-1)*t;
```

$$a := 6\,t$$

```
> for i from 1 to m do;
   A[i]:=b*t;
   E[i]:=`if`((-1)^i<0,E[0],E[90]):
  end do:
> n[0]:=(m+1)/2;
  n[90]:=(m-1)/2;
```

$$n_0 := 4$$

$$n_{90} := 3$$

```
> unassign('i');
```

INPUT parameters

```
> E[0]:=20000;
  E[90]:=1330;
  G[0]:=1250;
  G[90]:=125;
  t:=43;
  b:=1000;
```

$$E_0 := 20000$$

$$E_{90} := 1330$$

$$G_0 := 1250$$

$$G_{90} := 125$$

$$t := 43$$

$$b := 1000$$

OUTPUT to GSA beam-model

```
> EI[A]:=evalf[3](EI[A]);
  Iy[A]:=evalf[3](EI[A]/E[0]);
```

$$EI_A := 5.56\ 10^{11}$$

$$Iy_A := 2.78\ 10^{7}$$

```
> EI[B]:=evalf[4](EI[B]);
  Iy[B]:=evalf[4](EI[B]/E[0]);
```

$$EI_B := 3.265\ 10^{13}$$

$$Iy_B := 1.632\ 10^{9}$$

```
> GAs:=evalf[4](S);
  As:=evalf[5](S/G[0]);
```

$$GAs := 1.173\ 10^{8}$$

$$As := 93818.$$

```
> Iy:=1/12*b*t^3:W:=1/6*b*t^2:
```

INPUT from GSA-model

```
> M[A]:=1016E3;
  M[B]:=57110e3;
  V[A]:=558;
  V[B]:=28500;
  Nw:=8295;
```

$$M_A := 1.016\ 10^6$$

$$M_B := 5.7110\ 10^7$$

$$V_A := 558$$

$$V_B := 28500$$

$$Nw := 8295$$

Bending moment, Bending stress

```
> 'sigma[M,i]=M[i]/W';
  for i from 1 to m do
  M[i]:=evalf[4](E[i]*Iy/EI[A]*M[A]);
  end do:
```

$$\sigma_{M,\,i} = \frac{M_i}{W}$$

```
> 'sigma[M,i]=M[i]/W';
  for i from 1 to m do
  sigma[M,i]:=evalf[3](M[i]/W);
  end do;
```

$$\sigma_{M,\,i} = \frac{M_i}{W}$$

$$\sigma_{M,\,1} := 0.785$$

$$\sigma_{M,\,2} := 0.0522$$

$$\sigma_{M,\,3} := 0.785$$

$$\sigma_{M,\,4} := 0.0522$$

$$\sigma_{M,\,5} := 0.785$$

$$\sigma_{M,\,6} := 0.0522$$

$$\sigma_{M,\,7} := 0.785$$

Normal force (Steiner part), normal stress

```
> 'N[i]=E[i]*A[i]*abs(z[i])/EI[B]*M[B]+E[i]*A[i]/sum(E[j]*A[j],j=1..m)
  N[x]';
  for i from 1 to m do
  N[i]:=evalf[4](E[i]*A[i]*abs(z[i])/EI[B]*M[B]+E[i]*A[i]/sum(E[j]*A[j
  ,j=1..m)*Nw):
  end do:
```

$$N_i = \frac{E_i A_i \ |z_i| \ M_B}{EI_B} + \frac{E_i A_i N_x}{\sum_{j=1}^{m} E_j A_j}$$

```
> 'sigma[n,i]=N[i]/A[i]';
  for i from 1 to m do
  sigma[n,i]:=evalf[4](N[i]/A[i]);
  end do;
```

$$\sigma_{n,\,i} = \frac{N_i}{A_i}$$

$$\sigma_{n,\,1} := 4.558$$

$$\sigma_{n,\,2} := 0.2031$$

$$\sigma_{n,\,3} := 1.551$$

$$\sigma_{n,\,4} := 0.003056$$

$$\sigma_{n,\,5} := 1.551$$

$$\sigma_{n,\,6} := 0.2031$$

$$\sigma_{n,\,7} := 4.558$$

```
>
```

Shear stress

```
> 'tau[A,i]=[E[i]*Iy/EI[A]]*V[A]*[3/(2*A[i])]';
  for i from 1 to m do;
   tau[A,i]:=E[i]*Iy/EI[A]*V[A]*3/(2*A[i]);
  end do:
```

$$\tau_{A,\,i} = \left[\frac{E_i\, Iy}{EI_A}\right] V_A \left[\frac{3}{2\,A_i}\right]$$

```
> 'tau[B,i-1,i]=V[B]/EI[B]*sum(E[j]*A[j]*z[j],j=1..i-1)/b';
  tau[B,0,1]:=0:
  for i from 1 to m-1 do;
    tau[B,i,i+1]:=evalf[3](V[B]/EI[B]*sum(E[j]*A[j]*z[j],j=1..i)/b);
  end do:
  tau[B,m,m+1]:=0:
```

$$\tau_{B,\,i-1,\,i} = \frac{V_B \left(\sum_{j=1}^{i-1} E_j\, A_j\, z_j\right)}{EI_B\, b}$$

```
> 'tau[1,i]=min(tau[B,i-1,i],tau[B,i,i+1])';
  for i from 1 to m do;
  tau[1,i]:=evalf[3](min(tau[B,i-1,i],tau[B,i,i+1]));
  end do:
```

$$\tau_{1,\,i} = \min(\tau_{B,\,i-1,\,i}, \tau_{B,\,i,\,i+1})$$

```
> 'tau[2,i]=abs(tau[B,i-1,i]-tau[B,i,i+1])';
  for i from 1 to m do;
  tau[2,i]:=evalf[3](abs(tau[B,i-1,i]-tau[B,i,i+1]));
  end do:
```

$$\tau_{2,\,i} = \left|\tau_{B,\,i-1,\,i} - \tau_{B,\,i,\,i+1}\right|$$

```
>
```

```
> for i from 1 to m do;
   tau[max,i]:=evalf[3](
                `if`(tau[A,i]>tau[2,i]/4,
                tau[A,i]+tau[1,i]+tau[2,i]/2+tau[2,i]^2/(16*tau[A,i]),
                tau[1,i]+tau[2,i]));
  end do;
```

$$\tau_{\max,\,1} := 0.0970$$
$$\tau_{\max,\,2} := 0.101$$
$$\tau_{\max,\,3} := 0.134$$
$$\tau_{\max,\,4} := 0.134$$
$$\tau_{\max,\,5} := 0.134$$
$$\tau_{\max,\,6} := 0.101$$
$$\tau_{\max,\,7} := 0.0970$$

```
> ODD:=seq(1+2*i,i=0..(m-1)/2);
```

$$ODD := 1, 3, 5, 7$$

```
> EVEN:=seq(2+2*i,i=0..(m-2)/2);
```

$$EVEN := 2, 4, 6$$

Max stress parralel layers

```
> 'm'=(m);
```

$$m = 7$$

```
> sigma[M,max,0]:=max(seq(sigma[M,i],i=ODD));
```

$$\sigma_{M,\ \mathrm{max},\ 0} := 0.785$$

```
> sigma[n,max,0]:=max(seq(sigma[n,i],i=ODD));
```

$$\sigma_{n,\ \mathrm{max},\ 0} := 4.558$$

```
> tau[n,max,0]:=max(seq(tau[max,i],i=ODD));
```

$$\tau_{n,\ \mathrm{max},\ 0} := 0.134$$

Max stress perpendicular layers

```
> 'm'=(m);
```

$$m = 7$$

```
> sigma[M,max,90]:=max(seq(sigma[M,i],i=EVEN));
```

$$\sigma_{M,\ \mathrm{max},\ 90} := 0.0522$$

```
> sigma[n,max,90]:=max(seq(sigma[n,i],i=EVEN));
```

$$\sigma_{n,\ \mathrm{max},\ 90} := 0.2031$$

```
> tau[n,max,90]:=max(seq(tau[max,i],i=EVEN));
```

$$\tau_{n,\ \mathrm{max},\ 90} := 0.134$$

```
>
```

B.4 CLT Joint Resistance

Strength Fastener

```
> restart;
> Ru:=N[ef]*min(seq(FM[i],i=1..4))*m:
```

Number of Fasteners

```
> N[ef]:=N[x]*N[y];
```

$$N_{ef} := N_x N_y$$

Failure Mechanisms

```
> FM[1]:=f[h]*t[1]*d;
```

$$FM_1 := f_h t_1 d$$

```
> FM[2]:=0.5*f[h]*t[2]*d;
```

$$FM_2 := 0.5 f_h t_2 d$$

```
> FM[3]:=(f[h]*t[1]*d)/(2+beta)*sqrt(2*beta*(1+beta)+4*beta*(2+beta)
  *M[y,Rk]/(f[h]*t[1]^2)-beta);
```

$$FM_3 := \frac{f_h t_1 d \sqrt{2\beta(1+\beta) + \frac{4\beta(2+\beta) M_{y,Rk}}{f_h t_1^2} - \beta}}{2+\beta}$$

```
> FM[4]:=sqrt(2*beta/(1+beta))*sqrt(2*M[y,Rk]*f[h]*d);
```

$$FM_4 := 2\sqrt{\frac{\beta}{1+\beta}}\sqrt{M_{y,Rk} f_h d}$$

```
> beta:=1;
  for i from 1 to 4 do
  FM[i];
  end do;
```

$$\beta := 1$$

$$f_h t_1 d$$

$$0.5 f_h t_2 d$$

$$\frac{1}{3} f_h t_1 d \sqrt{3 + \frac{12 M_{y,Rk}}{f_h t_1^2}}$$

$$\sqrt{2}\sqrt{M_{y,Rk} f_h d}$$

Yield Capacity Fastener

```
> M[y,Rk]:=identify(8/10*1/6)*f[u,k]*d^3;
```

$$M_{y,Rk} := \frac{2}{15} f_{u,k} d^3$$

```
>
```

Parameters

```
> f[u,k]:=360;
  rho[k]:=900;
  t[1]:=2*43;
  t[2]:=5*43;
  m:=2;
  f[h]:=51.6;
  d:=12;
```

$$f_{u,\ k} := 360$$
$$\rho_k := 900$$
$$t_1 := 86$$
$$t_2 := 215$$
$$m := 2$$
$$f_h := 51.6$$
$$d := 12$$

Fastener Resistance

```
> unassign('i');
> for i from 1 to 4 do
  R[i]:=evalf[3](FM[i])/1e3;
  'kN'
> end do;
```

$$R_1 := 53.3$$
$$kN$$
$$R_2 := 66.5$$
$$kN$$
$$R_3 := 42.2$$
$$kN$$
$$R_4 := 10.1$$
$$kN$$

```
>
```

Maximum Joint Resistance (Neff=20, m=2)

```
> N[y]:=2;
  N[x]:=20;
```

$$N_y := 2$$

$$N_x := 20$$

```
> 'R[v,j,max]'=evalf[4](Ru)/1e3;'kN';
```

$$R_{v,\,j,\,\mathrm{max}} = 810.8$$

$$kN$$

Minumum Joint Resistance (Neff=5, m=2)

```
> N[y]:=1;
  N[x]:=5;
```

$$N_y := 1$$

$$N_x := 5$$

```
> 'R[v,j,min]'=evalf[4](Ru)/1e3;'kN';
```

$$R_{v,\,j,\,\mathrm{min}} = 101.4$$

$$kN$$